**REPUBLIC OF TÜRKİYE**

**YILDIZ TECHNICAL UNIVERSITY**

**GRADUATE SCHOOL OF SCIENCE AND ENGINEERING**

# HYPHENATED ANALYTICAL METHODS FOR HIGH ACCURACY, SENSITIVITY AND INNOVATIVE APPROACHES IN ISOTOPE DILUTION METHOD

**Sezin ERARPAT BODUR**

DOCTOR OF PHILOSOPHY THESIS

Department of Chemistry

Analytical Chemistry Program

Supervisor

Prof. Dr. Sezgin BAKIRDERE

May, 2024

**REPUBLIC OF TÜRKİYE**

**YILDIZ TECHNICAL UNIVERSITY**

**GRADUATE SCHOOL OF SCIENCE AND ENGINEERING**

# HYPHENATED ANALYTICAL METHODS FOR HIGH ACCURACY, SENSITIVITY AND INNOVATIVE APPROACHES IN ISOTOPE DILUTION METHOD

A thesis submitted by Sezin ERARPAT BODUR in partial fulfillment of the requirements for the degree of DOCTOR OF PHILOSOPHY is approved by the committee on 16.05.2024 in Department of Chemistry, Analytical Chemistry Program.

Prof. Dr. Sezgin BAKIRDERE

Yıldız Technical University

Supervisor

**Approved By the Examining Committee**

Prof. Dr. Sezgin BAKIRDERE, Supervisor
Yıldız Technical University _____

Prof. Dr. Yücel ŞAHİN, Member
Yıldız Technical University _____

Assoc. Prof. Dr. Nizamettin ÖZDOĞAN, Member
Zonguldak Bülent Ecevit University _____

Prof. Dr. Mustafa Reşat APAK, Member
İstanbul University Cerrahpaşa _____

Prof. Dr. Şule DİNÇ ZOR, Member
Yıldız Technical University _____

I hereby declare that I have obtained the required legal permissions during data collection and exploitation procedures, that I have made the in-text citations and cited the references properly, that I haven't falsified and/or fabricated research data and results of the study and that I have abided by the principles of the scientific research and ethics during my Thesis Study under the title of "Hyphenated Analytical Methods for High Accuracy, Sensitivity and Innovative Approaches in Isotope Dilution Method" supervised by my supervisor, Prof. Dr. Sezgin BAKIRDERE. In the case of a discovery of false statement, I am to acknowledge any legal consequence.

Sezin ERARPAT BODUR

Signature

This work was supported by Health Institutes of Türkiye (TÜSEB) and The Scientific and Technological Research Council of Türkiye (TÜBİTAK). Project numbers: 2020CV01-8946 (TÜSEB) and 122Z041 (TÜBİTAK).

*Dedicated to my husband*

*and my family*

# ACKNOWLEDGEMENTS

First, I would like to express my gratitude to my advisor Prof. Dr. Sezgin BAKIRDERE for his academic and spiritual supports and always believing in me. It is very valuable for me that he always encouraged me and has shared his valuable knowledge and experiences during my undergraduate, master's and doctoral processes. I am very proud to be his student and I would like to express my endless gratitude to my supervisor for holding my hand in my progress towards science.

I would like to thank my beloved husband and colleague Res. Asst. Süleyman BODUR, whose presence I felt every second during my doctorate journey, for all his help and efforts. Choosing a laboratory partner is as difficult as choosing a spouse. I found both my laboratory partner and my husband with whom I will share my life in the same person. I feel very lucky to work with such a hardworking and intelligent partner.

I would like to thank Assoc. Prof. Dr. Ömer Tahir Günkara, whom I felt very lucky to have known during my undergraduate life and to have been his student. He made great contributions to my thesis, especially regarding derivatization and isotope studies. We achieved successful results thanks to his excellent syntheses.

I would also like to thank my thesis committee; Prof. Dr. Yücel ŞAHİN and Assoc. Prof. Dr. Nizamettin ÖZDOĞAN for their insightful comments and encouragement.

I am grateful to Health Institutes of Türkiye (TÜSEB) and The Scientific and Technological Research Council of Türkiye (TÜBİTAK) for their support the projects found in this thesis.

I would like to thank Bakırdere Research Group members especially to Dr. Dotse Selali CHORMEY, Asst. Prof. Dr. Elif ÖZTÜRK ER, Asst. Prof. Dr. Hakan SERBEST, Dr. Buse Tuğba ZAMAN, Merve FIRAT AYYILDIZ, Elif YAZICI, Bedrihan KARTOĞLU, Aleyna BAHÇIVAN, Bahar KARADEMİR TUTAR, they have been with me in my difficult times and made me smile during this difficult period.

I would like to express my endless gratitude to my family Tülin KORKMAZ, Fatih ERARPAT, Müge ERARPAT, Merve ERARPAT, from whom I received the greatest financial and moral support throughout my life and never left me alone.

Sezin ERARPAT BODUR

# TABLE OF CONTENTS

**LIST OF SYMBOLS** **xi**
**LIST OF ABBREVIATIONS** **xiii**
**LIST OF FIGURES** **xviii**
**LIST OF TABLES** **xxii**
**ABSTRACT** **xxv**
**ÖZET** **xxvii**
**1 INTRODUCTION** **1**
1.1 Literature Review ..... 1
1.2 Objective of the Thesis ..... 3
1.3 Hypothesis ..... 3
**2 GENERAL INFORMATION** **5**
2.1 Chromium ..... 5
2.2 Cobalamin (Vitamin B12) ..... 7
2.3 Chloroquine ..... 9
2.4 Hydroxychloroquine ..... 11
2.5 Capsaicin ..... 12
2.6 Instrumental Methods ..... 14
2.6.1 Spectroscopic Methods ..... 14
2.6.2 Absorption spectrometry ..... 16
2.6.3 Flame atomic absorption spectrometry (FAAS) ..... 16
2.6.4 Emission spectroscopy ..... 18
2.6.5 Inductively Coupled Plasma Spectrometry ..... 19
2.6.6 Chromatographic Methods ..... 21
2.6.7 Gas chromatography (GC) ..... 22
2.6.8 Liquid chromatography (LC) ..... 23
2.6.9 Mass Spectrometry ..... 27
2.6.10 Hyphenated Methods ..... 32
2.7 Sample Preparation Methods ..... 34
2.7.1 Solid phase extraction (SPE) ..... 34
2.7.2 Liquid-liquid extraction (LLE) ..... 35
2.8 Derivatization ..... 40
2.9 Speciation Analysis ..... 42

2.10 Isotope Dilution Methods ..... 44
2.11 Multivariate Optimization Strategies ..... 49
**3 MATERIALS AND METHODS** **52**
3.1 Quantification of Chromium (III) and Chromium (VI) in Water, Soil and Grass Samples by HPLC-ICP-OES System ..... 52
3.1.1 Reagents and chemicals ..... 52
3.1.2 Instrumentation ..... 53
3.1.3 HPLC-ICP-OES conditions ..... 54
3.1.4 Samples ..... 55
3.2 Quantification of Cobalamin in Vitamin Drug Tablets by HPLC-FAAS System ..... 56
3.2.1 Reagents and chemicals ..... 56
3.2.2 Instrumentation ..... 56
3.2.3 Samples ..... 58
3.3 Quantification of Chloroquine in Human Urine, Saliva and Serum Samples by SB-FDF-LPME-ID$^4$-GC-MS System ..... 59
3.3.1 Reagents and chemicals ..... 59
3.3.2 Instrumentation ..... 60
3.3.3 SB-FDF-LPME Procedure ..... 61
3.3.4 Samples for accuracy and suitability tests ..... 61
3.3.5 Calibration and sample mixtures for SB-FDF-LPME-ID$^4$-GC-MS method ..... 62
3.3.6 Synthesis of chloroquine acetamide-*d3* (CA-*d3*) ..... 66
3.4 Quantification of Hydroxychloroquine in Human Urine, Saliva and Serum Samples by SSB-LPME-ID$^4$-GC-MS System ..... 67
3.4.1 Reagents and chemicals ..... 67
3.4.2 Instrumentation ..... 68
3.4.3 SSB-LPME Procedure ..... 69
3.4.4 Samples for accuracy and suitability tests ..... 69
3.4.5 Calibration and sample mixtures for SSB-LPME-ID$^4$-GC-MS method…. ..... 70
3.4.6 Synthesis of hydroxychloroquine methyl acetate-*d3* (HMA-$d_3$) ..... 74
3.5 Quantification of Capsaicin in Green Pepper, Wastewater and Human Saliva Samples by SB-FDF-LPME-ID$^4$-GC-MS System ..... 75
3.5.1 Reagents and chemicals ..... 75
3.5.2 Instrumentation ..... 76
3.5.3 SB-FDF-LPME Procedures ..... 77

3.5.4 Samples for accuracy and suitability tests ..... 78
3.5.5 Calibration and sample mixtures for SB-FDF-LPME-ID$^4$-GC-MS method..... 79
**4 RESULTS AND DISCUSSION 85**
4.1 Quantification of Chromium (III) and Chromium (VI) in Water, Soil and Grass Samples by HPLC-ICP-OES System ..... 85
4.1.1 Optimization studies ..... 85
4.1.2 System analytical performance for HPLC-ICP-OES method..... 93
4.1.3 Accuracy and suitability tests ..... 95
4.1.4 Comparison with other studies in literature ..... 97
4.2 Quantification of Cobalamin in Vitamin Drug Tablets by HPLC-FAAS System ..... 98
4.2.1 Optimization studies ..... 98
4.2.2 System analytical performance for HPLC-FAAS method..... 104
4.2.3 Accuracy and suitability tests ..... 105
4.2.4 Comparison with other studies in literature ..... 107
4.3 Quantification of Chloroquine in Human Urine, Saliva and Serum Samples by SB-FDF-LPME-ID$^4$-GC-MS System ..... 108
4.3.1 Characterization of chloroquine acetamide and its isotopic material…….. 108
4.3.2 Optimization Studies..... 109
4.3.3 System analytical performance for SB-FDF-LPME-GC-MS method…..... 114
4.3.4 Accuracy and suitability tests ..... 115
4.3.5 Integration of ID$^4$ and SB-FDF-LPME-GC-MS ..... 116
4.3.6 Comparison with other studies in literature ..... 119
4.4 Quantification of Hydroxychloroquine in Human Urine, Saliva and Serum Samples by SSB-LPME-ID$^4$-GC-MS System ..... 120
4.4.1 Characterization of chloroquine acetamide and its isotopic material…….. 121
4.4.2 Optimization studies ..... 122
4.4.3 Box Behnken Design ..... 124
4.4.4 System analytical performance for SSB-LPME-GC-MS method .... 129
4.4.5 Accuracy and suitability tests ..... 130
4.4.6 Integration of ID$^4$ and SSB-LPME-GC-MS ..... 131
4.4.7 Comparison with other studies in literature ..... 134
4.5 Quantification of Capsaicin in Green Pepper, Wastewater and Human Saliva Samples by SB-FDF-LPME-ID$^4$-GC-MS System ..... 135

4.5.1 Optimization studies ..... 135
4.5.2 System analytical performance for SB-FDF-LPME-GC-MS method…..... 143
4.5.3 Accuracy and suitability tests ..... 145
4.5.4 Integration of $ID^4$ and SB-FDF-LPME-GC-MS ..... 147
4.5.5 Comparison with other studies in literature ..... 149
**5 CONCLUSION** **151**
**REFERENCES** **154**
**PUBLICATIONS FROM THE THESIS** **177**

# LIST OF SYMBOLS

| | |
|---|---|
| % | Percentage |
| < | Less than |
| > | Greater Than |
| ± | Plus or Minus |
| ≤ | Less Than or Equal to |
| ≥ | Greater Than or Equal to |
| $^{o}$C | Degree Celsius |
| µg | Microgram |
| µL | Microliter |
| µm | Micrometer |
| cm | Centimeter |
| eV | Electronvolt |
| g | Gram |
| *g* | Gravitational Force |
| kg | Kilogram |
| L | Liter |
| log | Logarithm |
| m | meter |
| m/z | Mass to Charge Ratio |
| MΩ | Megaohm |
| mA | Milliampere |
| mg | Milligram |
| min | Minute |
| mL | Milliliter |
| mm | Millimeter |
| mmol | Millimol |
| mol | Mol |
| nm | Nanometer |
| s | second |

| | |
|---|---|
| v/v | Volume/Volume |
| w/w | Weight/Weight |

# LIST OF ABBREVIATIONS

| | |
|---|---|
| %RSD | Percent Relative Standard Deviation |
| A | Analyte |
| A* | Standard Solution of Analyte |
| A*B-x | Calibration Mixture (x: 1,2 or 3) |
| AB | Sample Mixture |
| Ac | Acetic Acid |
| ACN | Acetonitrile |
| ANOVA | Analysis of Variance |
| APCI | Atmospheric Pressure Chemical Ionization |
| B | Isotopic Material |
| BSA | N,O-bis(trimethylsilyl)acetamide |
| BSTFA | N,O-bis(trimethylsilyl)trifluoroacetamide |
| CE | Capillary Electrophoresis |
| CE | Capillary Electrophoresis |
| CI | Chemical Ionization |
| CoV | SARS-Associated Coronaviruses |
| COVID19 | Coronavirus Disease of 2019 |
| CPE-HPLC | Cloud Point Extraction-High-Performance Liquid Chromatography |
| DESs | Deep Eutectic Solvents |
| DLLME | Dispersive Liquid-Liquid Microextraction |
| DMA | Dimethyarsinic Acid |
| DMBA | N,N-dimethylbenzylamine |
| DMSPE-HPLC | Dispersive Micro-Solid Phase Extraction High Performance Liquid Chromatography |
| ECD | Electron Capture Detector |
| EDTA | Ethylenediaminetetraacetic acid |
| EI | Electron Ionization |
| ELCD | Electrolytic Conductivity Detector |
| ESI | Electrospray Ionization |

| | |
|---|---|
| ETAAS | Electrothermal Atomic Absorption Spectrometry |
| FAAS | Flame Atomic Absorption Spectrophotometry |
| FID | Flame Ionization Detector |
| FT-IR | Fourier-Transform Infrared Spectroscopy |
| GC | Gas Chromatography |
| GC-AAS | Gas Chromatography-Atomic Absorption Spectrometry |
| GC-ICP-MS | Gas Chromatography-Inductively Coupled Plasma-Mass Spectroscopy |
| GC-ICP-OES | Gas Chromatography-Inductively Coupled Plasma-Optical Emission Spectroscopy |
| GC-MS | Gas Chromatography-Mass Spectrometry |
| GLC | Gas-Liquid Chromatography |
| GSC | Gas-Solid Chromatography |
| HCL | Hollow Cathode Lamp |
| HF-LPME | Hollow Fiber-Based Liquid-Phase Microextraction |
| HG-AAS | Hydride Generation-Atomic Absorption Spectrometry |
| HID | Helium Ionization Detector |
| HPLC | High Performance Liquid Chromatography |
| HPLC-FAAS | High Performance Liquid Chromatography-Flame Atomic Absorption Spectrophotometry |
| HPLC‑FL | High Performance Liquid Chromatography With Fluorescence Detector |
| HPLC-ICP-AES | High-Performance Liquid Chromatography-Inductively Coupled Plasma-Atomic Emission Spectrometry |
| HPLC-ICP-MS | High Performance Liquid Chromatography-Inductively Coupled Plasma-Mass Spectrometry |
| HPLC-ICP-OES | High Performance Liquid Chromatography-Inductively Coupled Plasma-Optical Emission Spectrometry |
| HPLC-UV | High-Performance Liquid Chromatography-Ultraviolet Detector |
| HPLC-UV/VIS | High Performance Liquid Chromatography-Ultraviolet/Visible Detection |
| IC-ICP-AES | Ion Chromatography-Inductively Coupled Plasma-Atomic Emission Spectrometry |
| ICP-AES | Inductively Coupled Plasma-Atomic Emission Spectrometry |

| | |
|---|---|
| ICP-MS | Inductively Coupled Plasma-Mass Spectrometry |
| ICP-OES | Inductively Coupled Plasma-Optical Emission Spectrometry |
| ID | Isotope Dilution |
| ID2 | Double or Reverse Isotope Dilution |
| ID3 | Triple Isotope Dilution |
| ID4 | Quadruple Isotope Dilution |
| Ils | Ionic Liquids |
| IUPAC | International Union of Pure and Applied Chemistry |
| LC | Liquid Chromatography |
| LC-AAS | Liquid Chromatography-Atomic Absorption Spectrophotometry |
| LC-FAAS | Liquid Chromatography-Flame Atomic Absorption Spectrophotometry |
| LC-ICP-MS | Liquid Chromatography- Inductively Coupled Plasma Mass Spectrometry |
| LC-IR | Liquid Chromatography-Infrared Spectrometry |
| LC-MS | Liquid Chromatography-Mass Spectrometry |
| LC-MS/MS | Liquid Chromatography-Tandem Mass Spectrometry |
| LC–NMR | Liquid Chromatography-Nuclear Magnetic Resonance |
| LLE | Liquid–Liquid Extraction |
| LLLME-HPLC-UV | Liquid-Liquid-Liquid Microextraction-High Performance Liquid Chromatography-UV Detection |
| LLOD | Lower Limit of Detection |
| LLOQ | Lower Limit of Quantitation |
| LOD | Limit of Detection |
| LOQ | Limit of Quantitation |
| LPME | Liquid Phase Microextraction |
| LWR | Linear Working Range |
| m | Slope |
| MALDI | Matrix-Assisted Laser Desorption Ionization |
| MMA | Monomethylarsonic Acid |
| MS | Mass Spectrometry |
| MSPE | Magnetic Solid Phase Extraction |

| | |
|---|---|
| MSTFA | N-methyl-N-(trimethylsilyl)trifluoroacetamide |
| MTBSTFA | N-methyl-N-(tert-butyldimethylsilyl)trifluoroacetamide |
| NaAc | Sodium Acetate |
| NMR | Nuclear Magnetic Resonance Spectroscopy |
| P1 | Banana Pepper Sample |
| P2 | Kıl Pepper Sample |
| P3 | Sivri Pepper Sample |
| P4 | Samandağ Pepper Sample |
| PA | Peak Area |
| PFBBr | Pentafluorobenzyl Bromide |
| pH | Power of Hydrogen |
| PID | Photoionization Detector |
| PTFE | Polytetrafluoroethylene |
| R2 | Correlation Coefficient |
| S.D. | Standard Deviation |
| S1 | Saliva sample 1 |
| S2 | Saliva sample 2 |
| SB-FDF-LPME | Spraying Based Fine Droplet Formation Liquid Phase Microextraction |
| SB-FDF-LPME-ID$^4$-GC-MS | Spraying Based Fine Droplet Formation Liquid Phase Microextraction-Quadruple Isotope Dilution-Gas Chromatography-Mass Spectrometry |
| SDME | Single Drop Microextraction |
| SIM | Selected Ion Monitoring |
| SPE | Solid Phase Extraction |
| SPME-GC-MS | Solid Phase Microextraction–Gas Chromatography–Mass Spectrometry |
| SQT | Slotted Quartz Tube |
| SS | Standard Deviation Value Of The Lowest Concentration In The Calibration Plot |
| SSB-LPME | Smart Solvent-Based Liquid Phase Microextraction |
| SSB-LPME-ID$^4$-GC-MS | Smart Solvent Based Liquid Phase Microextraction-Quadruple Isotope Dilution-Gas Chromatography-Mass Spectrometry |

| | |
|---|---|
| SSs | Smart Solvents |
| TBA | Tetrabutylammonium Hydroxide |
| TCD | Thermal Conductivity Detector |
| TEA | Triethylamine |
| TID | Thermionic Ionization Detector |
| TLC | Thin Layer Chromatography |
| TRPV1 | Transient Receptor Potential Vanilloid Subtype 1 |
| T-SQT | T-Shaped Slotted Quartz Tube |
| UHPLC-HRMS | Ultra-High Performance Liquid Chromatography With High Resolution Mass Spectrometry |
| UHPLC-MS/MS | Ultrahigh Performance Liquid Chromatography-Tandem Mass Spectrometry |
| UPW | Ultrapure Water |
| USEPA | United States Environmental Protection Agency |
| UV-Vis | Ultraviolet-Visible |
| W1 | Wastewater Sample 1 |
| W2 | Wastewater Sample 2 |
| X | Acetic Anhydride Volume |
| Y | Smart Solvent Volume |
| Z | Sodium Hydroxide Volume |

# LIST OF FIGURES

**Figure 2.1** The entry mechanism of chromium (VI) to cell membrane (left) and electron transfer reaction to produce chromium intermediates and free radicals [27], [33] ..... 6
**Figure 2.2** The molecular structure of cobalamin [41] ..... 8
**Figure 2.3** The molecular structure of chloroquine [53] ..... 10
**Figure 2.4** The molecular structure of hydroxychloroquine [53] ..... 11
**Figure 2.5** Scoville scale index. The highest Scoville index belongs to pure capsaicin while the lowest index to bell peppers [90] ..... 13
**Figure 2.6** The molecular structure of capsaicin [83] ..... 13
**Figure 2.7** A summary of spectroscopic methods [100] ..... 15
**Figure 2.8** The diagram for a) Atomic emission b) atomic absorption c) atomic fluorescence spectrometers [100] ..... 15
**Figure 2.9** A schematic diagram of FAAS system [105] ..... 16
**Figure 2.10** T-shaped slotted quartz tube [118] ..... 18
**Figure 2.11** The schematic presentation of a torch in ICP sources [119] ..... 20
**Figure 2.12** The schematic diagram of ICP-OES system [121] ..... 21
**Figure 2.13** The family tree of chromatographic methods [125] ..... 22
**Figure 2.14** A schematic diagram of GC system [129] ..... 22
**Figure 2.15** High performance liquid chromatography system a) Mobile phase reservoir b) pump; c) sample introduction; d) analytical column, e) detector(s); f) data collection and processing; g) drain [139] ..... 27
**Figure 2.16** The general diagram of MS system [145] ..... 28
**Figure 2.17** The schematic presentation of ESI [147] ..... 29
**Figure 2.18** The schematic diagram of quadrupole mass analyzer [147] ..... 30
**Figure 2.19** The orbitrap mass analyzer [151] ..... 31
**Figure 2.20** The schematic diagram of a discrete dynode electron multiplier [147] ..... 31
**Figure 2.21** A diagram for the application of SPE method [173] ..... 35
**Figure 2.22** A schematic diagram for DLLME method [181] ..... 36
**Figure 2.23** A schematic presentation of SB-FDF-LPME taken from Dikmen et. al [9] ..... 37

**Figure 2.24** A schematic presentation of SSB-LPME method [8].....40
**Figure 2.25** Catch and release method that constitutes the principle of ID method [234].....45
**Figure 2.26** Isotopic compositions of sample and isotopic material.....46
**Figure 2.27** The schematic presentation of all ID methods .....49
**Figure 2.28** The graphical presentation for two (a) and three (b) parameters in central composite design [243] .....51
**Figure 2.29** The cubic view of Box-Behnken design [245].....51
**Figure 3.1** A schematic presentation of HPLC-ICP-OES system for the determination of chromium species .....53
**Figure 3.2** HPLC-FAAS system with the novel nebulizer system (A) and dimensions for T-SQT and nebulizer system (B) [251].....58
**Figure 3.3** Synthesis of CA-$d_3$ [252].....67
**Figure 3.4** Synthesis of HMA-$d_3$ .....75
**Figure 4.1** Optimization of nebulizer gas flow rate (The constant parameters were 15 L/min plasma gas flow rate, 0.20 L/min auxiliary gas flow rate)..85
**Figure 4.2** Optimization of plasma gas flow rate (The constant parameters were 0.60 L/min nebulizer gas flow rate, 0.20 L/min auxiliary gas flow rate) .....86
**Figure 4.3** A chromatogram obtained by the optimized HPLC-ICP-OES system with 30 mmol/L ammonium nitrate solution (pH 7.0).....88
**Figure 4.4** A chromatogram obtained by the optimized HPLC-ICP-OES system with 30 mmol/L ammonium nitrate and 3.0% methanol solution (pH 7.0) as mobile phase.....89
**Figure 4.5** Optimization of methanol concentration (Constant conditions: anion exchange column, 0.60 L/min nebulizer gas flow rate, 0.20 L/min auxiliary gas flow rate, 14 L/min plasma gas flow rate, 1.0 mL/min mobile phase flow rate, chromium (III) 9.04 mg/kg, chromium (VI) 6.27 mg/kg).....90
**Figure 4.6** Optimization of pH value for mobile phase (Constant conditions: anion exchange column, 0.60 L/min nebulizer gas flow rate, 0.20 L/min auxiliary gas flow rate, 14 L/min plasma gas flow rate, 1.0 mL/min mobile phase flow rate, chromium (III) 33.61 mg/kg, chromium (VI) 4.28 mg/kg).....91

**Figure 4.7** A chromatogram obtained by the optimized HPLC-ICP-OES system with 1.0 mL/min mobile phase flow rate ..... 92
**Figure 4.8** Optimization of injection volume (Constant conditions: anion exchange column, 0.60 L/min nebulizer gas flow rate, 0.20 L/min auxiliary gas flow rate, 14 L/min plasma gas flow rate, 1.0 mL/min mobile phase flow rate, chromium (III) 20.31 mg/kg, chromium (VI) 10.04 mg/kg) ..... 93
**Figure 4.9** Calibration plot for the determination of chromium (III) by the developed HPLC-ICP-OES system ..... 94
**Figure 4.10** Calibration plot for the determination of chromium (VI) by the developed HPLC-ICP-OES system ..... 94
**Figure 4.11** A plot of mobile phase flow rate against absorbance values (n= 3 error bars)..... 99
**Figure 4.12** Chromatographic separation of cobalt and cobalamin at the flow rate of 1.75 mL/min [251]..... 99
**Figure 4.13** A plot of nebulizer gas flow rate against absorbance values (n= 3 error bars)..... 100
**Figure 4.14** A plot of T-SQT height from burner head against absorbance values (n= 3 error bars) ..... 101
**Figure 4.15** A plot of injection volume against absorbance values (n= 3 error bars) ..... 102
**Figure 4.16** A plot of log[Ac]/[NaAc] against absorbance values (n= 3 error bars) ..... 103
**Figure 4.17** A plot of mobile phase concentration against absorbance values (n= 3 error bars)..... 104
**Figure 4.18** Calibration plot for the determination of cobalamin by HPLC-FAAS system ..... 105
**Figure 4.19** Standard addition calibration plots for vitamin drugs ..... 106
**Figure 4.20** GC-MS chromatograms (A and B) and mass spectrum (C) for CA derivative (black (219.2), orange (247.2), red (204.1), blue (332.3) and purple (86.2)) ..... 108
**Figure 4.21** GC-MS chromatogram (A) and mass spectrum (B) for CA-*d3* (black (222.2), purple (335.3) blue (292.1)) ..... 109
**Figure 4.22** Optimization of extraction solvent type ..... 110

**Figure 4.23** Optimization of spraying cycle ..... 110
**Figure 4.24** Optimization of sodium hydroxide concentration ..... 111
**Figure 4.25** Optimization of sodium hydroxide volume ..... 112
**Figure 4.26** Optimization of mixing type ..... 113
**Figure 4.27** Optimization of acetic anhydride concentration ..... 114
**Figure 4.28** Calibration plot for the developed SB-FDF-LPME-GC-MS method ..... 115
**Figure 4.29** GC-MS chromatogram (A) and mass spectrum (B) for HMA derivate ..... 121
**Figure 4.30** GC-MS chromatogram (A) and mass spectrum (B) for HMA-$d_3$ ..... 122
**Figure 4.31** The effect of mixing type ..... 123
**Figure 4.32** The effect of mixing period ..... 123
**Figure 4.33** The effect of sodium hydroxide concentration ..... 124
**Figure 4.34** Normal probability of internally studentized residuals ..... 128
**Figure 4.35** 3D surface plot showing the interaction between X and Y (Z was fixed at 2.75 mL) ..... 128
**Figure 4.36** Calibration plot for the SSB-LPME-GC-MS method ..... 130
**Figure 4.37** Optimization of extraction solvent type ..... 136
**Figure 4.38** Optimization of spraying cycle ..... 137
**Figure 4.39** Optimization of pH value ..... 137
**Figure 4.40** Optimization of buffer solution volume ..... 138
**Figure 4.41** Optimization of mixing type for extraction step ..... 139
**Figure 4.42** Optimization of mixing period for extraction step ..... 139
**Figure 4.43** Optimization of mixing type for derivatization step ..... 140
**Figure 4.44** Optimization of mixing period for derivatization step ..... 141
**Figure 4.45** Optimization of salt effect ..... 141
**Figure 4.46** Optimization of acetic anhydride volume ..... 142
**Figure 4.47** Optimization of initial sample volume ..... 143
**Figure 4.48** Calibration plot for the determination of capsaicin by GC-MS system ..... 144
**Figure 4.49** Calibration plot for the determination of capsaicin by SB-FDF-LPME-GC-MS system ..... 145
**Figure 4.50** Effect of equilibrium period for isotopes ..... 148

# LIST OF TABLES

**Table 2.1** Notations for isotope dilution formulas ..... 46
**Table 3.1** Reagents and chemicals used in this study ..... 52
**Table 3.2** HPLC-ICP-OES conditions for the determination of chromium species ..... 54
**Table 3.3** Reagents and chemicals used for HPLC-FAAS method ..... 56
**Table 3.4** HPLC-FAAS conditions for the determination of cobalamin ..... 57
**Table 3.5** All Reagents and chemicals used for the determination of chloroquine by SB-FDF-LPME-ID$^4$-GC-MS method ..... 59
**Table 3.6** GC-MS conditions for the determination of chloroquine by SB-FDF-LPME-ID$^4$-GC-MS method ..... 60
**Table 3.7** Theoretical mass values used for the preparation of calibration and sample mixtures ..... 62
**Table 3.8** Calibration mixture compositions (The concentration levels of A* and B solutions were 20.03 and 18.24 mg/kg, respectively)..... 63
**Table 3.9** Sample mixtures (The concentration of B was 72.17 mg/kg.)..... 63
**Table 3.10** Sample mixture dilutions after the protein precipitation for the process in Table 3.9 ..... 64
**Table 3.11** Calibration mixture compositions (The concentration levels of A* and B solutions were 40.62 and 36.11 mg/kg, respectively) ..... 65
**Table 3.12** Sample mixtures (The concentration of B was 144.60 mg/kg.)..... 65
**Table 3.13** Sample mixture dilutions after the protein precipitation for the process in Table 3.12 ..... 66
**Table 3.14** All reagents and chemicals used for the determination of hydroxychloroquine by SSB-LPME-ID$^4$-GC-MS method ..... 67
**Table 3.15** GC-MS conditions for the determination of hydroxychloroquine by SSB-LPME-ID$^4$-GC-MS method..... 68
**Table 3.16** The theoretical compositions of calibration and sample mixtures..... 70
**Table 3.17** Calibration and sample mixtures for 1.0 mg/kg of hydroxychloroquine sulfate spiked samples..... 71
**Table 3.18** Second dilutions for 1.0 mg/kg of hydroxychloroquine spiked samples ..... 72

**Table 3.19** Calibration and sample mixtures for 1.0 mg/kg of hydroxychloroquine sulfate spiked samples....73
**Table 3.20** Second dilutions for 2.0 mg/kg of hydroxychloroquine spiked samples ....74
**Table 3.21** All reagents and chemicals used for the determination of capsaicin by SB-FDF-LPME-ID$^4$-GC-MS method....75
**Table 3.22** GC-MS conditions for the determination of capsaicin by SB-FDF-LPME-ID$^4$-GC-MS method....77
**Table 3.23** Preparation of pepper samples....79
**Table 3.24** Second dilution process for P2 and P3 samples....80
**Table 3.25** Preparation of A solutions for pepper and wastewater samples....80
**Table 3.26** Protein precipitation for saliva samples....81
**Table 3.27** Dilution process for saliva samples after protein precipitation....81
**Table 3.28** Theoretical mass values used for the preparation of calibration and sample mixtures....81
**Table 3.29** Calibration and sample mixtures for 25 µg/kg of capsaicin in the spiked samples....82
**Table 3.30** Calibration and sample mixtures for 50 µg/kg of capsaicin in the spiked samples....83
**Table 4.1** Columns studied in the optimization of column type....87
**Table 4.2** Retention times obtained in the optimization of methanol concentration ....89
**Table 4.3** Retention times obtained in the optimization of mobile phase flow rate ....92
**Table 4.4** Analytical performance of the presented HPLC-ICP-OES method....94
**Table 4.5** Percent recoveries for water, soil, and grass samples....96
**Table 4.6** Analytical performance of the developed HPLC-FAAS method....104
**Table 4.7** Percent recoveries calculated for the spiked drug samples....106
**Table 4.8** Analytical performance of the developed SB-FDF-LPME-GC-MS method....114
**Table 4.9** Recovery results for the spiked samples....116
**Table 4.10** Calibration and sample mixtures for SB-FDF-LPME-ID$^4$-GC-MS method....117

**Table 4.11** Peak area ratios for the calibration and sample mixtures (4.5 mg/kg) ..... 117
**Table 4.12** Peak area ratios for the calibration and sample mixtures (9.2 mg/kg) ..... 118
**Table 4.13** Percent recoveries for the selected samples analyzed by the SB-FDF-LPME-ID$^4$-GC-MS method ..... 119
**Table 4.14** The constructed Box-Behnken experimental design and the results obtain from GC-MS system ..... 125
**Table 4.15** ANOVA results for Box-Behnken experimental design studied ..... 126
**Table 4.16** Analytical performance of the developed SSB-LPME-GC-MS method ..... 129
**Table 4.17** Recovery results for the spiked samples ..... 130
**Table 4.18** The derivatized analyte peak area/the labelled material peak area ratio for the mixtures. (low level) ..... 131
**Table 4.19** The derivatized analyte peak area/the labelled material peak area ratio for the mixtures (high level) ..... 132
**Table 4.20** Percent recoveries for the selected samples analyzed by the SSB-LPME-ID$^4$-GC-MS method ..... 134
**Table 4.21** Analytical performance of the developed SB-FDF-LPME-GC-MS method ..... 144
**Table 4.22** Recovery results for pepper, saliva and wastewater samples ..... 145
**Table 4.23** Percent recoveries and relative standard deviation for the ID$^4$-SFDF-LPME-GC-MS method ..... 149

# ABSTRACT

## Hyphenated Analytical Methods for High Accuracy, Sensitivity and Innovative Approaches in Isotope Dilution Method

Sezin ERARPAT BODUR

Department of Chemistry

Doctor of Philosophy Thesis

Supervisor: Prof. Dr. Sezgin BAKIRDERE

Hyphenated systems have been indispensable instrumental methods for the development of analytical strategies due to the presence of target analyte(s) at trace levels in complicated sample matrices. In this sense, this thesis comprises several hyphenated methods for the quantitation of inorganic and organic compounds in environmental and biological matrices. In the first study, chromium (III) and (VI) in water, soil and grass samples were chromatographically separated and detected by high performance liquid chromatography (HPLC) coupled to inductively coupled plasma optical emission spectrometry (ICP-OES). Good linearity ($R^2 \geq 0.9991$) and low limit of detection (LOD) values (0.27 and 0.05 mg/kg) were obtained for each analyte. The second study in this thesis belongs to the determination of cobalamin in vitamin drug samples by the help of HPLC system coupled to flame atomic absorption spectrophotometry (FAAS). A novel nebulizer system was produced using T-shaped slotted quartz tube (T-SQT). Under the optimum HPLC-FAAS conditions, LOD value was found as 1.6 mg/kg cobalamin as cobalt.

Precision and accuracy are important analytical parameters that researchers are willing to achieve excellent precision and accuracy for any analytical method. Isotope dilution (ID) methods have been performed to improve these analytical parameters. Within the scope of this thesis, chloroquine, hydroxychloroquine and capsaicin were individually determined by quadruple isotope dilution ($ID^4$) method combined with green microextraction methods. Gas chromatography-mass spectrometry (GC-MS) was used as hyphenated method for the separation and detection of these three analytes. Spraying based fine droplet formation liquid phase microextraction (SB-FDF-LPME) was used to enrich chloroquine and capsaicin when smart solvent-based liquid phase microextraction (SSB-LPME) method was performed for the preconcentration of hydroxychloroquine. In these three studies, trace level LOD values and high percent recoveries with low standard deviation values were obtained. The microextraction methods provided trace detection limits while $ID^4$ method boosted precision and accuracy of the developed methods.

**Keywords:** Hyphenated analytical methods, chromatography, spectroscopy, microextraction, speciation.

# ÖZET

## Yüksek Doğruluk, Duyarlılık Elde Etmeye Yönelik Birleştirilmiş Analitik Yöntemler ve İzotop Seyreltme Yönteminde Yenilikçi Yaklaşımlar

Sezin ERARPAT BODUR

Kimya Anabilim Dalı

Doktora Tezi

Danışman: Prof. Dr. Sezgin BAKIRDERE

Hedef analit(ler)in karmaşık örnek matrikslerinde eser seviyelerde bulunmasından dolayı birleştirilmiş sistemler analitik stratejilerin geliştirilmesi için vazgeçilmez enstrümantal yöntemler olmuşlardır. Bu bağlamda bu tez inorganik ve organik bileşiklerin çevresel ve biyolojik örneklerde kantitatif tayini için birçok birleştirilmiş yöntemler içermektedir. İlk çalışmada su, toprak ve çimen örneklerinde krom(III) ve (VI) yüksek performanslı sıvı kromatografisi (HPLC) ile birleştirilmiş indüktif eşleşmiş plazma optik emisyon spektrometrisi (ICP-OES) ile kromatografik olarak ayrılmış ve tayin edilmiştir. İyi bir doğrusallık ($R^2 \geq 0,9991$) ve düşük gözlenebilme limiti (GL) değerleri (0,27 ve 0,05 mg/kg) her bir analit için elde edilmiştir. Bu tezin ikinci çalışması HPLC ile birleştirilmiş alevli atomik absorpsiyon spektrofotometrisi (AAAS) yardımıyla vitamin örneklerinde kobalamin tayinine aittir. T-şekilli yarıklı kuvars tüp (T-YKT) kullanarak yeni bir sisleştirici sistem üretilmiştir. Optimum HPLC-AAAS koşulları altında GL değeri kobalt cinsinden kobalamin için 1,6 mg/kg olarak bulunmuştur.

Doğruluk ve kesinlik, araştırmacıların herhangi bir analitik yöntem için mükemmel doğruluk ve kesinliğe ulaşmaya istekli oldukları önemli analitik parametrelerdir. İzotop seyreltme (İS) yöntemleri bu analitik parametrelerin iyileştirilmesi için

kullanılmaktadır. Bu tez kapsamında klorokin, hidroksiklorokin ve kapsaisinin çevreci mikroekstraksiyon yöntemleri ile birleştirilmiş dörtlü izotop seyreltme ($IS^4$) aracılığıyla ayrı ayrı tayin edilmiştir. Gaz kromatografi-kütle spektrometrisi (GC-MS) bu üç analitin ayrılması ve tespiti için birleştirilmiş yöntem olarak kullanılmıştır. Spreyleme esaslı ince damlacık oluşturma sıvı faz mikroekstraksiyon (SE-İDO-SFME) klorokin ve kapsaisinin zenginleştirilmesi için kullanılırken akıllı çözücü esaslı sıvı faz mikroekstraksiyon (AÇE-SFME) hidroksiklorokinin önderiştirilmesi için uygulanmıştır. Bu üç çalışmada eser seviyede GL değerleri ve düşük standart sapma değerleri ile yüksek yüzde geri kazanım sonuçları elde edilmiştir. Mikroekstraksiyon yöntemleri eser gözlenebilme limitleri sağlarken $İS^4$ yöntemi geliştirilen yöntemlerin kesinliğini ve doğruluğunu arttırmaktadır.

**Anahtar kelimeler:** Birleştirilmiş analitik yöntemler, kromatografi, spektroskopi, mikroekstraksiyon, türlendirme.

# 1
# INTRODUCTION

## 1.1 Literature Review

In recent years, hyphenation of chromatographic and spectroscopic methods has been a powerful approach for the qualitative and quantitative determination of organic and inorganic analytes at trace levels. Chromatographic methods like liquid chromatography (LC), gas chromatography (GC) and capillary electrophoresis (CE) are coupled to spectroscopic methods like Fourier-transform infrared (FT-IR), ultraviolet-visible (UV–Vis) absorbance or fluorescence emission, mass spectroscopy (MS), and nuclear magnetic resonance spectroscopy (NMR) [1]. Among them, MS system coupled to GC or LC systems are fascinating combinations which have various applications such as microcontaminants, clinical chemistry, sports doping, forensics and/or toxicology, biomacromolecules, natural products and so on. MS systems allow to characterize chemical species found in complex sample matrices [2]. Another hyphenated method is high performance liquid chromatography (HPLC) coupled to flame atomic absorption spectrophotometry (FAAS). This system is generally used for speciation analysis [3]. Inductively coupled plasma-optical emission spectrometry (ICP-OES) can be linked to liquid chromatographic systems to enhance elemental detection ability and enable multi-elemental detection after a chromatographic separation [4]. In this thesis, three hyphenated analytical methods (GC-MS, HPLC-FAAS and HPLC-ICP-OES) were used to simultaneously separate and detect the target analytes in complex biological and environmental matrices.

An analytical method consists of some main stages such as sampling, sample preparation, measurement and data analysis. Sample preparation has great importance due to its ability to remove matrix interferences, enrich the analyte(s) and make the sample compatible with the instrument being used [5]. Traditional extraction methods such as liquid–liquid extraction (LLE), solid phase extraction (SPE) and Soxhlet extraction are still used in routine analytical procedures but these methods have been modified to minimize their disadvantages such as high consumption of organic solvents, formation of emulsions, excess dilution of the

analytes for LLE and high sample throughput for SPE [6]. Spraying based fine droplet formation liquid phase microextraction (SB-FDF-LPME) [7] and smart solvent-based liquid phase microextraction (SSB-LPME) [8] methods are two new generation extraction methods with green extraction steps and high preconcentration factors. SB-FDF-LPME method includes the preconcentration of analyte by a few microliter of organic solvent which is introduced to the sample solution via a simple spraying system [9]. SSB-LPME is also known as green microextraction method due to the usage of smart solvents [10]. Hence, SB-FDF-LPME and SSB-LPME were used as preconcentration methods prior to GC-MS measurements.

Some analytical procedures need to change the chemical form of analytes which called as derivatization in order to boost the sensitivity and accuracy of the developed methods. Derivatization is commonly used prior to GC analysis to obtain analyte derivatives with good thermal stability and low boiling points and derivatives without polar groups and active hydrogens [11]. Acetic anhydride was used for the acetylation of analytes in both aqueous and non-aqueous mediums [12] to protect -OH (alcohols, polyols, phenols, enols), NH (amines, amides) and -SH (thiols) groups [13]. It is low-cost chemical and has low boiling point and low molecular weight [14]. Hence, hydroxychloroquine, chloroquine and capsaicin were acetylated using acetic anhydride prior to their chromatographic separation.

Several calibration methods such as external, internal, standard addition methods [15] and matrix matching calibration methods [16] have been used in literature to quantify the target analyte(s). Isotope dilution (ID) has an exceptional quantitation method with high precision and accuracy [17]. It is based on the detection of isotope ratio for a mixture containing sample (A) and isotopic material (B) of the analyte. Today, four different isotope dilution methods are available but the latest one '*quadruple isotope dilution (ID$^4$)*' has higher precision and accuracy due to its formula being independent from the terms with high uncertainty [18]. For this reason, quadruple isotope dilution was implemented prior to preconcentration and measurement steps to achieve high accurate and precise results for chloroquine, hydroxychloroquine and capsaicin at trace levels.

## 1.2 Objective of the Thesis

The main purpose of this thesis was to establish hyphenated analytical methods for sensitive and accurate determination of organic and inorganic analytes at low concentration levels. Matrix effects and trace concentration of analytes make the researchers to use an efficient separation method and a sensitive detection method. For this reason, some hyphenated methods such as HPLC-ICP-OES, HPLC-FAAS and GC-MS were used throughout this thesis. In addition, some liquid phase microextraction methods were used to concentrate the target analytes to achieve high signal/noise ratios in the related hyphenated instrument. Within the scope of this thesis, chloroquine, hydroxychloroquine and capsaicin were determined by isotope dilution method in order to obtain high precision and accuracy. The integration of isotope dilution and microextraction methods allows to reach high precision and accuracy at trace levels of the analytes. All hyphenated methods were elaborately optimized, and their analytical performances were evaluated using the following parameters: linear working range (LWR), limit of detection (LOD), limit of quantitation (LOQ), coefficient of determination ($R^2$), percent relative standard deviation (%RSD). Following that recovery studies were implemented to assess suitability and accuracy of the proposed hyphenated methods.

## 1.3 Hypothesis

Chromium speciation is an important area in analytical chemistry due to the difference of chromium hazards according to its oxidation states. For this reason, HPLC system was coupled to ICP-OES system to separate chromium species on an anion exchange column. The developed hyphenated method was applied to water, soil and grass samples.

Cobalamin is an essential vitamin for human bodies and its deficiency can lead to several disorders. For this reason, its amount in drug tablets has substantial role to make up its deficiency when it is prescribed. Hence, HPLC system was combined with FAAS system to separate and detect cobalamin by the help of its cobalt content. Here, a novel nebulizer interface was used to combine HPLC and FAAS system without traditional nebulizer interfaces. The proposed method was applied to vitamin drug tablets to quantify the analyte.

Chloroquine and hydroxychloroquine are antimalarial drugs used for the treatment of malaria and coronavirus disease of 2019 (COVID-19) diseases. However, these chemicals have various side effects depending on their daily dosages. Capsaicin is a chemical being responsible for the pungency of peppers. Its high consumption can lead to different problems in human bodies. For these reasons, it is important to establish accurate and sensitive analytical methods for these organic compounds at low concentration levels. GC-MS system was used for the separation and detection of these chemicals. Spraying based fine droplet formation liquid phase microextraction (SB-FDF-LPME) method was used to preconcentrate chloroquine and capsaicin while smart solvent-based liquid phase microextraction (SSB-LPME) method was performed for the extraction of hydroxychloroquine. In these studies, acetic anhydride was utilized as derivatizing reagent to improve extraction yield and/or obtain isotopic material that needed for ID method. Under the optimum microextraction and derivatization conditions, analytical performance, recovery and ID studies were implemented.

# 2
# GENERAL INFORMATION

## 2.1 Chromium

Chromium (Cr) is one of the transition elements in the periodic table and has a ground state electronic configuration as $Ar3d^5 4s^1$. It was discovered in crocoite mineral in 1798 by Louis-Nicolas Vauquelin [19]. It is a steel-gray, hard, brittle, and lustrous metal that give high polish property. It is generally used as protective corrosion inhibitor due to its resistivity to oxidizing chemicals [20]. This element has been used for a long time to give shiny appearance to metal surfaces and produce paints in dyeing industry. Other important usage areas for this element include leather tanning, wood preservation and stainless steel production [21].

As for its inorganic chemistry, its oxidation states varied between –II and +VI but chromium (III) and chromium (VI) are more prevalent ones in the environment. In natural waters, chromium (III) hydroxo complexes such as $Cr(OH)_2^+$, $CrOH^{2+}$, $Cr(OH)_3^0$, $Cr_2(OH)_2^{4+}$, $Cr(OH)_4^-$ and $Cr_3(OH)_4^{5+}$ are expected as the dominant species but there are some reports in literature about the presence of polynuclear complexes of chromium in natural water systems. In addition, chromium (VI) may be found in water systems as dichromate ($Cr_2O_7^{2-}$), chromate ($CrO_4^{2-}$), dihydrogen chromate (chromic acid, $H_2CrO_4$), hydrogen chromate ($HCrO_4^-$), trichromate ($Cr_3O_{10}^{2-}$), hydrogen dichromate ($HCr_2O_7^-$) and tetrachromate ($Cr_4O_{13}^{2-}$) [20].

Metallic elements with higher density than 5.0 $g/cm^3$ are named as heavy metals [22] and these elements are notorious for their toxicity even at trace levels [23]. However, chromium has a different story in spite of heavy metal nature. It has both toxic and beneficial effects on human health depending on its oxidation state, chemical form and exposure way [24], [25]. Chromium (III) has relatively benign properties while chromium (VI) has toxic impacts on human bodies [20]. It is known that chromium (III) is classified as pharmacologically active element due to its significant positive effects on nucleic acid structural integrity, glucose and lipid metabolism [26]. Hence, it is essential element for human bodies in proper concentration levels [27]. However, chromium (VI) leads to different problems including kidney damage, cytotoxicity, genotoxicity, dermal sensitivity, and

neurodegeneration. According to in vivo and in vitro studies, this element causes the excess production of reactive oxygen species and free radicals [28], [29]. Chromium (VI) can pass through the cell membrane and react with intracellular reducing agents such as cytochrome P450 reductase, superoxide dismutase, ascorbate and GSH for the production of intermediates like chromium (III), chromium (V), chromium (IV) and free radicals [28], [30], [31], [32]. This process is demonstrated in Figure 2.1 The entry mechanism of chromium (VI) to cell membrane (left) and electron transfer reaction to produce chromium intermediates and free radicals [27], [33]

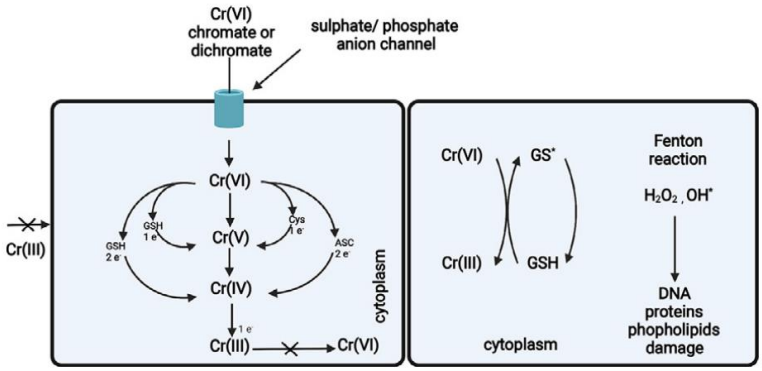


**Figure 2.1** The entry mechanism of chromium (VI) to cell membrane (left) and electron transfer reaction to produce chromium intermediates and free radicals [27], [33]

Chromium (V) is converted to chromium (VI) and produces reactive oxygen species which interfere with DNA-protein complexes [31], [34]. In addition, chromium (VI) can change redox homeostasis due to its production of reactive oxygen species and consumption of physiological antioxidants [35]. All these processes including oxidative damage, high amount of reactive oxygen species and DNA–protein crosslinks lead to cellular necrosis [33], [36]. For these reasons, it is essential to separate and detect chromium (III) and chromium (VI) to evaluate their impacts rather than total chromium detection.

It is also reported that mostly these two species are found in air, soil and water medium. Chromium strongly binds to soil and sediment that follows its dissolution in water and then leach from soil to groundwater. Its exposure to human bodies generally occurs via the consumption of chromium contaminated foods, well water

or the inhalation of chromium dust and skin contact during its usage in industrial places [21]. Chromium (III) takes part in food chain by plants that passively withdraw chromium (III) from soil medium [37]. In addition, the oxidation process of chromium (III) to chromium (VI) can be affected by high manganese content and high pH levels in soil medium [38]. Hence, the detection of chromium species in plants, soil and water systems are important to monitor their effects and consequences on environment and human health.

According to one survey in 2019, there are approximately 100 chromium discharged places in our world that put at risk 1.5 million people in terms of chromium exposure [33]. The United States Environmental Protection Agency (USEPA) has set a permissible limit for chromium (VI) and chromium (III) in drinking water as 0.050 and 0.10 mg/L, respectively [39]. Nevertheless, the abundance of chromium in our environment is a great concern for human health [40]. All these problems prove the need of sensitive and accurate analytical methods to separate and detect chromium species in environmental matrices.

## 2.2 Cobalamin (Vitamin B12)

Cobalamin or Vitamin $B_{12}$ is a general term for cobalt-containing corroids. It has a corrin core and cobalt atom at the center of the molecule. Among all vitamins, only cobalamin has metallic ion in its structure. It is also surrounded by four reduced pyrrole rings, nucleotide-like compounds and some variable compounds (R). The molecular structure of cobalamin is given in Figure 2.2 The molecular structure of cobalamin [41]. R group can be -CN, -OH, –5'-Deoxyadenosy, $-CH_3$, $-H_2O$, $-NO_2$ [41].

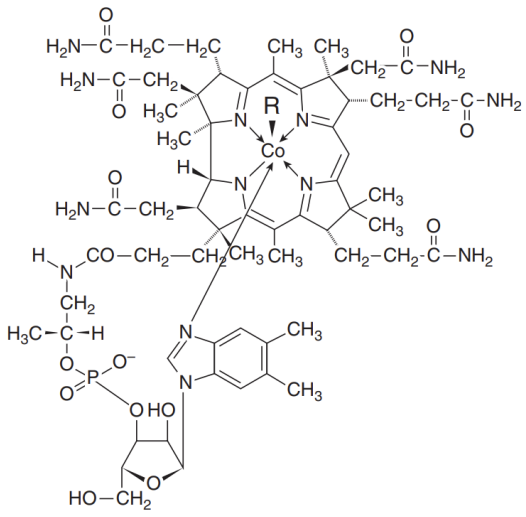

**Figure 2.2** The molecular structure of cobalamin [41]

Its isolation and characterization date back to the end of 19th century. After the discovery of pernicious anemia, Minot and Murphy found its treatment by nourishment with light cooked liver and Whipple also discovered this treatment for dogs before. Nobel prize was given to these three scientists in 1934 due to their contribution to medicine. Another Nobel prize was also given to Dorothy Hodgkin in 1964 thanks to the discovery of cobalamin via X-ray crystallography [42].

Its synthesis is only performed by microorganisms and some animal species have an appropriate medium in their intestinal systems for its production. As for human bodies, only small amount of this vitamin is synthesized in the colonic part of intestine and the required amount of this vitamin is supplied form animal-derived foodstuffs. For example, egg, salmon, beef, ox kidney, ox liver contain 19, 29, 50, 330 and 650 ng cobalamin/g, respectively [43].

Cobalamin is a vital reactant in two important reactions in human metabolism. These are known as isomerization of methyl-malonyl CoA and transmethylation of homocysteine. The former occurs in mitochondria and needs deoxyadenosylcobalamin. The latter necessitates methylcobalamin as coenzyme and catalyzed by the enzyme methionine synthase found in the cytosol. If these two vitamins are not enough in human bodies, the synthesis of methionine and its derivative S-adenosylmethionine and normal cellular functions are interrupted [43]. According to Dietary Reference Intakes, the required daily intake of cobalamin is estimated as 2.4 μg for adults [44]. Cobalamin deficiency is generally monitored in

vegans and their infants [42]. Some of the reasons for cobalamin deficiency can be listed as chronic atrophic gastritis, gastrectomy (partial or total), defects of the gastric mucosa (loss of parietal cells), intestinal stasis, malabsorption in the ileum, congenital disturbances of cobalamin metabolism, age, intestinal parasites, and sucklings if the pregnant women lack for vitamin B12 deficiency [43]. Its deficiency leads to pernicious anemia and neuropathy [45]. Other clinical symptoms observed in its deficiency are weight loss, megaloblastic gut, glossitis of the tongue, mental changes, and even infertility [46], [47]. Its effects on infants are different from those on adults. For example, failure to grow, movement disorders, irritability, and insufficient brain growth resulting in permanent developmental delay in some conditions are some consequences of cobalamin deficiency infants [47], [48].

The cobalamin deficiency is treated via the administration of hydroxycobalamin and cyanocobalamin. However, there are also adverse effects of parenteral administration of hydroxycobalamin or cyanocobalamin including urticaria, mild diarrhea, anaphylactic reactions and skin rash [49]. Today, people are recommended to use vitamin tablets to prevent cobalamin deficiency. Various kinds of vitamin drugs are commercially available and this triggers researchers to develop sensitive analytical methods for cobalamin in vitamin tablets [50].

## 2.3 Chloroquine

Chloroquine is a 4-aminoquinolone drug that has been used for the treatment of malaria, rheumatoid arthritis, hepatic amebiasis and some parasitic infections. It is known that chloroquine is relatively safe at appropriate dosages [51]. It has bitter taste and slightly yellow colored crystal powder. Chloroquine is soluble at pH 4.5 and has four different forms as chloroquine diphosphate, chloroquine phosphate, chloroquine sulfate and chloroquine dihydrochloride [52]. Its molecular structure is shown in Figure 2.3. It is utilized for the remediation of malaria since World War II and its dangerous side effects especially ocular toxicity are monitored during its chronic usage [53]. This drug has antimalarial and anti-inflammatory properties. It is rapidly absorbed and almost totally from the intestine. Its peak serum concentration is reached within 1.0 or 2.0 hours [54]. Its parenteral administration is no longer recommended because it may reach temporarily toxic concentrations.

Approximately 60% chloroquine is bound to plasma proteins and its two metabolites desethylchloroquine and bisdiethylchloroquine are produced after its biotransformation by the hepatic cytochrome P450 system. A 65-70% of chloroquine is eliminated from the body via the urinary system [51].

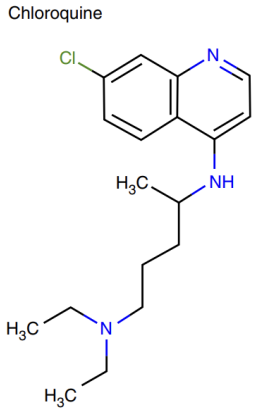


**Figure 2.3** The molecular structure of chloroquine [53]

In malaria treatment, chloroquine behaves as blood schizonticide and blocks heme polymerization in the parasites [55]. According to in vitro studies, chloroquine can be effective to minimize the viral replication of other infections like SARS-associated coronaviruses (CoV) and Middle East respiratory syndrome coronavirus (MERS-CoV) [56], [57], [58]. For this reason, it was recommended as potential drug for the treatment of COVID-19 disease [59]. In February 2020, the National Health Commission of China reported the use of chloroquine as a treatment for COVID-19 with two tablets of 500 mg daily for 10 days [60]. However, this dosage was reduced due to the safety issues [61]. In the early stages of COVID-19, there were great clinical trials in France and China about the suppression of Severe acute respiratory syndrome coronavirus 2 (SARS-CoV-2) infection [62]. After then, its usage was reduced due to the risk of adverse cases and mortality and the lack of efficacy [63], [64], [65], [66]. There are still controversies about the safety and efficacy of this drug for the treatment of COVID-19 disease [61].

The common side effects of chloroquine is kidney failure, blindness, cerebral edema, arrhythmias, and cardiac arrest [52]. Irreversible retinopathy and ototoxicity are other damaging effects observed during the daily administration of this drug higher than 250 mg. Its toxic effects are generally monitored in the central nervous system and cardiovascular system including confusion, convulsions, coma,

vasodilatation, hypotension, cardiac arrhythmias, suppressed myocardial function, and eventually cardiac arrest [51]. However, it was used during COVID-19 pandemic in China, Italy, South Korea and Türkiye [67]. There are also clinical trials for its efficacy in cancer [68] and human immunodeficiency virus type 1 (HIV-1) [69]. Hence it is necessary to determine chloroquine in biological fluids and drug formulations due to its wide clinical potential [67].

## 2.4 Hydroxychloroquine

Hydroxychloroquine is a synthetic 4-aminoquinolines synthesized to minimize the toxic effect of chloroquine. Its synthesis contains the addition of β-hydroxyl group to N-ethyl group found in the chloroquine molecule. This drug was approved for the treatment of malaria in 1955 by Food and Drug Administration. The molecular structure of hydroxychloroquine is given in Figure 2.4 The molecular structure of hydroxychloroquine [53][53]. It is also used to cure for systemic lupus erythematosus, rheumatoid arthritis, and chronic graft-versus-host disease. Its main side effect is gastrointestinal disturbances and other side effects are itching, intravascular hemolysis, retinal toxicity, bone marrow suppression and rashes [70].

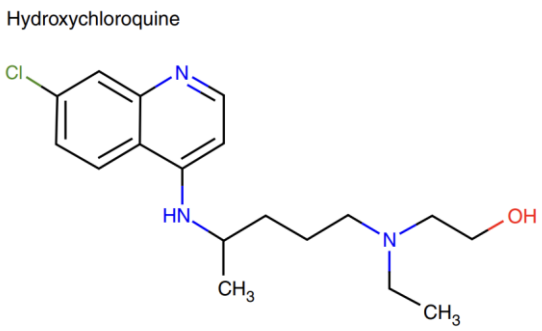


**Figure 2.4** The molecular structure of hydroxychloroquine [53]

Hydroxychloroquine is less toxic and has fewer side effects and more water miscible than chloroquine [71]. It is rapidly absorbed by gastrointestinal tract and eliminated by kidneys. When it is orally administered, it enters to the circulatory system and its plasma concentration is rapidly raised to maximum level [72]. Based on the in vitro studies, this drug can hinder entrance, replication and transmission of viruses [73], [74]. It increases the pH of cellular endosomes for the inhibition of viral entrance, glycosylation and replication of angiotensin-converting enzyme 2

(ACE-2) [75]. In addition to its antiviral activity, hydroxychloroquine has anti-inflammatory properties, immune modulation, and regulation in pro-inflammatory cytokines like interleukin 1 & 6, tumor necrosis factors and antioxidant activities [76]. It is metabolized in human bodies by oxidative deamination of the primary amines and N-dealkylation of the tertiary amine. The next step for its metabolization was the formation of its carboxylic acid derivatives, desethylhydroxychloroquine and desethylchloroquine [53].

In COVID-19 pandemic, hydroxychloroquine sulfate was one of the first-line drugs for the remediation of SARS-CoV-2 virus. In March 2020, United Stated Food and Drug Administration gave authorization to use hydroxychloroquine sulfate and chloroquine (di)phosphate [77]. It was firstly used in China to decrease recovery period of COVID-19 and boost pneumonia regression [78]. Even though this drug was prescribed with or without azithromycin during the COVID-19 pandemic [79], there are various debates regarding the usage of hydroxychloroquine to fight against SARS-CoV-2 virus due to the lack of safety and efficacy [80]. Its side effects can be listed as diarrhoea, vomiting, and gastrointestinal disorders, retinopathy and QTc interval prolongation [81]. For these reasons, its maximum daily intake was established as 6.5 mg/kg to prevent human eyes from retinotoxicity [82]. A sensitive and accurate analytical method for the detection of hydroxychloroquine in biological fluids are essential to investigate the chemical for future clinical studies.

## 2.5 Capsaicin

Capsaicin with IUPAC chemical name as 8-methyl-N-vanillyl-6-nonenamide is one of the active components found in chili peppers (*Capsicum genus*) [83]. It is an oil-soluble compound with melting point of 62-65 $^{o}$C [84]. Its molecular weight is 305.4 g/mol [85]. Capsaicin and other capsaicinoids give pungency flavor to chili peppers [86]. The amount of capsaicin in dried chilies are higher than that in the fresh chilies. It is also present in cilantro, oregano and cinnamon spices [83]. Capsaicin and dihydrocapsaicin are responsible for the pungency of peppers and these chemicals are 77-98% of the capsaicinoids in peppers [86] and capsaicin content in peppers determines the quality of the product [87].

Scoville Organoleptic Test is a conventional method to quantify the heat level of pungency and hot sauces. It was proposed by an American scientist Wilbur Scoville

in 1912 [88]. This test consists of two stages: 1) capsaicinoids in the pepper is extracted using alcoholic solution and 2) it is diluted with sugar containing solution until the pungency or heat is not detectable by human tongues belonging to five different specially trained volunteers. The dilution level of the capsaicinoid extract by sugar containing solution determines the Scoville unit of the pepper [89]. Scoville scale index is shown in Figure 2.5.

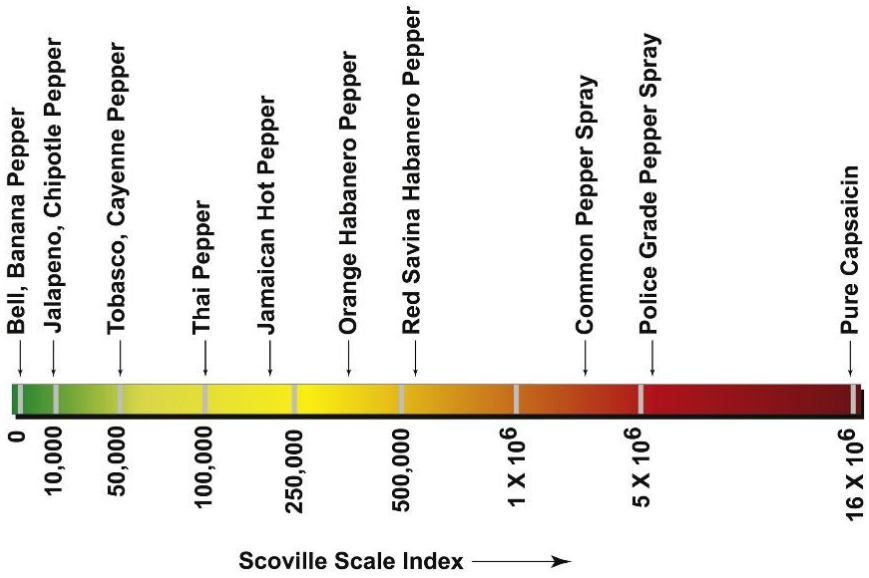


**Figure 2.5** Scoville scale index. The highest Scoville index belongs to pure capsaicin while the lowest index to bell peppers [90]

Capsaicin is a vanillin amide alkaloid (Figure 2.6) examined for its pharmacologic and health effects [91]. There are several reports about the positive effect of capsaicin on human lipid metabolism [92]. This chemical also utilized for the ailment of diabetes and obesity [93]. The other benefits of capsaicin are its anti-inflammatory, cardio-protective, thermogenic, antilithogenic and analgesic properties [94].

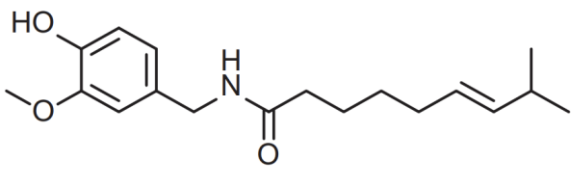


**Figure 2.6** The molecular structure of capsaicin [83]

On the other hand, there are negative effects of capsaicin on human skin, eyes and other organs. Its topical application can result in burning sensation and irritation. Intense tearing, pain, conjunctivitis and blepharospasm are observed after its exposure to human eyes. Its excess oral intake leads to vomiting, nausea, burning diarrhea and abdominal pain [84].

Capsaicin affects trigeminal sensation in the mouth cavity and actuates transient receptor potential vanilloid subtype 1 (TRPV1) that is responsible for the sensation of burning and hotness. In literature, this chemical suppresses the taste of foods due to its masking impact on olfactory and gustatory sensations [95], [96]. As for its pain reducing effect, it is thought that capsaicin depletes the sensory neurons of Substance P and inhibit the transfer of pain information from Substance P to its receptor. Therefore, it is commercially available in cream, gel or lotions and used topically to provide the relief of pain [97].

Capsaicin is also one of the components in food waste because it is highly consumed in some countries especially Southeast Asia, southwestern China and Latin American countries. Based on the published report in literature, the concentration of capsaicin in food waste can be reached to 25 g/kg [98]. It is also known that food wastes have high risks for human health and environment if these wastes are not treated [99]. For these reasons, capsaicin in saliva, pepper and wastewater should be determined by a sensitive and accurate analytical method to be used for the evaluation of its effects on human health, environmental pollution and food quality.

## 2.6 Instrumental Methods

### 2.6.1 Spectroscopic Methods

Spectroscopic methods are important analytical techniques to obtain elemental information and categorized into three distinct groups based on the particles detected in the system: 1) photons in optical atomic spectroscopy, 2) ions in inorganic (atomic or elemental) mass spectrometry, 3) electrons in electron spectroscopy (Figure 2.7). The absorbed photons or emitted photons by the sample are measured as a function of photon energy in optic atomic spectroscopic systems [100].

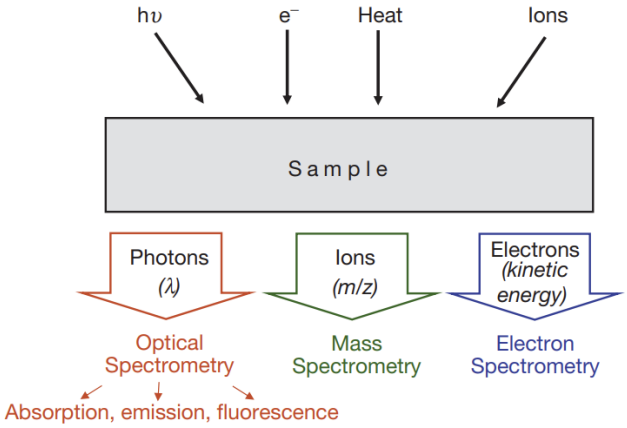


**Figure 2.7** A summary of spectroscopic methods [100]

The absorption or emission lines in atomic spectroscopic methods (Figure 2.8) result from the electron transition from one electron orbital to another in an atom. *Absorption* phenomena occurs if the exact energy to excite the orbital electron from the ground state to the excited state is sent to the atom. On the other hand, *emission* phenomena is the process that the excited atom with high energy emits electromagnetic radiation when falling back to the ground state [101].

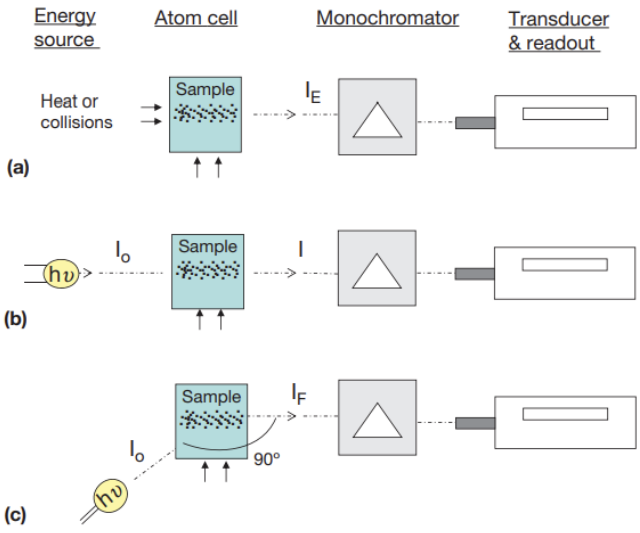


**Figure 2.8** The diagram for a) Atomic emission b) atomic absorption c) atomic fluorescence spectrometers [100]

*Fluorescence* is based on the process that the analyte atom in flame, glow discharge, plasma or furnace is excited by a monochromatic radiation and the fluorescence

radiation at the same wavelength of the excitation wavelength or longer is measured [102]. Atomic fluorescence spectroscopy is more sensitive than atomic absorption for a group of elements due to low background. Before fluorometric detections, hydride generation or cold vapor formation reduce the detection limit of some elements to parts per trillion levels [100].

### 2.6.2 Absorption spectrometry

Atomic absorption spectrometry is used to qualify and quantify metals and metalloids by means of the measurement of absorbed radiation by the atomized analyte at a specific wavelength. In the first step, analyte(s) should be converted into atoms by a proper atomization source. The ideal atomization source should be efficient for a complete atomization process regardless of the sample matrix components. In addition, the excitation process of the atoms should be minimal in order to avoid the emission noise of analyte and background. Flames and electrothermal atomization sources have been accepted as the common methods for the generation of atoms [103].

### 2.6.3 Flame atomic absorption spectrometry (FAAS)

Flame atomic absorption spectrometry depends on the measurement of absorption after the atomization of elements by a flame source. The electromagnetic radiation at a specific wavelength passes through the flame, monochromator and lastly detector which is the counter for the amount of light absorbed by the atomized element [104]. A flow chart belonging to the FAAS system is given in Figure 2.9.

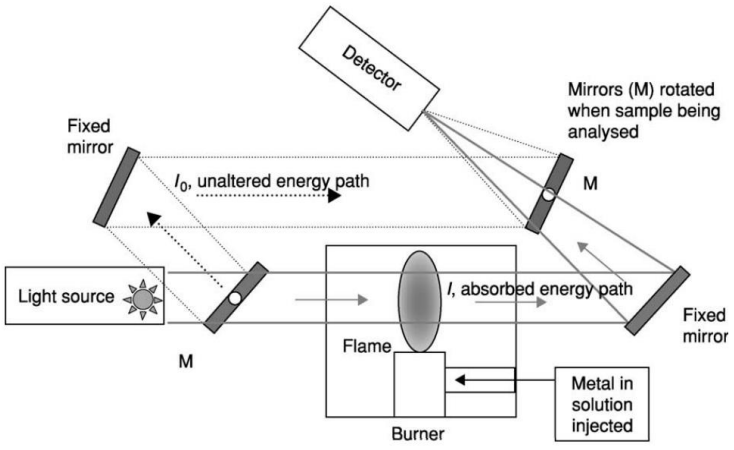


**Figure 2.9** A schematic diagram of FAAS system [105]

Air-propane (2200K), air-acetylene (2450 K), $N_2O$-acetylene (3200 K), air hydrogen (3200 K), $N_2O$-hydrogen (2900 K), $N_2O$-propane (2900 K) are the flame types with their approximate temperatures to generate the flame source. Among all types, air-acetylene mixture is generally preferred due to its stability, easy operation and free from inter-element interferences [106]. $N_2O$-acetylene flame is used for the atomization of refractory elements like silicon and aluminum because these elements forms their heat-stable oxides if acetylene-air flame is used [107].

In FAAS systems, the liquid sample solution is converted into fine aerosol droplets and large droplets are eliminated. Pneumatic nebulizers are generally used to obtain tiny droplets of the sample solution (1-50 μm droplet diameter). After the separation of large and tiny droplets, only about 10% of the sample solution mix with the fuel and oxidant gases. When the droplets mixed with these gases reach to the atomization region, a sequence of complicated process starts: (1) desolvation of the droplets, (2) vaporization of the molten or solid particles, (3) dissociation of molecules to produce atoms, and (4) possible ionization of atoms [107].

FAAS has lower sensitivity for several elements due to the fact that maximum 10% of the sample solution reach to the atomization region. In addition, the residence time of the atoms in this region is quietly limited as nearly $10^{-3}$ seconds [108]. Slotted quartz tube has been utilized in literature to solve the sensitivity problem of FAAS systems. The sensitivity of this instrument can be enhanced to 2-5-fold by means of SQT [109]. The usage of SQT was firstly performed by Watling in 1970s [110]. Here, one cylindric quartz tube with two slots were placed onto the atomization region and the absorbance signal was recorded after the sample was nebulized by ordinary process [111]. After the introduction of SQT, a water-cooled U tube was proposed to trap the analyte atoms on the surface of U-shaped quartz tube. A peak-shape signal was observed after the application of high temperature to the quartz tube for the atomization of the analyte atoms found in the inner surface of the tube. The atom trap used in this study can be recognized as online enrichment or preconcentration method [112]. U tube trap in an SQT [113], flame alteration, organic solvent aspiration/atomization [114] are other attempts to enhance the sensitivity of FAAS system.

Atom trapping has been popular in literature due to the opportunity to achieve ppb/ppt level detection limits by FAAS systems [115], [116]. These methods have

two distinct steps; atom trapping and revolatilization steps. In the atom trapping step, the analyte atoms are collected on the surface of quartz tube using lean flame composition. Next, an organic solvent is introduced to the system to change the flame composition [114], [116]. Not only organic solvents are used for the revolatilization process, but hydrogen gas is also employed to release the trapped atoms from the quartz surface. Hydrogen gas is directly sent to the quartz tube by means of a small quartz tube being perpendicular to the quartz tube. This new design is known as T-shaped slotted quartz tube (T-SQT, Figure 2.10). This system eliminates the combustion products and non-stable flame condition resulting from the usage of organic solvent for the revolatilization [117].

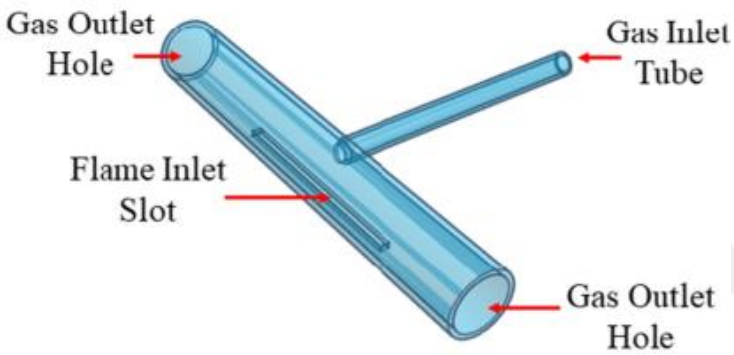


**Figure 2.10** T-shaped slotted quartz tube [118]

### 2.6.4 Emission spectroscopy

Atomic emission spectroscopy is a reliable and sensitive instrumental method for the determination of metals and non-metals in various kinds of samples. Atomic spectroscopic instruments mainly consist of an excitation source, a spectrometer, a detector, some forms of signal and data processing [119].

Atomic or ionic species can be obtained via high energy sources such as flame, plasma and electrical discharge techniques. When the energy of these sources is enough for the excitation process, electrons are excited and then go back to the ground state with a narrow line emission. The wavelength of the emission is unique for each excited element [120]. The emission spectra of an element are quite complicated due to various emission lines reflecting different electronic transitions occurred after the excitation of the element. As for sensitivity, it is sufficient for the

elements with low and middle atomic numbers but it is not proper for the elements with high atomic number due to the complex orbital energy diagrams and a larger choice of electronic transitions for these elements that yields lower intensity lines [101].

### 2.6.5 Inductively Coupled Plasma Spectrometry

Inductively coupled plasma optical emission spectrometry (ICP-OES) sometimes called as inductively coupled plasma-atomic emission spectrometry (ICP-AES) [121] and inductively coupled plasma-mass spectrometry (ICP-MS) have become more popular analytical methods for the simultaneous detection of several elements. ICP source-based methods have better sensitivity than FAAS system, wider linear ranges (up to 8 orders of magnitude), lower interference effects due to higher atomization temperature than flame (about 2-3 times greater). ICP-MS is also suitable for isotopic determination of elements [104], [122]. The most important advantage of ICP-based instruments is to obtain reproducible and efficient vaporization, atomization, excitation and ionization processes [123].

Flame can be used to atomize low excitation potential elements like alkali elements but the common atomization method in atomic emission spectroscopy is to use electrically generated plasmas [100]. The plasma is produced in an assembly of three concentric fused-silica tubes which is known as *torch* Figure 2.11. A long spiral copper coil connected to a RF generator is found at the top of the torch. The coil generates a dense electromagnetic field at the top of the torch. When the flow of plasma is obtained in the torch, a spark with high voltage is sent to the argon gas that yields chain reaction belonging to the ionization of argon gas. Argon atoms, argon ions and electrons are found at the end of this process [124]. During the production of plasma, RF generator is generally operated at 27 or 40 MHz to avoid from the interferents coming from normal communication channels [123].

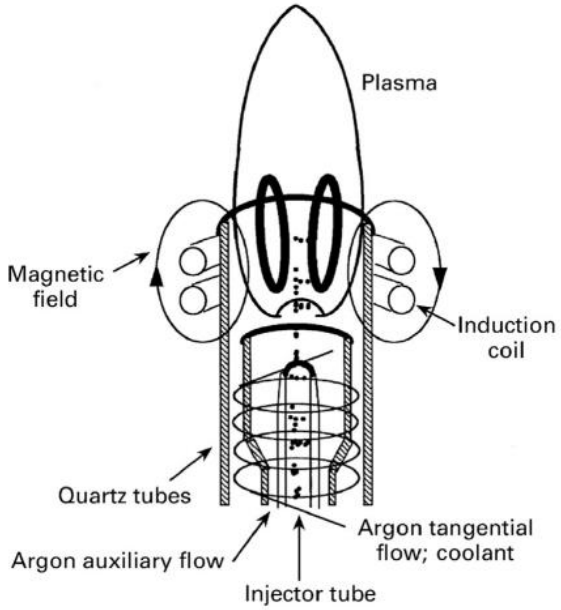


**Figure 2.11** The schematic presentation of a torch in ICP sources [119]

In conventional ICP-based instruments, axial and lateral viewing for the emitted radiation are possible. The axial viewing is chosen to improve the efficiency while the lateral one is used to prevent unwanted and intense background [123].

The vulnerable point of the system is the sample introduction process but several types of nebulizers and spray chambers can be used for the analysis slurry and liquid samples. Meinhard, ultrasonic, high efficiency, and microconcentric nebulizers are some examples of ICP nebulizers. Scott type and cyclonic spray designs are the most important spray chambers for ICP systems [100].

ICP-OES system given in Figure 2.12 is based on the measurement of the emitted electromagnetic radiation at a specific wavelength resulting from the movement of the excited electrons with high energy to the ground state with low energy. The intensity of the emitted radiation is proportional to the concentration of analyte in a sample. The optic system in ICP-OES systems separates the radiation which is specific for the element being determined [121].

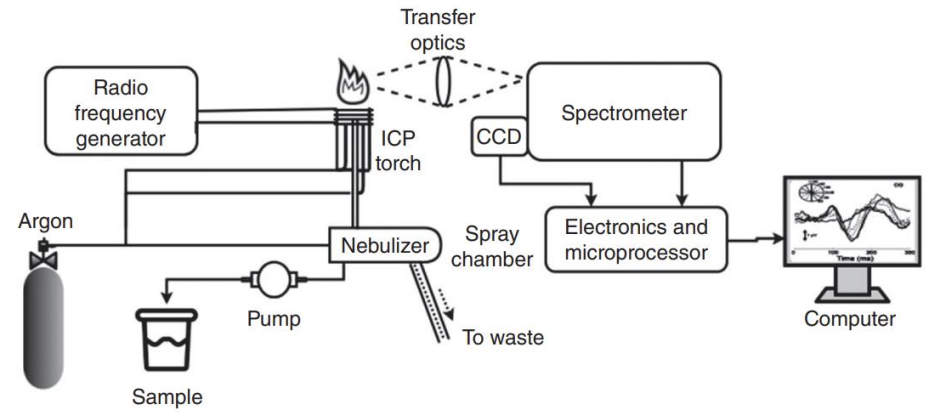


**Figure 2.12** The schematic diagram of ICP-OES system [121]

ICP-OES system can be useful for the multi-elemental analyses of biological and environmental samples, metals, alloys, electronic materials, oils, glass, ceramics, geological samples, and so on. It is also beneficial as a detector after a chromatographic system for speciation analysis due to the multi-elemental capacity and sensitivity. Some examples for the hyphenated instruments used for speciation analysis are gas chromatography-inductively coupled plasma optical emission spectrometry (GC-ICP-OES), high performance liquid chromatography-inductively coupled plasma optical emission spectrometry (HPLC-ICP-OES) and high performance liquid chromatography- inductively coupled plasma-mass spectrometry (HPLC-ICP-MS) systems [124].

### 2.6.6 Chromatographic Methods

Separation is a general term including all chemical and physical processes to separate one or more components from any mixture. Separation methods consist of crystallization, solvent extraction, selective precipitation, distillation, and chromatography [120]. Chromatography is one of the physical separation methods that a mixture is separated according to its distribution between two distinct phases; one is a bulk liquid, a porous bed, layer or film and the other is a liquid which flows through the system. The successive sorption and desorption events during the analyte transfer with mobile phase through the stationary phase provided the separation of analyte. A general classification of chromatographic methods is shown in Figure 2.13 [125].

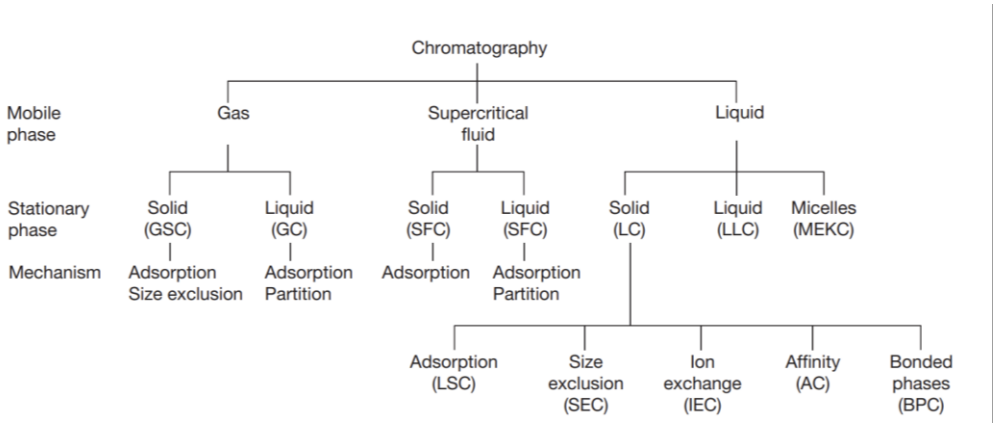


**Figure 2.13** The family tree of chromatographic methods [125]

According to the physical state of mobile phase, chromatography is divided into three main groups: gas chromatography (GC), liquid chromatography (LC) and supercritical fluid chromatography (SFC) [125].

### 2.6.7 Gas chromatography (GC)

Gas chromatography (GC, Figure 2.14) has been an indispensable analytical method for petrochemical industry, pollution control, pharmaceuticals, agricultural industry, medicine and so on. According to the stationary phase, GC system is categorized into two main groups; gas-solid chromatography (GSC) and gas -liquid chromatography (GLC) [126]. The mobile phase or carrier gas for GC systems can be nitrogen, hydrogen or helium gases which are responsible for the movement of the sample vapor to the detector [127]. The stationary phase is a microscopic layer of a polymer coated on the solid support found in the glass or metal column [128]. The analyte being separated by GC systems should have relatively high vapor pressure [127].

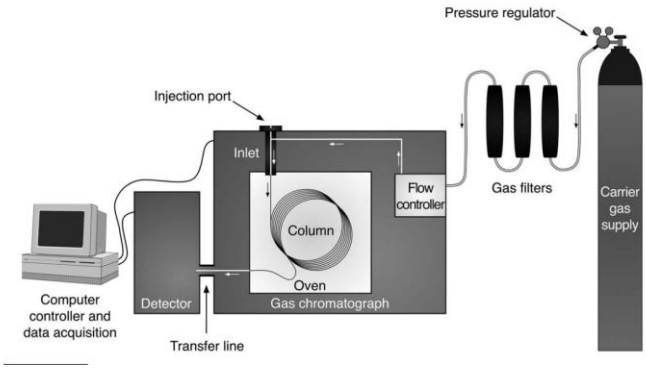


**Figure 2.14** A schematic diagram of GC system [129]

In GC systems, analytes with different boiling points, polarities and adsorption properties can be effectively separated. Firstly, the sample is converted into its vapor form and mixed with the carrier gas. The sample vapor is transferred to the stationary phase and then the partition of sample vapor between the carrier gas and the stationary phase occurs under a suitable temperature program. Next, the analyte vapors leave the column based on their vapor pressures and affinities to the stationary phase. The eluted analyte vapors are directed to the detector that convert the chemical information to electrical signal [130].

GC detectors can be mainly categorized into four distinct types; bulk physical property, ionization, electrochemical and optical detectors [131]. Flame ionization detector (FID), photoionization detector (PID), electron-capture detector (ECD), thermionic ionization detector (TID), and the helium ionization detector (HID) are examples for ionization detectors [132]. In these types of detectors, the conductivity in the absence and presence of the charged species is counted. Thermal conductivity detector (TCD) is a bulky physical type of detector and works depending on the thermal conductivity of the mobile phase (carrier gas) with and without the analyte. Optical detectors used in GC systems are flame photometric detector, chemiluminescence detector and atomic emission detector [131]. Approximately 28 elements including sulfur and phosphorous can be determined by flame photometric detectors [133]. Electrolytic conductivity detector (ELCD) is an electrochemical detector and used for sulfur-, nitrogen-and halogen-containing compounds [131].

### 2.6.8 Liquid chromatography (LC)

Liquid chromatography (LC) is one of the oldest separation methods which dates back to the early 20$^{th}$ century. A Russian botanist discovered a new technique to separate plant pigments [134]. Six different pigments (chlorophylls and xanthophylls) were obtained when petroleum ether was added into the column with calcium carbonate. This new technique was named as *chromatography* that means '*colored writing*' in Greek language [135]. In 1960s, the diameter of the packing particle was decreased and the mobile phase velocity was increased with an increasing pressure that yielded enhanced resolution and short analysis time [134], [136], [137].

An analyte has a critical relationship with stationary phase (s) and mobile phase (m). This relationship can be weak interactions like adsorption, solvation, etc. and strong interactions like the generation of chemical bond between the analyte and one phase like high-performance chelating ion chromatography. The distribution of analyte between mobile and stationary phases (Equation 2.1) can occur [135]:

$$Analyte_m \leftrightharpoons Analyte_s \tag{2.1}$$

The analyte is sorbed and desorbed in the chromatographic column and migrated through the column with the flow of mobile phase. The equilibrium of analyte in both phases can be expressed by distribution coefficient (Equation 2.2) [135]:

$$K_D = \frac{[Analyte]_s}{[Analyte]_m} \tag{2.2}$$

where [Analyte] is the molar concentration of analyte in the related phase. $K_D$ determines the retention of analyte in the chromatographic column. If $K_D$ is high for an analyte, the retention of the analyte is also high [135].

There are different stationary phases used if the mobile phase is liquid. The stationary phase can be a solid, a porous solid coated with a film of insoluble liquid, a solid of controlled pore size, a solid with immobilized ionic groups, a solid with immobilized molecular recognition sites, a solid with a surface containing chemically bonded organic groups used in liquid-solid chromatography, liquid-liquid chromatography, size exclusion chromatography, ion exchange or ion chromatography, affinity chromatography, bonded-phase chromatography, respectively [125]. The retention mechanism of liquid-solid chromatography depends on the adsorption of analytes onto the outer surface and active sites of the solid stationary phase. Liquid-liquid chromatography depends on the distribution of analyte between two immiscible phases. In ion exchange chromatography, the charged particles in sample solution interact electrostatically with the charged particles found on the surface of the stationary phase. In addition, a porous column with a specific range of pore diameter is used to retain the analytes according to their sizes. A ligand is immobilized onto the column surface in affinity chromatography to retain the analyte by specific interactions with the ligand (antibody, etc.) [135].

A stationary phase should possess the following properties: 1) pressure resistance, 2) immiscibility in mobile phases, 3) well-designed surface area, 4) reversible interaction with analytes. A small number of materials has these properties. Silica ($SiO_2$) and alumina ($Al_2O_3$) are used as polar stationary phase for normal phase chromatography and thin layer chromatography. In addition, silica surface is chemically modified by chloro- and alkoxy- silanes with the functional groups of thiol (–SH), primary amino ($–NH_2$) and cyano (–CN) for the production of polar bonded silica. The reaction between reactive silanol groups with alkylchlorosilanes yields non-polar bonded silica. The most common types are octyl- ($–C_8H_{17}$) or octadecyl -($–C_{18}H_{37}$) bonded silica [138].

Liquid-liquid chromatography and liquid solid chromatography have two modes as normal phase and reverse phase [138]. In normal phase mode, a polar stationary phase like silica is used with a non-polar mobile phase like chloroform and dichloromethane. In reverse phase mode, a non-polar stationary phase and a polar mobile phase are used to separate target analytes. Polar analytes are firstly eluted from the column due to less interaction with the non-polar stationary phase. However, non-polar analytes interacts with the non-polar stationary phase more strongly that results in greater retention for these analytes [139].

Anion and cation exchange columns are used as stationary phases in ion exchange chromatography. Positively charged ions are found on the surface of anion exchange column while negatively charged ions on the surface of cation exchange column. The analyte ion can be retained on the column with oppositely charged ions. The cationic analyte and cationic eluent components compete to bind the negatively charged stationary phase. For the cation exchange column, the following mechanism (Equation 2.3) occurs [140]:

$$S - X^- C^+ + M^+ \leftrightarrow S - X^- M^+ + C^+ \quad (2.3)$$

Here, S is the chromatographic support, $M^+$ is the cationic eluent components, $X^-$ is the anionic functional group, $C^+$ is the cationic analyte. In anion exchange column, the following reversible reaction (Equation 2.4) follows [140]:

$$S - X^+ A^- + B^- \leftrightarrow S - X^+ B^- + A^- \quad (2.4)$$

In which S is the chromatographic support, $B^-$ is the anionic eluent components, $X^+$ is the cationic functional group, $A^-$ is the anionic analyte [140]. Sulfonic acid group

and carboxylic acid group are the most common functional groups used in cationic stationary phases while tertiary amine and primary amine groups are the most common functional groups for the anion exchangers [15].

Ion chromatography is a different mode of LC systems that separates ionic or ionizable analytes [141]. The retention of ionic analyte depends on its charge and ionic radius. For example, sulphate ion ($SO_4^{2-}$) strongly retains than chloride ion ($Cl^-$) due to its higher charge. As for ionic radius, bromide ion ($Br^-$) strongly binds to the anion exchanger than chloride ion ($Cl^-$) due to its higher ionic radius [138].

Four different types of stationary phases are used in ion chromatography. These are [142]:

- Synthetic ion-exchange resins
- Dextran-, cellulose-, or agarose-based ion exchangers
- Inorganic ion exchangers
- Carbonaceous ion-exchangers

Poly(styrene-divinylbenzene), poly(vinyl alcohol) and poly(methacrylate) are some examples for synthetic ion exchange resins. Hydroxyapatite (hydrated calcium phosphate), zeolites (crystalline hydrated aluminosilicates), salts of some heteropolyacids (ammonium molybdophosphate, etc.), acid salts of polyvalent metal ions (like zirconium phosphate, nickel hexacyanoferrate (II), titanium tungstate, etc.) are based on inorganic ion exchangers. Activated carbon as carbon based ion exchanger is also used after its modification with ion exchange groups [142]. As for mobile phases in ion chromatography, detectors used in these systems limit the number of mobile phases due to the specific requirements of the detectors. As an example, hydroxide or hydronium based mobile phases are preferred in suppressed ion chromatography which the detector response to the eluent components is minimized [143].

As for the instrumentation for LC systems, these systems have similar designs. The basic parts of LC systems are mobile phase reservoir, pump, sample introduction, analytical column, detector, connective tubing and fittings as shown in Figure 2.15. Mobile phase reservoirs should be made from inert materials to mobile phase systems. Solvents used as mobile phase should be filtered and degassed before their usage in order to achieve reproducible flow rates of mobile phase and minimize

baseline fluctuation [134]. Isocratic mobile phase system which consists of the same solvent composition during the chromatographic separation is generally preferred due to its low-cost, simplicity and robustness. In addition, gradient elution is another mobile phase mode that used to separate analytes with different polarities by changing the polarity of mobile phase system throughout the chromatographic analysis [144].

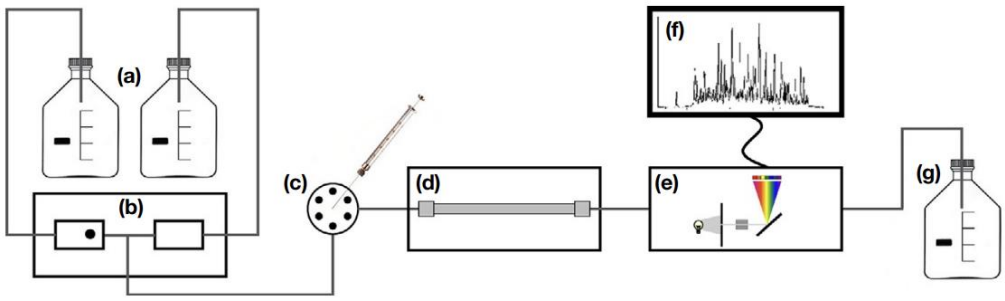


**Figure 2.15** High performance liquid chromatography system a) Mobile phase reservoir b) pump; c) sample introduction; d) analytical column, e) detector(s); f) data collection and processing; g) drain [139]

The ideal detector should produce response for $10^{-8}$-$10^{-15}$ g analyte/s and have reproducible and stable responses, wide linear range, short response time, nondestructive to the sample, easy operation and so on. Refractive index, UV-Vis absorbance, conductivity, electrochemical, evaporative light scattering are some detectors used in LC systems. Hyphenated methods like liquid chromatography-mass spectrometry (LC-MS), liquid chromatography-infrared spectrometry (LC-IR), liquid chromatography-nuclear magnetic resonance (LC–NMR) are used for multiple purposes [134].

### 2.6.9 Mass Spectrometry

Mass spectrometry (MS) depends upon the ionization and fragmentation of analyte(s) in the gas phase that follows the separation and detection of ions according to their mass to charge (m/z) ratios. The beginning of MS system dates back to the early years of twentieth century. J.J. Thomson and his colleagues studied on electrical discharges in gas phase that is regarded as the first footsteps for the development of MS system. A parabola spectrograph known as the first MS system was produced by Thomson in 1912 who performed this system for isotopic

measurements [145]. According to IUPAC, m/z is a dimensionless and positive that consists of the mass of ion (m) and charge of ion (z) [146].

A classical mass spectrometer consists of a vacuum source, an ionization or ion source, a mass analyzer, an ion detector and data processing system as shown in Figure 2.16 [145].

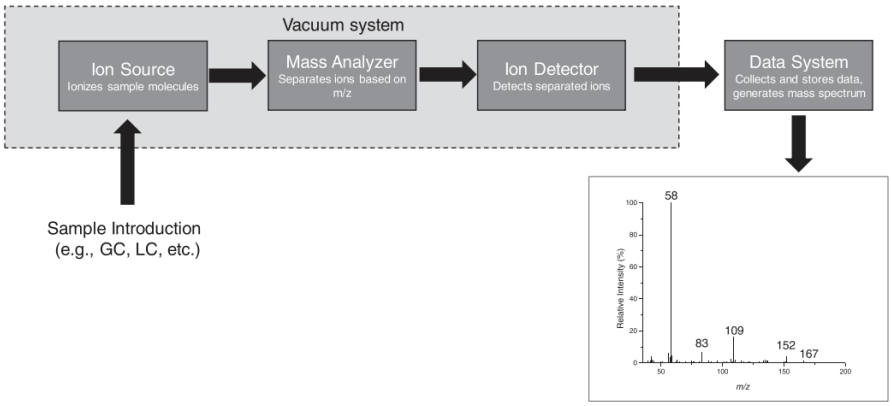


**Figure 2.16** The general diagram of MS system [145]

Several ionization techniques are used to obtain the ionic species of the analyte(s). Some of these techniques are chemical ionization (CI), electron ionization (EI), matrix-assisted laser desorption ionization (MALDI), atmospheric pressure chemical ionization (APCI) and electrospray ionization (ESI) [147].

EI is the first ionization source, and it is proper for MS systems with GC as sample introduction method. High energetic electrons produced by a heated filament collide with the analyte molecules at gas phase. The energy of the electrons is 70 eV which is enough to ionize most of the organic molecules. The energetic electrons remove electron form the analyte molecule that yields positively charged analyte molecule [145].

CI is one of the ionization sources depending on the ionization of analytes by a reagent gas which is bombarded with high energetic electrons. In general applications of CI, ammonia and methane gases are used as reagent gas and produce $NH_4^+$ and $CH_5^+$ ions. The reagent gas transfers its proton(s) to the gaseous analyte(s). In addition, water vapor is used as reagent gas but proton subtraction occurs in the analyte molecule due to the proton affinity of hydroxide ion produced by the reagent gas [147].

ESI (Figure 2.17) is convenient for the ionization of macromolecules, polar, non-volatile and ionic compounds because these analytes have low vapor pressure and high boiling points due to dipole-dipole, dipole-ion and coulombic attractive interactions that inhibit thermal vaporization of these analytes required for EI and CI systems. The analyte solution is introduced to a stainless-steel capillary at the flow rate of 1-10 µL/min. High voltage (2-5 kV) is applied to the tip of capillary and the polarity of voltage determines the charge of analytes. Positive capillary voltage results in positively charged ions and vice versa [146].

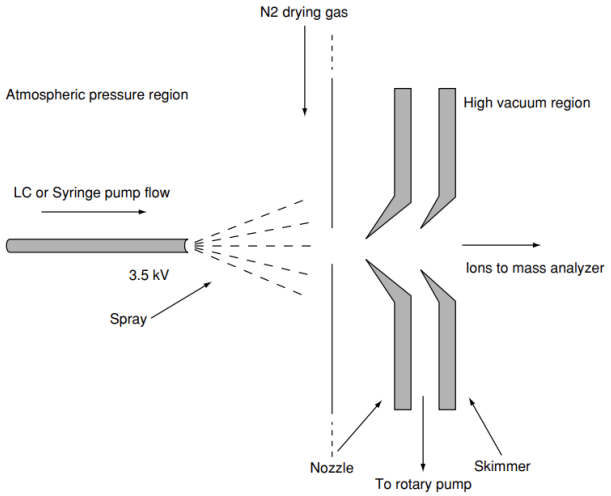


**Figure 2.17** The schematic presentation of ESI [147]

APCI is employed as ionization source in LC-MS systems. A nebulizing gas like nitrogen is utilized to obtain fine droplets of the column effluent. Next, the droplets move to a heated chamber for the desolvation and vaporization processes. The ionization process takes place in corona discharge electrode like CI process that previously described [145].

MALDI is suited for the quantitation of oligonucleotides, proteins, peptides, and other biological and synthetic compounds. In this system, the analyte is mixed with excess amount of matrix consisting of some chromophore groups absorbing laser light. The matrix produces plasma by the help of the laser energy and vaporization and ionization of the analyte occur [148]. Some examples for matrixes used in MALDI are picolinic acid, 3-Hydroxypicolinic acid for DNA and RNA, α-Cyano-4-hydroxycinnamic acid for peptides, lipids, oligonucleotides, sinapinic acid for proteins and 6,7-Dihydroxycoumarin for lipids [149].

Other important part of MS system is mass analyzer that used to separate the charged analyte(s) based on the m/z values after the ionization of analyte(s) [147]. Some of the important mass analyzers are quadrupole, ion trap, orbitrap and time of flight systems [148].

Quadrupole mass analyzer (Figure 2.18) includes four rods parallel to the ion direction (z axis). An electric field with high frequency is obtained between the rods by changing the voltage. Analyte ions are alternately repelled or attracted by the rods having opposite polarity [149]. This mass analyzer is known for its simplicity, robustness and low cost. However, it possesses low resolution (<3000), limited mass range (up to 3000 amu) and poor mass accuracy (<100 ppm). It is commonly used in LC-MS and GC-MS systems due to high scanning rate and the need of low vacuum [148]. Selected ion monitoring (SIM) can be performed in order to increase the sensitivity and it is only interested in the analyte ions at certain m/z values. Hence, a great amount of the specific ions reaches to the detector that boosts the sensitivity of the system [145].

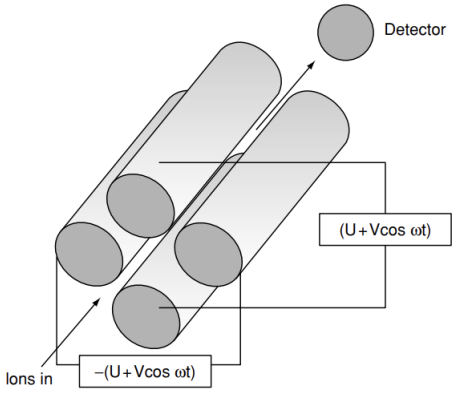


**Figure 2.18** The schematic diagram of quadrupole mass analyzer [147]

Time of flight mass analyzer depends on the different travel rates of the analyte ions with the same energy. In this system, the ionic particles expedite via electrostatic field, therefore the particles have the same kinetic energy. Next, a drift path is used to separate these particles because the heavier ones arrive the detector after the lighter ones [148].

Ion trap mass analyzer consists of a three dimensional quadrupole with a hyperbolic ring electrode and two hyperbolic end electrodes [150]. Analyte ions are trapped by the help of AC voltage applied to the hyperbolic ring electrode. Helium is used as

dampening gas to cool down the ions. Next, ions are directed to the detector in order of the increasing m/z values [148].

Orbitrap mass analyzer (Figure 2.19) includes an inner spindle electrode and two hollow outer concave electrodes. Ions in the inner electrode have a continuous spinning movement and oscillate forward and back along the axis of the inner electrode. The oscillation of the analyte ions are measured by Fourier transform and mass spectrum of the analyte can be achieved [151].

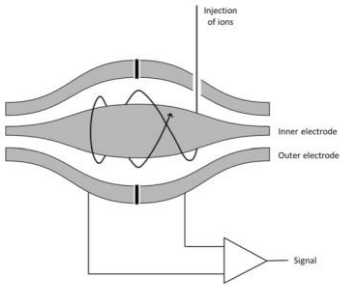


**Figure 2.19** The orbitrap mass analyzer [151]

In MS system, several ion detectors such as electron multiplier, array detector, scintillation detector, Faraday cup detectors are carried out. Electron multiplier detector can improve the ion beam up to the order of $10^6$. It has two different types as a discrete dynode and a continuous dynode type. In a discrete dynode (Figure 2.20), the ion beam collides to the first dynode with negative potential of several kilovolts and this process produces secondary electrons which then strikes to the second dynode. All these steps generate more electrons and so on [147].

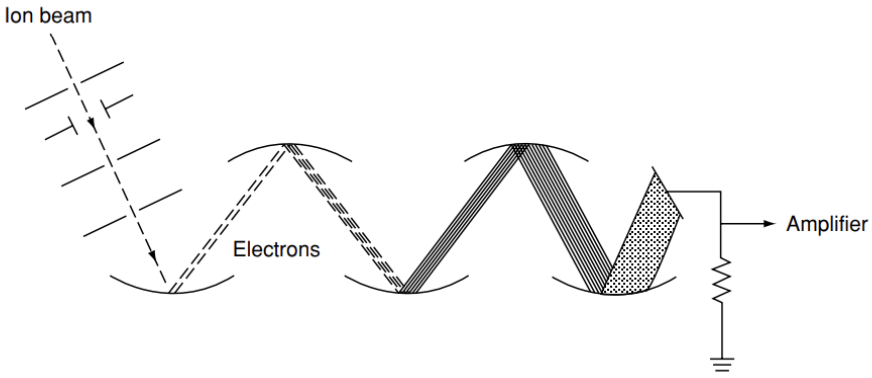


**Figure 2.20** The schematic diagram of a discrete dynode electron multiplier [147]

### 2.6.10 Hyphenated Methods

The term '*hyphenation*' is firstly proposed by Tomas Hirschfeld in 1980s and one separation method was combined with one or more spectroscopic methods in this study [152]. *Hyphenation* is to bring two or more techniques together in order to separate and detect analytes presented in a solution [153]. Chromatographic and spectroscopic methods are combined/hyphenated in order to take advantage of both methods. Chromatographic methods provide pure or almost pure fractions of analyte(s) found in a complicated sample matrix. Spectroscopic methods give information about the identity of analyte(s) by the help of standards and library spectrums [154]. Today, one of the most favorite hyphenated methods is chromatographic separation (LC or GC) coupled to mass spectrometry-based detection. In these methods, signal to noise ratio of the analyte(s) is enhanced due to low noise. In addition, sample loss and sample contamination can be eliminated by the help of online combinations of these methods [155].

Gas chromatography-mass spectrometry (GC-MS) is one of the most popular hyphenated methods consisting of GC for the separation stage and MS for the detection stage. MS provides structural information due to its ability to produce analyte fragments [153]. This hyphenated method is proper for the analytes that can be vaporized. GC and MS are compatible with each other because both methods require the vaporized sample. However, the main problem for the combination of GC and MS is the pressure difference that GC works at high pressures (760 torr) while MS at low pressures ($10^{-5}$–$10^{-6}$ torr). For this reason, a proper interface is used to couple GC and MS systems [156].

Liquid chromatography-mass spectrometry (LC-MS) is the combination of LC or HPLC systems with MS system. Generally, soft ionization techniques are performed in LC-MS systems that provides molecular ion of the analyte with some fragment ions [153]. When interfacing LC and MS systems, the major problem is the requirement of high vacuum conditions for MS system and the usage of high water-based solutions in LC systems. For this reason, the mobile phase used in LC system is removed before the entrance of the analytes into MS system or it is used to help the ionization of the analytes. There are two categories for the interfaces used in LC-MS systems: transport devices and unique ionization phenomena. Direct liquid introduction, moving belt (wire), particle beam are known as transport

devices while atmospheric pressure chemical ionization (APCI), electrospray (ESI) and thermospray are categorized in unique ionization phenomena [157]. The interfaces used in LC-MS system should have good nebulization and vaporization of the eluate, eliminate excess amount of sample vapor and ionize the sample [156].

HPLC systems can be combined with AAS methods by the introduction of liquid eluate to flame, graphite furnace or quartz tube after hydride generation process. Elements forming their volatile hydrides (As, Se, Sb, Sn, Pb, etc.) can be determined by the hyphenation of HPLC and HG-AAS methods. Not only the elements producing their volatile hydrides, but also other metals can be determined by the combination of HPLC-AAS methods. Direct or heated silica capillary interfacing HPLC-AAS [158] and thermospray nebulization [159] are some interfaces to combine HPLC and AAS methods. FAAS system is a rapid, accurate, reliable and robust spectroscopic method. After the achievements in AAS technology, more sensitive options like electrothermal AAS (ETAAS) with Zeeman correction have been developed [160]. In literature, the coupling of AAS and chromatographic systems (LC-AAS, GC-AAS) is more attractive for analytical chemists. When ETAAS is used for the detection method after the separation by LC system, a drying and ashing step should be performed. However, FAAS system does not require additional steps and liquid eluate from LC system can be directly sent to FAAS system [160], [161], [162].

ICP-OES and ICP-MS systems are popular plasma based spectroscopic methods for the determination of trace elements due to their excellence of accuracy, precision and sensitivity. ICP-OES system is favored among scientist due to its ability to conduct simultaneous measurement of elements [163]. Further, the high temperature of plasma removes the organic content of the samples which makes the structural analysis difficult. The combination of ICP-OES system with HPLC system offers low detection limits and multielement detection after the chromatographic separation [4]. HPLC-ICP-OES system has been used for the elemental speciation such as iron (Fe(II) and Fe(III)) [164], arsenic (As(III)), As(V), monomethylarsonic and dimethylarsinic acids, arsenocholine and arsenobetaine) [165] and vanadium (V(IV) and V(V)) [166]. In addition, organometallic compounds like cobalamin was determined by this system [167].

## 2.7 Sample Preparation Methods

Sample preparation is one of the most essential stages in analytical procedures and it is certainly a necessity before the instrumental measurements even for the sophisticated instruments in order to have analyte(s) separation from sample matrices [168]. It is carried out to simplify matrix effects, clean up the sample and enrich the analyte(s) [169]. There are several sample preparation methods in literature based on mechanics, gravity, magnetic field, size exclusion, electrochemistry, derivatization or labelling, degradation, filtration, membrane separation, phase partition and sorption [170]. The separation of analyte from sample matrices generally includes analyte partition between aqueous phase and extracting phase that can be volatile organic solvents or solid phases. When the partition of analyte is achieved, the extracting phase is taken from the aqueous medium to be analyzed by an instrumental method [168].

### 2.7.1 Solid phase extraction (SPE)

Solid phase extraction is one of the most frequently used method that consists of the sample introduction to a short column filled with solid adsorbent, adsorption of analyte(s) to the surface of the adsorbent and elution of analyte by a suitable solvent [171]. The short column is an open syringe barrel with the sorbent (50-60 μm particle size) which packed between plastic frits or porous metal [172].

Figure 2.21 summarizes the experimental steps for SPE method [173]. Octadecyl ($C_{18}$), octyl ($C_8$), cyclohexyl, phenyl, cyano (CN), amino ($NH_2$), silicagel (-SiOH), florisil ($Mg_2SiO_3$), alumina ($Al_2O_3$) are examples of sorbents used in SPE method [174].

SPE has some benefits in terms of the low solvent consumption and less waste production, but there are some serious problems in SPE method. These are insufficient uniformity of the packaging materials, limited selectivity of the adsorbent, competition of analyte with sample matrix components for adsorption [171].

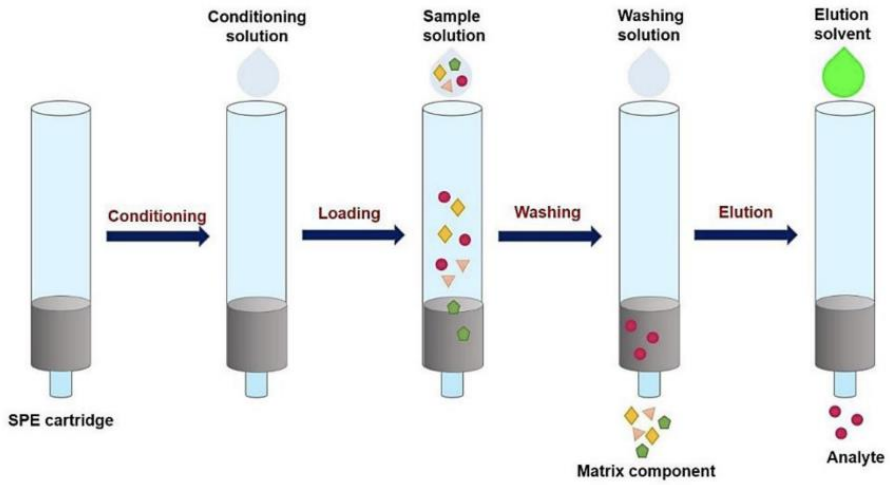


**Figure 2.21** A diagram for the application of SPE method [173]

### 2.7.2 Liquid-liquid extraction (LLE)

Liquid-liquid extraction is another important extraction method with comprehensive applications. Based on the definition declared by International Union of Pure and Applied Chemistry (IUPAC), LLE is a chemical process to transfer the dissolved substance from one aqueous phase to immiscible or partially immiscible liquid [175]. Analyte(s) are unequally distributed between two immiscible phases due to the solubility differences of the analyte(s) in the related phases. When the analyte transfer system is achieved to equilibrium state, most of the analyte remains in the phase that the analyte has higher solubility. There are some requirements in the selection of extraction solvent for this method. It should be non-reactive with the analyte, good dissolution property for the analyte, immiscible with water, sufficient density difference between the extraction solvent and water, low-cost and easily available at high purity [176].

Modern sample preparation methods make an effort to decrease the experimental steps and solvent usage and eliminate hazardous chemicals. Liquid phase microextraction (LPME) is a miniaturized form of LLE method which analytes are extracted form solid, liquid or gas samples into 100 µL or less volume of liquid [169]. LPME methods have been established to overcome the disadvantages of LLE method such as the high consumption of expensive, toxic and hazardous organic solvents, long extraction periods, exhausting and multiple processes [177]. Up to now, various LPME methods have been introduced and used in literature. Dispersive liquid-liquid microextraction (DLLME), solidified floating organic drop

microextraction, single drop microextraction (SDME), hollow fiber-based liquid-phase microextraction (HF-LPME) are different versions of LPME [178].

### 2.7.2.1 Dispersive liquid-liquid microextraction (DLLME)

Dispersive liquid-liquid microextraction was proposed by Rezaee and his coworkers in 2006 to preconcentrate polyaromatic hydrocarbons from surface, well and river water samples [179]. This method depends on the distribution of extraction solvent throughout the aqueous phase by the help of a second organic solvent that has miscible property in both phases. In practice, water immiscible solvent (extraction solvent) containing water miscible solvent (dispersive solvent) is injected into aqueous sample solution. The cloudy solution is then centrifuged to stop the distribution of extraction solvent and facilitate the phase separation. Finally, the analyte rich phase is taken by a micro syringe [180]. Its application is summarized in Figure 2.22.

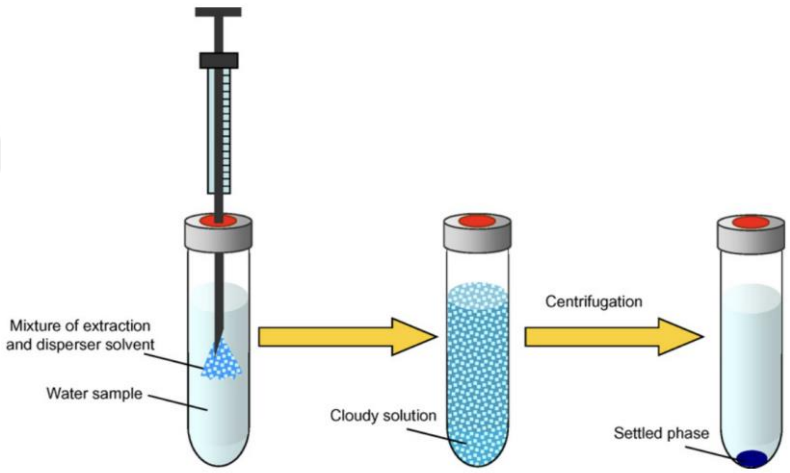


**Figure 2.22** A schematic diagram for DLLME method [181]

Although DLLME has been frequently by researchers, it has some important handicaps. First, the usage of polar solvents as dispersive solvents makes difficult to transfer the analyte(s) to extraction solvent due to the relatively high analyte solubility in dispersive solvents. In addition, the usage of dispersive solvents in the milliliter range is not an environmental action [182]. For these reasons, there are some attempts to overcome the handicaps of DLLME method. For example, ultrasound-assisted emulsification [183], [184], ultrasound-assisted surfactant-enhanced emulsification microextraction [185], [186], effervescence assisted

DLLME [187] and air-assisted DLLME [188] are some examples to reduce the impact of dispersive solvent usage in DLLME method.

#### 2.7.2.2 Spraying based fine droplet formation liquid phase microextraction (SB-FDF-LPME)

Spraying based fine droplet formation liquid phase microextraction (SB-FDF-LPME) was introduced to literature in 2020 to put an end for the usage of dispersive solvents to distribute the extraction solvent throughout the aqueous solution [9]. In SB-FDF-LPME method, a lab-made apparatus called as *spraying system* is utilized to introduce the extraction solvent in the solvent tank to the sample solution as fine droplets. The spraying system consists of a solvent tank, spray head, centrifuge tube cap with a hole at its center to combine the cap with the spray head. The centrifuge tube containing the sample solution is bonded to the centrifuge tube cap placed on the spray head. Next, the spray head is moved to the direction that the spraying process occurs. A cloudy solution is observed at the end of the spraying process due to the production of tiny droplets of extraction solvent [9], [189]. Figure 2.23 describes all the procedure in SB-FDF-LPME method.

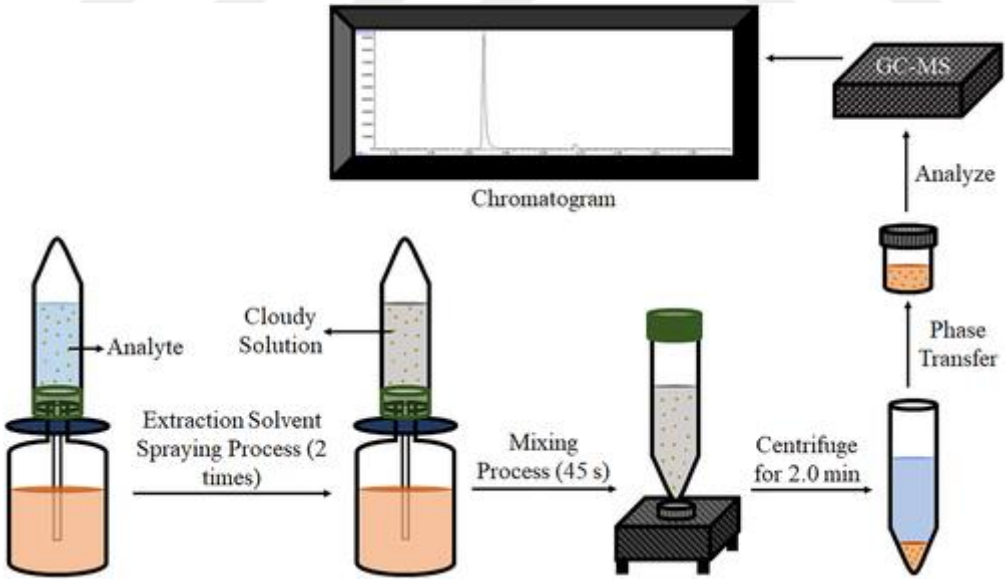


**Figure 2.23** A schematic presentation of SB-FDF-LPME taken from Dikmen et. al [9]

This system is dispersive-solvent free and compatible with other sample preparation and instruments. For example, ligand solutions or derivatizing agents can be easily transferred to the sample solution by the spraying system if the extraction solvent

is properly selected to dissolve these chemicals. Hence, simultaneous extraction and complexation or derivatization can be performed. Some examples for this process are copper complexation with N,N′-Bis(salicylidene)-1,2-phenylenediamine dissolved in chloroform [190], cadmium complexation with diphenlycarbazone dissolved in dichloromethane [189], cobalt complexation with a Schiff base ligand dissolved in chloroform [191], methamphetamine derivatized by acetic anhydride dissolved in 1,2-dichloroethane [192], fenuron derivatized by 2-naphthoyl chloride dissolved in chloroform [193]. SB-FDF-LPME method has been also used for the extraction of inorganic analytes from oil samples, but the extraction solvent should be water miscible solvents. For instance, cadmium and arsenic species in oil samples were extracted by the help of spraying system containing 2.0% nitric acid solution [7] and ultrapure water [194], respectively. According to these studies, SB-FDF-LPME method is a promising microextraction method in terms of its greenness, high efficiency and operational cost. For this reason, it is predicted that it will have different application areas in literature.

#### 2.7.2.3 Smart solvent-based liquid phase microextraction (SSB-LPME)

Organic solvents are carbon-based liquids that have ability to dissolve or disperse other chemicals. These solvents can be dangerous due to their carcinogenic and neurotoxic properties. Benzene, carbon tetrachloride or trichloroethylene are some examples for these solvents. In analytical methods, green solvents have taken the place of traditional organic solvents due to environmental concerns [195]. According to green chemistry, the amount of solvents should be reduced, it should be recycled, reused, regenerated or their usage can be rejected [196]. The usage of green solvents in analytical processes have gained momentum during the last century. Smart or switchable solvents (SSs), deep eutectic solvents (DESs) and ionic liquids (ILs) are well-known for their green nature. ILs are produced by anionic or cationic compounds with melting points lower than 100 $^{o}$C. These solvents have low volatility, wide liquid-state range, and low flammability [197]. DESs are composed of hydrogen acceptor and donor and found as liquid at room temperature. DESs have some benefits such as non-volatility, high thermal stability, good dissolution ability for organic and inorganic compounds [198]. SSs are known as their ability to change their hydrophobic nature to hydrophilic nature or vice versa [195], [199].

SSs were proposed by P.G. Jessop and his coworkers [200] in 2005. In their study, a polar ionic liquid was obtained after the mixture of two nonpolar solvents (1,8-diazabicyclo-[5.4.0]-undec-7-ene (DBU) and 1-hexanol) were mixed with carbon dioxide. It was also observed that the removal of carbon dioxide gas led to two distinct phases due to the alternation of polarity of the solvents to their original form [200]. This switchable property makes possible to separate polar compounds from non-polar compounds during the extraction process [201]. Up to now, SSs have been synthesized using amidine, ternary amines, medium chain saturated fatty acids. Some examples are N,N-dimethylbenzylamine (DMBA), triethylamine (TEA), 1-Ethylpiperidine, decanoic acid, octanoic acid and so on [202]. The reaction (Equation 2.5) between amine and water in the presence of carbon dioxide gas can be seen below [203].

$$NR_3 + H_2O + CO_2 \rightleftharpoons NR_3H^+ + HCO_3^- \quad (2.5)$$

As can be seen in the reaction, a protonation reaction of amine occurs when carbon dioxide is added to the mixture of amine and water [203]. As for the removal of carbon dioxide, various chemical and physical methods can be performed. Ultrasonic waves, heating, nitrogen addition, ion exchange resins are some examples for physical methods while the addition of salts, acids and bases are examples for chemical methods [201]. Among them, the usage of strong bases like sodium hydroxide is more popular owing to its fast carbon dioxide removal and minimal analyte loss [201], [204].

In practice, SSB-LPME method consists of four stages: 1) the addition of SS to the sample solution, (2) the addition of carbon dioxide removal agent, 3) the application of mixing process, 4) the separation and analysis of analyte rich phase [8]. All these steps are summarized in Figure 2.24.

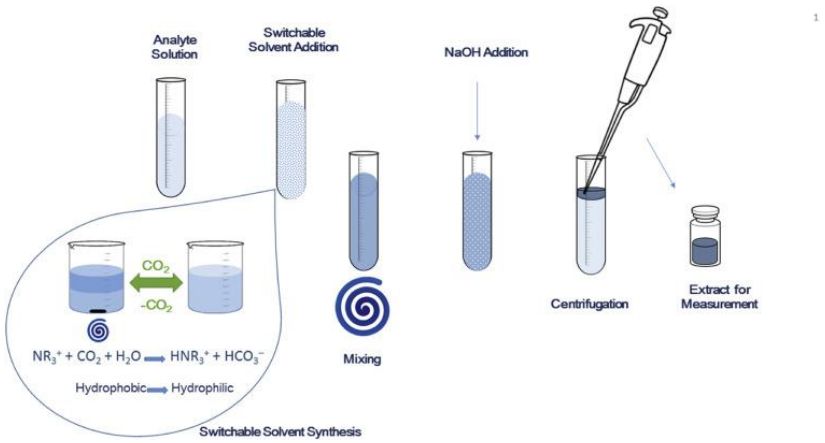


**Figure 2.24** A schematic presentation of SSB-LPME method [8]

SSB-LPME method has been performed for the extraction and preconcentration of organic and inorganic analytes from several sample matrices. For example, hormones and organochlorine pesticides from water and tea samples [205], cobalt from egg yolk [206], phthalic acid esters from water samples [207], polychlorinated biphenyls from beverages [208]. Based on the literature survey, SSs are excellent extraction solvents for organic and inorganic analytes due to their good solvent ability and wide application from biological to environmental matrices.

## 2.8 Derivatization

Derivatization process is performed to change physicochemical properties of analyte(s) into the desired one(s) [209]. Derivatization reagent or derivatizing agent is the chemical to modify target analyte(s) to be able to detect by GC or LC systems. An ideal derivatizing agent should have the following features: 1) it should react with analyte higher than 95% efficiency, 2) it should not lead to rearrangement or structural change during the production of analyte derivative, 3) it should not cause sample loss, 4) the produced derivative should not react with the stationary phase of GC system, 5) the produced derivative should be stable and should not change with time [210].

The major purpose of derivatization in GC system is to enhance volatility and change the analyte into a detectable form of analyte by the preferred detector [211]. The other main reason is to deactivate hydroxyl groups that interact with GC column and lead to peak tailing [209]. Other reasons are to enhance the peak shape of polar compounds, sensitivity of the analyte detection, chromatographic

separation of the analyte [212]. As for LC system, derivatization of the analyte(s) has less importance due to its suitability to a broad range analyte group. Derivatization in LC systems is generally performed to overcome the incompatibility of analyte and detector. There are several derivatizing reagents to convert the analyte into its UV, fluorescence, chemiluminescence or electrochemically active form [209].

The most well-known derivatization methods for GC system are silylation, acylation, alkylation and esterification [211].

*Silylation* is regarded as a simple and quick derivatization method for GC system. N,O-bis(trimethylsilyl)trifluoroacetamide (BSTFA), N-methyl-N-(trimethylsilyl)trifluoroacetamide (MSTFA), N,O-bis(trimethylsilyl)acetamide (BSA), N-methyl-N-(tert-butyldimethylsilyl)trifluoroacetamide (MTBSTFA) are some reagents used for silylation reaction [213]. Acidic hydrogen in analyte molecule is replaced by the alkylsilyl groups. For example, trimethylchlorosilane can be used as derivatizing agent for phenol. The reaction (Equation 2.6) can be seen below [211].

$$Ph - OH + (CH_3)_3SiCl \rightarrow Ph - O - Si(CH_3)_3 + HCl \qquad (2.6)$$

*Alkylation* is one of the most used derivatization reactions which protect the active hydrogen in analyte molecule by the displacement of active hydrogen by aliphatic and aromatic aliphatic groups (Equation 2.7) [210].

$$RCOOH + PhCH_2X \rightarrow RCOOCH_2Ph + HX \qquad (2.7)$$

where X is halogen or alkyl group R in the reaction above. Dialkylacetals, pentafluorobenzyl bromide (PFBBr), boron trifluoride ($BF_3$), tetrabutylammonium hydroxide (TBA) are some common reagents used in alkylation of analytes [210].

*Acylation* is also used to obtain volatile and less polar derivatives. It consists of the conversion of molecules with -OH, -NH and -SH into esters, amines and thioesters, respectively. One example for acylation reaction (Equation 2.8) is given below [211].

$$R - NH_2 + R^1COCl \rightarrow R - NH - COR^1 + HCl \qquad (2.8)$$

*Esterification* is the reaction between hydroxyl group of an alcohol and carboxyl group of an acid in the presence of a catalyst. It is useful to derivatize acidic groups

that has high reactivity and high polarity for GC system. Here, carbonyl oxygen is protonated and nucleophilic hydroxyl group attacks to the carbocation. This process yields the production of ester and water. The esterification reaction (2.9) is shown below [211].

$$RCOOH + R^1OH \rightleftharpoons RCOOR^1 + H_2O \quad (2.9)$$

In LC systems, UV absorbing property can be given by the reaction of some reagents such as 3,5-dinitrobenzoyl chloride (-OH), phenyl isocyanate (-OH), phenacyl bromide (-COOH), 2,4-dinitrophenylhydrazine (R-CO-R), 1-fluoro-2,4-dinitrobenzene (-$NH_2$, -$NHR_1$) and phenyl isothiocyanate (-$NH_2$, -$NHR_1$) [214]. Fluorescence detection in LC system is also popular due to its high sensitivity and selectivity. 2,6-Diaminopyridine-$Cu^{2+}$ (primary amine), 9-Fluorenylmethyl chloroformate ($1^o$ and $2^o$ amines), 2-p-Chlorosulfophenyl-3-phenylindone (amine, amino sugars), dansyl chloride (amines) are some reagents used for the florimetric derivatization of analytes [211]. Isoluminol, lucigenin and peroxyoxalate for chemiluminescence derivatization, isothiocyanates, ferrocene, aromatic nitro groups for electrochemical derivatization are also popular for the derivatization of analytes [212].

## 2.9 Speciation Analysis

Speciation comes from the Latin word "*species*" meaning species or species evolution [215]. According to IUPAC nomenclature, *speciation analysis* means the identification and measurement of one or more chemical species found in a sample. Different atomic and molecular species which derived from a same element are determined in speciation studies. These species can have different isotopic compositions, electronic or oxidation states, organic or inorganic compounds and their complexes, organometallic, macromolecular compounds [216]. In the last centuries, the total element concentration was regarded as sufficient for the evaluation of environmental and clinical processes. In spite of the importance of total element concentration in some areas, speciation analysis becomes extremely important field due to the changeable properties of chemical species such as toxicity, bioaccumulation, bioavailability, and mobility [217]. For example, arsenic is found as arsenobetaine or arsenosugars in seafoods and these compounds are not toxic for human bodies when compared to inorganic arsenic species which are

known as toxic for human organisms. Hence, it is not proper to make a conclusion only with total arsenic concentration and this may lead to economic problems [218]. Methylated arsenic species like monomethylarsonic acid (MMA) and dimethyarsinic acid (DMA) are also less toxic than arsenite (As(III)) and arsenate (As(V)) [219]. Chromium (III) is also known as essential element while chromium (VI)is highly toxic for human bodies. Vanadium (V) is more toxic than vanadium (IV) [220]. Other example is that inorganic tin is regarded as non-toxic while its organometallic species such as tripropyl-, tributyl- and triphenyltins are highly dangerous chemicals for living organisms [221].

Speciation analysis is essential for the following areas: 1) Biogeochemical behaviors of chemical species, 2) ecotoxicity or toxicity of some elements, 3) food quality control, 4) medical and pharmaceutical products, 5) clinical analysis, 6) occupational exposure, 7) process control and 8) effect of technological materials on the environment [222].

Sampling is the first challenge in speciation analysis because chemical species should not change during the sampling and storage. Another challenge is the concentration of species in natural samples which are generally at parts per billion or lower concentration levels [223]. The presence of oxidizing reducing agents, ionic strength, pH, temperature or bacterial activities should be taken into account during the sampling process. Water samples can be collected into polypropylene, polycarbonate, high density polyethylene or PTFE containers. It is better to record color, cloudiness, smell, pH, clarity of the sample after the sampling process because the liquid samples highly contact with the wall of containers which may lead to contamination or analyte loss [224]. Plastic containers are regarded as safe to store samples but some metals like chromium or nickel can be used during the production of these materials. It is found in literature that high density polyethylene containers can release a significant amount of barium, strontium or zinc to the sample solution [224], [225].

Solid and biota samples are preserved after their freezing process. Water samples are generally stored at 4.0 $^{o}$C in dark conditions and freezing is not desired due to the precipitation of some particles and the rupture of cells. In site selective preconcentration methods are also recommended for redox-sensitive species [223]. Liquid samples should be stored in amber or colored containers in order to avoid

any photochemical processes, algae and light-sensitive organism formation. Suspended particles should be removed by 0.20 or 0.45 μm membrane filters due to the possibility of its analyte adsorption or non-homogeneous sample formation [224], [226].

In speciation analysis, selectivity and sensitivity are most important analytical figures of merit to detect the target chemical species in the sample. Online coupling of separation methods and element selective detectors like atomic absorption, emission, fluorescence, mass spectrometry provide both selectivity and sensitivity for the determination of different species of the same element [222]. LC, GC, electrophoresis, and gel electrophoresis are some separation methods used before element selective detectors in online speciation analysis. ESI and MALDI methods are also useful for the structural information of molecular species [227]. Some examples for online coupling separation and element selective detectors are LC-MS, GC-MS, HPLC-FAAS, GC-AAS and GC-ICP-MS [222].

## 2.10 Isotope Dilution Methods

Isotope dilution (ID) is a well-recognized analytical method consisting of the measurement of isotopic composition of a sample that mixed with an isotopically enriched/labelled analyte beforehand [228]. It is considered as definitive analytical method due to its traceability to SI units, its excellent precision and accuracy not unsurpassed by other methods, its ability to compensate analyte loss and uncomplete extraction [229]. A typical ID analysis contains the following steps: 1) the weighing process of sample, 2) mixing the sample with a known amount of isotopically enriched/labelled material via gravimetric approach, 3) equilibrium and homogenization of the sample-isotopic material mixture, 4) chemical separation of the analyte and isotopic material, 5) measurement of isotopic composition of the mixture by MS system, 6) calculation of the analyte concentration in the sample using the known values such as the amount of sample and isotopic material and the isotopic composition of the mixture [230]. The advantages of ID method can be listed as [231]:

- Analyte loss is compensated once the equilibrium of sample-isotopic material mixture is reached.

- The adjustment of final volume in separation or preconcentration methods is not required due to the independence of isotope composition from concentration.
- Matrix effects are suppressed or eliminated because of the same positive and negative effects on the analyte and isotopic material [231].

On the other hand, there is a requirement to apply ID method. The analyte being determined should have two stable isotopes at least. For this reason, monoisotopic elements like F, Mn, Co, Au, Bi, P, Na, Al, As, Y, Sc, Nb, Rh, Ho, Tm, Pr, Tb cannot be determined by ID method. Some of the monoisotopic elements like Be, Th, I, Cs and Pa can be determined using their synthetic radioisotopes [230].

ID is an analytical method that enables the quantitative determination of both organic and inorganic species with high precision and accuracy [228]. The basis of this method was first developed by Etienne Roth. It was explained using the *'catch and release'* method (Figure 2.25) which aims to figure out the number of fish in a pond [232]. For this purpose, some of the fishes were caught and labelled to the pond. After a certain period to allow the distribution of all labelled fishes, another sampling was performed. The number of labelled and unlabeled fishes were counted and the total number of fishes in the pond was calculated using the ratio of labelled/unlabeled fishes and the total number of labelled fishes [233].

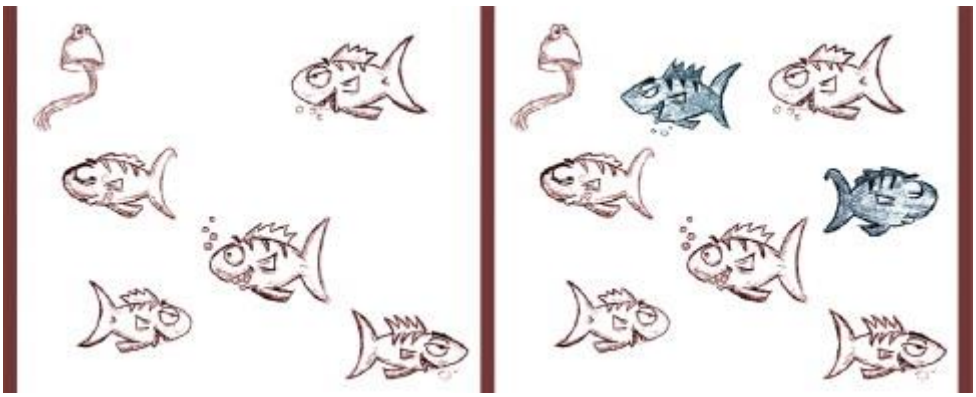

**Figure 2.25** Catch and release method that constitutes the principle of ID method [234]

ID is simply performed by mixing analyte (A) and its isotopic material (B) and measuring the isotopic composition of AB mixture. An equilibrium period is required before the MS based measurement due to the need of homogeneous isotope distribution throughout the AB mixture [235], [236]. There are four main ID

methods detailly explained by Vogl, Pritzkow and Pagliano. These are single (ID), double or reverse ($ID^2$), triple ($ID^3$) and quadruple ($ID^4$) isotope dilution methods [18], [237]. The compositions of sample and isotopic material can be seen in Figure 2.26.

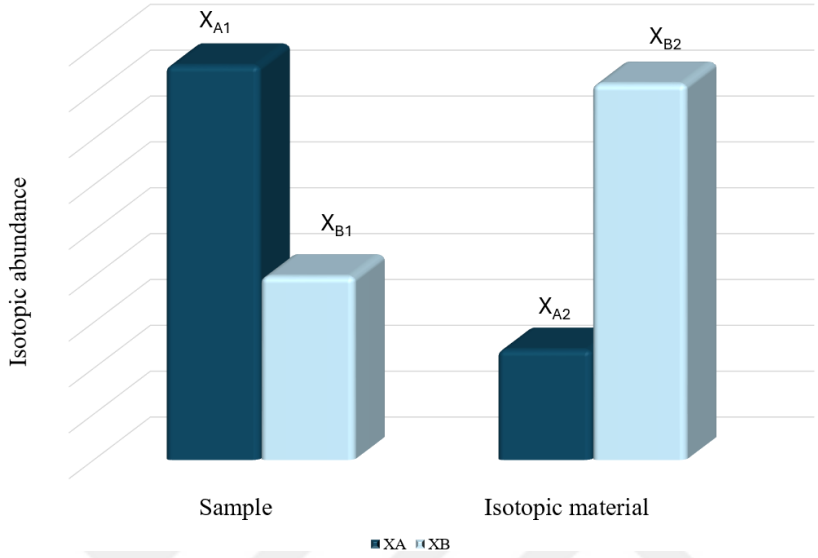


**Figure 2.26** Isotopic compositions of sample and isotopic material

**Table 2.1** Notations for isotope dilution formulas

| **Symbol** | **Definition** |
|---|---|
| A | Sample |
| A* | Standart solution of analyte |
| B | Isotopic material |
| AB | Sample mixture |
| A*B-a | Calibration mixture (a = 1, 2 or 3) |
| $n_x$ | Mole number of X (X =A, A* or B) |
| $M_x$ | Molecular weight of X (X = A, A* or B) |
| $w_{x-a}$ | Mass fraction of X (X = A, A* or B, a = 1,2 or 3) |

**Table 2.1** Notations for isotope dilution formulas (continued)

| | |
|---|---|
| $m_{x\text{-}a}(XY)$ | Mass of X in XY mixture (X,Y = A, A* or B, a = 1, 2 or 3) |
| $R_x$ | Isotope ratio of X (x = A, A*,B,1, 2 or 3) |
| $r_{x\text{-}a}$ | Isotope ratio measured by MS system (x = A, A* or B, a = 1, 2 or 3) |
| K | Mass bias factor |
| $\sum R_x$ | Total isotope ratio in mixtures (X = A, A* or B) |

Notations belonging to the isotope dilution methods can be seen in Table 2.1. The isotopic ratio of sample (Equation 2.10) and isotopic material (Equation 2.11) are as follows:

$$R_A = \frac{X_{A1}}{X_{B1}} \tag{2.10}$$

$$R_B = \frac{X_{A2}}{X_{B2}} \tag{2.11}$$

According to these equations, the isotopic ratio of the AB mixture (Equation 2.12) can be formulized as:

$$R_{AB} = \frac{n_A X_{A1} + n_B X_{A2}}{n_A X_{B1} + n_B X_{B2}} \tag{2.12}$$

When this equation is simplified, the equation will be as follows:

$$n_A = n_B \cdot \frac{(\frac{X_{A2}}{X_{B2}} - R_{AB})}{(R_{AB} - \frac{X_{A1}}{X_{B1}})} \cdot \frac{X_{B2}}{X_{B1}} \tag{2.13}$$

If the expression "$\frac{X_{B2}}{X_{B1}}$" is written as "$\frac{\sum R_A}{\sum R_B}$" [238]:

$$n_A = n_B \cdot \frac{(R_B - R_{AB})}{(R_{AB} - R_A)} \cdot \frac{\sum R_A}{\sum R_B} \tag{2.14}$$

The conversion of mole to mass fraction is carried out via the expression as $n_x = \frac{w_x \cdot m_x \cdot 10^6}{M_x}$ [238]. The equation above will be as follows:

$$w_A = w_B \cdot \frac{(R_B - R_{AB})}{(R_{AB} - R_A)} \cdot \frac{\sum R_A}{\sum R_B} \cdot \frac{m_{B(AB)}}{m_{A(AB)}} \cdot \frac{M_A}{M_B} \tag{2.15}$$

This equation belongs to single ID method. It is also corrected by mass bias factor 'k' due to the mass bias observed in MS systems. Hence, the expression '($R_x = K \cdot r_x$)' is applied to the equation above.

$$w_A = w_B \cdot \frac{(r_B - r_{AB})}{(r_{AB} - r_A)} \cdot \frac{\sum r_A}{\sum r_B} \cdot \frac{m_{i(AB)}}{m_{A(AB)}} \cdot \frac{M_A}{M_B} \tag{2.16}$$

According to the equation above, the mass fraction of isotopic material ($w_B$) should be known to calculate the concentration of analyte in the sample ($w_A$). An additional mixture called as *calibration mixture or blend* is prepared to eliminate the uncertainty contribution of $w_B$. This new mixture includes standard solution of the analyte (A*) and isotopic material (B). Therefore, the single ID formulations for AB and A*B mixtures generate the following formula below [18].

$$w_A = w_{A*} \cdot \frac{(r_A - r_{A*B})}{(r_{A*B} - r_B)} \cdot \frac{(r_B - r_{AB})}{(r_{AB} - r_A)} \cdot \frac{(m_{A*(A*B),aq})}{(m_{B(A*B),aq})} \cdot \frac{(m_{B(AB),aq})}{(m_{A(AB),aq})} \tag{2.17}$$

The usage of AB and A*B mixtures for the quantification of analyte in sample is known as double or reverse ID method. However, the isotopic composition of isotopic material ($r_B$) may also increase the uncertainty budget of the method. For this reason, a second calibration mixture (A*B-2) is added to the method in order to eliminate $r_B$ value from the formula. If the double ID formula is rearranged for A*B-1 and A*B-2 mixtures and two formulas obtained for each calibration mixture are equaled to each other, the following expression is obtained [18]:

$$w_A = \frac{w_{A*-2} \cdot \frac{m_{A*(A*B-2),aq}}{m_{B(A*B-2),aq}} (r_{AB} - r_{A*B-1}) \cdot (r_A - r_{A*B-2}) + w_{A*-1} \cdot \frac{m_{A*(A*B-1),aq}}{m_{B(A*B-1),aq}} (r_{AB} - r_{A*B-2}) \cdot (r_{A*B-1} - r_A)}{(r_{AB} - r_A) \cdot (r_{A*B-1} - r_{A*B-2})} \cdot \frac{m_{B(AB),aq}}{m_{A(AB),aq}} \tag{2.18}$$

The equation above is used in triple ID method. The last modification of ID method was proposed to cancel out the term as isotopic composition of sample ($r_A$) from the formula above. Hence, a third calibration mixture (A*B-3) is added to the method and the following equation is derived as [18]:

$$w_A = -\frac{m_{A*-2} \cdot m_{A*-3} \cdot k_1 + m_{A*-1} \cdot m_{A*-3} \cdot k_2 + m_{A*-1} \cdot m_{A*-2} \cdot k_3}{m_{A*-1} \cdot k_1 + m_{A*-2} \cdot k_2 + m_{A*-2} \cdot k_3} \tag{2.19}$$

$$m_{A*-x} = w_{A*-x} \cdot \frac{m_{A*(A*B-x)}}{m_{B(A*B-x)}} \tag{2.20}$$

$$k_1 = (r_{AB} - r_{A*B-1}) \cdot (r_{A*B-2} - r_{A*B-3}) \tag{2.21}$$

$$k_2 = (r_{AB} - r_{A*B-2}) \cdot (r_{A*B-3} - r_{A*B-1}) \quad (2.22)$$

$$k_3 = (r_{AB} - r_{A*B-3}) \cdot (r_{A*B-1} - r_{A*B-2}) \quad (2.23)$$

Isotope dilution methods is graphically summarized in Figure 2.27.

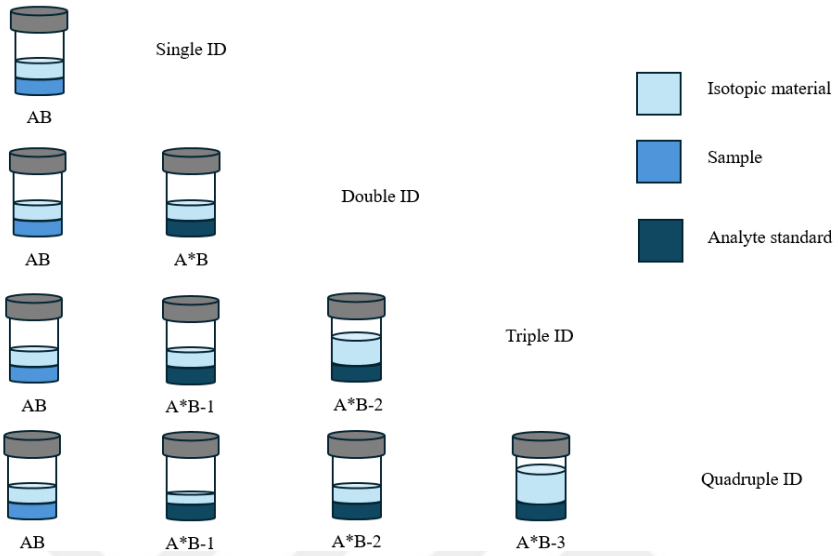


**Figure 2.27** The schematic presentation of all ID methods

This new approach is called as quadruple ID method [18]. In addition, exact matching can be used in all ID methods. In exact matching concept, the isotopic compositions of A*B and AB are equalized to eliminate the uncertainty effect of $r_B$ value and MS based measurement [18], [239].

In recent years, ID methods were used together with preconcentration methods. For example, quadruple ID method was used prior to DLLME method for the preconcentration of paracetamol from human serum and urine [240], binary solvent liquid phase microextraction for the preconcentration of bisphenol A from water samples [241], SB-FDF-LPME method for the preconcentration of methamphetamine from human urine and serum samples [192]. The integration of ID methods with preconcentration methods allows to achieve high precision and accuracy for target analytes at trace levels in complicated matrices.

## 2.11 Multivariate Optimization Strategies

Optimization is an imperative step during the development of analytical methods. It comprises a set of experimental studies to identify ideal conditions for an analytical method. Hence, accuracy, sensitivity, repeatability and detection limits

for an analytical method are improved as a result of optimization studies [242]. In general, one variable at a time approach is used by keeping all parameters constant except the tested one. However, this approach does not provide the effect of interaction between parameters and show the total effect of parameters on the response. The other drawback of this approach is the excess number of experiments that lead to high usage of chemicals and time consuming steps [243].

Chemometry is a discipline which process chemical data via statistical and mathematical fundamentals [244]. Response surface model is a chemometric tool that proposes quadratic models to determine critical experimental conditions. [244]. The simplest formula (Equation 2.24) for the quadratic model can be as follows [245]:

$$Y = \beta_0 + \beta_1 X_1 + \beta_2 X_2 + \beta_{12} X_1 X_2 + \beta_{11} X_1^2 + \beta_{22} X_2^2 \qquad (2.24)$$

Response surface model has important objectivities such as knowledge about the experimental processes, estimation of experimental variability (pure error), the production of response for the points that are not experimented, saving time and money [246]. In this model, there are some important terms which should be defined. *Factor or independent parameter* means that it can be independently undergone a change. Temperature, pH, concentration, flow rate can be independent parameters in a chemical system. Different values of a level that should be experimentally tested are known as *levels* of a parameter. It can be different pH levels from 4.0 to 7.0 if pH is an independent parameter. *Response* is the measured values like absorbance, electrical signal or emission while *residual* is the difference between experimental and predicted results. If the mathematical model is compatible with the experimental results, the model gives low residual values [243].

Central composite design and Box-Behnken design are the most popular response surface models in literature [245]. Central composite design investigates two or more parameters with five levels in general. It consists of a star design, a central point and two level full factorial design. The number of experiments required for this design can be calculated via $N= 2^k + 2k + C_0$, where k is the number of parameters and $C_0$ is the number of central points [244]. Figure 2.28 shows the graphical model for two and three parameters [243].

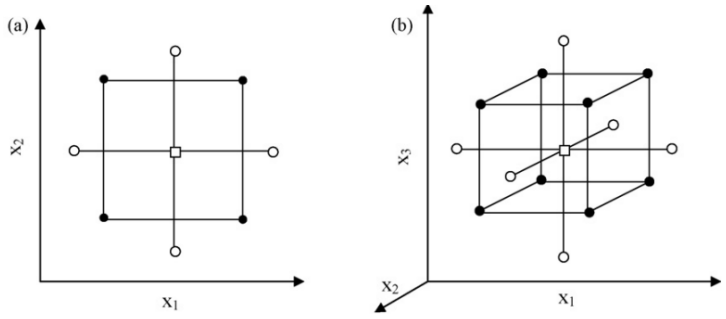


**Figure 2.28** The graphical presentation for two (a) and three (b) parameters in central composite design [243]

Box Behnken design is performed for three or more parameters with three levels. It is rotatable and spherical design with a cubic view [247]. The formula to find the number of experiments in Box-Behnken design is $N=2k(k-1)+C_0$ where k is the number of parameter and $C_0$ is the number of central points [248]. As shown in Figure 2.29, this design avoids the corner of the cube and deals with the combination of extreme levels and center. In summary, it is not interested in parameters with extreme levels [245].

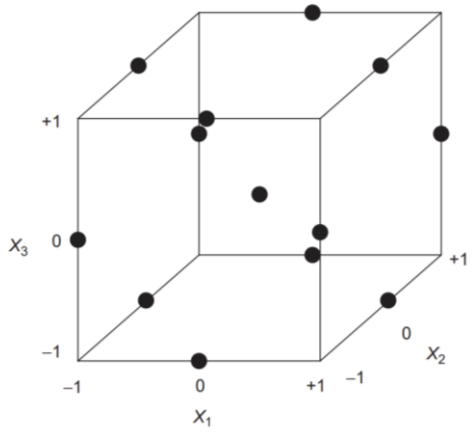


**Figure 2.29** The cubic view of Box-Behnken design [245]

Box Behnken design has lower number of experiments for three of more parameters if compared to central composite design. In addition, it is proper for three or more parameters and optimum conditions predicted in the range of studied levels [249].

# 3
# MATERIALS AND METHODS

## 3.1 Quantification of Chromium (III) and Chromium (VI) in Water, Soil and Grass Samples by HPLC-ICP-OES System

This study was published in Environmental Monitoring and Assessment in 2022 [250]. Ethical approval was obtained from Yıldız Technical University Social Sciences and Humanities Research Ethics Committee on 21.09.2022 with meeting number 2022/9.

### 3.1.1 Reagents and chemicals

Reagents and chemicals utilized during the optimization and other studies for the determination of chromium (III) and chromium (VI) are listed in Table 3.1. A 100 mg/kg of chromium (III) and chromium (VI) standard solutions were individually prepared by diluting the main stock solution of analytes. The mixture of two chromium species was prepared by diluting 100 mg/kg stock solution with 30 mmol/L ammonium nitrate solution at pH 7.2. Ultrapure water (UPW) (18.2 MΩ.cm, 25 $^{o}$C) obtained by a water purifying system (Elga Flex 3) was used in dilution and cleaning purposes.

**Table 3.1** Reagents and chemicals used in this study

| Chemical Name | Purity | Supplier |
|---|---|---|
| **Chromium (III)** | - | High Purity Standards (USA) |
| **Chromium (VI)** | - | |
| **Ammonium nitrate ($NH_4NO_3$)** | ≥ 98% | Merck (Germany, Darmstadt) |
| **Methanol** | ≥ 99.9% | |

Argon and nitrogen gases with high purity purchased from a local gas supplier (İstanbul, Türkiye) were used as plasma and cooling gases in ICP-OES system, respectively. A UC-20SDII model ultrasonicator, pH meter, Waring 8010E model blender, IKA A11 model grinding mill were purchased from BIOBASE (China, Zhangqiu), Mettler-Toledo GmbH (Greifensee, Switzerland), Waring Commercial (Connecticut, USA) and IKA Laboratory Equipment (Staufen, Germany), respectively.

### 3.1.2 Instrumentation

Chromatographic separation and elemental detection of chromium species were conducted by the combination of a LC20A Shimadzu HPLC system and a 2100DV model Perkin Elmer ICP-OES system. The hyphenated system consists of an autosampler (SIL-20A HT), a column oven (CTO-10AS) in HPLC system and peristaltic pump, air compressor in ICP-OES system. Table 3.2 summarizes all optimum conditions used in HPLC-ICP-OES system and Figure 3.1 demonstrates the combination of HPLC and ICP-OES systems used in this study.

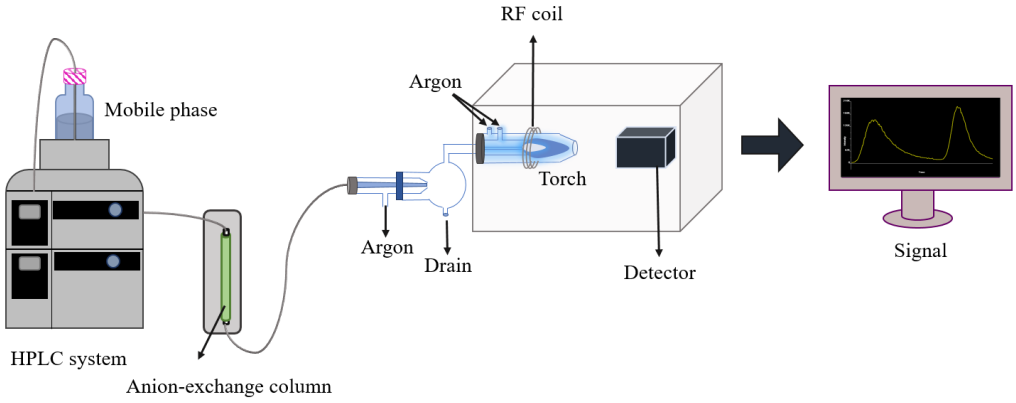


**Figure 3.1** A schematic presentation of HPLC-ICP-OES system for the determination of chromium species

**Table 3.2** HPLC-ICP-OES conditions for the determination of chromium species

| Parameter | Condition/Value |
|---|---|
| **Analytical column** | Anion-exchange LC column (7.0 µm of particle size, 4.6 i.d. x 150 mm, Alltech Allsep) |
| **Mobile phase system** | 30 mmol/L $NH_4NO_3$, %3.0 Methanol (pH 6.0) |
| **Flow rate of mobile phase system** | 1.0 mL/min |
| **Sample injection volume** | 50 µL |
| **Radiofrequency (RF) power** | 1400 W |
| **Working wavelength** | 267.716 nm |
| **The pressure of plasma, cooling and shear gases** | 8.0, 4.0, 5.0 bar |
| **The flow rate of plasma, nebulizer and auxiliary gas** | 14.0, 0.6, 0.2 L/min |

Peristaltic pump and air compressor were used to introduce liquid sample solution to the nebulizer and generate dry air to be used as shear gas in ICP-OES system, respectively. In HPLC-ICP-OES system, the liquid sample was injected and separated on anion exchange LC column. The separated substances were directly transferred to the ICP-OES system with the help of a capillary tubing placed between the outlet of the analytical column and nebulizer part of the ICP-OES system. Peak intensities observed in ICP-OES system were taken into account for the quantitation of chromium species.

### 3.1.3 HPLC-ICP-OES conditions

A 50 µL of sample or standard solution was introduced to the HPLC system via the autosampler. The chromium species were separated using quaternary ammonium

based anion exchange column as the stationary phase and 30 mmol/L ammonium nitrate including 3.0% methanol (pH 6.0) as mobile phase. The mobile phase was sent to the HPLC-ICP-OES system at the flow rate of 1.0 mL/min in order to achieve a good resolution of each peak belonging to the analytes. The separated analytes were delivered to the ICP-OES system with the aid of capillary tube linked the outlet of the analytical column to the inlet of nebulizer system. The monochromator in ICP-OES system was fixed to the emission wavelength of chromium as 267.716 nm in order to record the peak intensities of each analyte.

### 3.1.4 Samples

The collection of water, soil and grass samples were done from the roadside of factory buildings situated in Tuzla Organized Industrial Region (Tuzla, İstanbul). Filtration with 0.45-µm syringe filters was performed for the water samples before their analyses. A 5.0 g water sample was measured into a clean 50 mL centrifuge tube and diluted to 10 g with the solution containing 30 mmol/L ammonium nitrate at pH 7.0. Next, 0.20 g water sample was spiked to the different concentration values using 20 and 10 mg/kg mix standard solutions and then diluted to 0.75 g with 30 mmol/L ammonium nitrate solution at pH 7.0.

Drying process in a vacuum oven at 50 $^{o}$C for one day was implemented for soil and grass samples. After the samples were dried, homogenization and grinding process were applied to the solid samples.

A 2.0 g of dried soil sample was measured and admixed with 10 g of 30 mmol/L ammonium nitrate solution at pH 7.0. The sample solution was mixed by the help of orbital shaker for 10 min and then centrifuged at 4420 *g* for 10 min to facilitate the separation of solid particles and supernate phase. After the supernate phase was filtered by 0.45-µm syringe filters and transferred to a clean centrifuge tube, 0.50 g supernate solution was spiked and diluted to 1.0 g with 30 mmol/L ammonium nitrate solution at pH 7.0.

A 2.0 g of dried grass sample was mixed with 18 g of 30 mmol/L ammonium nitrate solution at pH 7.0. The solution was mixed by orbital shaker for 10 min and vortex for 5.0 min. The solid grass powder and supernate phase were separated by centrifuging at 4420 *g* for 10 min. The supernate was filtered through 0.45-µm

syringe filters. A 0.50 g supernate was diluted to 0.75 g with 30 mmol/L ammonium nitrate solution at pH 7.0 after the spiking procedure.

## 3.2 Quantification of Cobalamin in Vitamin Drug Tablets by HPLC-FAAS System

This study was published in Journal of Pharmaceutical and Biomedical Analysis in 2022 [251]. Ethical approval was obtained from Yıldız Technical University Social Sciences and Humanities Research Ethics Committee on 21.09.2022 with meeting number 2022/9.

### 3.2.1 Reagents and chemicals

Whole reagents and chemicals made use for the determination of cobalamin by HPLC-FAAS system are given in Table 3.3. Cobalamin main stock solution was dissolved in UPW and used to prepare working standard solutions. Gravimetric sample/standard preparation approach was followed during all experiments and OHAUS brand analytical balance (0.1 mg resolution, PA214C model) was used for the preparation of sample/standard solutions. UPW was used to prepare standard/sample solutions and mobile phases.

**Table 3.3** Reagents and chemicals used for HPLC-FAAS method

| Chemical Name | Purity | Supplier |
|---|---|---|
| **Cobalamin** | >98% | A pharmaceutical company (İstanbul, Türkiye) |
| **Sodium acetate trihydrate** | 99.0–101.0% | Merck (Germany, Darmstadt) |
| **Acetic acid** | 100% | |

### 3.2.2 Instrumentation

Cobalamin and free cobalt were separated using a Thermo HPLC system with AS3000 autosampler and P1500 pump. The detection of cobalamin and free cobalt

was obtained by an ATI UNICAM 929 AA model FAAS system equipped with cobalt hollow cathode lamp (HCL) and deuterium lamp. Air-acetylene flame was used for the atomization of cobalt found in cobalamin. Table 3.4 shows all instrumental parameters for HPLC-FAAS system.

**Table 3.4** HPLC-FAAS conditions for the determination of cobalamin

| Parameter | Condition/Value |
|---|---|
| **Analytical column** | Anion-exchange LC column (7.0 µm of particle size, 4.6 i.d. x 150 mm, Alltech Allsep) |
| **Mobile phase system** | Acetic acid/sodium acetate buffer system (34 mmol/L Ac/3.4 mmol/L NaAc) |
| **Flow rate of mobile phase system** | 1.75 mL/min |
| **Sample injection volume** | 75 µL |
| **HCL current** | 15 mA |
| **Working wavelength** | 240.8 nm |
| **Spectral bandwidth** | 0.20 nm |

T-SQT was designed and manufactured in our research laboratory in order to promote the interaction between analyte atoms and HCL light, and extend the dwell time of atoms. When T-SQT system was placed on the flame region, horizontal and sharp flame was observed at the edges of tube. For this reason, two air knives were used to protect FAAS system from this sharp flame.

A novel nebulizer system was also designed in our research laboratory and consisted of nebulizer gas input, sample input and concentric tube. The nebulizer system had an inner tube that was responsible for the transportation of liquid sample to the flame region by the help of a polytetrafluoroethylene (PTFE) capillary tubing (84.4 cm length × 0.76 mm outer diameter × 0.30 mm internal diameter) that also

linked to the outlet of the analytical column in HPLC system. Air used as nebulizer gas at the flow rate of 4.8 L/min was sent to the outer of the inner tube to obtain fine droplets of liquid sample before the atomization. Dimensions for T-SQT and nebulizer system are given in Figure 3.2.

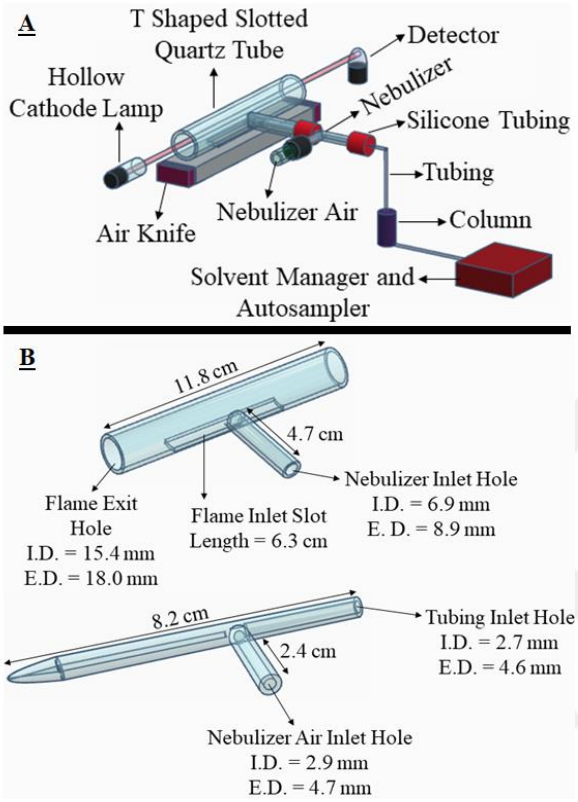


**Figure 3.2** HPLC-FAAS system with the novel nebulizer system (A) and dimensions for T-SQT and nebulizer system (B) [251]

### 3.2.3 Samples

In this study, two different brands of vitamin drugs containing thiamine, pyridoxine and cobalamin vitamins were purchased from local drug stores located in İstanbul, Türkiye. Five drug tablets of each brand drug were taken into a mortar and crushed to obtain fine particles of tablets. A 1.5087 g (A brand) and 1.3056 g (B brand) samples were measured and diluted to 10 g with UPW. Following that, the resulting solutions were subjected to ultrasonic waves for 5.0 min and filtered by 0.45 µm syringe filters. In the final step, 0.40 g filtered sample solution was spiked to different concentrations and then completed to 0.50 g with UPW.

## 3.3 Quantification of Chloroquine in Human Urine, Saliva and Serum Samples by SB-FDF-LPME-ID$^4$-GC-MS System

This study was published in Journal of Chromatography A in 2021 [252]. Ethical approval was obtained from Yıldız Technical University Social Sciences and Humanities Research Ethics Committee on 21.09.2022 with meeting number 2022/9.

### 3.3.1 Reagents and chemicals

All reagents and chemicals used in the presented study were of analytical grade. Table 3.5 summarizes all chemicals with their purities. In this study, all standard solutions were prepared based on the gravimetric approach. UPW with resistivity of 18.2 MΩ cm at room temperature was utilized to prepare standard solutions and other reagents.

**Table 3.5** All Reagents and chemicals used for the determination of chloroquine by SB-FDF-LPME-ID$^4$-GC-MS method

| Chemical Name | Purity | Supplier |
|---|---|---|
| **Chloroquine phosphate** | 99.4% assay | Abdi İbrahim Pharmaceutical Company (İstanbul, Türkiye) |
| **Acetic anhydride** | ≥99% purity | Sigma Aldrich (Darmstadt, Germany) |
| **Acetic anhydride-*d6*** | 99% | |
| **Chloroform** | ≥ 99.0% | Merck (Darmstadt, Germany) |
| **Dichloromethane** | 99.9% | |
| **1,2-dichloroethane** | ≥ 99.5% | |
| **Acetonitrile** | ≥ 99.8% | |
| **Methanol** | ≥ 99.9% | |

**Table 3.5** All Reagents and chemicals used for the determination of chloroquine by SB-FDF-LPME-ID$^4$-GC-MS method (continued)

| | | |
|---|---|---|
| **Ammonia solution** | 25.0 – 30.0% assay | Merck (Darmstadt, Germany) |
| **Sodium hydroxide** | 98% | Ak Kimya (Yalova, Türkiye) |

### 3.3.2 Instrumentation

An Agilent 6890 Gas Chromatograph (CA, USA) was coupled to an Agilent 5973 mass spectrometer (CA, USA) for the separation and detection of chloroquine acetamide (CA) and its isotopic derivative. The stationary phase in the system was an Agilent HP-5MS column (30 m x 250 µm x 0.25 µm) (CA, USA). Other GC-MS parameters were given in Table 3.6. The fragment ions used for the quantitation of CA and chloroquine acetamide-*d3* (CA-*d3*) were determined as 219 and 336 m/z, respectively.

**Table 3.6** GC-MS conditions for the determination of chloroquine by SB-FDF-LPME-ID$^4$-GC-MS method

| **Parameter** | **Value** |
|---|---|
| **Mobile phase and its flow rate** | Helium, 2.8 mL/min |
| **Inlet temperature** | 290 ºC |
| **Injection mode** | Splitless |
| **Injection volume** | 1.0 µL |
| **Temperature program** | Initial temperature was 100 °C and then increased to 290 °C (60 °C/min) and held for 4.33 min |
| **Electron impact ionization energy** | 70 eV |

**Table 3.6** GC-MS conditions for the determination of chloroquine by SB-FDF-LPME-ID$^4$-GC-MS method (continued)

| | |
|---|---|
| **MS transfer line, source and quadrupole temperature** | 280, 230 and 150 °C |

### 3.3.3 SB-FDF-LPME Procedure

A 12 mL of standard or sample solution was pipetted into a clean centrifuge tube. Next, sodium hydroxide solution (0.75 mL, 3.0 mol/L) was added to obtain basic medium for the removal of phosphate group. Acetic anhydride solution (20%, v/v) was prepared in 1,2-dicloroethane and then the spraying system was filled with this solution. The acetic anhydride solution found in the spraying system was sprayed only one time into the standard/sample solution. The separation of 1,2-dichloroethane phase from the aqueous phase was facilitated by centrifuging for 2.0 min at 3461 *g*. After the liquid part was removed from the centrifuge tube, the organic phase was taken into an insert vial for its analysis by GC–MS system.

### 3.3.4 Samples for accuracy and suitability tests

All biological samples taken by healthy volunteers in our laboratory were treated with a protein precipitation procedure. All samples were kept at −20 °C before applying the developed SB-FDF-LPME-GC-MS method. For this purpose, 3.0 g liquid sample was spiked with target analyte at different concentration values. Next, 5.40 g acetonitrile was added into the spiked sample solution and then diluted to 9.0 g with UPW. After centrifuging the diluted sample, 6.0 g supernate phase was completed to 40 g with UPW. The acetonitrile content in the sample solution was 12.5% (w/w) after the addition of 1.40 g acetonitrile to the diluted solution.

The protein precipitation process for urine sample had also concentrated ammonia solution. For this purpose, 3.0 g urine sample was spiked with proper standard solution of analyte and 4.30 g acetonitrile and 1.2 g concentrated ammonia were pipetted into the spiked sample. The final volume of the solution was fixed to 9.0 g with UPW. After centrifuging the diluted sample for 10 minutes, 6.0 g supernate and 1.10 g acetonitrile were mixed in a conical centrifuge tube. Next, the solution was diluted to 40 g with UPW before analyzing by SB-FDF-LPME-GC-MS method.

### 3.3.5 Calibration and sample mixtures for SB-FDF-LPME-ID$^4$-GC-MS method

Calibration mixtures (A*B-1, A*B-2, A*B-3) were prepared using chloroquine phosphate standard solution (A*) and CA-*d3* standard solution (B). Sample mixtures were prepared by the addition of sample solution (A) and CA-*d3* standard solution (B) with the protein precipitation reagents as acetonitrile and concentrated ammonia. SB-FDF-LPME-GC-MS method was performed on all samples spiked to two different concentration values. In the first step, all samples were spiked to about 80 (low level) and 160 (high level) mg/kg. In addition, 72.17 and 144.60 mg/kg CA-*d3* solution were used in the preparation of sample mixtures. Table 3.7 summarizes the mass values used in the preparation of calibration and sample mixtures. After the preparation of sample mixtures, 30 s vortex was applied to mix the mixtures and centrifugation process for 10 minutes was performed to separate the solid particles from the liquid part. The supernate phase (3.25 g) was diluted to 13 g with UPW prior to the SB-FDF-LPME-GC-MS method.

**Table 3.7** Theoretical mass values used for the preparation of calibration and sample mixtures

| | Mixtures | A*, g | A, g | B, g | Acetonitrile, g | Ammonia, g | UPW, g | Total, g |
|---|---|---|---|---|---|---|---|---|
| **Calibration Mixtures** | A*B-1 | 4.0 | - | 2.0 | - | - | 7.0 | 13.0 |
| | A*B-2 | 3.0 | - | 3.0 | - | - | 7.0 | 13.0 |
| | A*B-3 | 2.0 | - | 4.0 | - | - | 7.0 | 13.0 |
| **Serum (Sample Mixture)** | AB | - | 3.0 | 3.0 | 6.5 | - | 0.50 | 13.0 |
| **Urine (Sample Mixture)** | AB | - | 3.0 | 3.0 | 5.1 | 1.4 | 0.50 | 13.0 |
| **Saliva (Sample Mixture)** | AB | - | 3.0 | 3.0 | 6.5 | - | 0.50 | 13.0 |

Calibration mixtures for low level were prepared with chloroquine phosphate standard solution (A*, 20.03 mg/kg) and CA-*d3* solution (B, 18.24 mg/kg). In addition, calibration mixtures for high levels were obtained with chloroquine phosphate standard solution (A*, 40.62 mg/kg) and CA-*d3* solution (B, 36.11 mg/kg). Finally, 12 mL portion of all mixtures was separately taken into clean centrifuge tubes and the developed microextraction method was performed.

The experimental mass values belonging to calibration and sample mixtures for low concentration level are given in Table 3.8, Table 3.9 and Table 3.10.

**Table 3.8** Calibration mixture compositions (The concentration levels of A* and B solutions were 20.03 and 18.24 mg/kg, respectively)

| Mixture | A*, g | B, g | Total, g |
|---|---|---|---|
| **A*B-1-a** | 4.0029 | 2.0037 | 13.0440 |
| **A*B-1-b** | 4.0757 | 2.0012 | 13.0114 |
| **A*B-1-c** | 4.0055 | 2.0058 | 13.0649 |
| **A*B-2-a** | 3.0054 | 2.9998 | 13.0400 |
| **A*B-2-b** | 3.0031 | 3.0055 | 13.0070 |
| **A*B-2-c** | 3.0016 | 3.0121 | 13.0291 |
| **A*B-3-a** | 2.0337 | 3.9796 | 13.0361 |
| **A*B-3-b** | 2.0052 | 3.9977 | 13.0179 |
| **A*B-3-c** | 2.0055 | 3.9960 | 13.0330 |

A*: Chloroquine phosphate standard solution, B: CA-*d3*

**Table 3.9** Sample mixtures (The concentration of B was 72.17 mg/kg.)

| Sample | Mixture | A, g | B, g | ACN, g | $NH_3$, g | Total, g |
|---|---|---|---|---|---|---|
| **Serum** | AB-a | 3.0063 | 3.0231 | 6.5334 | - | 13.0011 |
| | AB-b | 3.0020 | 3.0366 | 6.4686 | - | 13.0195 |

**Table 3.9** Sample mixtures (The concentration of B was 72.17 mg/kg.) (continued)

| | | | | | | |
|---|---|---|---|---|---|---|
| **Serum** | AB-c | 3.0032 | 3.0173 | 6.5066 | - | 13.0138 |
| **Urine** | AB-a | 3.0020 | 3.0018 | 5.1134 | 1.4134 | 13.0077 |
| | AB-b | 3.0059 | 3.0281 | 5.1034 | 1.4074 | 13.0174 |
| | AB-c | 3.0195 | 3.0571 | 5.1131 | 1.4034 | 13.0026 |
| **Saliva** | AB-a | 3.0180 | 3.0360 | 6.4986 | - | 13.0153 |
| | AB-b | 3.0005 | 3.0153 | 6.4983 | - | 13.0073 |
| | AB-c | 3.0404 | 3.0626 | 6.5108 | - | 13.0170 |

A: The spiked sample, B: CA-*d3* ACN: acetonitrile.

**Table 3.10** Sample mixture dilutions after the protein precipitation for the process in Table 3.9

| **Sample** | **Mixture** | **Supernate, g** | **Total, g** | **A, mg/kg** | **Matrix Dilution** |
|---|---|---|---|---|---|
| **Serum** | AB-a | 3.2552 | 13.0658 | 4.64 | 4.0 |
| | AB-b | 3.2760 | 13.0150 | | |
| | AB-c | 3.2512 | 13.0400 | | |
| **Urine** | AB-a | 3.2639 | 13.0268 | 4.47 | 4.0 |
| | AB-b | 3.2536 | 13.2116 | | |
| | AB-c | 3.2529 | 13.0821 | | |
| **Saliva** | AB-a | 3.2530 | 13.0021 | 4.91 | 4.0 |
| | AB-b | 3.2592 | 13.0280 | | |
| | AB-c | 3.2605 | 13.0799 | | |

The experimental mass values belonging to calibration and sample mixtures for high concentration level are given in Table 3.11, Table 3.12 and Table 3.13.

**Table 3.11** Calibration mixture compositions (The concentration levels of A* and B solutions were 40.62 and 36.11 mg/kg, respectively)

| Mixture | A*, g | B, g | Total, g |
|---|---|---|---|
| **A*B-1-a** | 4.0078 | 2.0125 | 13.0124 |
| **A*B-1-b** | 4.0042 | 2.0049 | 13.0557 |
| **A*B-1-c** | 4.0099 | 2.0276 | 13.0215 |
| **A*B-2-a** | 3.0085 | 3.0027 | 13.0328 |
| **A*B-2-b** | 3.0089 | 2.9981 | 13.1486 |
| **A*B-2-c** | 3.0042 | 2.9999 | 13.0293 |
| **A*B-3-a** | 2.0024 | 4.0174 | 13.0388 |
| **A*B-3-b** | 2.0120 | 3.9952 | 13.0625 |
| **A*B-3-c** | 2.0009 | 4.0107 | 13.0470 |

A*: Chloroquine phosphate standard solution, B: CA-*d3*

**Table 3.12** Sample mixtures (The concentration of B was 144.60 mg/kg.)

| Sample | Mixture | A, g | B, g | ACN, g | $NH_3$, g | Total, g |
|---|---|---|---|---|---|---|
| **Serum** | AB-a | 3.0008 | 3.0235 | 6.5247 | - | 13.0131 |
| | AB-b | 3.0102 | 2.9917 | 6.5314 | - | 13.0092 |
| | AB-c | 3.0825 | 3.0052 | 6.4994 | - | 13.0069 |
| **Urine** | AB-a | 3.0148 | 3.0090 | 5.1017 | 1.4038 | 13.0106 |
| | AB-b | 3.0013 | 3.0089 | 5.1050 | 1.4000 | 13.0110 |

**Table 3.12** Sample mixtures (The concentration of B was 144.60 mg/kg.) (continued)

| | | | | | | |
|---|---|---|---|---|---|---|
| **Urine** | AB-c | 3.0029 | 3.0027 | 5.1069 | 1.4105 | 13.0008 |
| **Saliva** | AB-a | 2.9991 | 3.0503 | 6.5502 | - | 13.0181 |
| | AB-b | 3.0062 | 3.0049 | 6.5269 | - | 13.0205 |
| | AB-c | 3.0027 | 3.0227 | 6.5051 | - | 13.0191 |

A: The spiked sample, B: CA-*d3* ACN: acetonitrile.

**Table 3.13** Sample mixture dilutions after the protein precipitation for the process in Table 3.12

| **Sample** | **Mixture** | **Supernate, g** | **Total, g** | **A, mg/kg** | **Matrix Dilution** |
|---|---|---|---|---|---|
| **Serum** | AB-a | 3.2613 | 13.0328 | 9.46 | 4.0 |
| | AB-b | 3.2544 | 13.0114 | | |
| | AB-c | 3.2590 | 13.0090 | | |
| **Urine** | AB-a | 3.2522 | 13.0376 | 9.14 | 4.0 |
| | AB-b | 3.2556 | 13.0174 | | |
| | AB-c | 3.2643 | 13.0102 | | |
| **Saliva** | AB-a | 3.2503 | 13.0202 | 9.27 | 4.0 |
| | AB-b | 3.2598 | 13.0102 | | |
| | AB-c | 3.2616 | 13.0213 | | |

### 3.3.6 Synthesis of chloroquine acetamide-*d3* (CA-*d3*)

The isotopically labelled material was synthesized using 1.0 mmol chloroquine phosphate, 3.0 mL of 1,2-dichloroethane, 1.0 mmol sodium hydroxide and 1.2

mmol acetic anhydride-*d6*. All the chemicals were mixed in a single neck flask and kept in ultrasonication bath for 30 min. The reaction was controlled by thin layer chromatography (TLC) analyses. After the reaction was completed, the organic solvent was evaporated under the reduced pressure. Figure 3.3 shows the reaction of chloroquine and acetic anhydride-*d6* below.

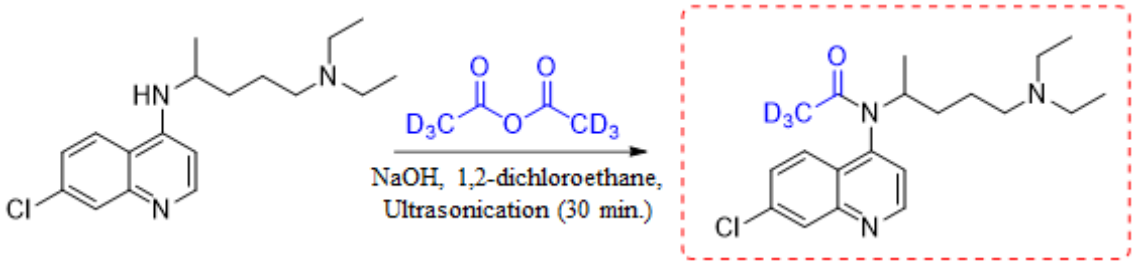


**Figure 3.3** Synthesis of CA-$d_3$ [252]

## 3.4 Quantification of Hydroxychloroquine in Human Urine, Saliva and Serum Samples by SSB-LPME-ID$^4$-GC-MS System

This study was published in Rapid Communications in Mass Spectrometry in 2022 [253]. Ethical approval was obtained from Yıldız Technical University Social Sciences and Humanities Research Ethics Committee on 21.09.2022 with meeting number 2022/9.

### 3.4.1 Reagents and chemicals

All reagents and chemicals used for the quantitation of hydroxychloroquine are given in Table 3.14. A water purification system (Elga Flex 3, High Wycombe, UK) was used throughout the study to produce UPW. The preparation and dilution of all stock and working standard solutions of the analyte were done using UPW.

**Table 3.14** All reagents and chemicals used for the determination of hydroxychloroquine by SSB-LPME-ID$^4$-GC-MS method

| Chemical Name | Purity | Supplier |
|---|---|---|
| **Hydroxychloroquine sulfate** | 98.6% assay | Neutec Pharmaceutical Company (İstanbul, Türkiye) |

**Table 3.14** All reagents and chemicals used for the determination of hydroxychloroquine by SSB-LPME-ID$^4$-GC-MS method (continued)

| | | |
|---|---|---|
| **Acetic anhydride** | ≥99% | Sigma Aldrich (Darmstadt, Germany) |
| **Acetic anhydride-*d6*** | 99% | |
| **N,N-dimethylbenzylamine** | ≥98.0% | Merck (Darmstadt, Germany) |
| **Acetonitrile** | ≥ 99.8% | |
| **Methanol** | ≥ 99.9% | |
| **Ammonia solution** | 25.0 – 30.0% assay | |
| **Sodium hydroxide** | 98% | Ak Kimya (Yalova, Türkiye) |

### 3.4.2 Instrumentation

An Agilent HP6890 series gas chromatograph was used to separate hydroxychloroquine methyl acetate (HMA) derivative and its isotopic material. An Agilent HP5973 series mass spectrometer connected to GC system was employed as a mass selective detector to separate both compounds in terms of m/z values. The stationary phase used in GC-MS system was HP5MS column with 30 m length, 250 µm inner diameter and 0.25 µm film thickness. All instrumental parameters belonging to GC-MS system are presented in Table 3.15.

**Table 3.15** GC-MS conditions for the determination of hydroxychloroquine by SSB-LPME-ID$^4$-GC-MS method

| **Parameter** | **Value** |
|---|---|
| **Mobile phase and its flow rate** | Helium, 2.8 mL/min |
| **Inlet temperature** | 290 ºC |
| **Injection mode** | Splitless |

**Table 3.15** GC-MS conditions for the determination of hydroxychloroquine by SSB-LPME-ID$^4$-GC-MS method (continued)

| | |
|---|---|
| **Injection volume** | 1.0 μL |
| **Temperature program** | Initial temperature was 100 °C and then increased to 290 °C (60 °C/min) and held for 4.33 min |
| **Electron impact ionization energy** | 70 eV |
| **MS transfer line, source and quadrupole temperature** | 280, 230 and 150 °C |

The analyte was separated and detected by GC-MS system after its derivatization by acetic anhydride and extraction by SSB-LPME method. The derivatization product in the final step was found as HMA. During all experiments in this study, 144.2/87.2 and 147.2/90.2 used as the quantifier/qualifier ions for HMA and hydroxychloroquine methyl acetate-*d3* (HMA-*d3*), respectively.

### 3.4.3 SSB-LPME Procedure

8.0 mL of liquid sample solution was pipetted into a conical centrifuge tube consisting of 199.1 μL of concentrated acetic anhydride solution. A 0.75 mL of smart solvent and 2.75 mL of 2.0 mol/L sodium hydroxide solution were sequentially added into the centrifuge tube to extract the derivatized analyte. The solution in the tube had a cloudy and white appearance after the addition of sodium hydroxide. Next, it was placed into an ultrasonic bath for 2.0 min to accelerate the hydroxychloroquine mass transfer from aqueous phase to smart solvent phase. In order to achieve a clear and distinct phase separation, the solution was centrifuged for 2.0 min at 3461 *g*. The analyte-rich phase was taken by a micropipette and placed into a glass insert vial to analyze by GC-MS system.

### 3.4.4 Samples for accuracy and suitability tests

Human urine, saliva and serum samples were taken from volunteers worked in our research laboratory. Protein content in all samples was removed or decreased by a protein precipitation process. A 2.0 g of human saliva and serum samples were

spiked with proper standard solutions and 3.60 g acetonitrile was added into the spiked samples. All solutions were completed to 6.0 g with UPW. As for urine samples, 2.0 g of urine sample was spiked with a proper concentration of analyte solution. A 2.80 g acetonitrile and 0.80 g ammonia were added to the spiked urine sample and then it was diluted to 6.0 g with UPW. All these solutions were mixed by vortex for 30 s to obtain a uniform precipitation process. A centrifugation process was also implemented for 10 min at 4420 *g* to separate the solid particles form supernate phase. After the centrifugation step, 4.50 g of supernate phase was gravimetrically transferred into a conical-bottom centrifuge tube and completed to 30 g with UPW. The developed SSB-LPME method was performed on the diluted supernate solutions.

### 3.4.5 Calibration and sample mixtures for SSB-LPME-ID$^4$-GC-MS method

A hydroxychloroquine sulfate standard solution (A*), a HMA-*d3* standard solution (B) and spiked sample solutions (A) were prepared to be used in calibration and sample mixtures. Two concentration levels (1.0 and 2.0 mg/kg) were used during the application of SSB-LPME-ID$^4$-GC-MS method. Table 3.16 presents all compositions for calibration and sample mixtures. When the calibration mixtures for low level (1.0 mg/kg) were prepared, 4.62 mg/kg hydroxychloroquine and 4.64 mg/kg HMA-*d3* were used as A* and B solutions, respectively. The sample mixtures for low level were prepared using 18.67 mg/kg hydroxychloroquine spiked sample and 18.41 mg/kg HMA-*d3* as A and B solutions, respectively. The calibration mixtures for high level (2.0 mg/kg) were prepared using 9.21 mg/kg hydroxychloroquine and 9.10 mg/kg HMA-*d3.* The sample mixtures for high level consisted of 37.49 mg/kg hydroxychloroquine spiked sample as A solution and 36.79 mg/kg HMA-*d3* as B solution.

**Table 3.16** The theoretical compositions of calibration and sample mixtures

| | **Mixture** | **A*, g** | **A, g** | **B, g** | **ACN, g** | **$NH_3$, g** | **UPW, g** | **Total, g** |
|---|---|---|---|---|---|---|---|---|
| **Calibration mixtures** | A*B-1 | 3.0 | - | 1.0 | - | - | 5.0 | 9.0 |
| | A*B-2 | 2.0 | - | 2.0 | - | - | 5.0 | 9.0 |

**Table 3.16** The theoretical compositions of calibration and sample mixtures (continued)

| | | | | | | | | |
|---|---|---|---|---|---|---|---|---|
| **Calibration mixtures** | A*B-3 | 1.0 | - | 3.0 | - | - | 5.0 | 9.0 |
| **Urine** | AB | - | 2.0 | 2.0 | 3.5 | 1.0 | 0.50 | 9.0 |
| **Saliva** | AB | - | 2.0 | 2.0 | 4.5 | - | 0.50 | 9.0 |
| **Serum** | AB | - | 2.0 | 2.0 | 4.5 | - | 0.50 | 9.0 |

The mixture preparation followed the mixing for 30 s and centrifugation for 10 min to obtain homogeneous distribution of isotopic material and analyte and a clear phase separation, respectively. A 2.5 g of supernate solution was taken into a conical centrifuge tube and completed to 10 g with UPW. All diluted solutions had a fixed acetonitrile concentration because different amounts of organic solvent could result in different volumes of analyte-rich phase after the SSB-LPME method. Hence urine, saliva and urine samples had 12.5%, 9.7% and 12.5% acetonitrile, respectively. An 8.0 mL of the diluted supernate solutions was treated with the developed SSB-LPME method.

The experimental mass values for calibration and sample mixtures for low concentration level are presented in Table 3.17 and Table 3.18.

**Table 3.17** Calibration and sample mixtures for 1.0 mg/kg of hydroxychloroquine sulfate spiked samples

| | **Mixture** | **A*, g** | **A, g** | **B, g** | **ACN, g** | **$NH_3$, g** | **Total, g** |
|---|---|---|---|---|---|---|---|
| **Calibration mixtures** | A*B-1-a | 3.0096 | - | 0.9926 | - | - | 9.0451 |
| | A*B-1-b | 3.0157 | - | 1.0175 | - | - | 9.0215 |
| | A*B-1-c | 3.0144 | - | 1.0112 | - | - | 9.0484 |
| | A*B-2-a | 2.0082 | - | 2.0048 | - | - | 9.0622 |
| | A*B-2-b | 2.0056 | - | 2.0071 | - | - | 9.0380 |

**Table 3.17** Calibration and sample mixtures for 1.0 mg/kg of hydroxychloroquine sulfate spiked samples (continued)

| | | | | | | | |
|---|---|---|---|---|---|---|---|
| **Calibration mixtures** | A*B-2-c | 2.0112 | - | 2.0034 | - | - | 9.0951 |
| | A*B-3-a | 1.0027 | - | 3.0266 | - | - | 9.0248 |
| | A*B-3-b | 1.0051 | - | 3.0178 | - | - | 9.0199 |
| | A*B-3-c | 1.0119 | - | 3.0070 | - | - | 9.0647 |
| **Serum** | AB-a | - | 2.0052 | 2.0132 | 4.4909 | - | 9.0223 |
| | AB-b | - | 2.0140 | 2.0033 | 4.4972 | - | 9.0184 |
| | AB-c | - | 2.0175 | 2.0046 | 4.4876 | - | 9.0051 |
| **Urine** | AB-a | - | 2.0182 | 2.0031 | 3.4875 | 1.0053 | 9.0152 |
| | AB-b | - | 2.0128 | 2.0028 | 3.5208 | 0.9670 | 9.0060 |
| | AB-c | - | 2.0028 | 2.0254 | 3.4879 | 0.9952 | 9.0039 |
| **Saliva** | AB-a | - | 2.0264 | 1.9902 | 4.5146 | - | 9.0153 |
| | AB-b | - | 2.0212 | 2.0127 | 4.5088 | - | 9.0037 |
| | AB-c | - | 2.0310 | 2.0118 | 4.5373 | - | 9.0375 |

**Table 3.18** Second dilutions for 1.0 mg/kg of hydroxychloroquine spiked samples

| **Sample** | **Mixture** | **Supernate, g** | **Total, g** | **A, mg/kg** | **Matrix dilution** |
|---|---|---|---|---|---|
| **Serum** | AB-a | 2.5039 | 10.1380 | 1.06 | 4.0 |
| | AB-b | 2.5148 | 10.0123 | | |
| | AB-c | 2.5108 | 10.0188 | | |
| **Urine** | AB-a | 2.5101 | 10.0344 | 1.04 | 4.0 |
| | AB-b | 2.5100 | 10.0587 | | |

**Table 3.18** Second dilutions for 1.0 mg/kg of hydroxychloroquine spiked samples (continued)

| | | | | | |
|---|---|---|---|---|---|
| **Urine** | AB-c | 2.5038 | 10.0564 | 1.04 | 4.0 |
| **Saliva** | AB-a | 2.5064 | 10.0399 | | |
| | AB-b | 2.5066 | 10.1363 | 1.03 | 4.0 |
| | AB-c | 2.5045 | 10.1713 | | |

The experimental mass values for calibration and sample mixtures for high concentration level are presented in Table 3.19 and Table 3.20.

**Table 3.19** Calibration and sample mixtures for 1.0 mg/kg of hydroxychloroquine sulfate spiked samples

| | **Mixture** | **A*, g** | **A, g** | **B, g** | **ACN, g** | **$NH_3$, g** | **Total, g** |
|---|---|---|---|---|---|---|---|
| **Calibration mixtures** | A*B-1-a | 3.0100 | - | 1.0092 | - | - | 9.0804 |
| | A*B-1-b | 3.0094 | - | 0.9924 | - | - | 9.1448 |
| | A*B-1-c | 3.0096 | - | 0.9969 | - | - | 9.0382 |
| | A*B-2-a | 2.0058 | - | 2.0105 | - | - | 9.0614 |
| | A*B-2-b | 2.0037 | - | 2.0084 | - | - | 9.0495 |
| | A*B-2-c | 2.0048 | - | 2.0092 | - | - | 9.0258 |
| | A*B-3-a | 1.0022 | - | 3.0003 | - | - | 9.0556 |
| | A*B-3-b | 1.0045 | - | 3.0128 | - | - | 9.0195 |
| | A*B-3-c | 1.0091 | - | 3.0055 | - | - | 9.0058 |
| **Serum** | AB-a | - | 2.0081 | 1.9929 | 4.5045 | - | 9.0260 |
| | AB-b | - | 2.0055 | 2.0120 | 4.4840 | - | 9.0066 |
| | AB-c | - | 2.0029 | 2.0114 | 4.4900 | - | 9.0065 |

**Table 3.19** Calibration and sample mixtures for 1.0 mg/kg of hydroxychloroquine sulfate spiked samples (continued)

| | | | | | | | |
|---|---|---|---|---|---|---|---|
| **Urine** | AB-a | - | 2.0104 | 2.0145 | 3.5073 | 1.0147 | 9.0071 |
| | AB-b | - | 2.0029 | 2.0164 | 3.4882 | 1.0115 | 9.0046 |
| | AB-c | - | 2.0175 | 2.0057 | 3.4899 | 0.9946 | 9.0089 |
| **Saliva** | AB-a | - | 2.0563 | 2.0053 | 4.4684 | - | 9.0099 |
| | AB-b | - | 2.0473 | 2.0249 | 4.4810 | - | 9.0017 |
| | AB-c | - | 2.0165 | 2.0012 | 4.5072 | - | 9.0216 |

**Table 3.20** Second dilutions for 2.0 mg/kg of hydroxychloroquine spiked samples

| Sample | Mixture | Supernate, g | Total, g | A, mg/kg | Matrix dilution |
|---|---|---|---|---|---|
| **Serum** | AB-a | 2.5169 | 10.0222 | 2.03 | 4.0 |
| | AB-b | 2.5160 | 10.0386 | | |
| | AB-c | 2.5018 | 10.0129 | | |
| **Urine** | AB-a | 2.5076 | 10.0736 | 2.09 | 4.0 |
| | AB-b | 2.5094 | 10.0736 | | |
| | AB-c | 2.5104 | 10.0047 | | |
| **Saliva** | AB-a | 2.5093 | 10.0136 | 2.07 | 4.0 |
| | AB-b | 2.5079 | 10.0066 | | |
| | AB-c | 2.5080 | 10.0148 | | |

### 3.4.6 Synthesis of hydroxychloroquine methyl acetate-*d3* (HMA-$d_3$)

HMA-*d3* was used as isotopically labelled material for the quantitation of hydroxychloroquine by ID$^4$ method. Its synthesis was performed in a Schlenk tube containing 1.0 mmol hydroxychloroquine, 1.50 mmol acetic anhydride-d6, 1.0 mL pyridine and 5.0 mL dichloromethane. The Schlenk tube was exposed to ultrasonic waves for 30 min and the reaction was complemented based on the result of thin

layer chromatography (TLC). Next, organic solvent was evaporated using a vacuum system. A white product was obtained at the end of the evaporation step. The synthesis scheme belonging to HMA-$d_3$ is given in Figure 3.4.

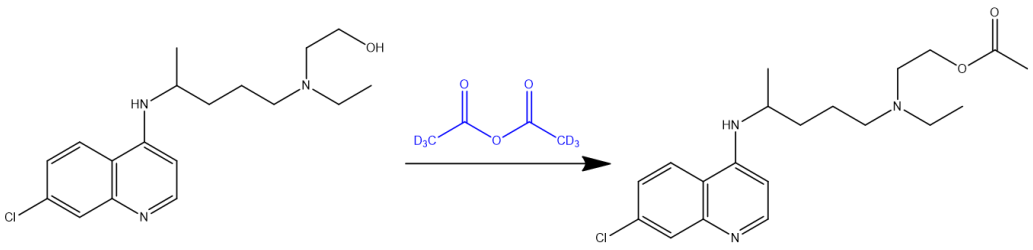


**Figure 3.4** Synthesis of HMA-$d_3$

## 3.5 Quantification of Capsaicin in Green Pepper, Wastewater and Human Saliva Samples by SB-FDF-LPME-ID$^4$-GC-MS System

Ethical approval was obtained from Yıldız Technical University Social Sciences and Humanities Research Ethics Committee on 21.09.2022 with meeting number 2022/9.

### 3.5.1 Reagents and chemicals

All reagents and chemicals consumed in this study are presented in Table 3.21. Approximately 1000 mg/kg capsaicin and capsaicin-*d3* standard solution were prepared in ethanol and these stock solutions were diluted by UPW to prepared working standard solutions. A water purification instrument with resistivity of 18.2 MΩ.cm at room temperature (Elga Flex 3 model, High Wycombe, United Kingdom) was used to supply UPW.

**Table 3.21** All reagents and chemicals used for the determination of capsaicin by SB-FDF-LPME-ID$^4$-GC-MS method

| Chemical Name | Purity | Supplier |
|---|---|---|
| **Capsaicin standard** | ≥95% | Sigma Aldrich (Darmstadt, Germany) |
| **Capsaicin-*d3*** | ≥99% deuterated form | Cayman Chemical (Ann Arbor, MI) |

**Table 3.21** All reagents and chemicals used for the determination of capsaicin by SB-FDF-LPME-ID$^4$-GC-MS method (continued)

| | | |
|---|---|---|
| **Acetic anhydride** | ≥98% | Merck (Darmstadt, Germany) |
| **Ethanol** | ≥99.9 % | IsoLab Laborgeräte GmbH (Eschau, Germany) |
| **Dichloromethane** | ≥99.8 % | |
| **1,2-dichloroethane** | ≥99.5% | Merck (Darmstadt, Germany) |
| **Chloroform** | 99.0 - 99.4 % | |
| **Acetonitrile** | ≥99.8% | |
| **Sodium chloride** | ≥99.0% | |
| **Potassium nitrate** | ≥99.0% | |
| **Potassium chloride** | ≥99.5% | |

### 3.5.2 Instrumentation

A Thermo Trace 1300 model gas chromatograph coupled to a Thermo ISQ QD model mass spectrometer was used to separate capsaicin derivative and its isotopic material. All instrumental conditions belonging to GC-MS system are given in Table 3.22. An HP5MS column with 60 m length, 250 µm inner diameter and 0.25 µm film thickness was placed into the oven part of the GC system. The scan range for the detector was fixed to 60-400 m/z. Quantifier ions for capsaicin derivative and its isotopically labelled material were selected as 137 and 140 m/z, respectively.

**Table 3.22** GC-MS conditions for the determination of capsaicin by SB-FDF-LPME-ID$^4$-GC-MS method

| Parameter | Value |
|---|---|
| **Mobile phase and its flow rate** | Helium, 2.0 mL/min |
| **Inlet temperature** | 290 ºC |
| **Injection mode** | Splitless |
| **Injection volume** | 1.0 µL |
| **Temperature program** | Initial temperature was 100 °C and then increased to 300 °C (40 °C/min) and held for 4.0 min |
| **Electron impact ionization energy** | 70 eV |
| **MS transfer line, source and quadrupole temperature** | 280, 230 and 150 °C |

### 3.5.3 SB-FDF-LPME Procedures

A 2.0 mL of pH 7.0 buffer solution was pipetted into 11.0 mL of analyte containing solution. Following that derivatization reaction was carried out by the addition of 30 µL of concentrated acetic anhydride solution. Mixing process was performed by vortex for 15 s to distribute the derivatizing agent. Next, the spraying system was filled with dichloromethane employed as extraction solvent in this study. The spraying system was attached to the centrifuge tube containing the derivatized analyte solution. Two sprays of dichloromethane were introduced to the centrifuge tube by the help of the spraying system. Another mixing process was done by ultrasonication for 30 s in an effort to promote the interaction between dichloromethane and analyte derivative. A centrifugation process for 2.0 min at 3461 *g* was implemented to separate the dichloromethane and aqueous phases. The bottom phase was withdrawn by a micropipette and placed into an insert vial for the GC-MS analysis.

### 3.5.4 Samples for accuracy and suitability tests

Green peppers (Banana (P1), Kıl (P2), Sivri (P3) and Samandağ (P4) peppers) were obtained from a local greengrocer in İstanbul, Türkiye. Whole samples were dried at 65 $^{o}$C for two weeks and grinded to make the samples into their powder form. Next, 0.40 g dried and powdered sample was placed into a plastic centrifuge tube and then completed to 10 g with ethanol for the extraction of capsaicin from pepper samples. The extraction process was accelerated by orbital shaker for 30 min. After the separation of pepper powders from the supernate by centrifugation for 10 min at 3461 *g*, the supernate was filtered using a syringe filter with 0.45 µm pore size. Further, P2, P3 and P4 samples were additionally diluted 248.2, 83.1 and 45.4-fold with ethanol because of their high concentration of capsaicin which did not fall into the LWR of the analyte in GC-MS system. A 0.20 g diluted supernate was spiked to about 15, 25, 75 and 100 µg/kg and diluted to 45 g with UPW. The developed SB-FDF-LPME-GC-MS method was performed on these spiked solutions.

Wastewater samples (W1 and W2) were supplied from Yıldız Technical University Environmental Engineering Department. All samples were removed from the solid or suspended particles by the filtration processes with quantitative filter paper and 0.45 µm syringe filter. Next, 2.0 g of wastewater sample was measured into a clean centrifuge tube and completed to 40 g with UPW after it was spiked to the different capsaicin concentrations in the range of 5.0 and 100 µg/kg. The developed microextraction method was then used to extract the analyte from wastewater samples.

Saliva samples (S1 and S2) were taken from two group members worked in our research laboratory. This study was verified by the ethics committee of Yıldız Technical University (approval number: 2022.03). Firstly, 0.50 g of saliva samples were individually spiked to about 15, 25, 50, 100 and 250 µg/kg. Next, 0.90 g of acetonitrile was pipetted into each solution to precipitate protein content and then diluted to 1.50 g with UPW. A centrifugation process for 10 min was done to obtain a clear supernate phase. In the final step, 1.0 g of saliva supernate was measured into a conical centrifuge tube and diluted to 40 g with UPW. The SB-FDF-LPME method was performed to extract the analyte from all diluted supernate solutions.

### 3.5.5 Calibration and sample mixtures for SB-FDF-LPME-ID$^4$-GC-MS method

In the SB-FDF-LPME-ID$^4$-GC-MS method, P1, S1 and W1 samples were spiked to two different concentration levels so as to assess precision and accuracy of the method. P2, P3 and P4 samples were not spiked, and their capsaicin concentrations were found by the developed SB-FDF-LPME-ID$^4$-GC-MS method. Sample solutions called as A in ID method were prepared as follows.

A 0.40 g of pepper sample in powder form was completed to 10 g with ethanol. The heterogeneous mixture was mixed by orbital shaker for 30 min and centrifuged for 10 min. After the filtration process by syringe filters with 0.45 μm pore size, only P2 and P3 pepper supernates were additionally diluted with ethanol. Hence, the total dilution for P1, P2, P3 and P4 samples were 25.2, 101.6, 31.7 and 16.5-fold. Following that 0.20 g of pepper supernate was diluted to 45 g with UPW and then analyzed by SB-FDF-LPME-ID$^4$-GC-MS method. Only P1 sample was separately spiked to 25 and 50 μg/kg in this stage for the control of accuracy and suitability for the developed method. In addition to pepper samples, 2.0 g of wastewater sample was also spiked to 25 and 50 μg/kg and completed to 40 g with UPW. The preparation of pepper, wastewater and water samples are summarized in Table 3.23, Table 3.24, Table 3.25, Table 3.26 and Table 3.27.

**Table 3.23** Preparation of pepper samples

| Sample | Powdered pepper, g | Total, g (Ethanol) | Matrix dilution |
|---|---|---|---|
| **P1** | 0.4003 | 10.0877 | 25.2 |
| **P2** | 0.4008 | 10.161 | 25.4 |
| **P3** | 0.3999 | 10.1676 | 25.4 |
| **P4** | 0.6051 | 10.0039 | 16.5 |

**Table 3.24** Second dilution process for P2 and P3 samples

| Sample | Pepper supernate, g | Total, g (Ethanol) | Total matrix dilution |
|---|---|---|---|
| **P2** | 2.502 | 10.022 | 101.6 |
| **P3** | 6.034 | 7.518 | 31.7 |

**Table 3.25** Preparation of A solutions for pepper and wastewater samples

| Sample | Capsaicin standard solution, g | Sample, g | Total (UPW) |
|---|---|---|---|
| **P1 Blank** | - | 0.2033 | 45.1542 |
| **P1 25 ppb** | 0.0581 | 0.2593 | 45.3257 |
| **P1 50 ppb** | 0.1172 | 0.2032 | 45.1140 |
| **P2** | - | 0.2024 | 45.2986 |
| **P3** | - | 0.212 | 45.0027 |
| **P4** | - | 0.2046 | 45.0333 |
| **W1 Blank** | - | 2.0103 | 40.1416 |
| **W1 25 ppb** | 0.0558 | 1.9998 | 40.0107 |
| **W1 50 ppb** | 0.1055 | 2.0238 | 40.7888 |

As for saliva samples, 0.50 g of sample was measured and then spiked to 0.10 and 2.3 mg/kg. Subsequently, 0.90 g of acetonitrile was added into the spiked samples for the precipitation of protein molecules. It was vortexed for 30 s after its dilution to 1.50 g with UPW. The slurry solution was then centrifuged for 10 min and 1.0 g of saliva supernate was taken into a clean centrifuge tube. The supernate was diluted

to 40 g with UPW that resulted in the final concentration of capsaicin as approximately 25 and 50 µg/kg.

**Table 3.26** Protein precipitation for saliva samples

| Spiked concentration, µg/kg | Saliva, g | Capsaicin standard solution, g | Acetonitrile, g | Total, g |
|---|---|---|---|---|
| **2272.50** | 0.5398 | 0.1025 | 0.868 | 1.510 |
| **987.02** | 0.5090 | 0.1008 | 0.917 | 1.527 |
| **Blank** | 0.5594 | - | 0.840 | 1.502 |

**Table 3.27** Dilution process for saliva samples after protein precipitation

| Capsaicin concentration, µg/kg | Supernate, g | Total, g (UPW) |
|---|---|---|
| **25 ppb** | 1.0406 | 40.1446 |
| **50 ppb** | 1.0011 | 42.0438 |
| **Blank** | 1.0089 | 40.4036 |

Calibration and sample mixtures were prepared using an analytical balance. Theoretical mixture preparation is presented in Table 3.28. A* and B solutions for low level (25 µg/kg) were fixed to 28.13 and 25.28 µg/kg, respectively. These solutions for high level (50 µg/kg) were 55.83 and 49.67 µg/kg, respectively.

**Table 3.28** Theoretical mass values used for the preparation of calibration and sample mixtures

| Mixture | A/A*, g | B, g |
|---|---|---|
| **AB** | 5.50 | 5.50 |
| **A*B-1** | 3.50 | 7.50 |

**Table 3.28** Theoretical mass values used for the preparation of calibration and sample mixtures (continued)

| | | |
|---|---|---|
| **A*B-2** | 5.50 | 5.50 |
| **A*B-3** | 7.50 | 3.50 |

Table 3.29 gives the experimental composition of all calibration and sample mixtures for low level.

**Table 3.29** Calibration and sample mixtures for 25 μg/kg of capsaicin in the spiked samples

| | **Mixture** | **A*/A, g** | **B, g** | **r** |
|---|---|---|---|---|
| **Calibration mixtures** | A*B-1-a | 3.5032 | 7.5037 | 0.4837 |
| | A*B-1-b | 3.5035 | 7.5226 | 0.4911 |
| | A*B-1-c | 3.5055 | 7.4990 | 0.4750 |
| | A*B-2-a | 5.5156 | 5.4869 | 0.9524 |
| | A*B-2-b | 5.5099 | 5.5194 | 0.9705 |
| | A*B-2-c | 5.5139 | 5.4996 | 0.9490 |
| | A*B-3-a | 7.4932 | 3.5131 | 1.5118 |
| | A*B-3-b | 7.5044 | 3.5442 | 1.5323 |
| | A*B-3-c | 7.4939 | 3.5154 | 1.5123 |
| **P1** | AB-1-a | 5.5069 | 5.5021 | 0.9487 |
| | AB-1-b | 5.5063 | 5.5019 | 0.9547 |
| | AB-1-c | 5.5175 | 5.4990 | 0.9259 |
| **W1** | AB-1-a | 5.5020 | 5.5268 | 0.9765 |
| | AB-1-b | 5.5122 | 5.5008 | 0.9974 |

**Table 3.29** Calibration and sample mixtures for 25 µg/kg of capsaicin in the spiked samples (continued)

| | | | | |
|---|---|---|---|---|
| **W1** | AB-1-c | 5.4974 | 5.5083 | 0.9948 |
| **S1** | AB-1-a | 5.5123 | 5.5089 | 0.8963 |
| | AB-1-b | 5.5050 | 5.5478 | 0.9285 |
| | AB-1-c | 5.5027 | 5.5151 | 0.9111 |

Table 3.30 presents the experimental mass values for all calibration and sample mixtures for high level.

**Table 3.30** Calibration and sample mixtures for 50 µg/kg of capsaicin in the spiked samples

| | **Mixture** | **A*/A, g** | **B, g** | **r** |
|---|---|---|---|---|
| **Calibration mixtures** | A*B-1-a | 3.5010 | 7.5109 | 0.4547 |
| | A*B-1-b | 3.5056 | 7.4972 | 0.4246 |
| | A*B-1-c | 3.5017 | 7.7566 | 0.4419 |
| | A*B-2-a | 5.5173 | 5.4960 | 0.9462 |
| | A*B-2-b | 5.5007 | 5.5073 | 0.9552 |
| | A*B-2-c | 5.5194 | 5.4855 | 0.9457 |
| | A*B-3-a | 7.5066 | 3.4984 | 1.5402 |
| | A*B-3-b | 7.5129 | 3.4981 | 1.5482 |
| | A*B-3-c | 7.5108 | 3.5029 | 1.4545 |
| **P1** | AB-1-a | 5.5011 | 5.5225 | 0.9441 |
| | AB-1-b | 5.5162 | 5.5087 | 0.9392 |
| | AB-1-c | 5.5245 | 5.4902 | 0.9623 |
| **W1** | AB-1-a | 5.5176 | 5.4925 | 0.9460 |

**Table 3.30** Calibration and sample mixtures for 50 µg/kg of capsaicin in the spiked samples (continued)

| | | | | |
|---|---|---|---|---|
| **W1** | AB-1-b | 5.5014 | 5.5000 | 0.9347 |
| | AB-1-c | 5.5076 | 5.5014 | 0.9642 |
| **S1** | AB-1-a | 5.5219 | 5.4958 | 0.9515 |
| | AB-1-b | 5.5208 | 5.4856 | 0.9342 |
| | AB-1-c | 5.4970 | 5.5066 | 0.9540 |
| **P2** | AB-1-a | 5.4974 | 5.5151 | 0.9466 |
| | AB-1-b | 5.5181 | 5.4944 | 0.9545 |
| | AB-1-c | 5.5063 | 5.5238 | 0.9356 |
| **P3** | AB-1-a | 5.5016 | 5.5111 | 0.9763 |
| | AB-1-b | 5.5151 | 5.4997 | 0.9626 |
| | AB-1-c | 5.5070 | 5.5010 | 0.9875 |
| **P4** | AB-1-a | 5.5026 | 5.5174 | 0.9838 |
| | AB-1-b | 5.5034 | 5.5074 | 0.9311 |
| | AB-1-c | 5.5192 | 5.5039 | 0.9768 |

# 4
# RESULTS AND DISCUSSION

## 4.1 Quantification of Chromium (III) and Chromium (VI) in Water, Soil and Grass Samples by HPLC-ICP-OES System

### 4.1.1 Optimization studies

This study was published in Environmental Monitoring and Assessment in 2022 [250].

#### 4.1.1.1 Nebulizer gas flow rate

Nebulizer gas flow rate was optimized to achieve high signal to noise ratio for chromium. For this purpose, 0.25 mg/kg chromium (VI) standard solution was directly introduced to ICP-OES system with the nebulizer gas flow rate values between 0.50 and 0.80 L/min. As can be seen in Figure 4.1, 0.60 L/min had the highest intensity than other flow rate values. Therefore, 0.60 L/min was chosen as the optimum one for the studied parameter.

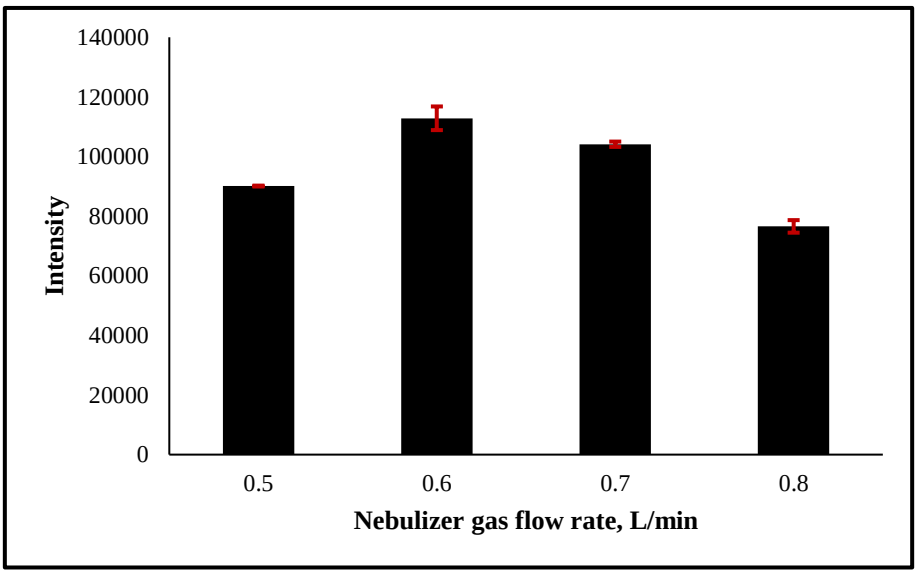


**Figure 4.1** Optimization of nebulizer gas flow rate (The constant parameters were 15 L/min plasma gas flow rate, 0.20 L/min auxiliary gas flow rate)

#### 4.1.1.2 Plasma gas flow rate

Argon gas was used as plasma gas in the developed hyphenated system. Its flow rate was tested in the range of 13 and 16 L/min. It is clear in Figure 4.2 that no significant difference between all flow rate values in terms of chromium intensities was. However, plasma instability was observed at 13 L/min and the optimum value was selected as 14 L/min.

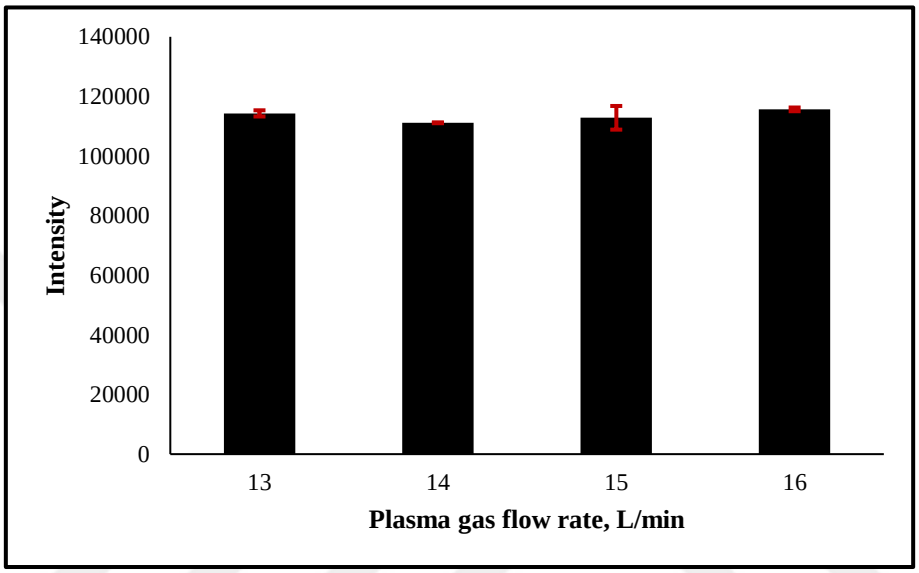


**Figure 4.2** Optimization of plasma gas flow rate (The constant parameters were 0.60 L/min nebulizer gas flow rate, 0.20 L/min auxiliary gas flow rate)

#### 4.1.1.3 Interconversion Experiments

It is well-defined in literature that the stability of chromium species is highly based on hydronium concentration, the presence of complexing and oxidizing/reducing agents. For example, chromium (VI) is easily reduced to chromium (III) in acidic medium but chromium (VI) is more stable against the redox reaction in basic medium [254]. For this reason, the stability of chromium species in the developed HPLC-ICP-OES system was checked by injecting the mixture of chromium (III) and chromium (VI) and their individual standard solutions at the same concentration found in the mixture. Mobile phase consisted of 30 mmol/L ammonium nitrate solution at pH 7.0. No significant change in the intensities of chromium species was observed. As a results, the mobile phase used in this experiment was used for the next experiments to maintain chromium species stable.

#### 4.1.1.4 Type of stationary phase

In this optimization, different stationary phases were tried to achieve better separation for the selected chromium species. For this purpose, anion exchange column, cation exchange column and octadecylsilane column were tested using the mixture consisting of 20.46 mg/kg chromium (III) and 5.85 mg/kg chromium (VI). Table 4.1 summarizes all testes stationary phases with their dimensions. Only anion exchange column gave two individual signals for chromium (III) and chromium (VI) but other two columns gave only one signal within 10 min which can be attributed to simultaneous elution of the chromium species or elution of one species. Hence, anion exchange column was selected to be optimum one for further experiments.

**Table 4.1** Columns studied in the optimization of column type

| Column | Stationary Phase | Dimensions |
|---|---|---|
| **Anion exchange** | Methacrylate based phase with quaternary ammonium functional groups | 150 mm × 4.6 i.d. × 7.0 µm particle size |
| **Cation exchange** | Benzene sulphonic acid groups | 250 mm × 4.6 i.d. × 10 µm particle size |
| **Octadecylsilane** | Octadecylsilane | 250 mm × 4.6 i.d. × 5.0 µm particle size |

#### 4.1.1.5 Concentration of ammonium nitrate in mobile phase

In this study, ammonium nitrate was used as the main constituent of mobile phase because there are several studies in literature that used this chemical as the mobile phase for the chromatographic separation of chromium species [255], [256], [257]. Here, ammonium nitrate concentration was optimized to achieve reasonable retention time and good resolution for the selected species. Four different concentration values between 10 and 40 mmol/L were tested and a good chromatographic separation was obtained when 30 mmol/L ammonium nitrate

solution was used as mobile phase (Figure 4.3). Retention times belonging to chromium (III) and chromium (VI) were found as 3.35 and 6.21 min, respectively. In addition, no separation observed for 10 and 20 mmol/L while plasma extinction was observed with 40 mmol/L ammonium nitrate solution.

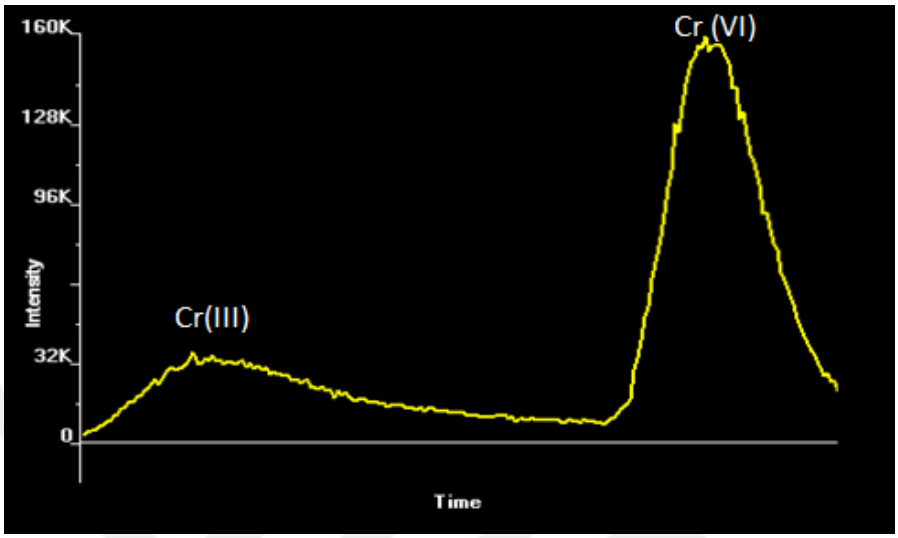


**Figure 4.3** A chromatogram obtained by the optimized HPLC-ICP-OES system with 30 mmol/L ammonium nitrate solution (pH 7.0)

#### 4.1.1.6 Concentration of methanol in mobile phase

The effect of organic solvent on the separation of chromium (III) and chromium (VI) was investigated by trying 0, 0.5, 1.0, 2.0 and 3.0% methanol in mobile phase. In addition, methanol was tried to improve the broad peak shape of chromium (III) that was obtained in the previous optimization (Figure 4.4). After testing all methanol concentration, peak resolution between chromium (III) and chromium (VI) was improved with the increase of methanol concentration (Figure 4.5). Peak intensities for both species were high for the highest methanol concentration. For this reason, the optimum methanol concentration for the mobile phase used for the next experiments was set at %3.0. The retention times attained from different mobile phase compositions are given in Table 4.2.

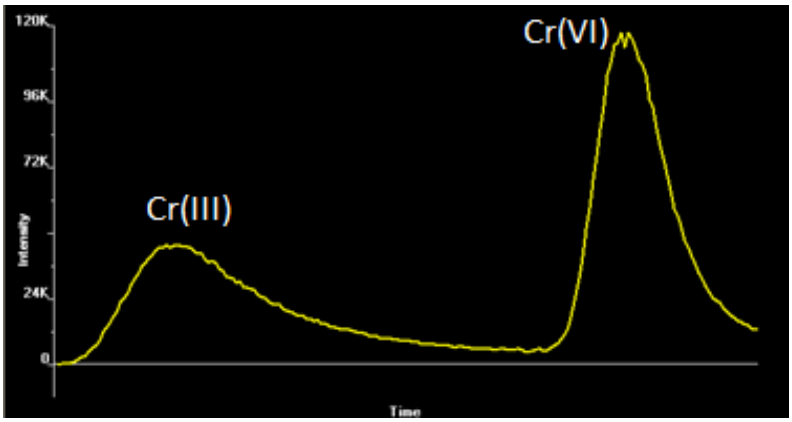


**Figure 4.4** A chromatogram obtained by the optimized HPLC-ICP-OES system with 30 mmol/L ammonium nitrate and 3.0% methanol solution (pH 7.0) as mobile phase

**Table 4.2** Retention times obtained in the optimization of methanol concentration

| **Methanol Concentration in Mobile Phase, %** | **Retention time for chromium (III)** | **Retention time for chromium (VI)** |
|---|---|---|
| **0** | 2.30 | 3.35 |
| **0.50** | 2.21 | 3.52 |
| **1.0** | 2.20 | 3.54 |
| **2.0** | 2.20 | 3.56 |
| **3.0** | 2.17 | 3.58 |

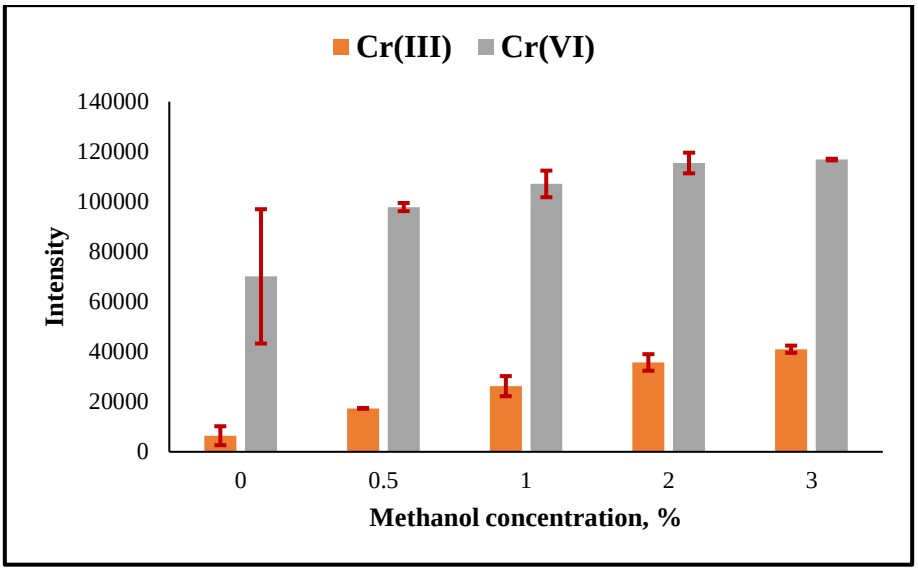


**Figure 4.5** Optimization of methanol concentration (Constant conditions: anion exchange column, 0.60 L/min nebulizer gas flow rate, 0.20 L/min auxiliary gas flow rate, 14 L/min plasma gas flow rate, 1.0 mL/min mobile phase flow rate, chromium (III) 9.04 mg/kg, chromium (VI) 6.27 mg/kg)

#### 4.1.1.7 pH value of mobile phase

Chromium (III) is found as $Cr(OH)^{2+}$ and $Cr(OH)_2^{+}$ in slightly acidic medium and $Cr(OH)_3$ precipitate in basic condition. Further, chromium (VI) is found as $HCrO_4^{-}$ or $Cr_2O_7^{2-}$ under slightly acidic solution and as $CrO_4^{2-}$ in basic solutions [254]. For this reason, pH value of mobile phase was one of the most important parameters that is needed to be optimized to achieve successful separation and sensitive analytical methods for the analytes. Next, pH value was investigated in the range of 3.0 and 8.0 by adding diluted nitric acid and ammonia solution to the mobile phase including 30 mmol/L ammonium nitrate and 3.0% methanol. It can be seen in Figure 4.6, conversion from chromium (VI) to chromium (III) was observed at low pH levels. Therefore, pH 6.0 was selected as the optimum pH level for the selected mobile phase due to the stability of chromium species, short retention times and proper resolution. Further, no signal was recorded for pH 3.0 and 8.0.

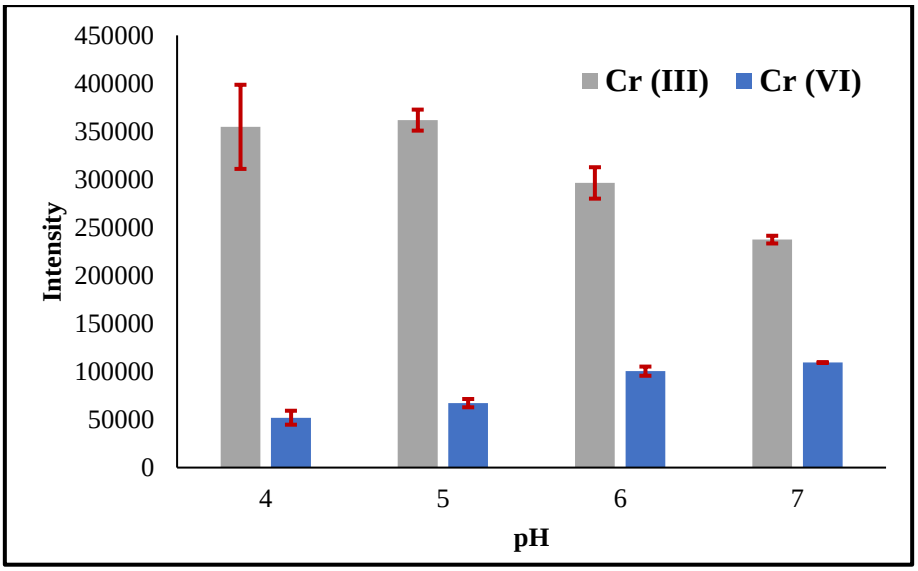


**Figure 4.6** Optimization of pH value for mobile phase (Constant conditions: anion exchange column, 0.60 L/min nebulizer gas flow rate, 0.20 L/min auxiliary gas flow rate, 14 L/min plasma gas flow rate, 1.0 mL/min mobile phase flow rate, chromium (III) 33.61 mg/kg, chromium (VI) 4.28 mg/kg)

#### 4.1.1.8 Flow rate of mobile phase

In this step, it was aimed to develop a separation and detection for the selected species by rapid and proper chromatographic system due to high argon gas consumption in ICP-OES system. Three different flow rates (0.75, 1.0 and 1.1 mL/min) were tried to obtain an efficient separation and proper resolution for the selected analytes. As shown in Figure 4.7, sharp and narrow peaks were recorded for 1.0 mL/min flow rate. In addition, 1.1 mL/min was not examined owing to the presence of plasma instability and 0.75 mL/min led to increase the analysis period. For this reason, 1.0 mL/min was chosen as the optimum flow rate in terms of good resolution, sharp peak shapes, and lower analysis period than 0.75 mL/min. Table 4.3 presents the retention times belonging to chromium (III) and chromium (VI) obtained in the mobile phase flow rate optimization.

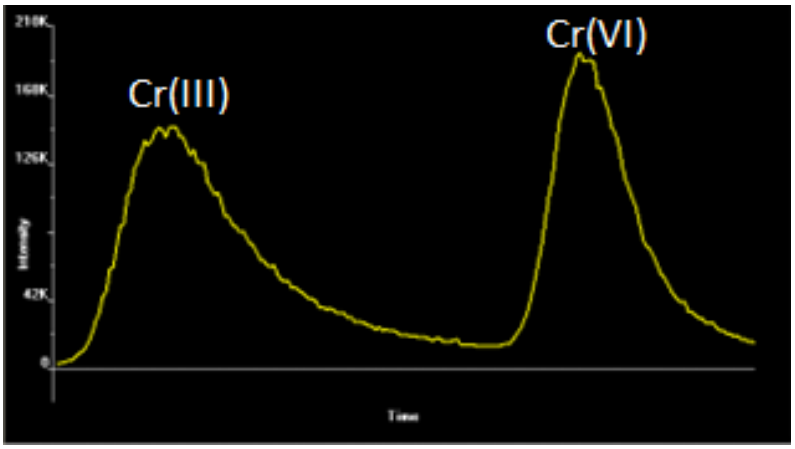


**Figure 4.7** A chromatogram obtained by the optimized HPLC-ICP-OES system with 1.0 mL/min mobile phase flow rate

**Table 4.3** Retention times obtained in the optimization of mobile phase flow rate

| Mobile phase flow rate, mL/min | Retention time for chromium (III) | Retention time for chromium (VI) |
|---|---|---|
| **0.75** | 3.31 | 5.50 |
| **1.0** | 2.35 | 4.05 |

#### 4.1.1.9 Sample injection volume

Sample injection volume was also optimized to increase the peak intensities of chromium species in the developed HPLC-ICP-OES system. The optimum injection volume was determined by testing different injection volumes including 20, 35 and 50 µL. As can be seen in Figure 4.8 that higher volumes gave higher peak intensities and no tailing for each analyte signal was observed. For this reason, the optimum sample injection volume selected for the developed hyphenated system was 50 µL.

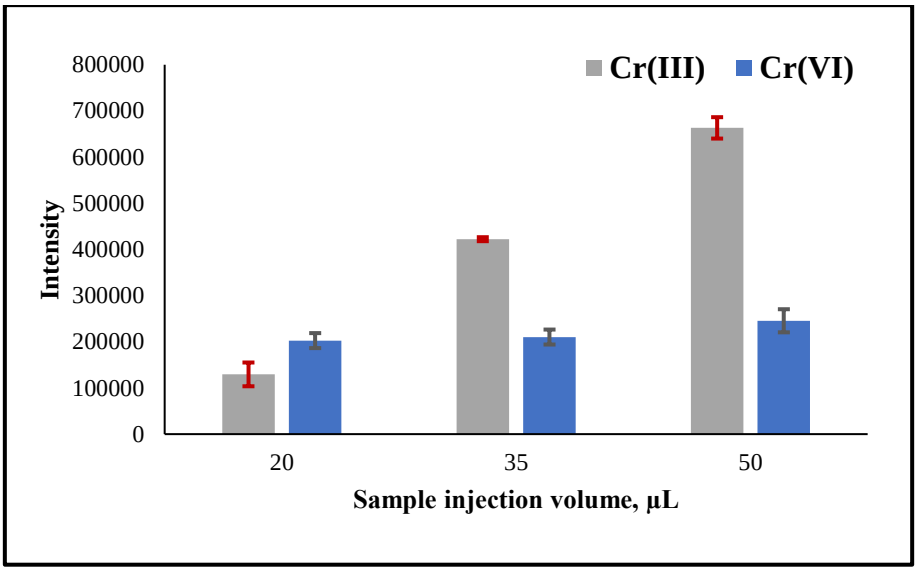


**Figure 4.8** Optimization of injection volume (Constant conditions: anion exchange column, 0.60 L/min nebulizer gas flow rate, 0.20 L/min auxiliary gas flow rate, 14 L/min plasma gas flow rate, 1.0 mL/min mobile phase flow rate, chromium (III) 20.31 mg/kg, chromium (VI) 10.04 mg/kg)

### 4.1.2 System analytical performance for HPLC-ICP-OES method

Under the optimum HPLC-ICP-OES conditions, the developed method was validated with a series of mixed standard solutions in terms of linear working ranges, LOD, LOQ and $R^2$ (Table 4.4). Linearity was achieved between 0.74 and 7.36 mg/kg for chromium (III) (Figure 4.9) and 0.13 and 2.32 mg/kg for chromium (VI) (Figure 4.10). LOD/LOQ values were 0.27/0.90 mg/kg for chromium (III) and 0.05/0.18 mg/kg for chromium (VI). Further, $R^2$ values were determined as 0.9993 and 0.9991 for chromium (III) and chromium (VI), respectively. The method precision was evaluated by %RSD values and these values were lower than 10% for each analyte.

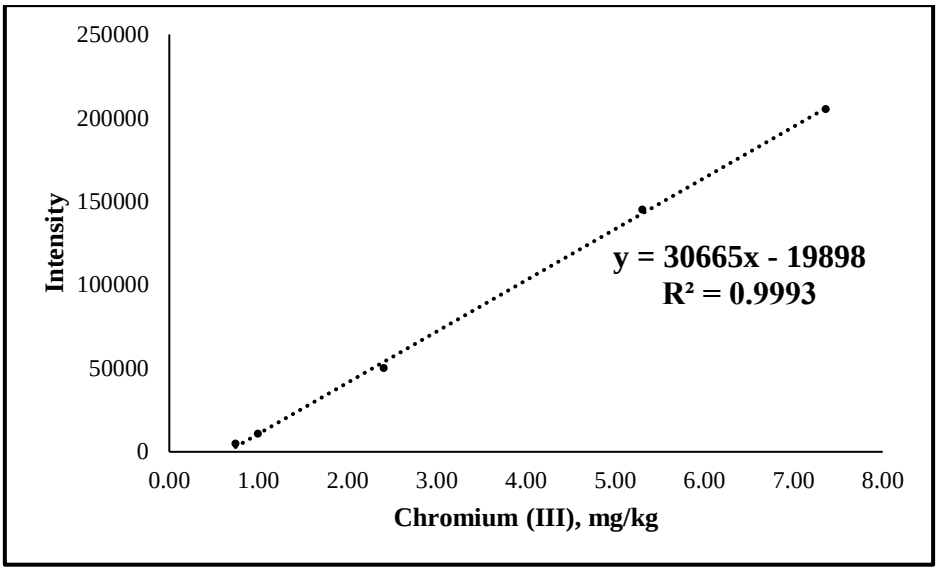


**Figure 4.9** Calibration plot for the determination of chromium (III) by the developed HPLC-ICP-OES system

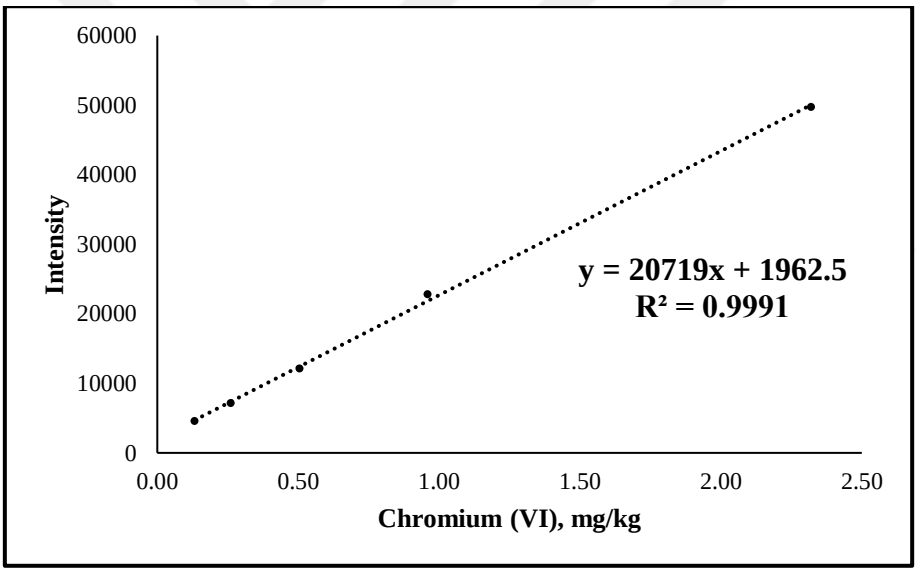


**Figure 4.10** Calibration plot for the determination of chromium (VI) by the developed HPLC-ICP-OES system

**Table 4.4** Analytical performance of the presented HPLC-ICP-OES method

| Parameter | Chromium (III) | Chromium (VI) |
|---|---|---|
| **LOD, mg/kg** | 0.27 | 0.05 |
| **LOQ, mg/kg** | 0.90 | 0.18 |

**Table 4.4** Analytical performance of the presented HPLC-ICP-OES method (continued)

| | | |
|---|---|---|
| **LWR, mg/kg** | 0.74-7.36 | 0.13-2.32 |
| **$R^2$** | 0.9993 | 0.9991 |

### 4.1.3 Accuracy and suitability tests

The presented method was implemented to the spiked water, soil and grass samples in order to test the method suitability and accuracy. Firstly, all sample solutions were prepared according to the procedure detailed in Section 3.1.4 and then analyzed by the established HPLC-ICP-OES system. However, there was no detectable chromium (III) or chromium (VI) signal for all samples. Next, matrix matching calibration strategy was performed to equalize the matrix effect for all calibration and sample solutions. For this purpose, a certain amount of sample solution was spiked with proper standard solution of analyte and calibration plots were drawn after measuring the solutions containing a certain amount of sample solution and increasing concentration of analytes. Percent recoveries with their standard deviation values are presented in Table 4.5. The results showed that the developed hyphenated system was applicable to the studied environmental samples and good accuracy and suitability were achieved due to high percent recoveries close to 100%.

**Table 4.5** Percent recoveries for water, soil, and grass samples

| Analyte | Chromium (III) | | | Chromium (VI) | | |
|---|---|---|---|---|---|---|
| **Sample** | **Theoretical concentration, mg/kg** | **Experimental concentration, mg/kg** | **%Recovery ±S.D.** | **Theoretical concentration, mg/kg** | **Experimental concentration, mg/kg** | **%Recovery ±S.D.** |
| **Water** | 0.87 | 0.77 | 88.9 ± 3.6 | 0.84 | 0.86 | 102.0 ± 1.8 |
| | 3.92 | 3.60 | 91.7 ± 3.9 | 4.04 | 4.15 | 102.6 ± 2.2 |
| **Soil** | 0.77 | 0.68 | 88.2 ± 4.1 | 0.80 | 0.79 | 99.3 ± 0.5 |
| | 1.02 | 1.00 | 97.5 ± 21.9 | 1.06 | 1.03 | 97.9 ± 1.3 |
| **Grass** | 1.01 | 1.00 | 98.9 ± 5.3 | 0.98 | 1.00 | 102.0 ± 3.0 |
| | 1.20 | 1.25 | 104.1 ± 2.3 | 1.20 | 1.19 | 99.1 ± 0.2 |
| | 2.02 | 2.04 | 101.0 ± 3.1 | 2.03 | 2.01 | 99.1 ± 1.8 |

*Uncertainties (±): Standard deviation for n = 2.*

### 4.1.4 Comparison with other studies in literature

There are some studies regarding the determination of chromium species by hyphenated systems. One study conducted by Byrdy et al. [258] used high-performance liquid chromatography-inductively coupled plasma-atomic emission spectrometry (HPLC-ICP-AES) system to separate chromium (III) or chromium (VI). An anion exchange column was used as stationary phase while ammonium hydroxide (100 mM) and ammonium sulfate (250 mM) solution fixed to pH 9.2 was performed as mobile phase. The main advantage of our developed HPLC-ICP-OES system over the HPLC-ICP-AES is LOD and LOQ values. The developed HPLC-ICP-OES system gave 3.7 and 40 folds lower LOD values than HPLC-ICP-AES system.

Some studies used complex mobile phase systems which require additional chemicals and result in expensive analytical methods. For example, Prokisch et. al. [259] developed ion chromatography-inductively coupled plasma-atomic emission spectrometry (IC-ICP-AES) system and carried out a chromatographic system with potassium hydrogen phthalate, ethylene glycol and 2-propanol as mobile phase and a Polispher AN anion exchanger as stationary phase. However, ammonium nitrate and methanol were enough to separate the selected chromium species in our study. In addition, similar LOD values were recorded for each system as 0.25 and 0.27 mg/kg for chromium (III) and (VI) in IC-ICP-AES and 0.27 and 0.05 mg/kg in HPLC-ICP-OES system, respectively.

In literature, there are also chromium speciation studies conducted by complexing agents and extraction methods. Tang et. al. established an analytical method for chromium speciation using cloud point extraction-high-performance liquid chromatography (CPE-HPLC). Diethyldithiocarbamate was used in this study as complexing agent to convert chromium ions into their complexes. Trace LOD values were recorded for chromium (III) and (VI) as 3.4 and 5.2 μg/L, respectively. It can be concluded that this extraction method can be used prior to our developed HPLC-ICP-OES method in order to reach lower LOD values than CPE-HPLC method [260].

Another method conducted by Ali and Aboul-Eneinused [261] high-performance liquid chromatography-ultraviolet detector (HPLC-UV) for the separation and

detection of chromium species. Reverse phase mode was used in this study and Econosil C18 column with 10 mM ammonium acetate buffer (pH 6.0)–acetonitrile (10:90, v/v) were used as stationary and mobile phases, respectively. Under the optimum conditions, LOD values for chromium (III) and (VI) were found as 0.40 and 1.0 mg/L, respectively. Based on the LOD values, the developed HPLC-ICP-OES method produced lower LOD values than HPLC-UV method. Hence, HPLC-ICP-OES method is more sensitive than the proposed HPLC-UV method for chromium speciation.

## 4.2 Quantification of Cobalamin in Vitamin Drug Tablets by HPLC-FAAS System

### 4.2.1 Optimization studies

This study was published in Journal of Pharmaceutical and Biomedical Analysis in 2022 [251].

Univariate optimization studies were conducted to achieve experimental conditions for high signal to noise ratio and sharp signals for the determination of cobalamin. Flow rate of mobile phase, flow rate of nebulizer gas, T-SQT height from burner head, sample injection volume, pH of mobile phase, concentration of mobile phase components were studied to find their optimum values. Three measurement replicates were done for all parameters to calculate mean and standard deviation values. Optimum conditions were chosen according to highest absorbance, standard deviation and resolution of free cobalt and cobalamin.

Dry air was used as nebulizer gas instead of argon gas because there was no cobalamin signal when argon was used to nebulize the eluate to the flame region. Argon gas may lead to the temperature decrease of flame that resulted in insufficient decomposition of cobalamin in the flame region and atomization of cobalt.

#### 4.2.1.1 Flow rate of mobile phase

Acetic acid/sodium acetate buffer system that was found as the optimum mobile phase system in our previous study [167] was used throughout the study. Its flow rate was firstly optimized in this study. The effect of flow rate was examined by testing 1.25, 1.50, 1.75 and 2.0 mL/min. According to Figure 4.11, no significant

change in absorbance values was recorded, but 1.25 and 1.50 mL/min had longer retention times than 1.75 and 2.0 mL/min. In addition, background signal was not proper for 2.0 mL/min flow rate value. For this reason, 1.75 mL/min was selected as the optimum value for the next studies. A chromatogram belonging to the chromatographic separation of cobalt and cobalamin presents in Figure 4.12.

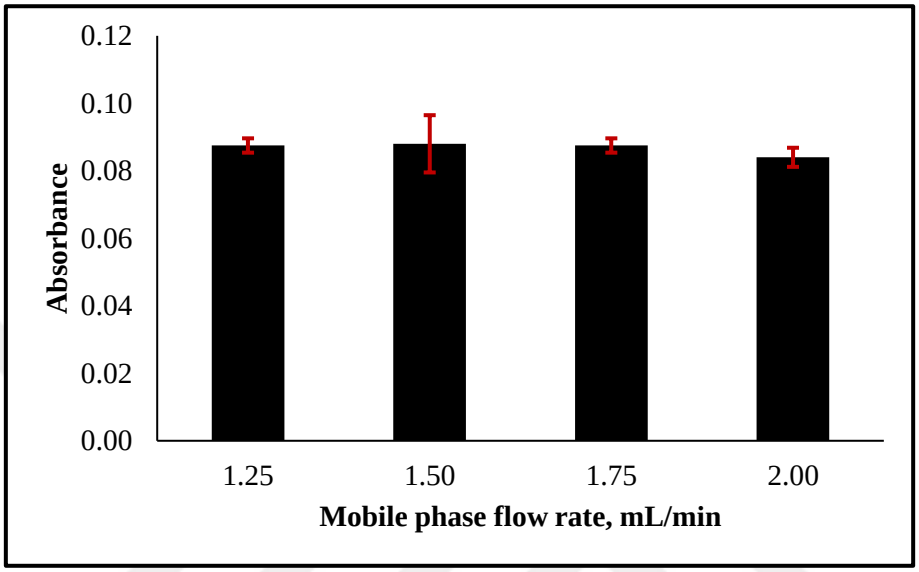


**Figure 4.11** A plot of mobile phase flow rate against absorbance values (n= 3 error bars)

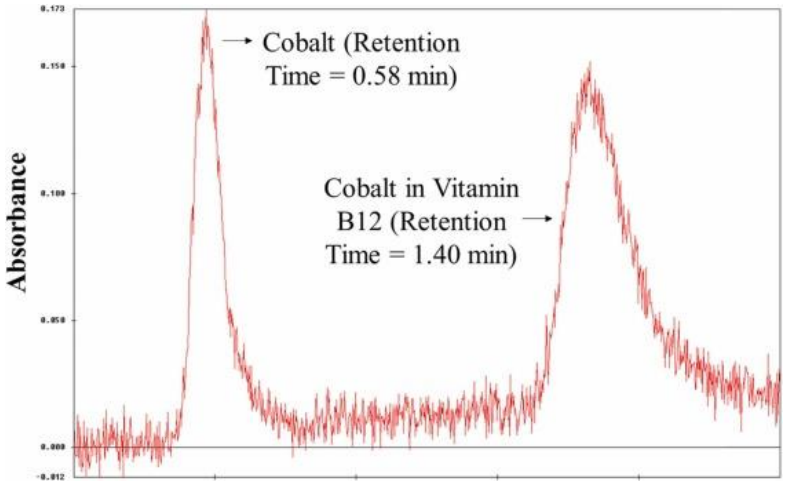


**Figure 4.12** Chromatographic separation of cobalt and cobalamin at the flow rate of 1.75 mL/min [251]

#### 4.2.1.2 Flow rate of nebulizer gas

The flow rate of nebulizer gas was an important parameter for HPLC-FAAS system because low flow rates may lead to low nebulization efficiency and inadequate

transfer of the eluate to the flame region and high flow rates may affect the atomization of the analyte. Therefore, three different flow rate values (1.9, 4.8 and 10.7 L/min) were tested to observe their nebulization efficiencies. Based on the absorbance values shown in Figure 4.13, high absorbance values with high precise results were recorded for 4.8 L/min. Hence, 4.8 L/min was determined as the optimum value for nebulizer gas flow rate.

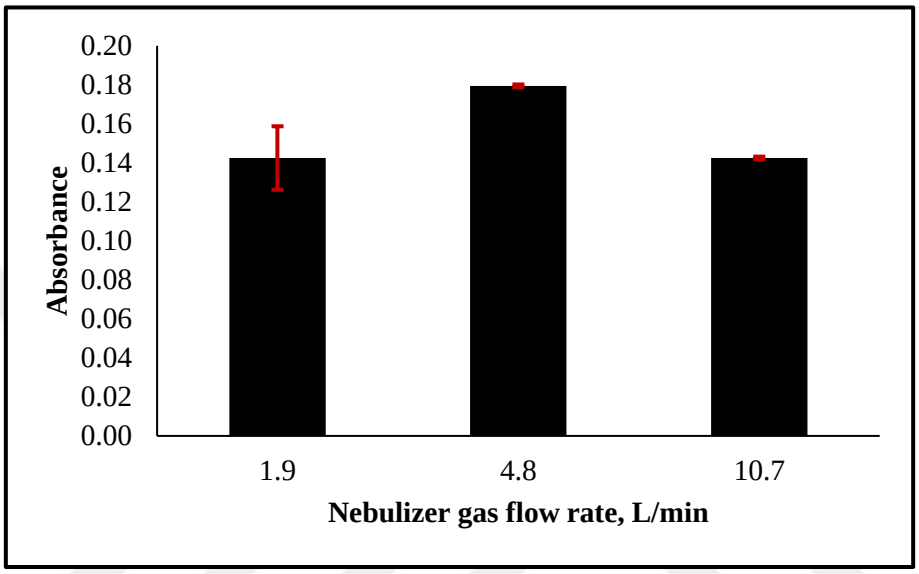


**Figure 4.13** A plot of nebulizer gas flow rate against absorbance values (n= 3 error bars)

#### 4.2.1.3 T-SQT height from burner head

T-SQT height from burner head affects the entrance of the eluate to the atomization region and interaction of analyte and hollow cathode lamp light. Therefore, T-SQT height from burner head was individually adjusted to 0.0, 1.0 and 2.0 mm and tested to monitor its effects on absorbance values. As shown in Figure 4.14, 0.0 mm gave the higher absorbance than 1.0 and 2.0 mm, and the lowest standard deviation value was obtained for 0.0 mm. Hence, further experiments were carried out with 0.0 mm T-SQT height from burner head.

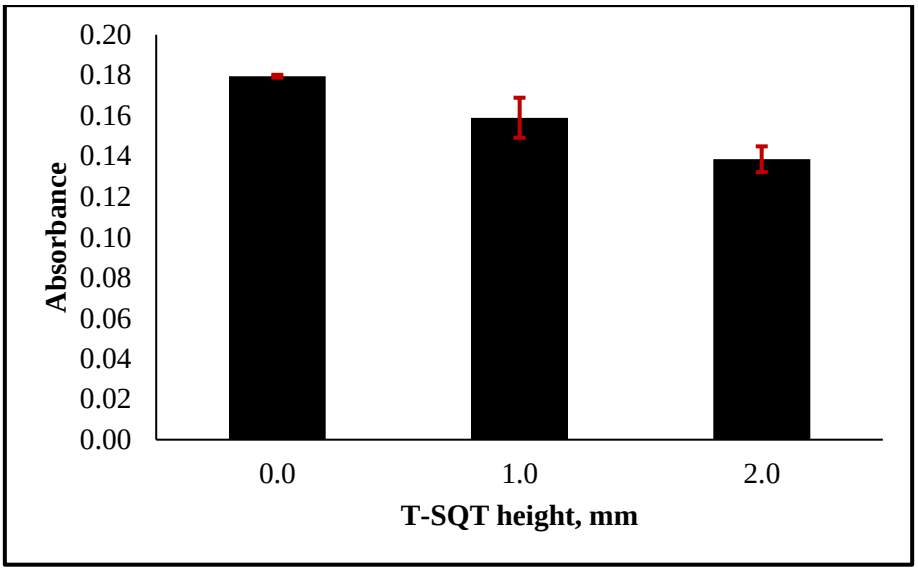


**Figure 4.14** A plot of T-SQT height from burner head against absorbance values (n= 3 error bars)

#### 4.2.1.4 Sample injection volume

Injection volume optimization was done to increase absorbance values for the analyte. For this purpose, 50, 75 and 100 µL sample solution were individually sent to the HPLC-FAAS system. Higher volumes than 100 µL was not tested due to the maximum loop size. According to the Figure 4.15, highest absorbance value was obtained for 100 µL but there was no significant difference between the absorbance values of 75 and 100 µL and increase in peak width was observed for 100 µL. For this reason, 75 µL was chosen to be optimum value for injection volume.

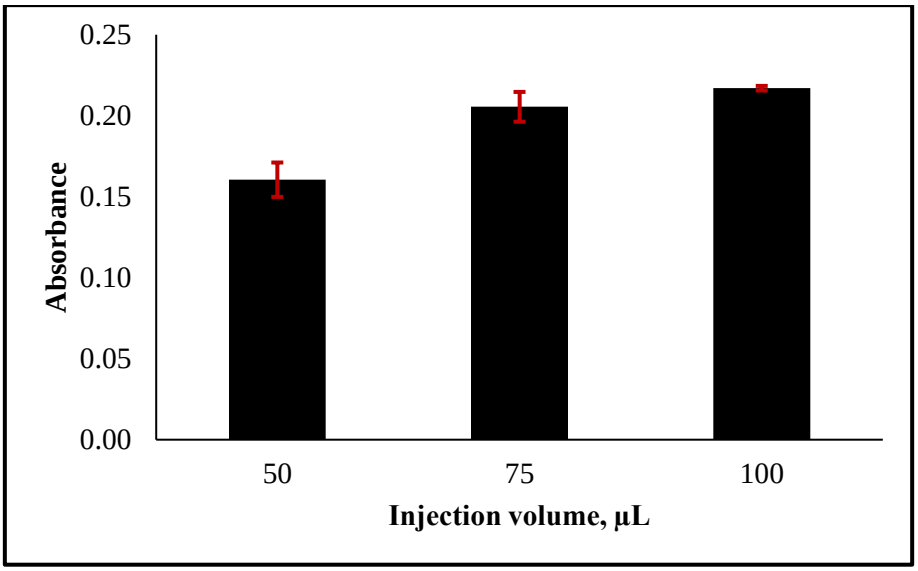


**Figure 4.15** A plot of injection volume against absorbance values (n= 3 error bars)

#### 4.2.1.5 pH of mobile phase

pH value of the mobile phase influences the separation of analytes on analytical column. For this purpose, acetic acid/sodium acetate buffer solutions were prepared by mixing different amounts of acetic acid (Ac) and sodium acetate (NaAc) (17 mmol/L Ac/1.7 mmol/L NaAc (pH 3.67), 1.75 mmol/L Ac/1.75 mmol/L NaAc (pH=4.59), 0.17 mmol/L Ac/1.7 mmol/L NaAc (pH=5.25)). As can be seen in Figure 4.16, absorbance values increased with the increase of acetic acid concentration. In addition, good resolution between free cobalt and cobalt in cobalamin was achieved via mobile phase with pH 3.67. For this reason, pH 3.67 was selected as the optimum pH value for mobile phase.

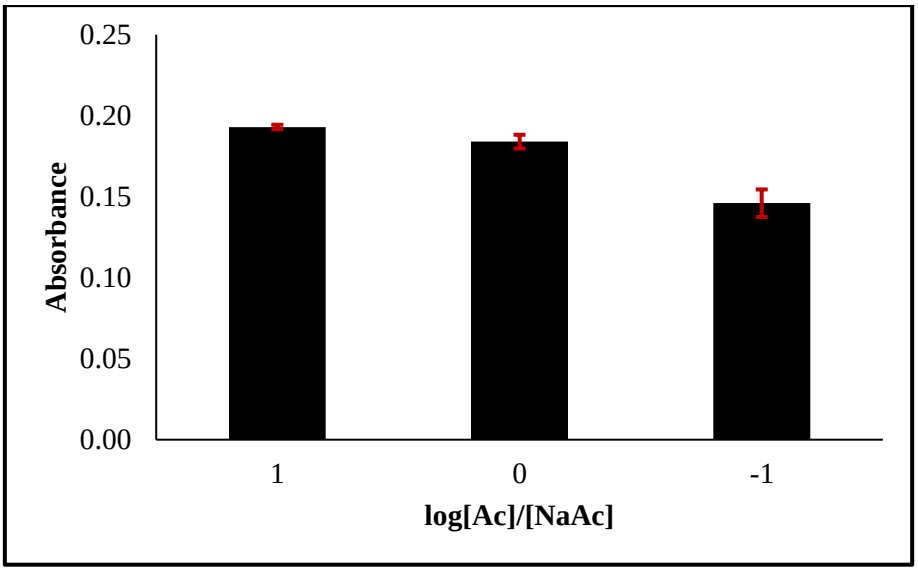


**Figure 4.16** A plot of log[Ac]/[NaAc] against absorbance values (n= 3 error bars)

#### 4.2.1.6 Concentration of mobile phase components

After optimizing pH value of the mobile phase, concentration of mobile phase components was optimized to fix the ionic strength of the mobile phase for the separation of free cobalt and cobalamin. Three different mobile phase system (17 mmol/L Ac/1.7 mmol/L NaAc, 34 mmol/L Ac/3.4 mmol/L NaAc and 51 mmol/L Ac/5.1 mmol/L NaAc) with pH 3.7 were tried to obtain sharp signals and high absorbance values with high peak resolution. However, there was no important change in absorbance values or peak shape, given in Figure 4.17. For this reason, 34 mmol/L Ac/3.4 mmol/L NaAc was determined as the optimum concentration of mobile phase components due to the higher buffer capacity than 17 mmol/L Ac/1.7 mmol/L NaAc. In addition, 51 mmol/L Ac/5.1 mmol/L NaAc was not chosen because of high concentration of mobile phase components that may damage analytical column and the developed system.

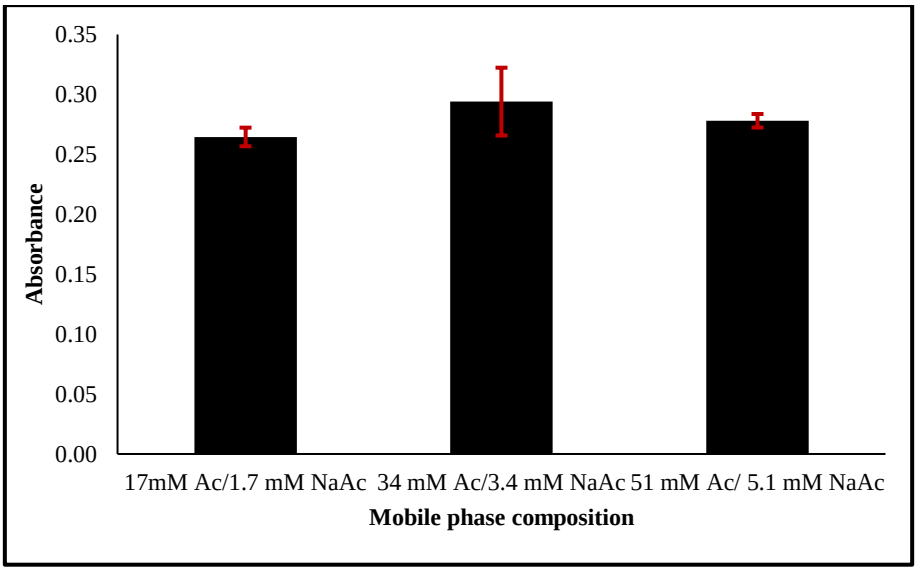


**Figure 4.17** A plot of mobile phase concentration against absorbance values (n= 3 error bars)

### 4.2.2 System analytical performance for HPLC-FAAS method

System analytical performance of the presented HPLC-FAAS system was evaluated based on LOD, LOQ, LWR and %RSD. Ten different standard solution in the range of 4.7 and 231.6 mg/kg cobalamin as cobalt were prepared and sent to the developed system. LWR was achieved between 4.7 and 92 mg/kg cobalamin as cobalt. LOD and LOQ were attained by the formulas as LOD: 3SS/m and LOQ:10SS/m, where SS: standard deviation belonging to the repetitive measurement of the lowest concentration in the calibration plot and m: slope acquired by the related calibration plot. LOD and LOQ values calculated according to these formulas were 1.6 and 5.3 mg/kg cobalamin as cobalt, respectively. %RSD value for the lowest concentration in the calibration plot was recorded as %5.3 that proved the precision of the developed system. Table 4.6 presents system analytical performance of the developed system and other studies found in literature for the determination of cobalamin. In addition, the calibration plot belonging to the cobalt in cobalamin obtained from HPLC-FAAS system can be seen in Figure 4.18.

**Table 4.6** Analytical performance of the developed HPLC-FAAS method

| Parameter | Cobalamin as cobalt |
|---|---|
| **LOD, mg/kg** | 1.6 mg/kg |

**Table 4.6** Analytical performance of the developed HPLC-FAAS method (continued)

| | |
|---|---|
| **LOQ, mg/kg** | 5.3 mg/kg |
| **LWR, mg/kg** | 4.7-92 mg/kg |
| **$R^2$** | 0.9989 |

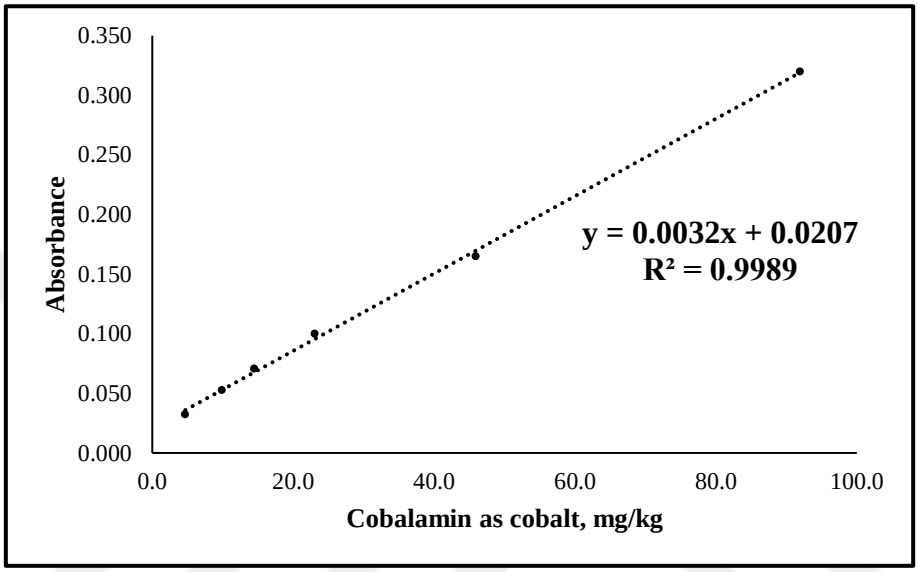


**Figure 4.18** Calibration plot for the determination of cobalamin by HPLC-FAAS system

### 4.2.3 Accuracy and suitability tests

Two different brands of vitamin drugs were prepared according to the procedure given in Section 3.2.3. Standard addition calibration strategy was performed to find the concentration of cobalamin in vitamin drug tablets. Calibration plots belonging to standard addition calibration plots for Brand A and Brand B samples are given in Figure 4.19. According to the calibration plots, cobalamin concentration was figured out as $1.53 \pm 0.03$ and $1.75 \pm 0.05$ mg/tablet for Brand A and B, respectively.

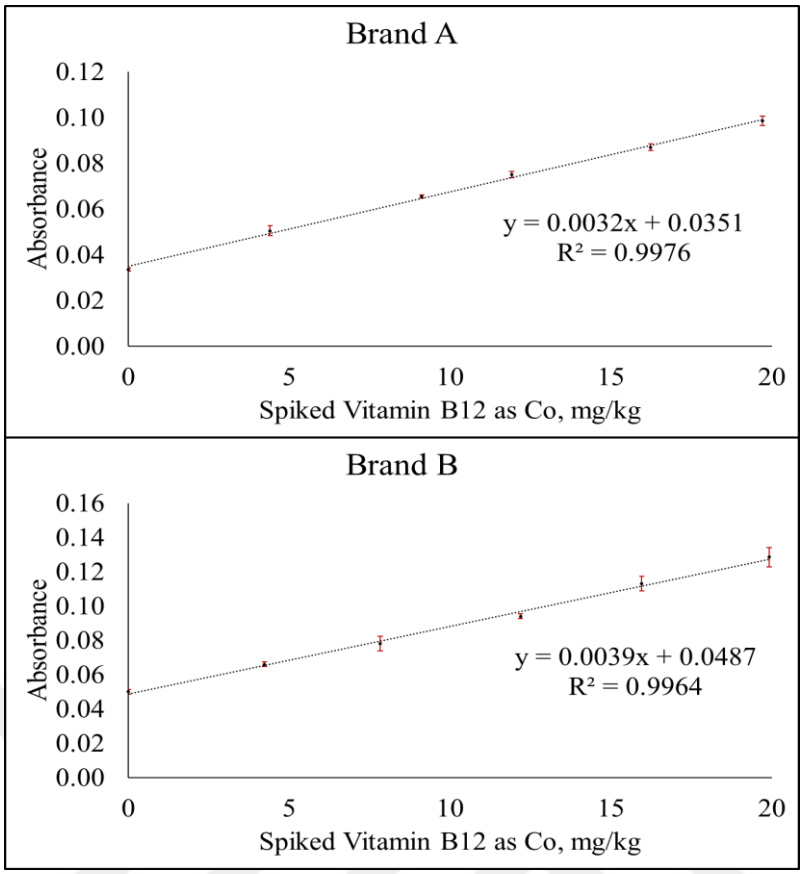


**Figure 4.19** Standard addition calibration plots for vitamin drugs

Accuracy and suitability of the developed HPLC-FAAS system were assessed by spiking drug samples with different concentration of cobalamin. Matrix matching calibration strategy was performed to depress or eliminate the interference effects of sample matrices. For this purpose, 0.40 g vitamin sample solution was taken into a clean vial and spiked with proper concentration of analyte. All solutions were diluted to 0.50 g with UPW. Percent recoveries (Table 4.7) were calculated using the calibration plot obtained by the spiked vitamin sample solutions after blank corrections. High recovery results between 92.9 and 112.4% were attained and these results demonstrated accuracy and suitability of the proposed HPLC-FAAS system.

**Table 4.7** Percent recoveries calculated for the spiked drug samples

| Vitamin Tablet | Spiked concentration, mg/kg (as Co) | %Recovery | ±S.D. |
|---|---|---|---|
| **Brand A** | 4.4 | 112.4 | 4.7 |

**Table 4.7** Percent recoveries calculated for the spiked drug samples (continued)

| | | | |
|---|---|---|---|
| **Brand A** | 9.1 | 95.4 | 1.0 |
| | 11.9 | 92.9 | 1.8 |
| **Brand B** | 4.2 | 95.2 | 2.0 |
| | 7.8 | 100.5 | 5.5 |
| | 12.2 | 106.9 | 1.6 |

### 4.2.4 Comparison with other studies in literature

The developed HPLC-FAAS system is an alternative analytical method to other traditional methods. For example, high performance liquid chromatography – inductively coupled plasma – optical emission spectrometry (HPLC-ICP-OES) method was proposed in 2021 [167] for the determination of cobalamin by means of its cobalt content. LOD, LOQ and LWR values for cobalamin as cobalt were 0.07, 0.24 and 0.27–40.2 mg/kg, respectively.

Liquid chromatography – inductively coupled plasma mass spectrometry (LC-ICP-MS) for the determination of cobalamin was developed by Raju et. al. [262] in 2013. In this study, mobile phase and stationary phase was 20 mmol/L ethylenediaminetetraacetic acid (EDTA) in 25:75 methanol–water mixture and an Atlantis T3 C18 column, respectively. LOD value and LWR for cobalamin as cobalt was 0.04 ng/g and 0.1-100 ng/g, respectively. Although LC-ICP-MS method had lower LOD value than HPLC-FAAS system, operational cost could be high due to high argon consumption for LC-ICP-MS system.

Viñas et al. [263] presented liquid chromatography-flame atomic absorption spectrophotometry (LC-FAAS) for the determination of cobalamin in pharmaceuticals. In this study, LC and FAAS systems were connected by the help of a T-piece placed between the outlet of the column and FAAS nebulizer. LOD values in LC-FAAS system (4.2 mg/L as Co) was not lower than that for the developed HPLC-FAAS method with novel nebulizer interface. It can be concluded that the novel interface boosted the sensitivity of HPLC-FAAS system for the determination of cobalamin.

## 4.3 Quantification of Chloroquine in Human Urine, Saliva and Serum Samples by SB-FDF-LPME-ID$^4$-GC-MS System

This study was published in Journal of Chromatography A in 2021 [252].

### 4.3.1 Characterization of chloroquine acetamide and its isotopic material

Chloroquine phosphate (200.0 mg/kg) was derivatized and preconcentrated under the optimum SB-FDF-LPME-GC-MS method. The GC-MS chromatogram and MS spectrum are given in Figure 4.20. Retention times belonging to chloroquine and its derivative were 4.63 and 6.22 min, respectively. According to these results, CA had a chromatographic signal having different retention time than chloroquine and it had five m/z values highlighted in Figure 4.20.

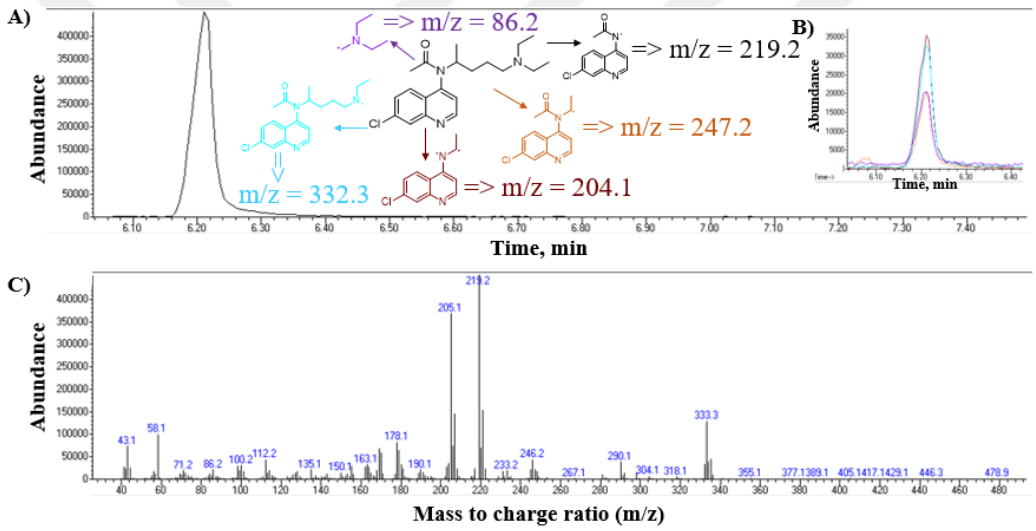


**Figure 4.20** GC-MS chromatograms (A and B) and mass spectrum (C) for CA derivative (black (219.2), orange (247.2), red (204.1), blue (332.3) and purple (86.2))

The synthesized CA-*d3* was also characterized by GC-MS system. It was dissolved in methanol and then sent to the GC-MS system. The GC-MS chromatogram and MS spectrum are given in Figure 4.21. Based on these results, the expected m/z values (222.2, 335.3 and 292.1) belonging to the fragments containing the acetamide-*d3* group were recorded.

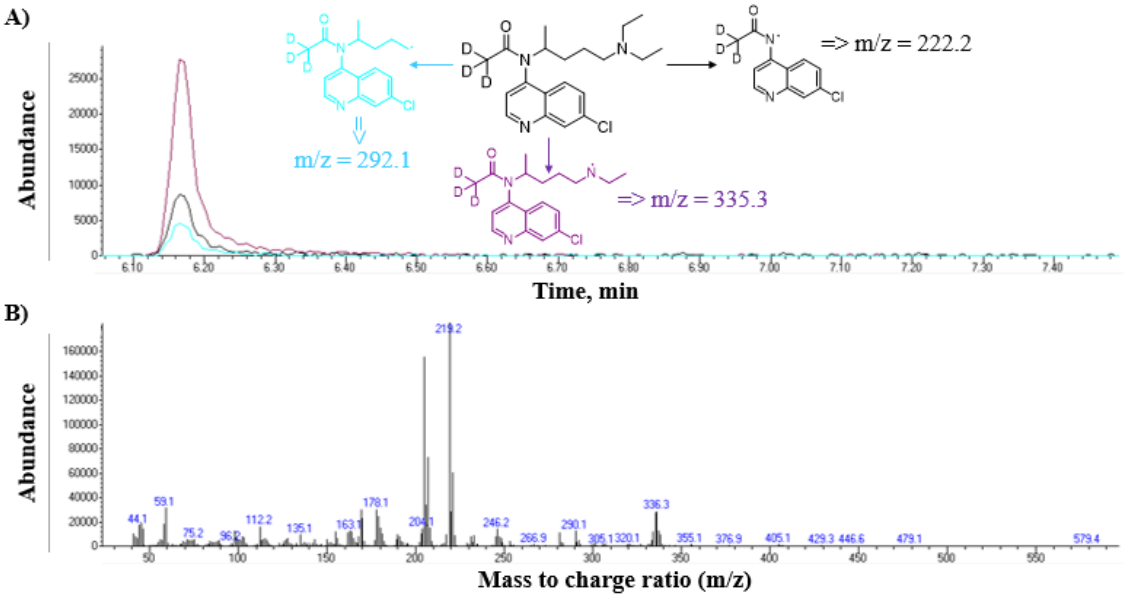


**Figure 4.21** GC-MS chromatogram (A) and mass spectrum (B) for CA-*d3* (black (222.2), purple (335.3) blue (292.1))

The m/z values for the quantification of chloroquine and CA-*d3* were 219 and 336, respectively. It should be noted that 219 m/z was found in the MS spectrum of CA-*d3* and its signal was subtracted from the signals obtained by CA-*d3* in the isotope dilution method.

### 4.3.2 Optimization Studies

#### 4.3.2.1 Type of extraction solvent

In LPME methods, extraction solvent type is an important parameter to enrich the interest of analyte(s) from aqueous sample solutions [264]. Dichloromethane, chloroform, 1,2-dichloroethane and their binary combinations were tested for the extraction of the analyte derivative. There was no signal for chloroform and dichloromethane-chloroform. Figure 4.22 shows the peak area values for all extraction solvents. The highest analytical signals were recorded for 1,2-dichloroethane as can be seen in Figure 4.22.

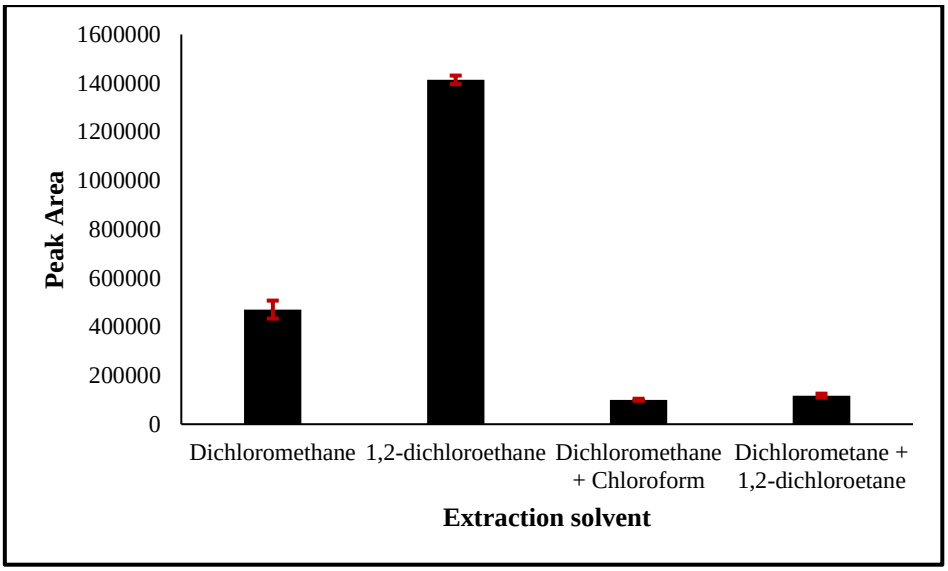


**Figure 4.22** Optimization of extraction solvent type

### 4.3.2.2 Number of spraying cycle

The spraying cycle directly affects the volume of extraction solvent introduced to the aqueous solution [265]. High spraying cycles lead to excess volume of extraction solvent and cause excessive dilution of analyte-rich phase. For this reason, spraying cycle was optimized by testing one and two sprays. According to the experimental results given in Figure 4.23, one spray was enough to reach high peak area values and selected as the optimum one for SB-FDF-LPME method.

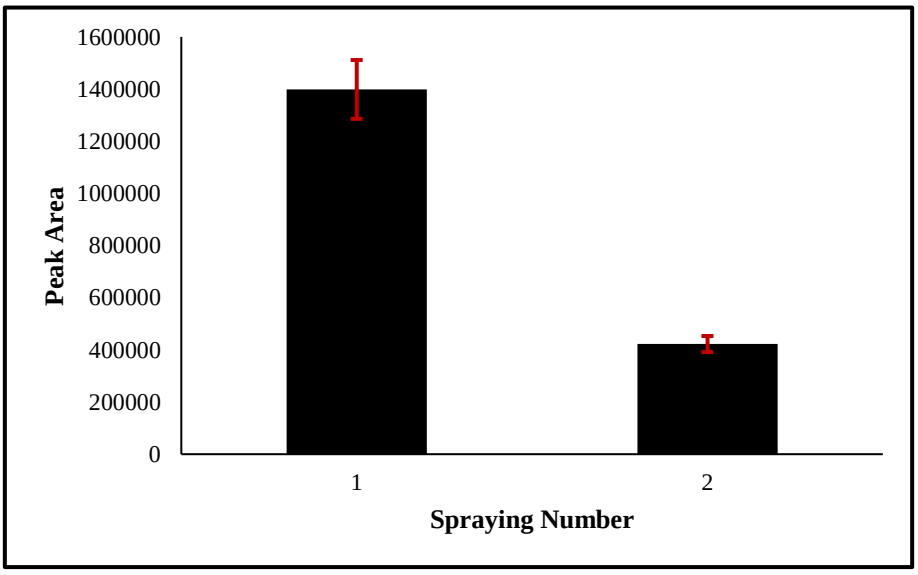


**Figure 4.23** Optimization of spraying cycle

#### 4.3.2.3 Concentration and volume of sodium hydroxide solution

Chloroquine is found as chloroquine phosphate in drug tablets and the phosphate group hindered the derivatization and extraction of chloroquine. Three replicates of standard solution without the addition of sodium hydroxide were extracted by SB-FDF-LPME method and there was no analytical signal for the analyte and this result proved the statement about the effect of phosphate group on its extraction. For this reason, sodium hydroxide was used in SB-FDF-LPME procedure, and its concentration and volume were optimized. Different concentrations of sodium hydroxide solutions in the range of 1.0 and 5.0 mol/L were studied and a Gaussian shape curve was observed in the experimental results shown in Figure 4.24. The highest signal to noise ratio was achieved for 3.0 mol/L sodium hydroxide solution and the optimum concentration was determined as 3.0 mol/L. In addition, three different volumes of sodium hydroxide solution as 0.50, 0.75 and 1.0 mL were tested. Based on the results given in Figure 4.25, 0.75 mL had higher peak area values than 0.50 and 1.0 mL, therefore, it was chosen as optimum volume for sodium hydroxide solution.

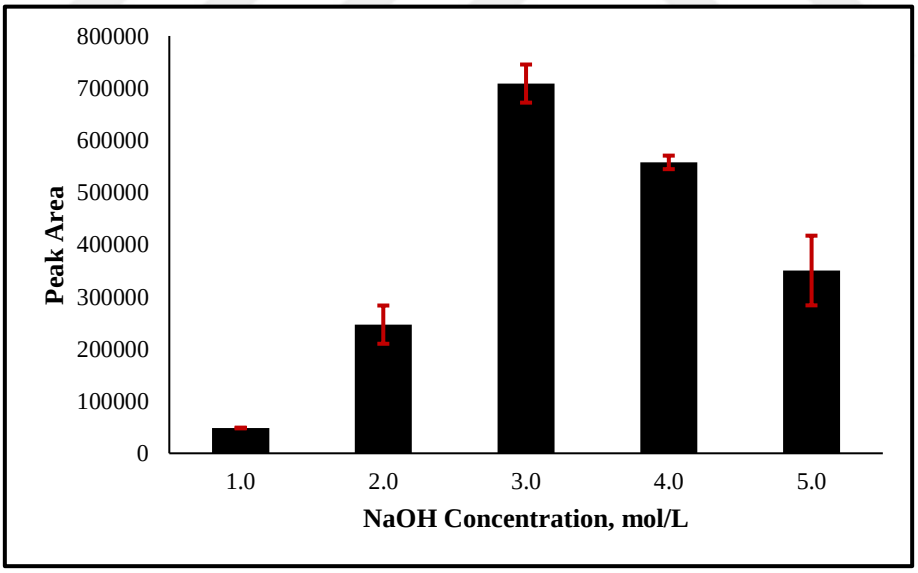


**Figure 4.24** Optimization of sodium hydroxide concentration

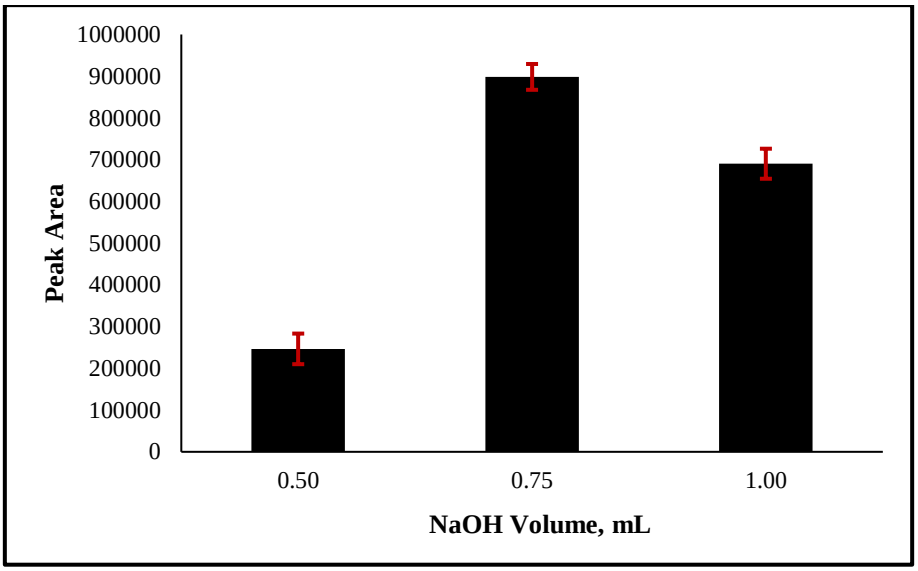


**Figure 4.25** Optimization of sodium hydroxide volume

#### 4.3.2.4 Type of mixing process

The spraying system provides the distribution of water-immiscible solvent throughout the sample solution, but several mixing processes have been used to enhance the extraction yield in literature [266]. For this reason, mixing effect on the derivatization and extraction of the analyte was investigated by testing vortex, ultrasonication and no mixing processes. As can be seen in Figure 4.26, no mixing gave the highest peak area values than vortex and ultrasonication. This result showed that there was a reversible mass transfer from the organic phase to the aqueous phase. No mixing was chosen as the optimum one due to its high analytical signals.

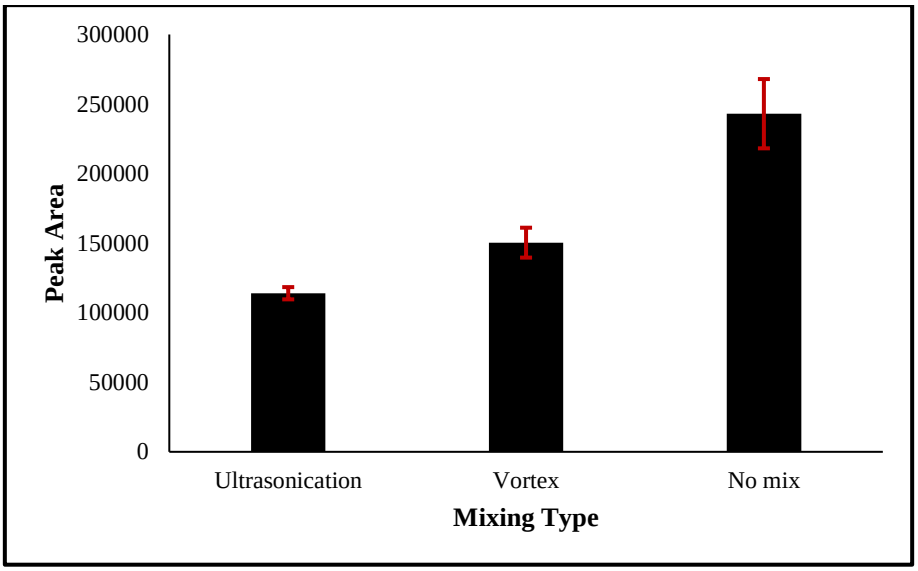


**Figure 4.26** Optimization of mixing type

#### 4.3.2.5 Concentration of acetic anhydride solution

In the presented study, acetic anhydride was utilized as derivatizing reagent for the production of acetamide derivative of the analyte. The reagent was dissolved in the selected extraction solvent to protect this chemical from its decomposition in aqueous medium and simultaneously derivatize and extract target analyte. Hence, 10, 15, 20 and 30 % (v/v) acetic anhydride solutions were tried to observe their effects on the SB-FDF-LPME method. As can be seen in Figure 4.27, high analytical signals were obtained for 20% (v/v) acetic anhydride. In addition, 30% (v/v) could inhibit the mass transfer from the water phase to 1,2-dichloroethane phase due to its high amount dissolved in the organic phase. Therefore, 20% (v/v) was selected as the optimum one.

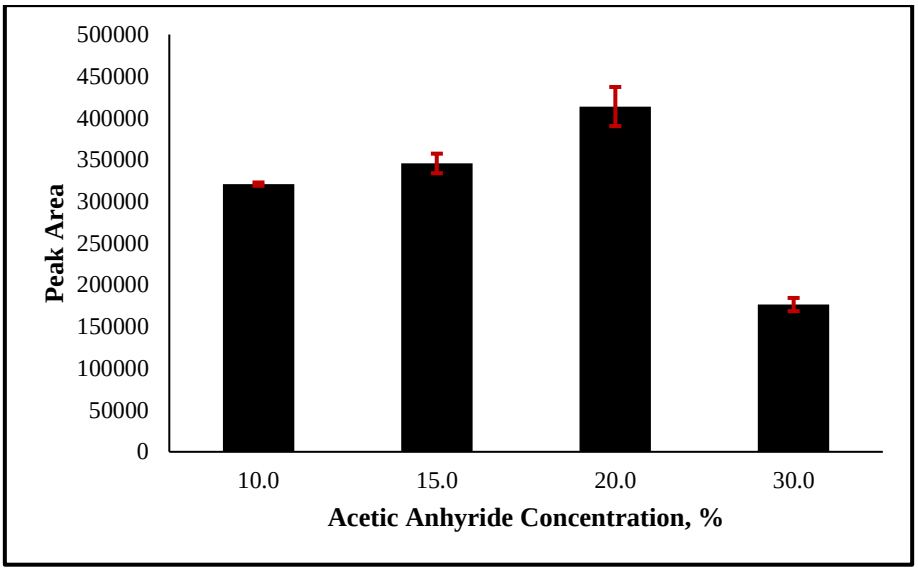


**Figure 4.27** Optimization of acetic anhydride concentration.

### 4.3.3 System analytical performance for SB-FDF-LPME-GC-MS method

In this step, system analytical performance for the developed method was investigated by calculating LOD, LOQ, %RSD and LWR. For this purpose, a series of chloroquine standard solutions approximately in the range of 0.50 and 100 mg/kg was prepared and treated with the developed microextraction method. According to the measurements in GC-MS system, LWR was observed between 0.52 and 49.25 mg/kg. LOD, LOQ, %RSD were determined as 0.16 mg/kg, 0.53 mg/kg and 8.2%, respectively. The linear equation and correlation coefficient were y=5448.2x+2281.8 and 0.9997, respectively. All these results demonstrated that the developed analytical method provided low LOD and LOQ values with wide linear range and high precision (%RSD ≤ 10). While the analytical figures of merit are summarized in Table 4.8, calibration plot obtained from SB-FDF-LPME-GC-MS for the analyte is given in Figure 4.28.

**Table 4.8** Analytical performance of the developed SB-FDF-LPME-GC-MS method

| Parameter | Value |
|---|---|
| **LOD, mg/kg** | 0.16 mg/kg |
| **LOQ, mg/kg** | 0.53 mg/kg |

**Table 4.8** Analytical performance of the developed SB-FDF-LPME-GC-MS method

| | |
|---|---|
| **LWR, mg/kg** | 0.52-49.25 mg/kg |
| **$R^2$** | 0.9997 |

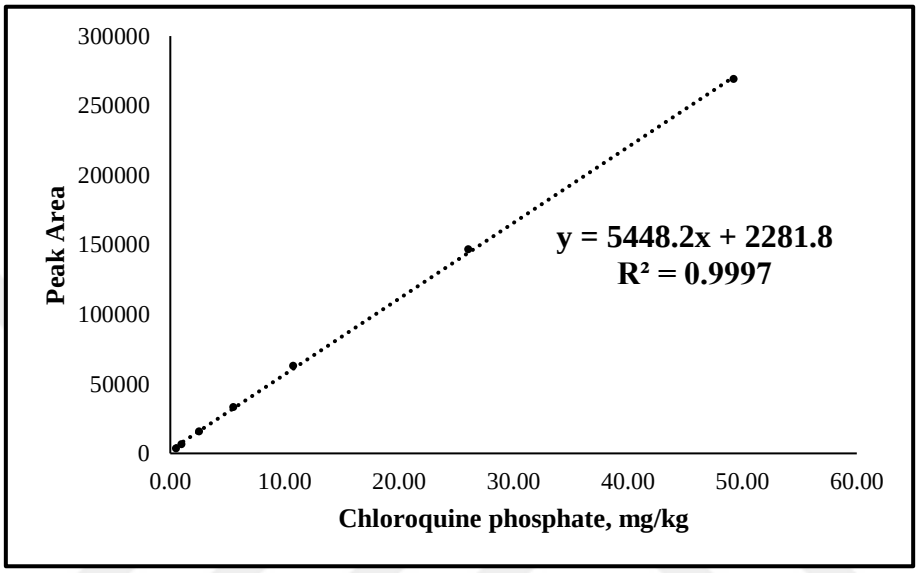


**Figure 4.28** Calibration plot for the developed SB-FDF-LPME-GC-MS method

### 4.3.4 Accuracy and suitability tests

The suitability and accuracy of the developed SB-FDF-LPME-GC-MS method were checked by recovery experiments carried out for urine, saliva and serum samples. First, all samples were treated with a protein precipitation process detailed in Section 3.3.4 and then analyzed by the developed method. There was no analyte in the analyzed samples according to the experimental results. For this reason, all samples were spiked to 20 and 40 mg/kg to conduct the recovery experiment. As can be seen in Table 4.9, percent recoveries were 103.2 – 108.6% for urine, 198.0 – 228.2% for saliva and 204.8 – 213.4% for serum samples. Based on the analytical results, positive interference effects were monitored for saliva and serum samples due to the percent recoveries higher than the acceptable values. These matrix effects could be compensated using isotope dilution methods.

**Table 4.9** Recovery results for the spiked samples

| Sample | Chloroquine phosphate, mg/kg | %Recovery ± SD* |
|---|---|---|
| **Urine** | 20.44 | 103.2 ± 7.0 |
| | 40.80 | 108.6 ± 3.4 |
| **Saliva** | 20.36 | 228.2 ± 6.4 |
| | 40.16 | 198.0 ± 11.8 |
| **Serum** | 20.17 | 213.4 ± 13.1 |
| | 40.09 | 204.8 ± 8.5 |

### 4.3.5 Integration of ID$^4$ and SB-FDF-LPME-GC-MS

In this study, ID$^4$ method was used to increase the precision and accuracy of the developed method and eliminate the matrix effects for the selected samples. For this purpose, the isotopically labelled chloroquine phosphate was synthesized in our research laboratory according to the procedure given in 3.3.6 Section. Next, calibration and samples mixtures were prepared using the analyte standard solution (A*), CA-*d3* solution (B) and sample solution (A). The selected samples were spiked to two different concentrations. As can be seen in Table 4.10, all sample mixtures were also treated with the protein precipitation process. A mixing process for 30 s and centrifugation process for 10 min were applied to the sample mixtures to separate the precipitates from the supernate phase. A 3.25 g of supernate phase was diluted to 13 g with UPW. Finally, 12 mL of the prepared mixtures were individually transferred into clean centrifuge tubes and the developed SB-FDF-LPME-GC-MS method was performed.

**Table 4.10** Calibration and sample mixtures for SB-FDF-LPME-ID$^4$-GC-MS method

| | Mixture | A*, g | A, g | B, g | ACN, g | $NH_3$, g | UPW, g | Total, g |
|---|---|---|---|---|---|---|---|---|
| **Calibration mixtures** | A*B-1 | 4.0 | - | 2.0 | - | - | 7.0 | 13.0 |
| | A*B-2 | 3.0 | - | 3.0 | - | - | 7.0 | 13.0 |
| | A*B-3 | 2.0 | - | 4.0 | - | - | 7.0 | 13.0 |
| **Urine** | AB | - | 3.0 | 3.0 | 5.1 | 1.4 | 0.50 | 13.0 |
| **Saliva** | AB | - | 3.0 | 3.0 | 6.5 | - | 0.50 | 13.0 |
| **Serum** | AB | - | 3.0 | 3.0 | 6.5 | - | 0.50 | 13.0 |

All $r_{AB}$ and $r_{A*B}$ values given in Table 4.11 and Table 4.12 were obtained by dividing the peak area of CA to CA-*d3*. These values were used in the formulation of quadruple isotope dilution detailed by Pagliano et al [18].

**Table 4.11** Peak area ratios for the calibration and sample mixtures (4.5 mg/kg)

| | Mixture | Analyte peak area/isotopically labelled material peak area |
|---|---|---|
| **Calibration mixtures** | A*B-1-a | 2.651 |
| | A*B-1-b | 2.673 |
| | A*B-1-c | 2.658 |
| | A*B-2-a | 1.946 |
| | A*B-2-b | 1.941 |
| | A*B-2-c | 1.956 |
| | A*B-3-a | 1.118 |
| | A*B-3-b | 1.108 |
| | A*B-3-c | 1.089 |

**Table 4.11** Peak area ratios for the calibration and sample mixtures (4.5 mg/kg) (continued)

| | | |
|---|---|---|
| **Sample mixtures** | AB-a (Urine) | 1.920 |
| | AB-b (Urine) | 1.903 |
| | AB-c (Urine) | 1.905 |
| | AB-a (Saliva) | 1.995 |
| | AB-b (Saliva) | 2.002 |
| | AB-c (Saliva) | 2.028 |
| | AB-a (Serum) | 1.944 |
| | AB-b (Serum) | 1.939 |
| | AB-c (Serum) | 1.940 |

**Table 4.12** Peak area ratios for the calibration and sample mixtures (9.2 mg/kg)

| | **Mixture** | **Analyte peak area/isotopically labelled material peak area** |
|---|---|---|
| **Calibration mixtures** | A*B-1-a | 2.764 |
| | A*B-1-b | 2.750 |
| | A*B-1-c | 2.747 |
| | A*B-2-a | 1.948 |
| | A*B-2-b | 1.954 |
| | A*B-2-c | 1.956 |
| | A*B-3-a | 1.096 |
| | A*B-3-b | 1.088 |
| | A*B-3-c | 1.062 |
| **Sample mixtures** | AB-a (Urine) | 1.926 |
| | AB-b (Urine) | 1.923 |
| | AB-c (Urine) | 1.938 |
| | AB-a (Saliva) | 1.932 |

**Table 4.12** Peak area ratios for the calibration and sample mixtures (9.2 mg/kg) (continued)

| | | |
|---|---|---|
| **Sample mixtures** | AB-b (Saliva) | 1.930 |
| | AB-c (Saliva) | 1.927 |
| | AB-a (Serum) | 1.917 |
| | AB-b (Serum) | 1.954 |
| | AB-c (Serum) | 1.976 |

After using the formula for all samples, percent recoveries given in Table 4.13 were close to %100 and standard deviation values were ranged from 0.6 to 1.6. All these results proved the precision and accuracy of the SB-FDF-LPME-ID$^4$-GC-MS method.

**Table 4.13** Percent recoveries for the selected samples analyzed by the SB-FDF-LPME-ID$^4$-GC-MS method

| **Sample** | **Chloroquine phosphate, mg/kg** | **%Recovery ± SD*** |
|---|---|---|
| **Urine** | 4.47 mg/kg | 100.9 ± 0.9 |
| | 9.14 mg/kg | 101.0 ± 0.6 |
| **Saliva** | 4.91 mg/kg | 100.4 ± 1.6 |
| | 9.27 mg/kg | 100.5 ± 1.1 |
| **Serum** | 4.64 mg/kg | 99.8 ± 0.8 |
| | 9.46 mg/kg | 99.4 ± 1.0 |

### 4.3.6 Comparison with other studies in literature

In literature, chloroquine in different matrices has been generally determined by LC systems. Some of these studies are summarized below.

Liquid chromatography-tandem mass spectrometry (LC-MS/MS) system was used to quantify chloroquine phosphate in human blood. Mobile phase and stationary

phase in this study were acetonitrile-ammonium formate 20 mmol/L with 1% formic acid (15–85, v/v) and a Zorbax SB-CN column. Percent recoveries and %RSD value were 95.0 – 104 ± 2.83% – 14.8% and 87.3 – 101 ± 2.67% – 3.46% for the spiked human blood at 6.03 and 1334 µg/L, respectively. According to these results, our developed SB-FDF-LPME-ID$^4$-GC-MS method recorded better recoveries and repeatability than LC-MS/MS method [267].

High performance liquid chromatography-ultraviolet/visible detection (HPLC-UV/VIS) was performed to separate and detect chloroquine in dried blood samples. SPE method was used to extract the analyte after a liquid phase extraction from filter paper. Under the optimum conditions, LWR was in the range of 150 and 2500 ng/mL while LOD and LOQ were 50 and 150 ng/mL, respectively. In this study, percent recoveries with %RSD values were found to be 97.6-99.3% ± 2.7-6.7% [268].

In another study, single drop liquid-liquid-liquid microextraction-high performance liquid chromatography-UV detection (LLLME-HPLC-UV) was developed by Daneshfar et. al. for the determination of chloroquine in urine and antimalaria tablets. LWR, LOD and LOQ values were recorded as 1 – 200, 0.3 and 1.0 µg/L, respectively. Percent recoveries for the selected samples varied from 94.6 and 101% with %RSD values as 1.0-3.2% [269]. When compared to our developed SB-FDF-LPME method, LLLME had tedious experimental steps and a special equipment.

Chloroquine was also separated and detected by GC system with nitrogen selective detector. Pentafluoropropionic anhydride was used to derivatize chloroquine prior to GC analysis. LOD value for the analyte was 5.0 µg/L but the developed method included sample treatment method with toxic organic solvents such as hexane, benzene and isoamyl alcohol [270]. However, the developed SB-FDF-LPME method only required a few microliters of 1,2-dichloroethane to preconcentrate the analyte.

## 4.4 Quantification of Hydroxychloroquine in Human Urine, Saliva and Serum Samples by SSB-LPME-ID$^4$-GC-MS System

This study was published in Rapid Communications in Mass Spectrometry in 2022 [253].

### 4.4.1 Characterization of chloroquine acetamide and its isotopic material

In the first step, 40 mg/kg hydroxychloroquine standard solution was derivatized by acetic anhydride solution and then concentrated by SSB-LPME method. Figure 4.29 presents GC-MS chromatogram, MS spectrum and the predicted fragments of the HMA. According to MS spectrum, the following m/z values 87.2, 144.2, 205.1, 219.1, 247.2 and 304.3 proved the success of the derivatization reaction and molecular identification of the derivatized molecule. Hence, the qualitative and quantitative determination of hydroxychloroquine can be done using the proposed derivatization method.

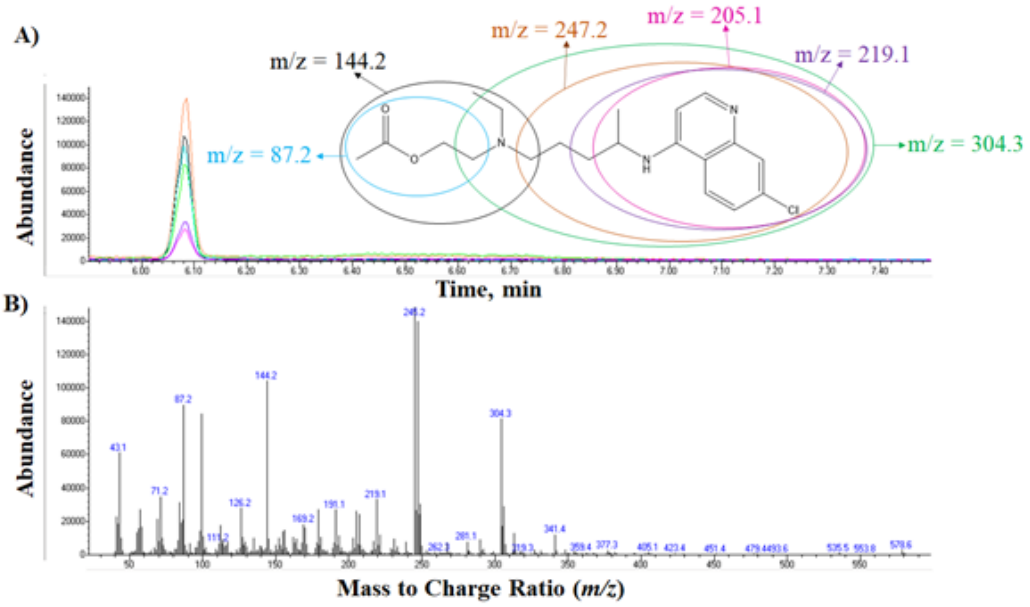


**Figure 4.29** GC-MS chromatogram (A) and mass spectrum (B) for HMA derivate

The product obtained in Section 3.4.6. was dissolved in UPW and concentrated by SSB-LPME method. It was sent to GC-MS system for the characterization of isotopic material. Figure 4.30 shows GC-MS chromatogram, MS spectrum and the predicted fragmentation of HMA-*d3*. If the MS spectrum is examined, the predicted fragments (90.2, 147.2 and 203.2) were compatible with the fragments in the spectrum.

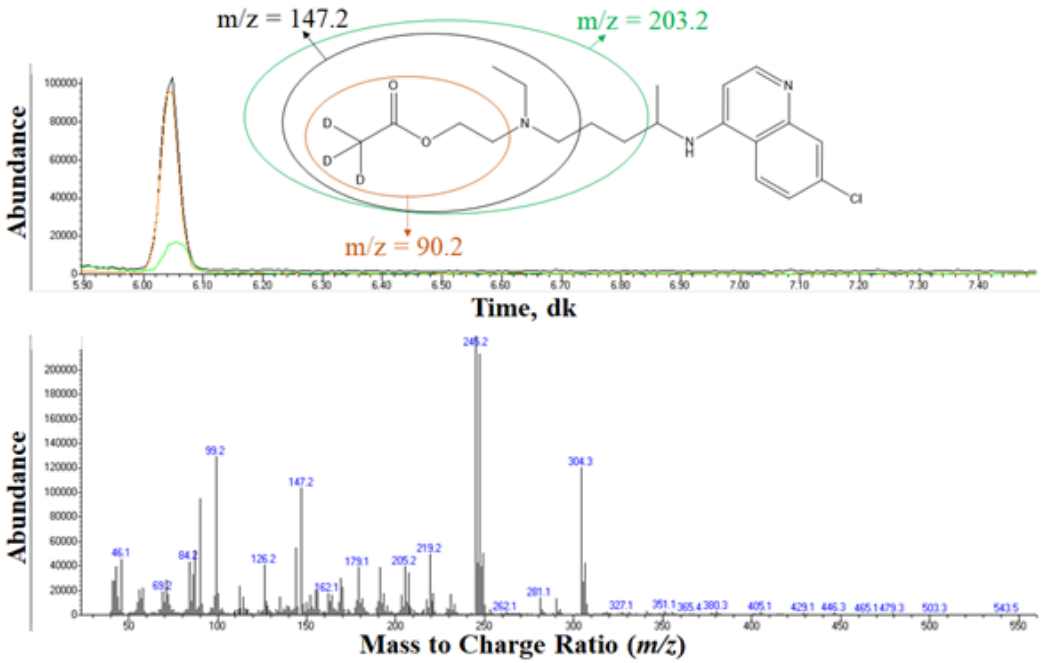


**Figure 4.30** GC-MS chromatogram (A) and mass spectrum (B) for HMA-$d_3$

### 4.4.2 Optimization studies

In this study, univariate approach was used to optimize type and period of mixing and concentration of sodium hydroxide solution. In addition, some parameters affecting the preconcentration factor and derivatization yield were optimized by Box Behnken Design.

#### 4.4.2.1 Type and period of mixing

Mixing process is one of the important steps in SSB-LPME because it accelerates homogeneous distribution of smart solvent and sodium hydroxide solution [271]. Vortex and ultrasonication were tested to monitor their effects on the extraction and derivatization yield. There was also one trial without any mixing process. According to the peak areas and standard deviation in Figure 4.31, there was no significant difference between ultrasonication and vortex. For this reason, ultrasonication was chosen as optimum mixing type due to its easy application and simplicity than vortex.

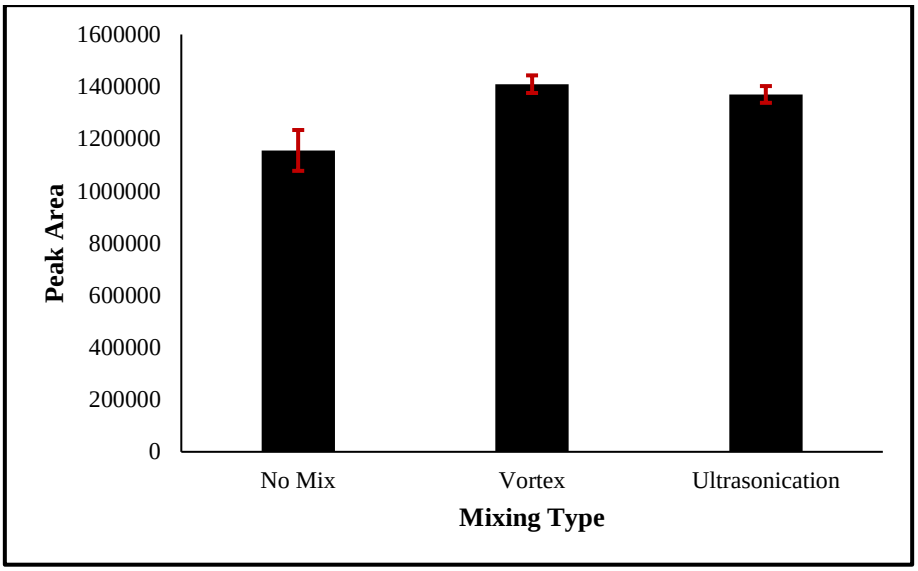


**Figure 4.31** The effect of mixing type

The period of ultrasonication process was also examined in this study. For this purpose, 1.0, 2.0, 5.0 and 10 min were tested to select the optimum ultrasonication period. As can be seen in Figure 4.32, no significant difference was observed after the application of 2.0 min ultrasonication because similar peak area values were recorded for 2.0, 5.0 and 10 min. Hence, 2.0 min was selected as the optimum ultrasonication period for the following experiments.

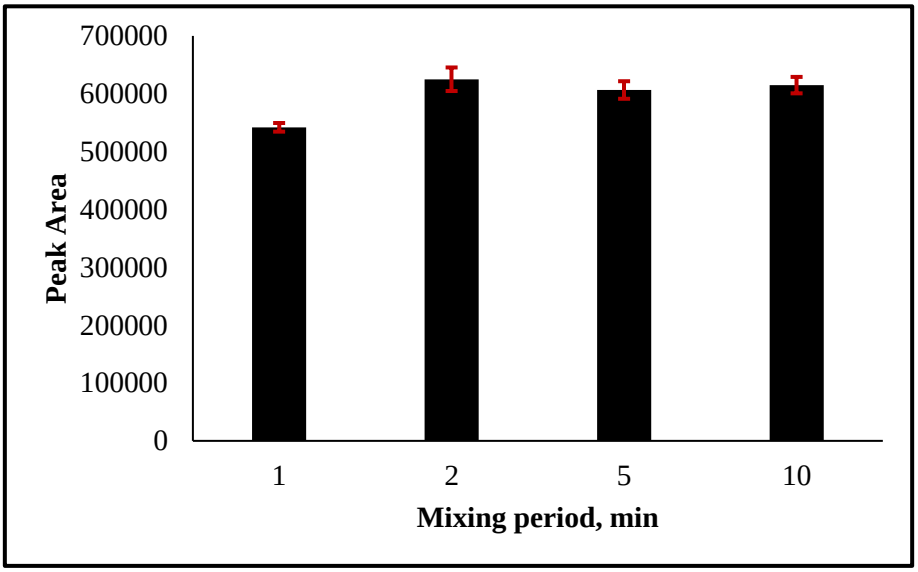


**Figure 4.32** The effect of mixing period

#### 4.4.2.2 Concentration of sodium hydroxide

The concentration of sodium hydroxide directly affects the phase separation of organic phase in SSB-LPME method. Its low volumes can lead to insufficient deprotonation of smart solvent while its high volumes can result in excess dilution of the analyte-rich phase due to the increase in the volume of organic phase [272]. Therefore, different concentration values in the range of 1.0 and 4.0 mol/L were studied in this optimization. No clear phase separation was observed for the trial with 1.0 mol/L sodium hydroxide solution. The highest signal to noise ratio was recorded for 2.0 mol/L sodium hydroxide solution (Figure 4.33). Other concentrations gave high volume of organic phase at the end of centrifugation step which causes excessive dilution of the analyte.

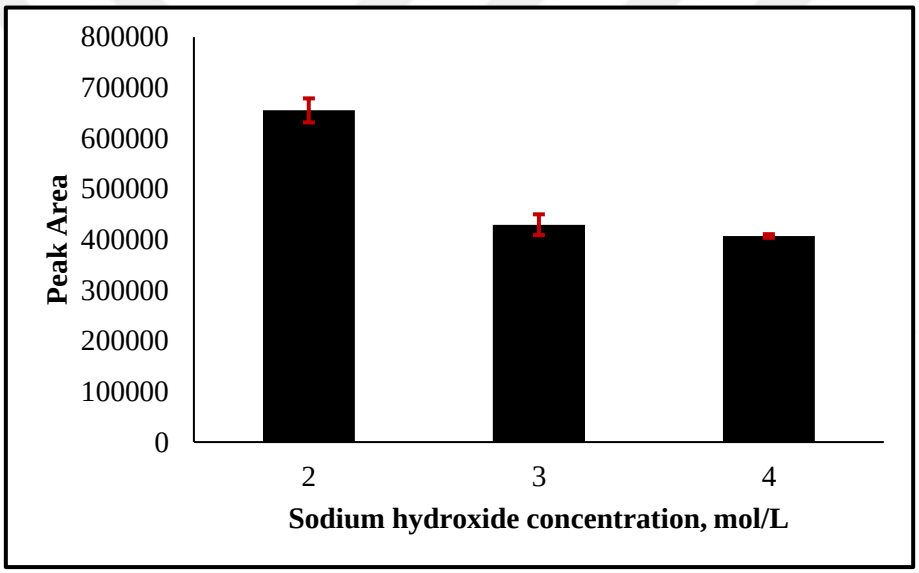


**Figure 4.33** The effect of sodium hydroxide concentration

### 4.4.3 Box Behnken Design

The volumes of acetic anhydride, smart solvent and sodium hydroxide were adjusted to their optimum values after their optimization studies by Box Behnken Design. Firstly, low (-1) and high (+1) levels of each parameter were determined by preliminary tests. Based on these tests, the low and high volumes for acetic anhydride, smart solvent and sodium hydroxide solution were determined as 50-200 µL, 0.75-1.50 mL and 2.0-3.0 mL, respectively. It should be noted that higher acetic anhydride volumes than 200 µL were not tested due to the momentary reaction between acetic anhydride and smart solvent. In addition to this information,

there was no distinct phase observed for the trial with smart solvent and sodium hydroxide lower than 0.75 mL and 2.0 mL, respectively. After the preliminary tests, Box Behnken Design was prepared using Design Expert software. Seventeen combinations with five center points were tested and peak area values are given in Table 4.14.

**Table 4.14** The constructed Box-Behnken experimental design and the results obtain from GC-MS system

| Order of sample preparation | Order of sample read | Acetic anhydride (X), µL | Smart solvent (Y), mL | Sodium hydroxide (Z), mL | PA* |
|---|---|---|---|---|---|
| **3** | 1 | 50 | 1.50 | 2.50 | 137798 |
| **4** | 2 | 200 | 1.50 | 2.50 | 307148 |
| **5** | 3 | 50 | 1.13 | 2.00 | 132892 |
| **9** | 4 | 125 | 0.75 | 2.00 | 804573 |
| **17** | 5 | 125 | 1.13 | 2.50 | 253401 |
| **6** | 6 | 200 | 1.13 | 2.00 | 717122 |
| **10** | 7 | 125 | 1.50 | 2.00 | 292053 |
| **16** | 8 | 125 | 1.13 | 2.50 | 212994 |
| **12** | 9 | 125 | 1.50 | 3.00 | 236034 |
| **8** | 10 | 200 | 1.13 | 3.00 | 510709 |
| **13** | 11 | 125 | 1.13 | 2.50 | 287906 |
| **11** | 12 | 125 | 0.75 | 3.00 | 592119 |
| **14** | 13 | 125 | 1.13 | 2.50 | 278162 |

**Table 4.14** The constructed Box-Behnken experimental design and the results obtain from GC-MS system

| | | | | | |
|---|---|---|---|---|---|
| **15** | 14 | 125 | 1.13 | 2.50 | 374428 |
| **7** | 15 | 50 | 1.13 | 3.00 | 126774 |
| **2** | 16 | 200 | 0.75 | 2.50 | 1266348 |
| **1** | 17 | 50 | 0.75 | 2.50 | 228285 |

**PA: Mean of peak area for triplicate measurements.*

Analysis of variance (ANOVA) test at 95% confidence level was implemented to evaluate the interaction of independent parameters. The quadratic equation obtained by ANOVA test is given in Equation 4.1.

$$Response = +3.216 \cdot 10^5 + 2.719 \cdot 10^5 \cdot X - 2.398 \cdot 10^5 \cdot Y - 60125.50 \cdot Z - 2.172 \cdot 10^5 \cdot X \cdot Y + 1.614 \cdot 10^5 \cdot Y^2 \quad \text{(Equation 4.1)}$$

Based on the equation, the volumes of acetic anhydride, smart solvent, sodium hydroxide, the interaction of the volume of acetic anhydride and smart solvent and quadratic effect of the volume of smart solvent were found as statistically important for the proposed equation. ANOVA results and regression model are given in Table 4.15.

**Table 4.15** ANOVA results for Box-Behnken experimental design studied

| **Source** | **Sum of squares** | **Degree of freedom** | **Mean squares** | **F-value** | **P-value** |
|---|---|---|---|---|---|
| **Model** | $1.380 \times 10^{12}$ | 5 | $2.759 \times 10^{11}$ | 50.43 | <0.0001 (significant) |
| **X** | $5.916 \times 10^{11}$ | 1 | $5.916 \times 10^{11}$ | 108.13 | <0.0001 |
| **Y** | $4.600 \times 10^{11}$ | 1 | $4.600 \times 10^{11}$ | 84.06 | <0.0001 |
| **Z** | $2.892 \times 10^{10}$ | 1 | $2.892 \times 10^{10}$ | 5.29 | 0.0421 |

**Table 4.15** ANOVA results for Box-Behnken experimental design studied (continued)

| | | | | | |
|---|---|---|---|---|---|
| **XY** | $1.887x10^{11}$ | 1 | $1.887x10^{11}$ | 34.48 | 0.0001 |
| **$Y^2$** | $1.104x10^{11}$ | 1 | $1.0104x10^{11}$ | 20.17 | 0.0009 |
| **Residual** | $6.019x10^{10}$ | 11 | $5.472x10^{9}$ | - | - |
| **Lack of fit** | $4.602x10^{10}$ | 7 | $6.574x10^{9}$ | 1.86 | 0.2872 (insignificant) |
| **Pure error** | $1.417x10^{10}$ | 4 | $3.543x10^{9}$ | - | - |
| **Cor. total** | $1.44x10^{12}$ | 16 | - | - | - |

X: Acetic anhydride volume; Y: Smart solvent volume; Z: Sodium hydroxide volume

According to p values in Table 4.15., X, Y, Z, XY, $Y^2$ had p values lower than 0.050 meaning that the related parameters were statistically important at 95% confidence level. The model produced coefficient of determination ($R^2$) value of 0.9582 and an adjusted $R^2$ value of 0.9392, which showed a high correlation between the observed and the predicted values. The experimental results were compatible with the polynomial regression due to high $R^2$ value (0.9582). Normality of the residuals were also controlled by the analysis of the obtained data. Normal distribution plot is also given in Figure 4.34. All data points were close to the straight line which supported the selection of significant parameters.

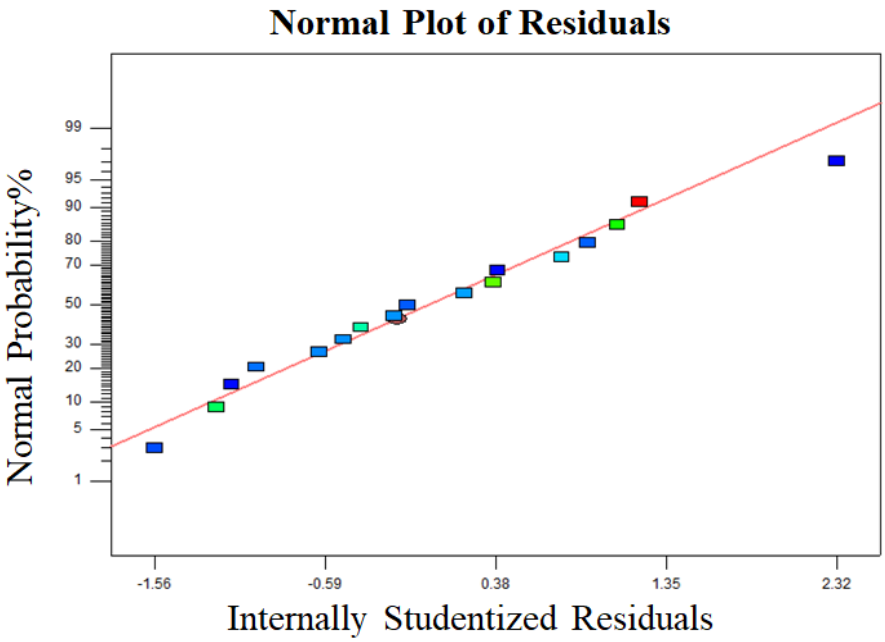


**Figure 4.34** Normal probability of internally studentized residuals

A three-dimensional graph is given in Figure 4.35. to show the interaction between the volumes of acetic anhydride and smart solvent. According to this graph, lower volumes of smart solvent with high volumes of acetic anhydride gave high responses. For this reason, optimum conditions were selected as 199.1 µL of acetic anhydride solution, 0.75 mL of smart solvent and 2.75 mL of sodium hydroxide solution.

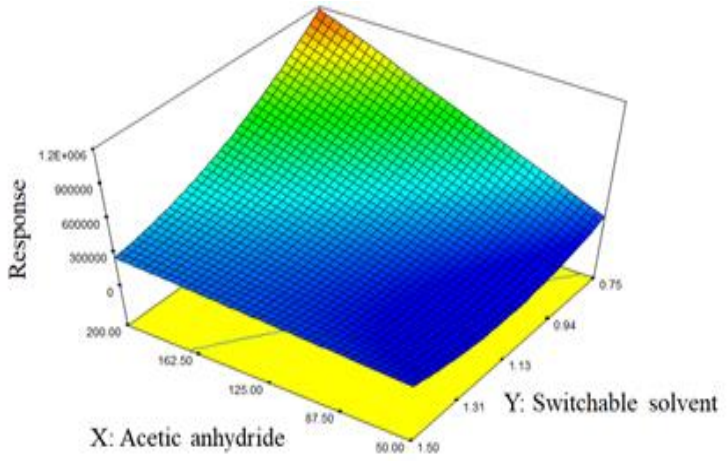


**Figure 4.35** 3D surface plot showing the interaction between X and Y (Z was fixed at 2.75 mL)

It should be noted that the optimum conditions were determined according to the protein precipitation method because acetonitrile was used as precipitating agent for urine, saliva and serum samples and acetonitrile content reduced the volume of organic phase after the SSB-LPME method. Lower volumes of sodium hydroxide than 2.75 mL resulted in insufficient phase separation. For this reason, optimum conditions were selected by considering the phase separation.

### 4.4.4 System analytical performance for SSB-LPME-GC-MS method

Analytical performance of the developed SSB-LPME-GC-MS method was assessed by applying the method to different hydroxychloroquine standard solutions between 0.11 and 49.38 mg/kg. Calibration plot belonging to the SSB-LPME-GC-MS method is given in Figure 4.36. LOD, LOQ, LWR and %RSD values were calculated as 0.03, 0.09, 0.11-49.38 mg/kg and 8.7%, respectively. The linear equation and $R^2$ value were found as y=18209x-3189.8 and 0.9996, respectively. According to these results, hydroxychloroquine at trace levels was separated and detected by GC-MS system after its derivatization with acetic anhydride and preconcentration by SSB-LPME method. All analytical performance values are given in Table 4.16.

**Table 4.16** Analytical performance of the developed SSB-LPME-GC-MS method

| Parameter | Value |
|---|---|
| **LOD, mg/kg** | 0.03 mg/kg |
| **LOQ, mg/kg** | 0.09 mg/kg |
| **LWR, mg/kg** | 0.11-49.38 mg/kg |
| **$R^2$** | 0.9996 |

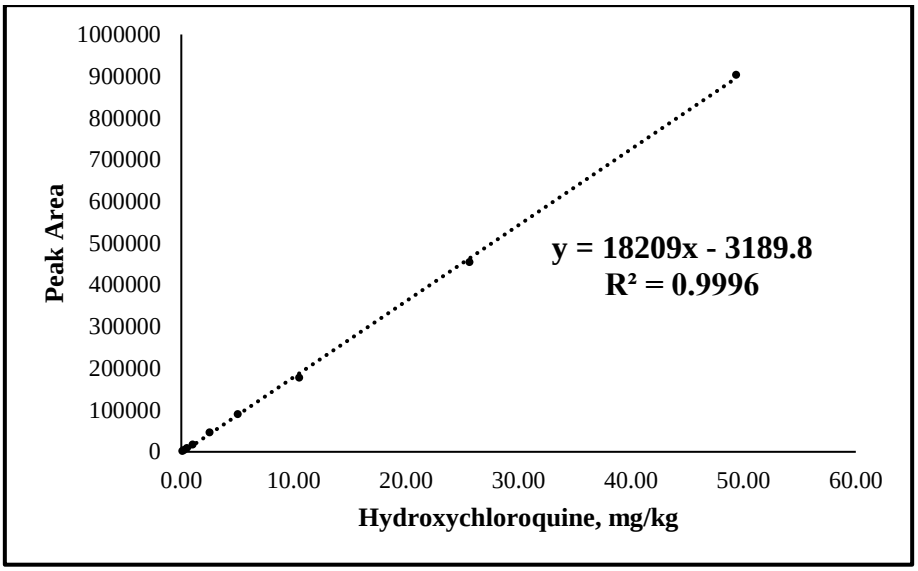


**Figure 4.36** Calibration plot for the SSB-LPME-GC-MS method

### 4.4.5 Accuracy and suitability tests

The developed SSB-LPME-GC-MS method was also tested in terms of its accuracy and suitability. For this purpose, human urine, saliva and serum samples were treated by the procedure detailed in Section 3.4.3. The analyte concentration in the tested samples were below the detection limit. Hence, all samples were spiked to three different concentration levels and analyzed under the optimum conditions of SSB-LPME-GC-MS method. Percent recoveries were calculated using the external calibration strategy.

As can be clearly seen in Table 4.17 that positive interference effects were observed for the spiked urine and serum samples while negative interference effects were monitored for the spiked saliva samples. For this reason, the developed preconcentration method was combined with $ID^4$ method to improve the recovery results and accuracy of the method.

**Table 4.17** Recovery results for the spiked samples

| Sample | Hydroxychloroquine, mg/kg | %Recovery ± SD* |
|---|---|---|
| Urine | 0.69 | 145.1 ± 12.2 |
| | 1.45 | 157.1 ± 6.9 |

**Table 4.17** Recovery results for the spiked samples (continued)

| | | |
|---|---|---|
| **Urine** | 2.75 | 151.7 ± 4.3 |
| **Saliva** | 0.44 | 70.5 ± 9.5 |
| | 1.11 | 57.0 ± 3.7 |
| | 2.55 | 52.7 ± 4.8 |
| **Serum** | 0.84 | 260.2 ± 17.9 |
| | 1.21 | 307.5 ± 28.8 |
| | 2.28 | 397.5 ± 14.5 |

### 4.4.6 Integration of ID$^4$ and SSB-LPME-GC-MS

Percent recoveries and standard deviation values found in Section 4.4.5 were not acceptable values for an accurate and precise analytical method. These results proved the presence of heavy matrix effects on the analytical results. Therefore, ID$^4$ and SSB-LPME-GC-MS method were performed together in order to boost the precision and accuracy of the developed method. HMA-*d3* was used as isotopic material in the preparation of calibration and sample mixtures which detailed in Section 3.4.5. Its synthesis and characterization are found in Section 3.4.6. In this study, two concentration levels (1.0 and 2.0 mg/kg) were prepared to validate the developed method. Table 4.18 and Table 4.19 summarize the peak area ratios of calibration and sample mixtures prepared for low and high concentration levels.

**Table 4.18** The derivatized analyte peak area/the labelled material peak area ratio for the mixtures. (low level)

| | **Mixture** | **The peak area of derivatized analyte/the peak area of labelled material ratio** |
|---|---|---|
| **Calibration mixtures** | A*B-1-a | 0.926 |
| | A*B-1-b | 0.930 |

**Table 4.18** The derivatized analyte peak area/the labelled material peak area ratio for the mixtures. (low level) (continued)

| | | |
|---|---|---|
| **Calibration mixtures** | A*B-1-c | 0.951 |
| | A*B-2-a | 0.359 |
| | A*B-2-b | 0.365 |
| | A*B-2-c | 0.371 |
| | A*B-3-a | 0.131 |
| | A*B-3-b | 0.135 |
| | A*B-3-c | 0.137 |
| **Sample mixtures** | AB-a (Serum) | 0.373 |
| | AB-b (Serum) | 0.370 |
| | AB-c (Serum) | 0.375 |
| | AB-a (Urine) | 0.366 |
| | AB-b (Urine) | 0.371 |
| | AB-c (Urine) | 0.363 |
| | AB-a (Saliva) | 0.365 |
| | AB-b (Saliva) | 0.362 |
| | AB-c (Saliva) | 0.365 |

**Table 4.19** The derivatized analyte peak area/the labelled material peak area ratio for the mixtures (high level)

| | **Mixture** | **The peak area of derivatized analyte/the peak area of labelled material ratio** |
|---|---|---|
| **Calibration mixtures** | A*B-1-a | 0.713 |
| | A*B-1-b | 0.718 |

**Table 4.19** The derivatized analyte peak area/the labelled material peak area ratio for the mixtures (high level) (continued)

| | | |
|---|---|---|
| **Calibration mixtures** | $A^*B$-1-c | 0.735 |
| | $A^*B$-2-a | 0.383 |
| | $A^*B$-2-b | 0.380 |
| | $A^*B$-2-c | 0.387 |
| | $A^*B$-3-a | 0.198 |
| | $A^*B$-3-b | 0.201 |
| | $A^*B$-3-c | 0.192 |
| **Sample mixtures** | AB-a (Serum) | 0.384 |
| | AB-b (Serum) | 0.384 |
| | AB-c (Serum) | 0.385 |
| | AB-a (Urine) | 0.386 |
| | AB-b (Urine) | 0.391 |
| | AB-c (Urine) | 0.386 |
| | AB-a (Saliva) | 0.389 |
| | AB-b (Saliva) | 0.388 |
| | AB-c (Saliva) | 0.387 |

After the application of SSB-LPME-ID$^4$-GC-MS method, excellent percent recoveries (99.6-101.3%) with low standard deviation values (S.D.≤1.8) were recorded for the selected biological samples (Table 4.20). In this way, positive and negative interference effects on the recovery results were compensated by the combined method. It is predicted that the developed method can be used for the determination of other drug active compounds in the following years due to the success of this method on biological matrices.

**Table 4.20** Percent recoveries for the selected samples analyzed by the SSB-LPME-ID$^4$-GC-MS method

| Sample | Hydroxychloroquine, mg/kg | %Recovery ± SD* |
|---|---|---|
| **Urine** | 1.04 | 99.9 ± 1.7 |
| | 2.09 | 99.8 ± 1.8 |
| **Saliva** | 1.03 | 99.6 ± 1.5 |
| | 2.07 | 101.0 ± 1.1 |
| **Serum** | 1.06 | 99.9 ± 1.6 |
| | 2.03 | 101.3 ± 1.2 |

### 4.4.7 Comparison with other studies in literature

In 2021, dispersive micro-solid phase extraction high performance liquid chromatography (DMSPE-HPLC) method was proposed to qualify and quantify hydroxychloroquine in human serum [273]. A new magnetic metal–organic framework molecularly imprinted polymer adsorbent was used in this study for the preconcentration of target analyte. Under the optimum conditions, linearity was achieved between 1 and 300 μg/L while LOD and LOQ values were calculated as 0.2 and 0.67 μg/L, respectively. Good recovery results (96-103%) with %RSD values lower than 3.5% was obtained for the spiked serum samples. Although analytical performance and recovery values were acceptable to obtain accurate and sensitive analytical method, chemicals used in the synthesis of the adsorbent are expensive and its synthesis requires laborious and multi-staged experiments.

Wang et al. [274] presented an analytical method for the determination of hydroxychloroquine in human blood samples by liquid chromatography tandem mass spectrometry (LC-MS/MS). At the end of the optimization of chromatographic system, LWR, LOD and LOQ were recorded as 5-2000, 2.0 and 5.0 ng/mL, respectively. Percent recoveries for the spiked human blood were in the range of 94 % and 107.6% and %RSD values were found as 1.9-8.0%. The

developed SSB-LPME-ID$^4$ method can be also combined with LC-MS/MS method to reach lower detection limits.

Capillary electrophoresis (CE) system was also used for the quantitation of hydroxychloroquine. For example, one study proposed by Oliveira et. al. [275] performed liquid-phase microextraction based on polypropylene hollow fibers (LPME) for the preconcentration of hydroxychloroquine from urine samples prior to CE analysis. Optimization studies was done to determine optimum conditions for LPME method. LWR for the LPME-CE method was obtained in the range of 10 and 1000 ng/mL with $R^2$ value as 0.9983. LOQ value in this study was calculated as 10 ng/mL. Recovery experiments were also done to check accuracy of the LPME-CE method and 85.1-87.5% percent recoveries with %RSD values lower than 9.8% were achieved for the spiked urine samples.

Charlier et. al. [276] established ion-pairing high performance liquid chromatography with fluorescence detector (HPLC-FL) method to separate and detect hydroxychloroquine found in whole blood samples. Lower limit of detection (LLOD) and lower limit of quantitation (LLOQ) were found to be 1.0 and 20 ng/mL, respectively. Linearity was obtained between 1.0 and 2500 ng/mL with $R^2$ value as 0.9953.

## 4.5 Quantification of Capsaicin in Green Pepper, Wastewater and Human Saliva Samples by SB-FDF-LPME-ID$^4$-GC-MS System

### 4.5.1 Optimization studies

Some prominent parameters including type of extraction solvent, spraying number, pH, the volume of buffer solution, type and period of mixing for extraction and derivatization methods, the effect of salt addition, the volume of derivatization agent, and the volume of initial sample were optimized to enhance extraction and derivatization outputs. One variable at a time approach was followed during the optimization studies.

#### 4.5.1.1 Type of extraction solvent

It is important to select a proper extraction solvent in order to avoid solvent loss during the extraction step. Solvent with high density than water can be used for this

purpose [277]. Hence, three different solvents denser than water were tried to find the optimum extraction solvent for the preconcentration of capsaicin acetamide. It can be clearly seen in Figure 4.37 that dichloromethane gave the highest peak area values than chloroform and 1,2-dichloroethane. It can be attributed to the volume of organic phase which was lowest for dichloromethane due to its high-water solubility than others. For this reason, dichloromethane was selected as optimum one for the subsequent experiments.

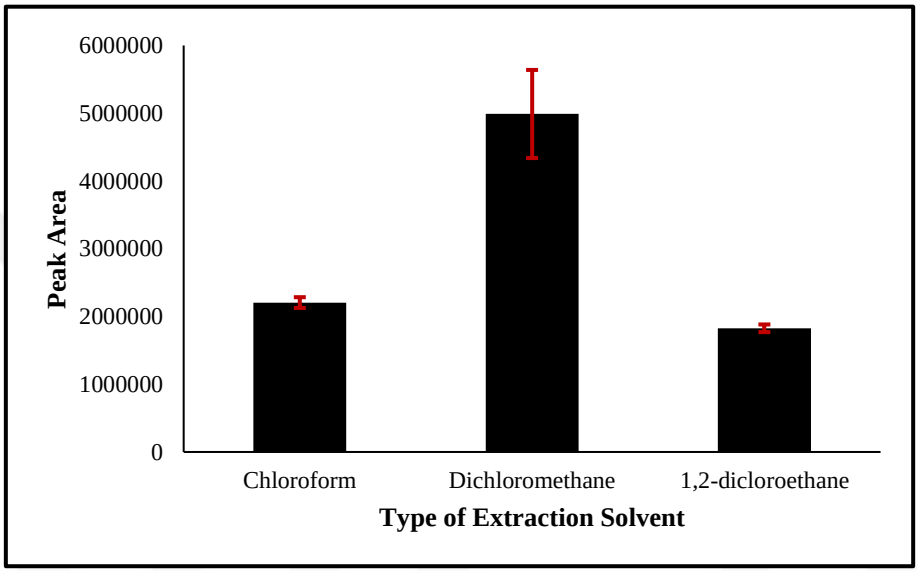


**Figure 4.37** Optimization of extraction solvent type

#### 4.5.1.2 Number of spraying cycle

Spraying cycle was investigated to improve the extraction output of the analyte derivative. Two, three and four spraying cycles were tested one by one, and the experimental results are given in Figure 4.38. Increasing the spraying cycle caused to a linear decrease in peak area values. Higher volumes than two cycles had high volumes of organic phases at the end of the extraction process meaning that diluted the analyte found in the organic phase. Hence, two spraying cycle was chosen to be used as optimum spraying cycle.

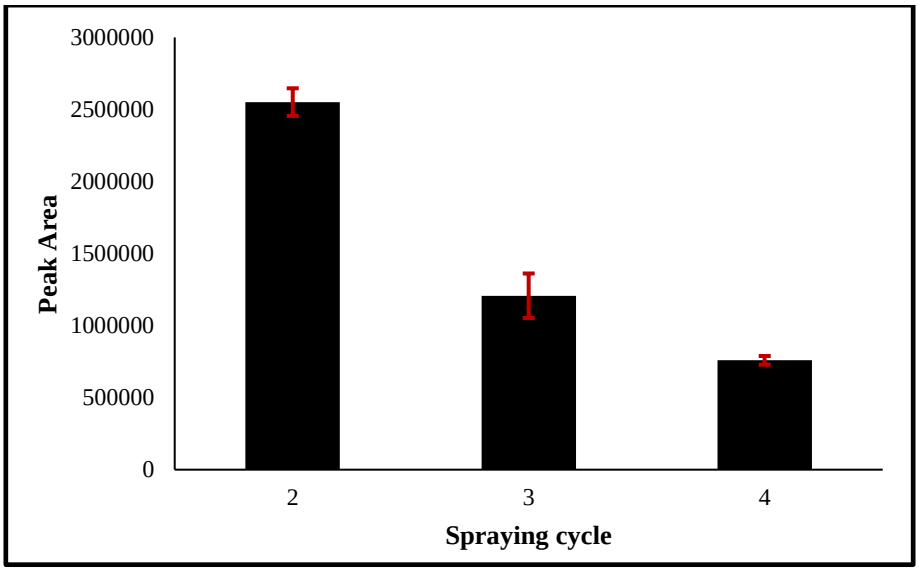


**Figure 4.38** Optimization of spraying cycle

#### 4.5.1.3 pH and volume of buffer solution

pH is one of the prominent extraction parameters changing the extraction efficiency [278]. pH effect was investigated between 4.0 and 12 in order to boost extraction and derivatization yields. There was also one experiment conducted without the addition of buffer solution. It was recorded in Figure 4.39 that basic pH levels had highest peak area values while acidic pH levels gave peak area values close to non-buffered solution. If the real sample extracts were considered, it was proper to select pH 7.0 as the optimum one due to neutral pH levels of real samples.

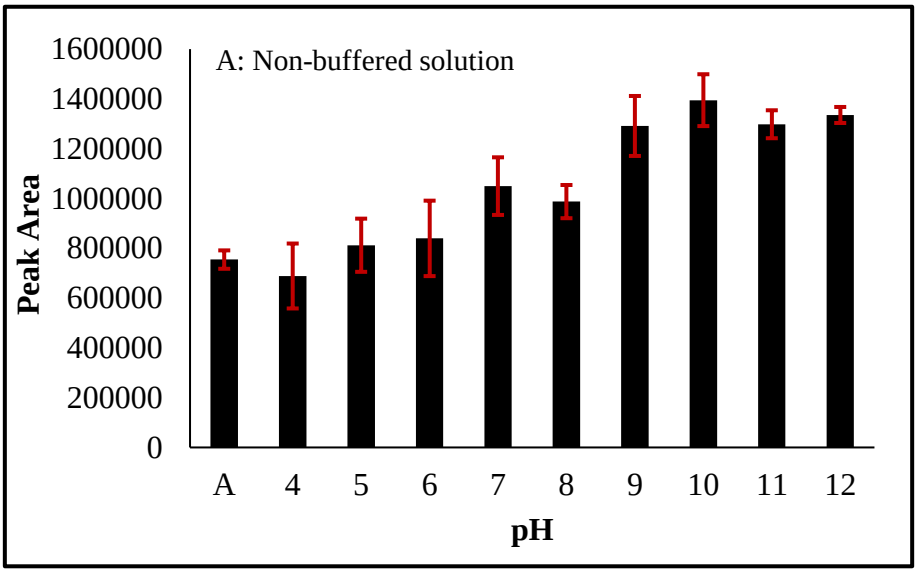


**Figure 4.39** Optimization of pH value

The volume of buffer solution was also optimized through univariate approach. Four different volume of pH 7.0 buffer solution were individually added to the aqueous solutions and the optimized method was performed. As depicted in Figure 4.40, the highest signal to noise ratio was achieved for 2.50 mL but blurry and unclear organic phase was obtained for this volume at the end of centrifugation process. Hence, optimum volume was determined as 2.0 mL due to its high peak area values than 1.0 and 1.50 mL.

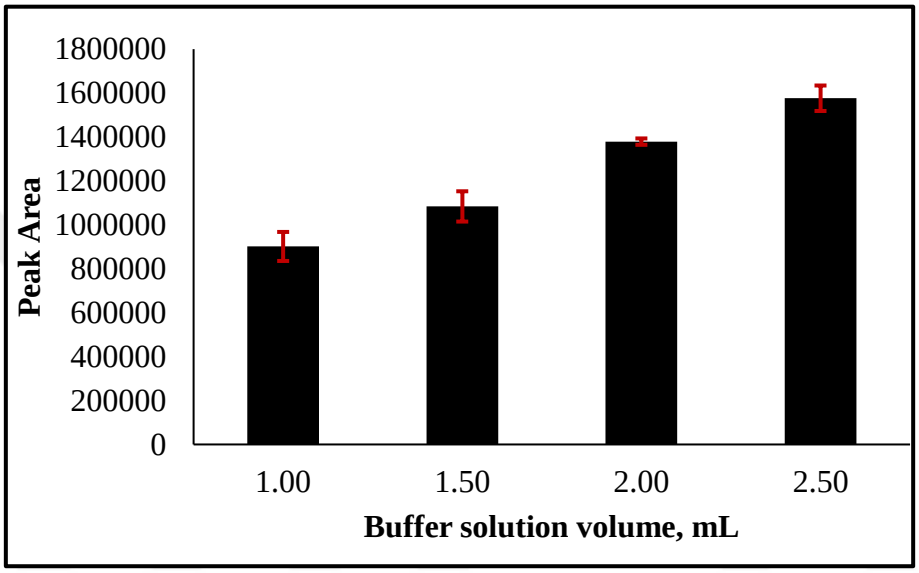


**Figure 4.40** Optimization of buffer solution volume

#### 4.5.1.4 Type and period of mixing for extraction step

It is known that type and period of mixing process are two dominant parameters affecting mass transfer of analyte from aqueous medium to organic medium [279]. Two mixing processes and no mixing were separately performed after the spraying process was completed. Based on the peak area values given in Figure 4.41, ultrasonication was marginally higher than vortex and no mixing processes. It is also clear that the lowest standard deviation value was recorded for ultrasonication. For this reason, ultrasonication was used for the further experiments.

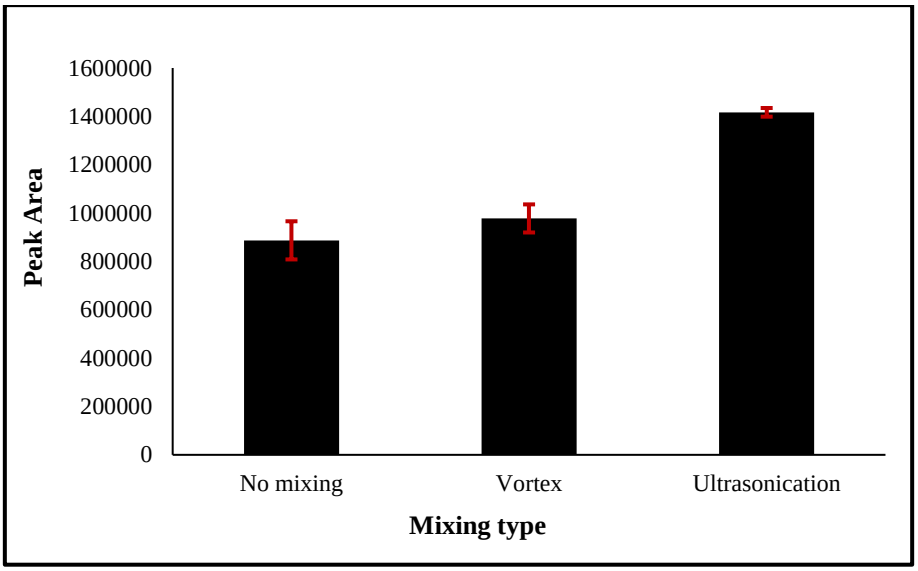


**Figure 4.41** Optimization of mixing type for extraction step

At the end of the optimization of mixing type for extraction step, mixing period was also studied to observe its effects on the capsaicin acetamide extraction. Mixing periods in the range of 15 and 60 s were tried to find the optimum period. It can be clearly seen in Figure 4.42 that 30 s was enough to reach high peak area values. Higher periods (45 and 60 s) had similar results with 30 s. Hence, 30 s was selected as optimum ultrasonication period for extraction step.

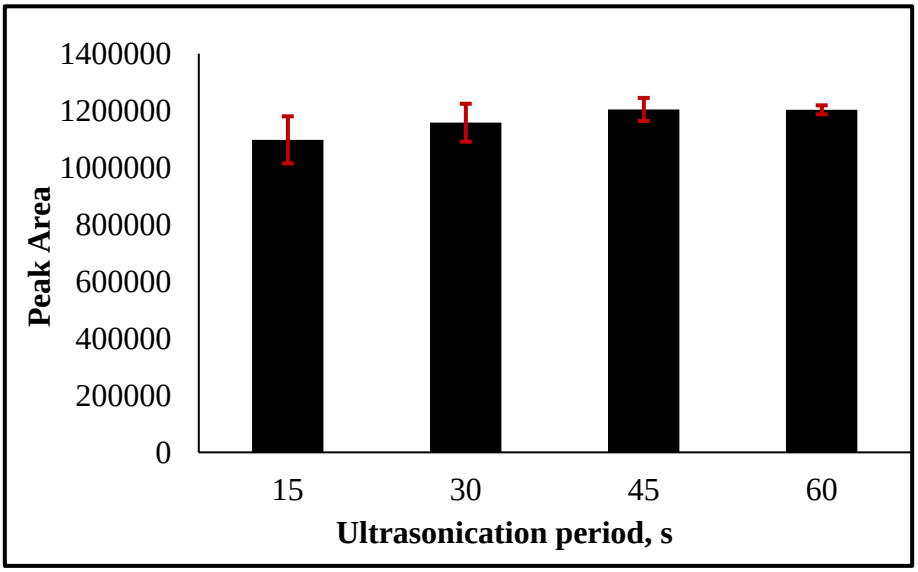


**Figure 4.42** Optimization of mixing period for extraction step

#### 4.5.1.5 Type and period of mixing for derivatization step

In this optimization, mixing effect was investigated due to its importance for derivatization yield and repeatability. Vortex, no mixing and ultrasonication were applied to the aqueous solutions containing the same amount of analyte, buffer solution and derivatizing agent. After the optimized SB-FDF-LPME-GC-MS method was carried out for the solutions non-mixed and mixed by vortex and ultrasonication, the non-mixed solution gave the highest results with high standard deviation value. Vortex was selected as the optimum mixing type due to its low standard deviation values than other two mixing processes (Figure 4.43).

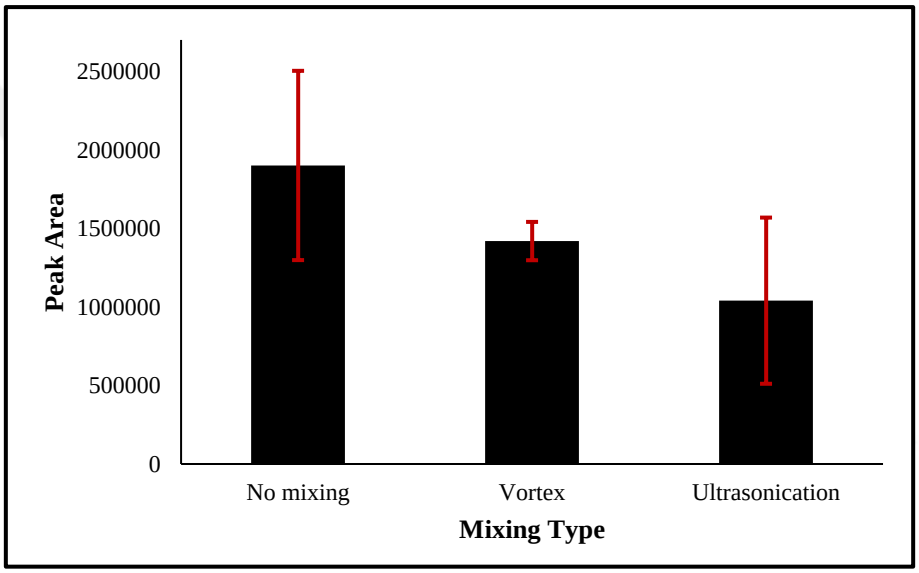


**Figure 4.43** Optimization of mixing type for derivatization step

Vortex period was then optimized in order to have maximum derivatization efficiency with minimum mixing period. For this purpose, the effect of vortex period was assessed at different mixing periods between 15 and 60 s. As can be seen in Figure 4.44, no significant increase was observed for the tested period. For this reason, 15 s was determined as optimum vortex period for derivatization step.

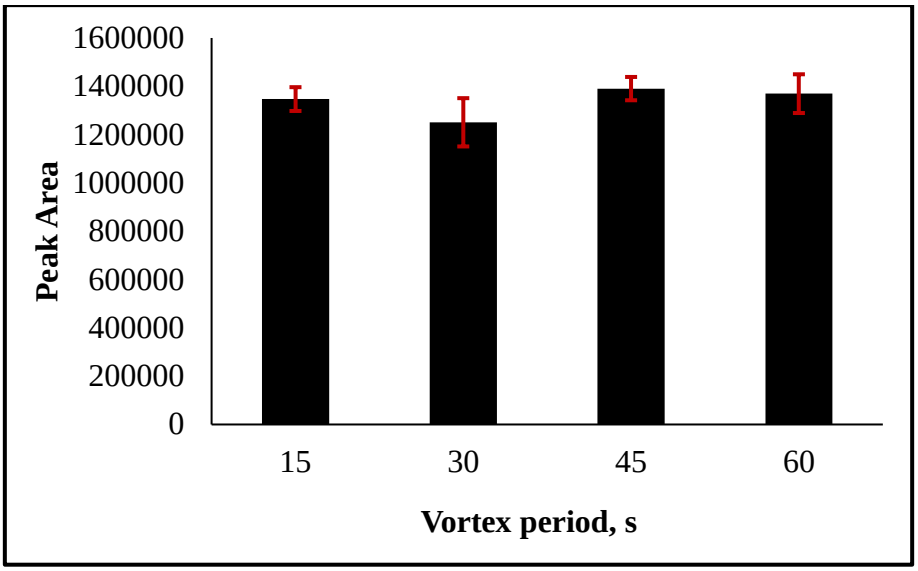


**Figure 4.44** Optimization of mixing period for derivatization step

#### 4.5.1.6 Effect of salt addition

In literature, different kinds of salts are used in extraction strategies to lower the solubility of analyte in aqueous medium [280]. Considering this fact, potassium chloride, potassium nitrate and sodium chloride were individually tested. In addition, one experiment was conducted without the addition of salt. Figure 4.45 shows that the addition of salt had no impact on the extraction outputs of target analyte. Therefore, no salt addition was selected as the optimum one in order to reduce the chemical usage in the developed method.

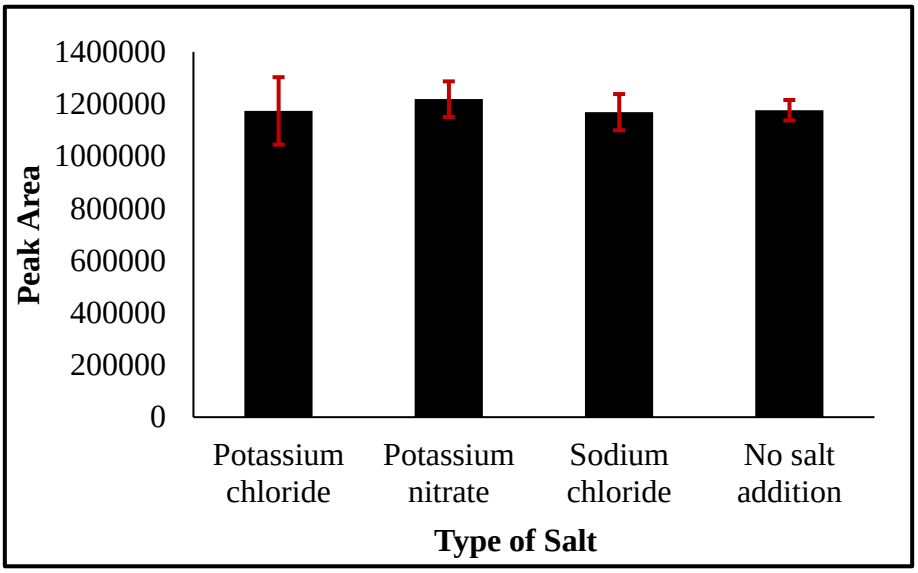


**Figure 4.45** Optimization of salt effect

#### 4.5.1.7 Volume of derivatization agent

The volume of derivatizing agent has an impact on reaction completeness and reaction speed [281]. A set of experiments were done to investigate the effect of derivatizing agent volume on the acylation reaction. For this purpose, it was examined by adding 20, 25, 30 and 35 µL derivatizing agent into analyte containing solution. A slightly higher results were obtained for 30 µL if compared to results for 20 and 25 µL. As presented in Figure 4.46, 30 and 35 µL had peak area values close to each other. For this reason, the optimum one was determined as 30 µL.

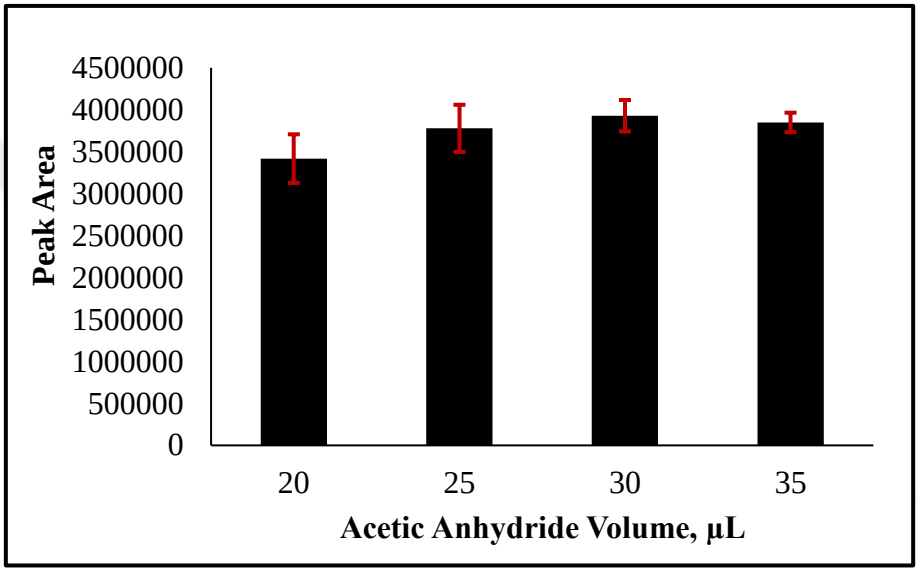


**Figure 4.46** Optimization of acetic anhydride volume

#### 4.5.1.8 Volume of initial sample

Analyte recovery and preconcentration factor can be enhanced by means of optimization studies for the volume of initial sample[282]. The optimum volume of initial sample was examined via extracting 8, 9, 10, 11 and 12 mL of sample solutions by the developed SB-FDF-LPME method. A Gaussian curve with a maximum peak area at 11 mL can be seen in Figure 4.47. According to these results, initial sample volumes lower than 11 mL had low preconcentration factors while higher volumes than 11 mL recorded low extraction yield due to insufficient extraction solvent. Higher volumes than 12 mL were not tried due to the maximum volume capacity of the centrifuge tube used in this study. Hence, 11 mL was chosen as the optimum volume of initial sample solution.

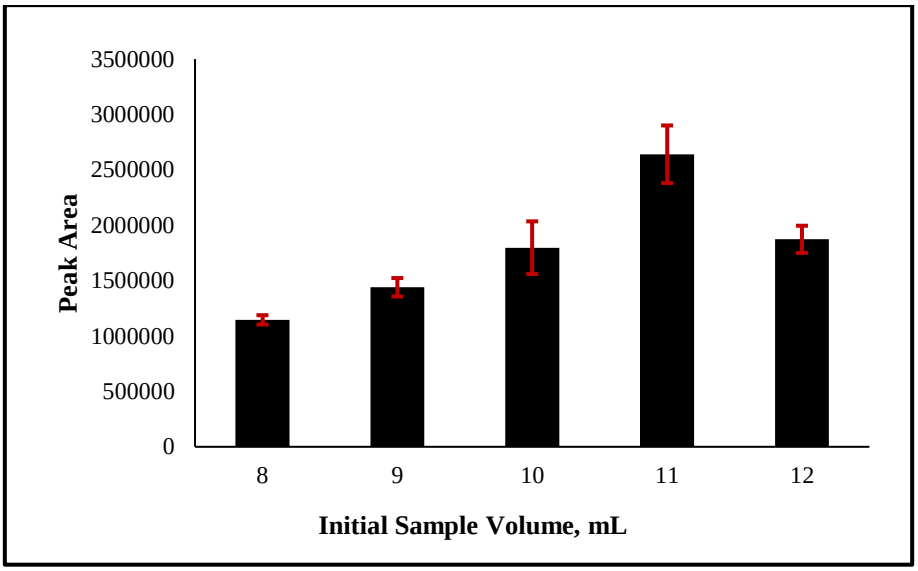


**Figure 4.47** Optimization of initial sample volume

### 4.5.2 System analytical performance for SB-FDF-LPME-GC-MS method

Under the optimum GC-MS and SB-FDF-LPME-GC-MS conditions, system analytical performance studies were performed by calculating LWR, LOD, LOQ and $R^2$ values. First, a series of capsaicin standard solutions between 9.92 and 252.46 mg/kg were sent to GC-MS system without derivatization and microextraction processes. LOD and LOQ for GC-MS system were found as 3.17 and 10.56 mg/kg, respectively. Calibration plot belonging to GC-MS system is given in Figure 4.48. Further, different capsaicin standard solutions in the concentration range of 1.03 and 507.0 µg/kg were prepared and extracted by the optimized SB-FDF-LPME method. LOD and LOQ values for the developed SB-FDF-LPME-GC-MS method were figured out to be 0.33 and 1.10 µg/kg, respectively. Calibration plot belonging to SB-FDF-LPME-GC-MS system is presented in Figure 4.49. Based on the LOD values for both systems, 9580-fold enhancement in detection power was recorded. All analytical performance parameters are given in Table 4.21.

**Table 4.21** Analytical performance of the developed SB-FDF-LPME-GC-MS method

| Parameter | GC-MS | SB-FDF-LPME-GC-MS |
|---|---|---|
| **LOD, mg/kg** | 3.17 mg/kg | 0.33 µg/kg |
| **LOQ, mg/kg** | 10.56 mg/kg | 1.10 µg/kg |
| **LWR, mg/kg** | 9.92 – 252.46 mg/kg | 1.03-507.0 µg/kg |
| **$R^2$** | 0.9994 | 0.9998 |

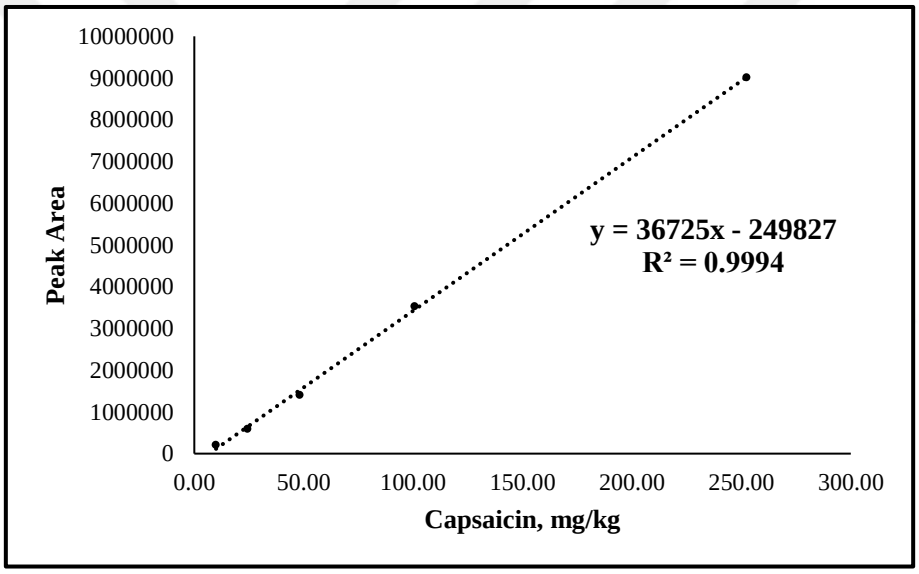


**Figure 4.48** Calibration plot for the determination of capsaicin by GC-MS system

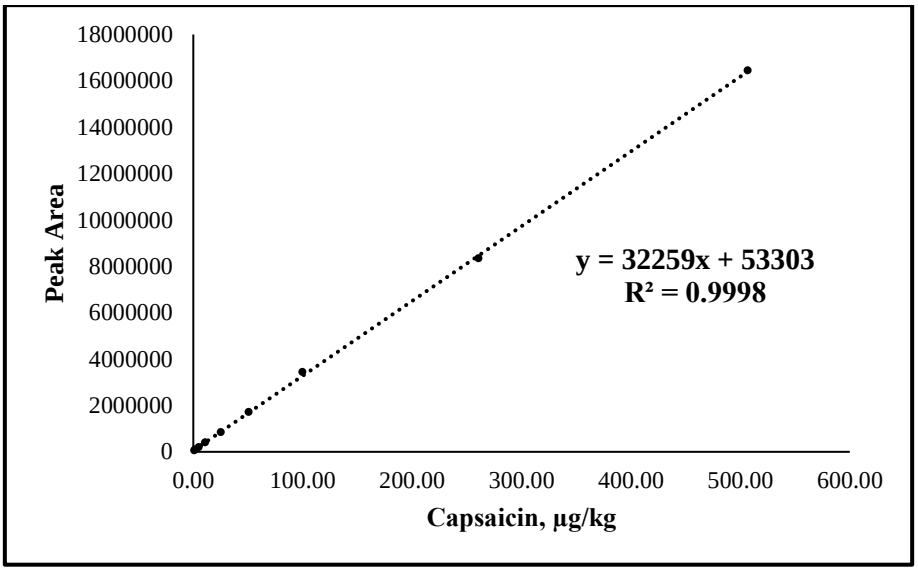


**Figure 4.49** Calibration plot for the determination of capsaicin by SB-FDF-LPME-GC-MS system

### 4.5.3 Accuracy and suitability tests

Here, accuracy and suitability of the developed SB-FDF-LPME-GC-MS method were assessed by spiking experiments. For this purpose, pepper, wastewater and saliva samples were prepared according to the procedure given in Section 3.5.4. Capsaicin concentration in pepper samples were found using standard addition calibration strategy. Banana (P1), Kıl (P2), Sivri (P3) and Samandağ (P4) peppers had 32.8 ± 5.0, 796.0 ± 88.2, 200.4 ± 17.6 and 137.4 ± 9.6 mg/kg capsaicin, respectively. Percent recoveries (Table 4.22) for pepper samples were calculated by matrix matching calibration strategy after blank correction was performed.

**Table 4.22** Recovery results for pepper, saliva and wastewater samples

| Sample | Spiked concentration, µg/kg | %Recovery | S.D. |
|---|---|---|---|
| **Kıl pepper** | 13.67 | 108.2 | 13.0 |
| | 28.27 | 117.9 | 12.0 |
| | 74.57 | 98.5 | 11.8 |

**Table 4.22** Recovery results for pepper, saliva and wastewater samples (continued)

| | | | |
|---|---|---|---|
| **Kıl pepper** | 98.87 | 101.2 | 8.3 |
| **Sivri pepper** | 14.57 | 90.6 | 4.5 |
| | 27.68 | 110.7 | 7.8 |
| | 76.12 | 94.8 | 5.6 |
| | 101.58 | 91.2 | 3.8 |
| **Samandağ pepper** | 13.16 | 114.4 | 4.4 |
| | 26.69 | 129.4 | 21.2 |
| | 74.72 | 120.4 | 7.7 |
| | 99.25 | 129.5 | 1.9 |
| **Saliva 1** | 26.1 | 96.0 | 15.9 |
| | 54.0 | 89.6 | 9.6 |
| | 102.4 | 84.1 | 3.4 |
| | 271.8 | 99.7 | 5.2 |
| **Saliva 2** | 28.4 | 131.7 | 8.5 |
| | 57.1 | 126.1 | 15.4 |
| | 108.7 | 111.0 | 11.8 |
| | 272.4 | 100.1 | 2.7 |
| **Wastewater 1** | 10.4 | 103.6 | 10.9 |
| | 25.0 | 97.1 | 1.0 |

**Table 4.22** Recovery results for pepper, saliva and wastewater samples (continued)

| | | | |
|---|---|---|---|
| **Wastewater 1** | 53.6 | 97.1 | 6.2 |
| | 102.2 | 98.5 | 5.3 |
| **Wastewater 2** | 10.4 | 96.2 | 5.2 |
| | 25.2 | 98.2 | 0.6 |
| | 51.6 | 95.3 | 9.2 |
| | 100.9 | 103.7 | 9.0 |

Percent recoveries for the spiked wastewater and saliva samples were also figured out by matrix matching calibration strategy. As shown in Table 4.22., percent recoveries were determined between 90.6-129.5% for pepper samples, 84.1-131.7% for saliva samples and 95.3-103.7% for wastewater samples. In addition, standard deviation values were ranged from 0.6 to 21.2. According to these results, recoveries and standard deviation values for all selected samples were not enough to reach high accurate and precise results. For this reason, $ID^4$ method was carried out prior to the developed SB-FDF-LPME-GC-MS method in order to achieve superior precision and accuracy.

### 4.5.4 Integration of $ID^4$ and SB-FDF-LPME-GC-MS

One of the requirements for the application of $ID^4$ method is the homogeneous distribution of all isotopes [234]. Therefore, equilibrium period for the homogeneous distribution of capsaicin and its isotopic material was examined in this optimization study. Seven different periods from 0 to 180 min were tested to have a stable isotope ratio. It is clear in Figure 4.50 that the stability in isotope ratios was achieved within 120 min. In addition, 150 and 180 min gave similar results with 120 min, but 120 min was selected as optimum equilibrium period to lessen the period for the homogeneous distribution of isotopes.

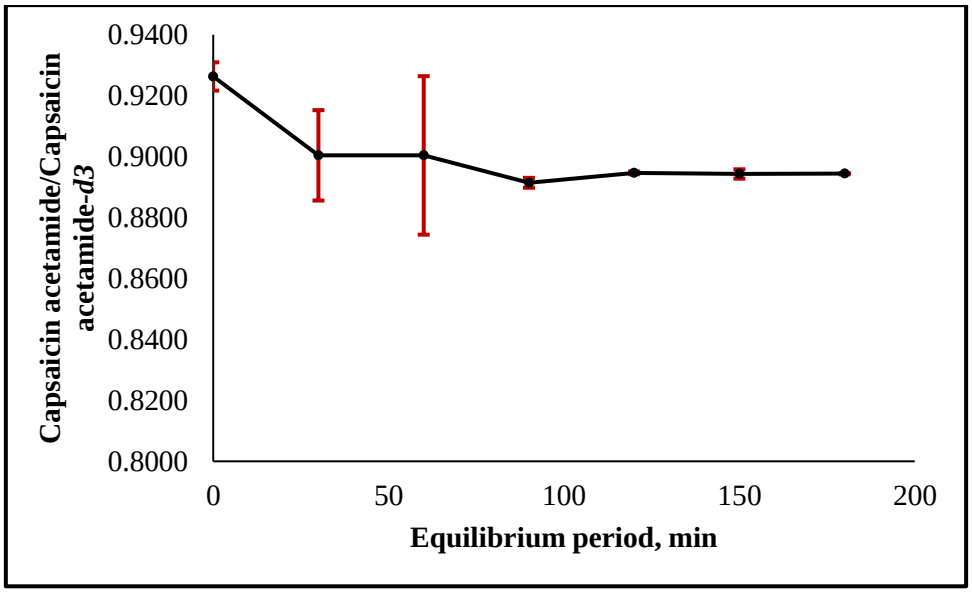


**Figure 4.50** Effect of equilibrium period for isotopes

P1, S1 and W1 samples were spiked to two different concentration levels detailed Section 3.5.5. After the preparation of sample and calibration mixtures for both concentration levels, SB-FDF-LPME-GC-MS method was performed on all mixtures. Capsaicin concentration in the spiked samples was calculated via the $ID^4$ formula given by Pagliano et. al. [18]. Capsaicin was not detected in blank solutions of wastewater and saliva samples according to blank measurements.

Table 4.23 summarizes all percent recoveries for P1, S1 and W1 samples found by SB-FDF-LPME-$ID^4$-GC-MS method. According to these results, excellent percent recoveries (94.9-104.0%) with low percent standard deviation (1.4-2.8%) values were recorded for all spiked samples. These results were better than the results obtained by SB-FDF-LPME-GC-MS method in terms of precision and accuracy. Therefore, high accurate and precise results were recorded for each matrix due to the usage of capsaicin-*d3*. Further, P2, P3 and P4 samples were analyzed by the proposed SB-FDF-LPME-$ID^4$-GC-MS method and their capsaicin concentration were determined as 1269.2±14.3, 390.6±6.6 and 208.3±6.7 mg/kg, respectively.

**Table 4.23** Percent recoveries and relative standard deviation for the ID$^4$-SFDF-LPME-GC-MS method

| Sample | Spiked concentration, µg/kg | Found concentration, | %Recovery | %RSD |
|---|---|---|---|---|
| **Banana pepper (Low Level)** | 28.69 | 27.65 | 96.4 | 2.3 |
| **Banana pepper (High Level)** | 58.15 | 55.94 | 96.2 | 1.4 |
| **Saliva (Low Level)** | 25.58 | 26.60 | 104.0 | 2.8 |
| **Saliva (High Level)** | 54.11 | 55.69 | 102.9 | 1.7 |
| **Wastewater (Low Level)** | 31.22 | 29.61 | 94.9 | 1.9 |
| **Wastewater (High Level)** | 57.89 | 55.90 | 96.6 | 1.9 |

### 4.5.5 Comparison with other studies in literature

There are several studies for the determination of capsaicin based on GC and LC systems. In 2009, solid phase microextraction–gas chromatography–mass spectrometry (SPME-GC-MS) was established by Alvarez et. al. [283]. Direct immerse SPME device was used with polydimethylsiloxane fiber. Under the optimum SPME conditions, there was linearity recorded between 0.109 and 1.323 µg/mL. LOD and LOQ values for the prosed SPME-GC-MS method were 0.014 and 0.069 µg/mL, respectively. Percent recoveries for the spiked pepper and pepper sauces were in the range of 36.1% and 88% (%RSD≤17).

Dispersive liquid–liquid microextraction (DLLME) was also used to extract capsaicin from urine sample prior to ultra-high performance liquid chromatography with high resolution mass spectrometry (UHPLC-HRMS). In this study, 1.5 mL of ethanol and 0.60 mL of methyl isobutyl ketone were used as dispersive and extraction solvents, respectively. At the end of the optimization of DLLME and UHPLC conditions, system analytical performance was evaluated by calculating LOD (1.5 μg/L) and LOQ (5.0 μg/L) for the analyte. Enrichment factor and %RSD value for the proposed method were 61 and 8.9%, respectively [284].

Lu et. al. [285] developed an analytical method in 2020 for the quantitative determination of capsaicin in soybean oil and rapeseed oil. Magnetic solid phase extraction (MSPE) was the preconcentration method to separate the analyte from complex sample matrices. Graphene oxide–$Fe_3O_4$ nanocomposite was used as adsorbent to collect the analyte found in the oil samples. Instrumental measurements were performed with ultrahigh performance liquid chromatography-tandem mass spectrometry (UHPLC-MS/MS). Based on the analytical performance studies, LOD, LOQ and LWR for target analyte were figured out to be 0.15, 0.40 and 0.4-200 μg/L, respectively. Percent recoveries for rapeseed and soybean oil samples were calculated as 71.2-84.3% and 81.2-103.3%, respectively. %RSD values were lower than 5.7% for the selected samples.

In 2012, reversed phase-HPLC with fluorescence detection was carried out for chromatographic separation and fluorometric detection of capsaicin in hot peppers. Excitation and emission wavelengths for the detection of capsaicin were 278 and 310 nm, respectively. Accelerated solvent extraction and SPE were sequentially used to extract the analyte from pepper samples. LOD and LOQ values for capsaicin in HPLC system were 0.008 and 0.01 μg/mL, respectively. Linearity was achieved between 1.0 and 25.0 μg/mL. %RSD values for repeatability and reproducibility tests were 3.99 and 4.84%, respectively. Percent recoveries for the pepper samples were ranged from 69.2 to 98.6% [286].

# 5
# CONCLUSION

The combination of HPLC and ICP-OES presented as a rapid and efficient separation for chromium (III) and chromium (VI) species in water, soil and grass samples. HPLC system was coupled to ICP-OES system by the help of plastic capillary tube from the out of column to the nebulizer part of ICP-OES system. ICP-OES and HPLC system parameters were optimized to attain high signal to noise ratio with a proper peak resolution and rapid analysis period. Under the optimum experimental conditions, LOD values were recorded as 0.27 and 0.05 mg/kg for chromium (III) and chromium (VI), respectively. Matrix matching calibration method was used to check suitability and accuracy of the developed HPLC-ICP-OES system. In addition, percent recoveries were found between 88.2 and 104.1% for water, soil and grass samples. As a results, a sensitive and accurate analytical method for chromium speciation in water, soil and grass samples was developed in the scope of this thesis.

A new method for the integration of HPLC and FAAS system was proposed to determine metal containing molecules. The proposed method was called as high-performance liquid chromatography-flame atomic absorption spectrophotometer (HPLC-FAAS) with a novel nebulizer system. Cobalamin was selected as the analyte in this study due to the presence of cobalt in cobalamin. Here, cobalamin was separated by HPLC system and then detected as cobalt by FAAS system. LOD and LOQ values were improved by optimizing several parameters such as flow rate of mobile phase, flow rate of nebulizer gas, T-SQT height from burner head, sample injection volume, pH of mobile phase, concentration of mobile phase components. Under the optimum HPLC-FAAS conditions, LOD and LOQ were recorded as 1.6 and 5.3 mg/kg cobalamin as cobalt, respectively. LWR with a good correlation coefficient ($R^2$=0.9989) was obtained for the developed system. In the final step, recovery studies were performed with the spiked vitamin drug samples to control accuracy and suitability of the proposed HPLC-FAAS system. Great recovery results close to %100 certified the accuracy and suitability of the method.

An accurate and sensitive microextraction method has been proposed for the determination of chloroquine phosphate at low concentration levels in human urine, saliva and samples. SB-FDF-LPME method was used to preconcentrate the analyte derivative from the aqueous solution. Acetic anhydride was used as the derivatizing reagent and introduced to the sample solution together with the extraction solvent. At the end of the optimization studies for the derivatization and preconcentration steps, system analytical performance study was fulfilled to determine LOD, LOQ, %RSD and LWR for the presented SB-FDF-LPME-GC-MS method. LOD, LOQ and LWR were found as 0.16, 0.53 and 0.52-49.25 mg/kg, respectively. However, the developed method did not compensate the matrix effects for the selected biofluid samples, $ID^4$ method was applied to the samples prior to SB-FDF-LPME-GC-MS method to boost the percent recoveries and eliminate the matrix effects coming from the complicated biological matrices. High percent recoveries (99.4-101%) were attained by the integration of $ID^4$ and SB-FDF-LPME-GC-MS method.

Another analytical method based on isotope dilution was developed for trace determination of hydroxychloroquine in human urine, saliva and serum samples. Acetic anhydride was also used as derivatizing agent to produce HMA derivative. Smart solvent (protonated N,N-dimethyl benzylamine) was used as extraction solvent in the preconcentration step by SSB-LPME method. Optimum conditions for SSB-LPME-GC-MS method were determined by univariate and Box Behnken Design approach. Under the optimum SSB-LPME-GC-MS conditions, LOD, LOQ, LWR and %RSD values were calculated as 0.03, 0.09, 0.11-49.38 mg/kg and 8.7%, respectively. Further, the developed method was coupled to $ID^4$ method in order to overcome heavy interference effects of the selected biological samples. Acceptable percent recoveries (99.6-101.3%) with considerably low standard deviation values ($SD \leq 1.8$) were achieved by the help of $ID^4$ and SSB-LPME-GC-MS method.

In the last study, a sensitive, rapid and accurate analytical method was established for the trace determination of capsaicin in pepper, wastewater and saliva samples. SB-FDF-LPME method was developed to derivatize and enrich the analyte in order to lower the detection limit in GC-MS system. The derivatizing agent in this study was acetic anhydride solution. Univariate optimization studies were conducted to find the optimum conditions for the extraction and derivatization steps. Under the optimum conditions, LOD, LOQ and LWR were found as 0.33, 1.10, 1.03-507

μg/kg, respectively. $ID^4$ method was used prior to SB-FDF-LPME-GC-MS method because percent recoveries and standard deviation values for SB-FDF-LPME-GC-MS method were not sufficient to obtain high accurate and precise analytical method. The spiked P1, W1 and S1 samples gave percent recoveries between 94.9 and 104%. In addition, %RSD values were ranged from 1.4 to 2.8%. These high recoveries with low %RSD values confirmed the accuracy, suitability and precision of the developed method.

Studies about $ID^4$ method provided excellent precision and accuracy for the determination of studied analytes. It reduced the matrix effects for the analytes more than matrix matching or external calibration strategies. This can be attributed to the usage of isotopic material being physically and chemically similar to the analyte and the usage of isotope ratios rather than absolute signal values. Acceptable percent recovery results were obtained due to the combination of $ID^4$ methods with the developed microextraction methods.

# REFERENCES


[1] S. D. Sarker and L. Nahar, “Hyphenated Techniques,” in *Natural Products Isolation*, Totowa, NJ: Humana Press, 2006, pp. 233–267. doi: 10.1385/1-59259-955-9:233.

[2] W. M. . Niessen, “Hyphenated Techniques, Applications of in Mass Spectrometry,” in *Encyclopedia of Spectroscopy and Spectrometry*, Elsevier, 2017, pp. 174–180. doi: 10.1016/B978-0-12-409547-2.05240-9.

[3] S.-G. Dai and C.-R. Jia, “Applications of Hyphenated Techniques in Environmental Analysis,” *Anal. Sci.*, vol. 12, no. 2, pp. 355–361, Apr. 1996, doi: 10.2116/analsci.12.355.

[4] J. Delafiori, G. Ring, and A. Furey, “Clinical applications of HPLC–ICP-MS element speciation: A review,” *Talanta*, vol. 153, pp. 306–331, Jun. 2016, doi: 10.1016/j.talanta.2016.02.035.

[5] Á. I. López-Lorente, F. Pena-Pereira, S. Pedersen-Bjergaard, V. G. Zuin, S. A. Ozkan, and E. Psillakis, “The ten principles of green sample preparation,” *TrAC Trends Anal. Chem.*, vol. 148, p. 116530, Mar. 2022, doi: 10.1016/j.trac.2022.116530.

[6] L. Ramos, “Critical overview of selected contemporary sample preparation techniques,” *J. Chromatogr. A*, vol. 1221, pp. 84–98, Jan. 2012, doi: 10.1016/j.chroma.2011.11.011.

[7] S. Bodur, S. Erarpat, Ö. F. Tutar, and S. Bakırdere, “A simple spray assisted extraction/preconcentration of cadmium from sunflower oil, olive oil and hazelnut oil samples prior to flame atomic absorption spectrometry determination,” *J. Food Compos. Anal.*, vol. 117, p. 105144, Apr. 2023, doi: 10.1016/j.jfca.2023.105144.

[8] D. S. Chormey, B. T. Zaman, N. A. Kasa, and S. Bakırdere, “Liquid phase microextraction strategies and their application in the determination of endocrine disruptive compounds in food samples,” *TrAC Trends Anal. Chem.*, vol. 128, p. 115917, Jul. 2020, doi: 10.1016/j.trac.2020.115917.

[9] Y. Dikmen, A. Güleryüz, B. Metin, S. Bodur, M. Öner, and S. Bakırdere, “A novel and rapid extraction protocol for sensitive and accurate determination of prochloraz in orange juice samples: Vortex-assisted spraying-based fine droplet formation liquid-phase microextraction before gas chromatography–mass spectrometry,” *J. Mass Spectrom.*, vol. 55, no. 10, Oct. 2020, doi: 10.1002/jms.4622.

[10] S. Bodur *et al.*, “Assessment of different isotope dilution strategies and their combination with switchable solvent-based liquid phase microextraction prior to the quantification of bisphenol A at trace levels via GC-MS,” *New J. Chem.*, vol. 44, no. 32, pp. 13685–13691, 2020, doi: 10.1039/D0NJ02706E.

[11] S. C. Moldoveanu and V. David, “Derivatization methods in GC and GC/MS,” in *Gas Chromatography-Derivatization, Sample Preparation, Application*, P. Kusch, Ed., IntechOpen, 2018, p. 9.

[12] G. B. Baker, R. T. Coutts, and A. Holt, “Derivatization with acetic anhydride:

Applications to the analysis of biogenic amines and psychiatric drugs by gas chromatography and mass spectrometry," *J. Pharmacol. Toxicol. Methods*, vol. 31, no. 3, pp. 141–148, Jun. 1994, doi: 10.1016/1056-8719(94)90076-0.

[13] V. G. Zaikin and J. M. Halket, "Derivatization in Mass Spectrometry—2. Acylation," *Eur. J. Mass Spectrom.*, vol. 9, no. 5, pp. 421–434, Oct. 2003, doi: 10.1255/ejms.576.

[14] B. Wang *et al.*, "Quantification of piperazine in chicken and pig tissues by gas chromatography–electron ionization tandem mass spectrometry employing pre-column derivatization with acetic anhydride," *J. Chromatogr. A*, vol. 1519, pp. 9–18, Oct. 2017, doi: 10.1016/j.chroma.2017.08.079.

[15] D. A. Skoog, F. J. Holler, and D. M. West, *Principles of Instrumental Analysis*, 6th ed. Cenage Learning, 2014.

[16] D. S. Chormey, Y. Karakuş, S. Karayaka, Ç. Özsöyler, A. E. Bozdoğan, and S. Bakırdere, "Multivariate optimization of dispersive liquid–liquid microextraction for the determination of paclobutrazol and triflumizole in water by GC–MS," *J. Sep. Sci.*, vol. 40, no. 23, pp. 4541–4548, Dec. 2017, doi: 10.1002/jssc.201700853.

[17] J. D. Fassett and P. J. Paulsen, "Isotope Dilution Mass Spectrometry for Accurate Elemental Analysis," *Anal. Chem.*, vol. 61, no. 10, pp. 643A-649A, May 1989, doi: 10.1021/ac00185a001.

[18] E. Pagliano, Z. Mester, and J. Meija, "Reduction of measurement uncertainty by experimental design in high-order (Double, triple, and quadruple) isotope dilution mass spectrometry: Application to GC-MS measurement of bromide," *Anal. Bioanal. Chem.*, vol. 405, no. 9, pp. 2879–2887, Mar. 2013, doi: 10.1007/s00216-013-6724-5.

[19] A. K. Shanker, "Chromium: Environmental Pollution, Health Effects and Mode of Action," in *Encyclopedia of Environmental Health*, Elsevier, 2019, pp. 624–633. doi: 10.1016/B978-0-12-409548-9.11575-1.

[20] M. Sperling, "Chromium," in *Reference Module in Chemistry, Molecular Sciences and Chemical Engineering*, Elsevier, 2014. doi: 10.1016/B978-0-12-409547-2.11125-4.

[21] S. C. Gad, "Chromium," in *Encyclopedia of Toxicology*, Elsevier, 2014, pp. 952–954. doi: 10.1016/B978-0-12-386454-3.00828-9.

[22] A. B. Fulke, A. Kotian, and M. D. Giripunje, "Marine Microbial Response to Heavy Metals: Mechanism, Implications and Future Prospect," *Bull. Environ. Contam. Toxicol.*, vol. 105, no. 2, pp. 182–197, Aug. 2020, doi: 10.1007/s00128-020-02923-9.

[23] S. Mishra and R. N. Bharagava, "Toxic and genotoxic effects of hexavalent chromium in environment and its bioremediation strategies," *J. Environ. Sci. Heal. Part C*, vol. 34, no. 1, pp. 1–32, Jan. 2016, doi: 10.1080/10590501.2015.1096883.

[24] A. Pechova and L. Pavlata, "Chromium as an essential nutrient: a review," *Vet. Med. (Praha).*, vol. 52, no. 1, pp. 1–18, Jan. 2007, doi: 10.17221/2010-VETMED.

[25] I. Moffat, N. Martinova, C. Seidel, and C. M. Thompson, "Hexavalent Chromium in Drinking Water," *J. AWWA*, vol. 110, no. 5, May 2018, doi: 10.1002/awwa.1044.

[26] J. B. Vincent, “New Evidence against Chromium as an Essential Trace Element,” *J. Nutr.*, vol. 147, no. 12, pp. 2212–2219, Dec. 2017, doi: 10.3945/jn.117.255901.

[27] G. Genchi, G. Lauria, A. Catalano, A. Carocci, and M. S. Sinicropi, “The Double Face of Metals: The Intriguing Case of Chromium,” *Appl. Sci.*, vol. 11, no. 2, p. 638, Jan. 2021, doi: 10.3390/app11020638.

[28] H. Sun, J. Brocato, and M. Costa, “Oral Chromium Exposure and Toxicity,” *Curr. Environ. Heal. Reports*, vol. 2, no. 3, pp. 295–303, Sep. 2015, doi: 10.1007/s40572-015-0054-z.

[29] S.-C. Fu *et al.*, “Cr(VI) induces ROS-mediated mitochondrial-dependent apoptosis in neuronal cells via the activation of Akt/ERK/AMPK signaling pathway,” *Toxicol. Vitr.*, vol. 65, p. 104795, Jun. 2020, doi: 10.1016/j.tiv.2020.104795.

[30] T. Pavesi and J. C. Moreira, “Mechanisms and individuality in chromium toxicity in humans,” *J. Appl. Toxicol.*, vol. 40, no. 9, pp. 1183–1197, Sep. 2020, doi: 10.1002/jat.3965.

[31] K. H. Cheung and J.-D. Gu, “Mechanism of hexavalent chromium detoxification by microorganisms and bioremediation application potential: A review,” *Int. Biodeterior. Biodegradation*, vol. 59, no. 1, pp. 8–15, Jan. 2007, doi: 10.1016/j.ibiod.2006.05.002.

[32] M. Costa, “Potential hazards of hexavalent chromate in our drinking water,” *Toxicol. Appl. Pharmacol.*, vol. 188, no. 1, pp. 1–5, Apr. 2003, doi: 10.1016/S0041-008X(03)00011-5.

[33] A. Monga, A. B. Fulke, and D. Dasgupta, “Recent developments in essentiality of trivalent chromium and toxicity of hexavalent chromium: Implications on human health and remediation strategies,” *J. Hazard. Mater. Adv.*, vol. 7, p. 100113, Aug. 2022, doi: 10.1016/j.hazadv.2022.100113.

[34] M. Pesti, Z. Gazdag, and J. BelÃ¡gyi, “In vivo interaction of trivalent chromium with yeast plasma membrane, as revealed by EPR spectroscopy,” *FEMS Microbiol. Lett.*, vol. 182, no. 2, pp. 375–380, Jan. 2000, doi: 10.1111/j.1574-6968.2000.tb08924.x.

[35] Y. Wang, H. Su, Y. Gu, X. Song, and J. Zhao, “Carcinogenicity of chromium and chemoprevention: a brief update,” *Onco. Targets. Ther.*, vol. Volume 10, pp. 4065–4079, Aug. 2017, doi: 10.2147/OTT.S139262.

[36] S. De Flora, M. Iltcheva, and R. M. Balansky, “Oral chromium(VI) does not affect the frequency of micronuclei in hematopoietic cells of adult mice and of transplacentally exposed fetuses,” *Mutat. Res. Toxicol. Environ. Mutagen.*, vol. 610, no. 1–2, pp. 38–47, Nov. 2006, doi: 10.1016/j.mrgentox.2006.06.011.

[37] A. Sharma *et al.*, “Chromium Bioaccumulation and Its Impacts on Plants: An Overview,” *Plants*, vol. 9, no. 1, p. 100, Jan. 2020, doi: 10.3390/plants9010100.

[38] D. M. Hausladen and S. Fendorf, “Hexavalent Chromium Generation within Naturally Structured Soils and Sediments,” *Environ. Sci. Technol.*, vol. 51, no. 4, pp. 2058–2067, Feb. 2017, doi: 10.1021/acs.est.6b04039.

[39] B. Dhal, H. N. Thatoi, N. N. Das, and B. D. Pandey, “Chemical and microbial remediation of hexavalent chromium from contaminated soil and mining/metallurgical solid waste: A review,” *J. Hazard. Mater.*, vol. 250–251, pp. 272–291, Apr. 2013, doi: 10.1016/j.jhazmat.2013.01.048.

[40] D. Singh, N. L. Sharma, C. K. Singh, S. K. Sarkar, I. Singh, and M. L. Dotaniya, “Effect of chromium (VI) toxicity on morpho-physiological characteristics, yield, and yield components of two chickpea (Cicer arietinum L.) varieties,” *PLoS One*, vol. 15, no. 12, p. e0243032, Dec. 2020, doi: 10.1371/journal.pone.0243032.

[41] D. Nohr and H. K. Biesalski, “Vitamin B12,” in *Reference Module in Food Science*, Elsevier, 2016. doi: 10.1016/B978-0-08-100596-5.01075-1.

[42] E. Lurz, “Vitamin B12; Absorption, Metabolism, and Deficiency,” in *Encyclopedia of Gastroenterology*, Elsevier, 2020, pp. 727–733. doi: 10.1016/B978-0-12-801238-3.11357-1.

[43] D. Nohr, H. K. Biesalski, and E. I. Back, “Vitamins|Vitamin B12,” in *Encyclopedia of Dairy Sciences*, Elsevier, 2011, pp. 675–677. doi: 10.1016/B978-0-12-374407-4.00484-2.

[44] Food and Nutrition Board, *Dietary Reference Intakes for Thiamin, Riboflavin, Niacin, Vitamin B6, Folate, Vitamin B12, Pantothenic Acid, Biotin, and Choline*. Washington, D.C.: National Academy Press, 1998.

[45] M. A. Bernard, P. A. Nakonezny, and T. M. Kashner, “The Effect of Vitamin B 12 Deficiency on Older Veterans and Its Relationship to Health,” *J. Am. Geriatr. Soc.*, vol. 46, no. 10, pp. 1199–1206, Oct. 1998, doi: 10.1111/j.1532-5415.1998.tb04534.x.

[46] S. P. Stabler, “Vitamin B 12 Deficiency,” *N. Engl. J. Med.*, vol. 368, no. 2, pp. 149–160, Jan. 2013, doi: 10.1056/NEJMcp1113996.

[47] S. P. Stabler, “Vitamin B12,” in *Present Knowledge in Nutrition*, Wiley, 2012, pp. 343–358. doi: 10.1002/9781119946045.ch22.

[48] S. M. Graham, O. M. Arvela, and G. A. Wise, “Long-term neurologic consequences of nutritional vitamin B12 deficiency in infants,” *J. Pediatr.*, vol. 121, no. 5, pp. 710–714, Nov. 1992, doi: 10.1016/S0022-3476(05)81897-9.

[49] J. Minigh, “Vitamin B12,” in *xPharm: The Comprehensive Pharmacology Reference*, Elsevier, 2007, pp. 1–6. doi: 10.1016/B978-008055232-3.62856-9.

[50] X. Luo, B. Chen, L. Ding, F. Tang, and S. Yao, “HPLC-ESI-MS analysis of Vitamin B12 in food products and in multivitamins-multimineral tablets,” *Anal. Chim. Acta*, vol. 562, no. 2, pp. 185–189, Mar. 2006, doi: 10.1016/j.aca.2006.01.073.

[51] E. Scholar, “Chloroquine,” in *xPharm: The Comprehensive Pharmacology Reference*, Elsevier, 2007, pp. 1–7. doi: 10.1016/B978-008055232-3.61444-8.

[52] M. Ramesh, S. Anitha, R. K. Poopal, and C. Shobana, “Evaluation of acute and sublethal effects of chloroquine (C18H26CIN3) on certain enzymological and histopathological biomarker responses of a freshwater fish Cyprinus carpio,” *Toxicol. Reports*, vol. 5, pp. 18–27, 2018, doi: 10.1016/j.toxrep.2017.11.006.

[53] M. Qozi and F. L. Cantrell, “Chloroquine/Hydroxychloroquine,” in *Encyclopedia of Toxicology*, Elsevier, 2014, pp. 913–915. doi: 10.1016/B978-0-12-386454-3.00710-7.

[54] F. L. Cantrell, “Chloroquine,” in *Encyclopedia of Toxicology*, Elsevier, 2005, pp. 573–574. doi: 10.1016/B0-12-369400-0/00224-6.

[55] E. Scholar, “Malaria,” in *Reference Module in Biomedical Sciences*, Elsevier,

2014. doi: 10.1016/B978-0-12-801238-3.05130-8.

[56] A. Savarino, J. R. Boelaert, A. Cassone, G. Majori, and R. Cauda, “Effects of chloroquine on viral infections: an old drug against today’s diseases,” *Lancet Infect. Dis.*, vol. 3, no. 11, pp. 722–727, Nov. 2003, doi: 10.1016/S1473-3099(03)00806-5.

[57] P. Colson, J.-M. Rolain, and D. Raoult, “Chloroquine for the 2019 novel coronavirus SARS-CoV-2,” *Int. J. Antimicrob. Agents*, vol. 55, no. 3, p. 105923, Mar. 2020, doi: 10.1016/j.ijantimicag.2020.105923.

[58] A. Cortegiani, G. Ingoglia, M. Ippolito, A. Giarratano, and S. Einav, “A systematic review on the efficacy and safety of chloroquine for the treatment of COVID-19,” *J. Crit. Care*, vol. 57, pp. 279–283, Jun. 2020, doi: 10.1016/j.jcrc.2020.03.005.

[59] S. Kamat and M. Kumari, “Repurposing Chloroquine Against Multiple Diseases With Special Attention to SARS-CoV-2 and Associated Toxicity,” *Front. Pharmacol.*, vol. 12, Apr. 2021, doi: 10.3389/fphar.2021.576093.

[60] M. Li *et al.*, “Comparison of the antiviral effect of Arbidol and Chloroquine in treating COVID-19,” *Ann. Palliat. Med.*, vol. 10, no. 3, pp. 3307–3312, Mar. 2021, doi: 10.21037/apm-21-400.

[61] X. Gao *et al.*, “Safety considerations of chloroquine in the treatment of patients with diabetes and COVID-19,” *Chem. Biol. Interact.*, vol. 361, p. 109954, Jul. 2022, doi: 10.1016/j.cbi.2022.109954.

[62] Z. Zhi, J. He, H. Hu, and X. Za, “Expert consensus on chloroquine phosphate for the treatment of novel coronavirus pneumonia,” *Chinese J. Tuberc. Respir. Dis.*, vol. 12, no. 43 (3), pp. 185–188, 2020.

[63] M. G. S. Borba *et al.*, “Effect of High vs Low Doses of Chloroquine Diphosphate as Adjunctive Therapy for Patients Hospitalized With Severe Acute Respiratory Syndrome Coronavirus 2 (SARS-CoV-2) Infection,” *JAMA Netw. Open*, vol. 3, no. 4, p. e208857, Apr. 2020, doi: 10.1001/jamanetworkopen.2020.8857.

[64] C. Axfors *et al.*, “Mortality outcomes with hydroxychloroquine and chloroquine in COVID-19 from an international collaborative meta-analysis of randomized trials,” *Nat. Commun.*, vol. 12, no. 1, p. 2349, Apr. 2021, doi: 10.1038/s41467-021-22446-z.

[65] R. C. Group *et al.*, “Effect of Hydroxychloroquine in Hospitalized Patients with Covid-19,” *N. Engl. J. Med.*, vol. 383, no. 21, pp. 2030–2040, Nov. 2020, doi: 10.1056/NEJMoa2022926.

[66] W. H. Self *et al.*, “Effect of Hydroxychloroquine on Clinical Status at 14 Days in Hospitalized Patients With COVID-19,” *JAMA*, vol. 324, no. 21, p. 2165, Dec. 2020, doi: 10.1001/jama.2020.22240.

[67] C. Saka, “Analytical Methods on Determination in Pharmaceuticals and Biological Materials of Chloroquine as Available for the Treatment of COVID-19,” *Crit. Rev. Anal. Chem.*, vol. 52, no. 1, pp. 19–34, Jan. 2022, doi: 10.1080/10408347.2020.1781592.

[68] J. B. De Sanctis, J. Charris, Z. Blanco, H. Ramírez, G. P. Martínez, and M. R. Mijares, “Molecular Mechanisms of Chloroquine and Hydroxychloroquine Used in Cancer Therapy,” *Anticancer. Agents Med. Chem.*, vol. 23, no. 10, pp. 1122–1144, Jun. 2023, doi: 10.2174/1871520622666220519102948.

[69] S. Naghipour, M. Ghodousi, S. Rahsepar, and S. Elyasi, “Repurposing of well-known medications as antivirals: hydroxychloroquine and chloroquine – from HIV-1 infection to COVID-19,” *Expert Rev. Anti. Infect. Ther.*, vol. 18, no. 11, pp. 1119–1133, Nov. 2020, doi: 10.1080/14787210.2020.1792291.

[70] “Chloroquine and hydroxychloroquine,” in *Meyler’s Side Effects of Drugs*, Elsevier, 2016, pp. 253–267. doi: 10.1016/B978-0-444-53717-1.00478-9.

[71] Z. Sahraei, M. Shabani, S. Shokouhi, and A. Saffaei, “Aminoquinolines against coronavirus disease 2019 (COVID-19): chloroquine or hydroxychloroquine,” *Int. J. Antimicrob. Agents*, vol. 55, no. 4, p. 105945, Apr. 2020, doi: 10.1016/j.ijantimicag.2020.105945.

[72] M. A. El Mhammedi *et al.*, “Current Trends in Analytical Methods for the Determination of Hydroxychloroquine and Its Application as Treatment for COVID-19,” *ChemistrySelect*, vol. 5, no. 46, pp. 14602–14612, Dec. 2020, doi: 10.1002/slct.202003361.

[73] X. Yao *et al.*, “In Vitro Antiviral Activity and Projection of Optimized Dosing Design of Hydroxychloroquine for the Treatment of Severe Acute Respiratory Syndrome Coronavirus 2 (SARS-CoV-2),” *Clin. Infect. Dis.*, vol. 71, no. 15, pp. 732–739, Jul. 2020, doi: 10.1093/cid/ciaa237.

[74] J. Liu *et al.*, “Hydroxychloroquine, a less toxic derivative of chloroquine, is effective in inhibiting SARS-CoV-2 infection in vitro,” *Cell Discov.*, vol. 6, no. 1, p. 16, Mar. 2020, doi: 10.1038/s41421-020-0156-0.

[75] J. Bajpai, A. Pradhan, A. Singh, and S. kant, “Hydroxychloroquine and COVID-19 – A narrative review,” *Indian Journal of Tuberculosis*. Tuberculosis Association of India, Jul. 2020. doi: 10.1016/j.ijtb.2020.06.004.

[76] Q. Ye, B. Wang, and J. Mao, “The pathogenesis and treatment of the `Cytokine Storm’ in COVID-19,” *J. Infect.*, vol. 80, no. 6, pp. 607–613, Jun. 2020, doi: 10.1016/j.jinf.2020.03.037.

[77] T. Y. Zhang and B. Zhong, “Meeting the potential emergency global drug supply challenge of hydroxychloroquine for COVID-19,” *Med. Drug Discov.*, vol. 5, p. 100036, Mar. 2020, doi: 10.1016/j.medidd.2020.100036.

[78] Z. CJH, Z. Z, J. S, H. S, Y. D, and Z. R, “Efficacy of hydroxychloroquine in patients with COVID-19: results ofa randomized clinical trial,” *MedRixv*, 2020, doi: https://doi.org/10.1101/2020.03.22.20040758.

[79] T. Rouamba *et al.*, “Safety of Chloroquine or Hydroxychloroquine Plus Azithromycin for the Treatment of COVID-19 Patients in Burkina Faso: An Observational Prospective Cohort Study,” *Ther. Clin. Risk Manag.*, vol. Volume 17, pp. 1187–1198, Nov. 2021, doi: 10.2147/TCRM.S330813.

[80] T. Rouamba *et al.*, “Assessment of Recovery Time, Worsening, and Death among Inpatients and Outpatients with COVID-19, Treated with Hydroxychloroquine or Chloroquine plus Azithromycin Combination in Burkina Faso,” *Int. J. Infect. Dis.*, vol. 118, pp. 224–229, May 2022, doi: 10.1016/j.ijid.2022.02.034.

[81] C. Wright, C. Ross, and N. Mc Goldrick, “Are hydroxychloroquine and chloroquine effective in the treatment of SARS-COV-2 (COVID-19)?,” *Evid. Based. Dent.*, vol. 21, no. 2, pp. 64–65, Jun. 2020, doi: 10.1038/s41432-020-0098-2.

[82] M. F. Marmor, R. E. Carr, M. Easterbrook, A. A. Farjo, and W. F. Mieler, “Recommendations on screening for chloroquine and hydroxychloroquine retinopathy,” *Ophthalmology*, vol. 109, no. 7, pp. 1377–1382, Jul. 2002, doi: 10.1016/S0161-6420(02)01168-5.

[83] I. Shah *et al.*, “Analysis of other phenolics (capsaicin, gingerol, and alkylresorcinols),” in *Recent Advances in Natural Products Analysis*, Elsevier, 2020, pp. 255–271. doi: 10.1016/B978-0-12-816455-6.00006-8.

[84] M. Hayman and P. C. A. Kam, “Capsaicin: A review of its pharmacology and clinical applications,” *Curr. Anaesth. Crit. Care*, vol. 19, no. 5–6, pp. 338–343, Oct. 2008, doi: 10.1016/j.cacc.2008.07.003.

[85] M. Reyes-Escogido, E. G. Gonzalez-Mondragon, and E. Vazquez-Tzompantzi, “Chemical and Pharmacological Aspects of Capsaicin,” *Molecules*, vol. 16, no. 2, pp. 1253–1270, Jan. 2011, doi: 10.3390/molecules16021253.

[86] G. F. Barbero, A. G. Ruiz, A. Liazid, M. Palma, J. C. Vera, and C. G. Barroso, “Evolution of total and individual capsaicinoids in peppers during ripening of the Cayenne pepper plant (Capsicum annuum L.),” *Food Chem.*, vol. 153, pp. 200–206, Jun. 2014, doi: 10.1016/j.foodchem.2013.12.068.

[87] Z. A. Al Othman, Y. B. H. Ahmed, M. A. Habila, and A. A. Ghafar, “Determination of Capsaicin and Dihydrocapsaicin in Capsicum Fruit Samples using High Performance Liquid Chromatography,” *Molecules*, vol. 16, no. 10, pp. 8919–8929, Oct. 2011, doi: 10.3390/molecules16108919.

[88] W. L. Scoville, “Note on Capsicums,” *J. Am. Pharm. Assoc.*, vol. 1, no. 5, pp. 453–454, May 1912, doi: 10.1002/jps.3080010520.

[89] R. T. Kachoosangi, G. G. Wildgoose, and R. G. Compton, “Carbon nanotube-based electrochemical sensors for quantifying the ‘heat’ of chilli peppers: the adsorptive stripping voltammetric determination of capsaicin,” *Analyst*, vol. 133, no. 7, p. 888, 2008, doi: 10.1039/b803588a.

[90] J. R. Friedman *et al.*, “Capsaicinoids: Multiple effects on angiogenesis, invasion and metastasis in human cancers,” *Biomed. Pharmacother.*, vol. 118, p. 109317, Oct. 2019, doi: 10.1016/j.biopha.2019.109317.

[91] A. E. Rosca, M. I. Iesanu, C. D. M. Zahiu, S. E. Voiculescu, A. C. Paslaru, and A.-M. Zagrean, “Capsaicin and Gut Microbiota in Health and Disease,” *Molecules*, vol. 25, no. 23, p. 5681, Dec. 2020, doi: 10.3390/molecules25235681.

[92] R. Li *et al.*, “Anti-obesity effects of capsaicin and the underlying mechanisms: a review,” *Food Funct.*, vol. 11, no. 9, pp. 7356–7370, 2020, doi: 10.1039/D0FO01467B.

[93] J. K. Mariwala *et al.*, “Accumulating evidence to support the safe and efficacious use of a proprietary blend of capsaicinoids in mediating risk factors for obesity,” *Food Sci. Nutr.*, vol. 9, no. 6, pp. 2823–2835, Jun. 2021, doi: 10.1002/fsn3.2122.

[94] K. Srinivasan, “Biological Activities of Red Pepper ( Capsicum annuum ) and Its Pungent Principle Capsaicin: A Review,” *Crit. Rev. Food Sci. Nutr.*, vol. 56, no. 9, pp. 1488–1500, Jul. 2016, doi: 10.1080/10408398.2013.772090.

[95] J. Prescott, “Effects of oral chemical irritation on tastes and flavors in frequent and infrequent users of chili,” *Physiol. Behav.*, vol. 58, no. 6, pp. 1117–1127, Dec. 1995, doi: 10.1016/0031-9384(95)02052-7.

[96] N. Yang, Q. Yang, J. Chen, and I. Fisk, “Impact of capsaicin on aroma release and perception from flavoured solutions,” *LWT*, vol. 138, p. 110613, Mar. 2021, doi: 10.1016/j.lwt.2020.110613.

[97] L. C. Murrin, “Capsaicin,” in *xPharm: The Comprehensive Pharmacology Reference*, Elsevier, 2007, pp. 1–6. doi: 10.1016/B978-008055232-3.61375-3.

[98] M. Du *et al.*, “Mitigation of the Toxicity of Capsaicin on Anaerobic Codigestion of Food Waste and Waste Activated Sludge Using Calcium Peroxide: A Comprehensive Analysis Using Computational and Biological Approaches,” *ACS Sustain. Chem. Eng.*, vol. 11, no. 4, pp. 1448–1458, Jan. 2023, doi: 10.1021/acssuschemeng.2c06015.

[99] M. Du *et al.*, “Understanding the fate and impact of capsaicin in anaerobic co-digestion of food waste and waste activated sludge,” *Water Res.*, vol. 188, p. 116539, Jan. 2021, doi: 10.1016/j.watres.2020.116539.

[100] A. Sanz-Medel, J. M. Costa, and R. Pereiro, “Atomic Spectrometry,” in *Reference Module in Chemistry, Molecular Sciences and Chemical Engineering*, Elsevier, 2013. doi: 10.1016/B978-0-12-409547-2.05348-8.

[101] P. J. Potts, “Principles of Atomic Spectroscopy,” in *Treatise on Geochemistry: Second Edition*, vol. 15, Elsevier Inc., 2013, pp. 171–180. doi: 10.1016/B978-0-08-095975-7.01411-X.

[102] J. A. C. Broekaert, “Atomic Fluorescence Spectrometry,” in *Analytical Atomic Spectrometry with Flames and Plasmas*, Wiley, 2005, pp. 332–338. doi: 10.1002/3527606653.ch7.

[103] A. K. Gilmutdinov, “Atomic Absorption, Theory,” in *Encyclopedia of Spectroscopy and Spectrometry*, Elsevier, 2017, pp. 44–51. doi: 10.1016/B978-0-12-803224-4.00100-X.

[104] C. Chagué-Goff, and H. K. Y. Wong, “14.23 Wet Chemical Methods (pH, Electrical Conductivity, Ion-Selective Electrodes, Colorimetric Analysis, Ion Chromatography, Flame Atomic Absorption Spectrometry, Inductively Coupled Plasma-Atomic Emission Spectroscopy, and Quadrupole Inductively Coupled,” in *Treatise on Geomorphology*, Elsevier, 2013, pp. 274–281. doi: 10.1016/B978-0-12-374739-6.00391-2.

[105] R. H. Worden, “ANALYTICAL METHODS | Geochemical Analysis (Including X-ray),” in *Encyclopedia of Geology*, Elsevier, 2005, pp. 54–76. doi: 10.1016/B0-12-369396-9/00096-4.

[106] S. J. Hill, “ATOMIC ABSORPTION SPECTROMETRY | Flame,” in *Reference Module in Chemistry, Molecular Sciences and Chemical Engineering*, 2013.

[107] B. Fernández, L. Lobo, and R. Pereiro, “Atomic Absorption Spectrometry: Fundamentals, Instrumentation and Capabilities,” in *Reference Module in Chemistry, Molecular Sciences and Chemical Engineering*, Elsevier, 2018. doi: 10.1016/B978-0-12-409547-2.14116-2.

[108] H. Matusiewicz, “Atom trapping and in situ preconcentration techniques for flame atomic absorption spectrometry,” *Spectrochim. Acta - Part B At. Spectrosc.*, vol. 52, no. 12, pp. 1711–1736, 1997, doi: 10.1016/S0584-8547(97)00089-X.

[109] G. Kaya and M. Yaman, “Online preconcentration for the determination of lead, cadmium and copper by slotted tube atom trap (STAT)-flame atomic absorption

spectrometry," *Talanta*, vol. 75, no. 4, pp. 1127–1133, 2008, doi: 10.1016/j.talanta.2008.01.008.

[110] R. J. Watling, "The use of a slotted quartz tube for the determination 0f arsenic, antimony, selenium and mercury," *Anal. Chim. Acta*, vol. 94, no. 1, pp. 181–186, Nov. 1977, doi: 10.1016/S0003-2670(01)83645-X.

[111] R. J. Watling, "The use of a slotted tube for the determination of lead, zinc, cadmium, bismuth, cobalt, manganese and silver by atomic absorption spectrometry," *Anal. Chim. Acta*, vol. 97, no. 2, pp. 395–398, Apr. 1978, doi: 10.1016/S0003-2670(01)93448-8.

[112] C. Lau, A. Held, R. S.- Canadian, and undefined 1976, "Sensitivity enhancements to flame AAS by use of a flame atom trap," *INC PO BOX 148, MORIN Height.*, Accessed: Aug. 11, 2018. [Online]. Available: https://scholar.google.com.tr/scholar?hl=tr&as_sdt=0%2C5&q=Lau%2C+C.%2C+Held%2C+A.%2C+Stephens%2C+R.+1976.+Sensitivity+enhancements+to+flame+AAS+by+use+of+a+flame+atom+trap.+Can.+J.+Spectrocs.%2C+21%3A100-104.%29.++&btnG=

[113] H. Matusiewicz and M. Kopras, "Methods for improving the sensitivity in atom trapping flame atomic absorption spectrometry: Analytical scheme for the direct determination of trace elements in beer," *J. Anal. At. Spectrom.*, vol. 12, no. 11, pp. 1287–1291, 1997, doi: 10.1039/a704407k.

[114] N. Ertaş, D. K. Korkmaz, S. Kumser, and O. Y. Ataman, "Novel traps and atomization techniques for flame AAS," *J. Anal. At. Spectrom.*, vol. 17, no. 10, pp. 1415–1420, 2002, doi: 10.1039/B206363H.

[115] Y. Arslan, E. Kendüzler, and O. Y. Ataman, "Indium determination using slotted quartz tube-atom trap-flame atomic absorption spectrometry and interference studies," *Talanta*, vol. 85, no. 4, pp. 1786–1791, 2011, doi: 10.1016/j.talanta.2011.07.006.

[116] I. Demirtaş, S. Bakirdere, and O. Y. Ataman, "Lead determination at ng/mL level by flame atomic absorption spectrometry using a tantalum coated slotted quartz tube atom trap," *Talanta*, vol. 138, pp. 218–224, 2015, doi: 10.1016/j.talanta.2015.02.044.

[117] H. Uslu *et al.*, "A novel analytical method for sensitive determination of lead: Hydrogen assisted T-shape slotted quartz tube-atom trap-flame atomic absorption spectrometry," *Microchem. J.*, vol. 137, pp. 155–159, 2018, doi: 10.1016/j.microc.2017.10.015.

[118] E. Yazıcı, Ç. Büyükpınar, S. Bodur, N. San, O. T. Komesli, and S. Bakırdere, "Ultrasonic assisted glass bead loaded gas liquid separator-photochemical vapor generation-T-shaped slotted quartz tube-flame atomic absorption spectrophotometry system for antimony determination in tap water and wastewater samples," *Chem. Pap.*, vol. 75, no. 4, pp. 1377–1386, Apr. 2021, doi: 10.1007/s11696-020-01392-y.

[119] S. L. Bonchin, G. K. Zoorob, and J. A. Caruso, "Atomic Emission Spectrometry|Methods and Instrumentation," in *Reference Module in Chemistry, Molecular Sciences and Chemical Engineering Encyclopedia of Analytical Science (Third Edition)*, 2017. doi: https://doi.org/10.1016/B978-0-08-101983-2.00101-8.

[120] U. J. Krull and M. Thompson, “Analytical Chemistry,” in *Reference Module in Chemistry, Molecular Sciences and Chemical Engineering*, Elsevier, 2013. doi: 10.1016/B978-0-12-409547-2.05433-0.

[121] R. S. Khandpur, “Inductively Coupled Plasma Optical Emission Spectrometer (ICP-OES),” in *Compendium of Biomedical Instrumentation*, Wiley, 2020, pp. 1057–1062. doi: 10.1002/9781119288190.ch196.

[122] A. Montaser, *Inductively Coupled Plasma Mass Spectrometry*. New York: Wiley-VCH, 1998.

[123] J. R. Dean, “The Inductively Coupled Plasma,” in *Practical Inductively Coupled Plasma Spectrometry*, Wiley, 2019, pp. 95–108. doi: 10.1002/9781119478775.ch5.

[124] M. L. Fernández-Sánchez, “Optical Atomic Emission Spectrometry—Inductively Coupled Plasma,” in *Reference Module in Chemistry, Molecular Sciences and Chemical Engineering*, Elsevier, 2018. doi: 10.1016/B978-0-12-409547-2.14542-1.

[125] C. F. Poole, “Chromatography,” in *Reference Module in Chemistry, Molecular Sciences and Chemical Engineering*, Elsevier, 2018. doi: 10.1016/B978-0-12-409547-2.04396-1.

[126] V. G. Berezkin, “Gas Chromatography/Gas–Solid Chromatography,” in *Reference Module in Chemistry, Molecular Sciences and Chemical Engineering*, Elsevier, 2018. doi: 10.1016/B978-0-12-409547-2.14102-2.

[127] R. A. Shellie, “Gas Chromatography,” in *Encyclopedia of Forensic Sciences*, Elsevier, 2013, pp. 579–585. doi: 10.1016/B978-0-12-382165-2.00245-2.

[128] A. Kuksis, “Gas Chromatography☆,” in *Reference Module in Chemistry, Molecular Sciences and Chemical Engineering*, Elsevier, 2015. doi: 10.1016/B978-0-12-409547-2.04805-8.

[129] E. Stauffer, J. A. Dolan, and R. Newman, “Gas Chromatography and Gas Chromatography—Mass Spectrometry,” in *Fire Debris Analysis*, Elsevier, 2008, pp. 235–293. doi: 10.1016/B978-012663971-1.50012-9.

[130] Y. Han, Y. Zhang, and H. Liu, “Gas Chromatography: Principles,” in *Reference Module in Chemistry, Molecular Sciences and Chemical Engineering*, Elsevier, 2017. doi: 10.1016/B978-0-12-409547-2.14348-3.

[131] C. F. Poole, “Gas Chromatography Detectors,” in *Reference Module in Chemistry, Molecular Sciences and Chemical Engineering*, Elsevier, 2016. doi: 10.1016/B978-0-12-409547-2.11719-6.

[132] C. F. Poole, “Ionization-based detectors for gas chromatography,” *J. Chromatogr. A*, vol. 1421, pp. 137–153, Nov. 2015, doi: 10.1016/j.chroma.2015.02.061.

[133] H. Jing and A. Amirav, “Pulsed flame photometric detector – a step forward towards universal heteroatom selective detection,” *J. Chromatogr. A*, vol. 805, no. 1–2, pp. 177–215, May 1998, doi: 10.1016/S0021-9673(97)01306-X.

[134] P. Campíns-Falcó, R. Herráez-Hernández, and P. Serra-Mora, “Liquid Chromatography—Instrumentation,” in *Reference Module in Chemistry, Molecular Sciences and Chemical Engineering*, Elsevier, 2018. doi: 10.1016/B978-0-12-409547-2.14218-0.

[135] P. N. Nesterenko and M. D. Palamareva, “Liquid Chromatography: Overview,” in *Reference Module in Chemistry, Molecular Sciences and Chemical Engineering*, Elsevier, 2018. doi: 10.1016/B978-0-12-409547-2.14214-3.

[136] I. Halász and I. Sebestian, “New Stationary Phase for Chromatography,” *Angew. Chemie Int. Ed. English*, vol. 8, no. 6, pp. 453–454, Jun. 1969, doi: 10.1002/anie.196904531.

[137] C. G. Horvath and S. R. Lipsky, “Peak capacity in chromatography,” *Anal. Chem.*, vol. 39, no. 14, pp. 1893–1893, Dec. 1967, doi: 10.1021/ac50157a075.

[138] P. N. Nesterenko and M. D. Palamareva, “Liquid Chromatography: Principles,” in *Reference Module in Chemistry, Molecular Sciences and Chemical Engineering*, Elsevier, 2018. doi: 10.1016/B978-0-12-409547-2.14215-5.

[139] H. Gika, G. Kaklamanos, P. Manesiotis, and G. Theodoridis, “Chromatography: High-Performance Liquid Chromatography,” in *Encyclopedia of Food and Health*, Elsevier, 2016, pp. 93–99. doi: 10.1016/B978-0-12-384947-2.00159-8.

[140] L. Bhattacharyya, “Ion Chromatography—Principles and Applications,” in *Applications of Ion Chromatography for Pharmaceutical and Biological Products*, Wiley, 2012, pp. 1–21. doi: 10.1002/9781118147009.ch1.

[141] B. Paull and R. Michalski, “Ion Exchange: Ion Chromatography Principles and Applications,” in *Reference Module in Chemistry, Molecular Sciences and Chemical Engineering*, Elsevier, 2018. doi: 10.1016/B978-0-12-409547-2.14502-0.

[142] P. N. Nesterenko, “Ion Exchange—Overview,” in *Reference Module in Chemistry, Molecular Sciences and Chemical Engineering*, Elsevier, 2018. doi: 10.1016/B978-0-12-409547-2.14440-3.

[143] C. A. Pohl, “Mechanisms: Ion Chromatography,” in *Reference Module in Chemistry, Molecular Sciences and Chemical Engineering*, Elsevier, 2016. doi: 10.1016/B978-0-12-409547-2.11724-X.

[144] J. R. Torres-Lapasió and M. C. García-Alvarez-Coque, “Liquid Chromatography: Strategies for Optimization,” in *Reference Module in Chemistry, Molecular Sciences and Chemical Engineering*, Elsevier, 2018. doi: 10.1016/B978-0-12-409547-2.14499-3.

[145] R. Waddell Smith, “Mass Spectrometry,” in *Encyclopedia of Forensic Sciences, Third Edition*, Elsevier, 2023, pp. 464–473. doi: 10.1016/B978-0-12-823677-2.00054-4.

[146] M. Schäfer, “Mass Spectrometry: Fundamentals and Instrumentation,” in *Reference Module in Chemistry, Molecular Sciences and Chemical Engineering*, Elsevier, 2018. doi: 10.1016/B978-0-12-409547-2.11258-2.

[147] F. A. Mellon, “MASS SPECTROMETRY | Principles and Instrumentation,” in *Encyclopedia of Food Sciences and Nutrition*, Elsevier, 2003, pp. 3739–3749. doi: 10.1016/B0-12-227055-X/00746-X.

[148] G. Kaklamanos, E. Aprea, and G. Theodoridis, “Mass Spectrometry: Principles and Instrumentation,” in *Encyclopedia of Food and Health*, Elsevier, 2016, pp. 661–668. doi: 10.1016/B978-0-12-384947-2.00447-5.

[149] C. H. Hocart, “Mass Spectrometry: An Essential Tool for Trace Identification and

Quantification," in *Comprehensive Natural Products II*, Elsevier, 2010, pp. 327–388. doi: 10.1016/B978-008045382-8.00187-8.

[150] A. Maccoll, "Mass Spectrometry, Historical Perspective," in *Encyclopedia of Spectroscopy and Spectrometry*, Elsevier, 2017, pp. 742–747. doi: 10.1016/B978-0-12-803224-4.00197-7.

[151] A. M. Haag, "Mass Analyzers and Mass Spectrometers," in *Modern Proteomics – Sample Preparation, Analysis and Practical Applications. Advances in Experimental Medicine and Biology*, 2016, pp. 157–169. doi: 10.1007/978-3-319-41448-5_7.

[152] T. Hirschfeld, "The hy-phen-ated methods," *Anal. Chem.*, vol. 52, no. 2, pp. 297A-312A, 1980.

[153] R. R. Joshi, K. R. Gupta, and S. S. Patil, "Hyphenated technique-A boon to analytical world," *Int. J. Pharm. Sci. Res.*, vol. 3, no. 11, p. 4184, 2012.

[154] K. N. Patel, J. K. Patel, M. P. Patel, G. C. Rajput, and H. A. Patel, "Introduction to hyphenated techniques and their applications in pharmacy," *Pharm. Methods*, vol. 1, no. 1, pp. 2–13, Oct. 2010, doi: 10.1016/S2229-4708(10)11002-4.

[155] W. M. . Niessen, "Hyphenated Techniques, Applications of in Mass Spectrometry," in *Encyclopedia of Spectroscopy and Spectrometry*, Elsevier, 2010, pp. 984–989. doi: 10.1016/B978-0-12-374413-5.00169-X.

[156] S. Nagajyothi, Y. Swetha, J. Neeharika, P. V. Suresh, and N. Ramarao, "Hyphenated techniques-a comprehensive review," *Int. J. Adv. Res. Dev.*, vol. 2, p. 4, 2017.

[157] D. L. Norwood, J. O. Mullis, and T. N. Feinberg, "Hyphenated techniques," in *Separation Science and Technology*, 2007, pp. 189–235. doi: 10.1016/S0149-6395(07)80013-4.

[158] O. Nygren, C. A. Nilsson, and W. Frech, "On-line interfacing of a liquid chromatograph to a continuously heated graphite furnace atomic absorption spectrophotometer for element-specific detection," *Anal. Chem.*, vol. 60, no. 20, pp. 2204–2208, 1988.

[159] J. S. Blais and W. D. Marshall, "Determination of ionic alkyllead compounds in water, soil and sediment by high-performance liquid chromatography-quartz tube atomic absorption spectrometry," *J. Anal. At. Spectrom.*, vol. 4, no. 3, p. 271, 1989, doi: 10.1039/ja9890400271.

[160] P. J. Parsons and F. Barbosa, "Atomic spectrometry and trends in clinical laboratory medicine," *Spectrochim. Acta Part B At. Spectrosc.*, vol. 62, no. 9, pp. 992–1003, Sep. 2007, doi: 10.1016/j.sab.2007.03.007.

[161] R. Cornelis, J. Caruso, H. Crews, and K. Heumann, *Handbook of Elemental Speciation: Techniques and Methodology*. Wiley, 2003. doi: 10.1002/0470868384.

[162] R. Cornelis, J. Caruso, H. Crews, and K. Heumann, *Handbook of Elemental Speciation II – Species in the Environment, Food, Medicine and Occupational Health*. Wiley, 2005. doi: 10.1002/0470856009.

[163] C. Douvris, T. Vaughan, D. Bussan, G. Bartzas, and R. Thomas, "How ICP-OES changed the face of trace element analysis: Review of the global application landscape," *Sci. Total Environ.*, vol. 905, p. 167242, Dec. 2023, doi:

10.1016/j.scitotenv.2023.167242.

[164] J. Proch and P. Niedzielski, “Iron species determination by high performance liquid chromatography with plasma based optical emission detectors: HPLC–MIP OES and HPLC–ICP OES,” *Talanta*, vol. 231, p. 122403, Aug. 2021, doi: 10.1016/j.talanta.2021.122403.

[165] M. B. Amran, F. Lagarde, and M. J. F. Leroy, “Determination of arsenic species in marine organisms by HPLC-ICP-OES and HPLC-HG-QFAAS,” *Mikrochim. Acta*, vol. 127, no. 3–4, pp. 195–202, Sep. 1997, doi: 10.1007/BF01242722.

[166] M. Hu and P. P. Coetzee, “Method for vanadium speciation in aqueous samples by HPLC-ICP-OES,” *South African J. Chem.*, vol. 60, pp. 113–117, 2007.

[167] S. Bodur, S. Erarpat, U. Balçık, and S. Bakırdere, “A rapid, sensitive and accurate determination of cobalamin with double monitoring system: HPLC-UV and HPLC-ICP-OES,” *Food Chem.*, vol. 340, p. 127945, Mar. 2021, doi: 10.1016/j.foodchem.2020.127945.

[168] S. N. Atapattu and J. M. Rosenfeld, “Solid phase analytical derivatization as a sample preparation method,” *J. Chromatogr. A*, vol. 1296, pp. 204–213, Jun. 2013, doi: 10.1016/j.chroma.2013.03.020.

[169] A. Przyjazny, “Liquid-Phase Microextraction,” in *Reference Module in Chemistry, Molecular Sciences and Chemical Engineering*, Elsevier, 2017. doi: 10.1016/B978-0-12-409547-2.12678-2.

[170] Y. Chen, Z. Guo, X. Wang, and C. Qiu, “Sample preparation,” *J. Chromatogr. A*, vol. 1184, no. 1–2, pp. 191–219, Mar. 2008, doi: 10.1016/J.CHROMA.2007.10.026.

[171] A. Aly and T. Górecki, “Green Approaches to Sample Preparation Based on Extraction Techniques,” *Molecules*, vol. 25, no. 7, p. 1719, Apr. 2020, doi: 10.3390/molecules25071719.

[172] C. F. Poole, “EXTRACTION | Solid-Phase Extraction,” in *Reference Module in Chemistry, Molecular Sciences and Chemical Engineering*, Elsevier, 2016. doi: 10.1016/B978-0-12-409547-2.12175-4.

[173] S. Salve, Y. Bahiram, A. Jadhav, R. Rathod, and R. K. Tekade, “Nanoplatform-Integrated Miniaturized Solid-Phase Extraction Techniques: A Critical Review,” *Crit. Rev. Anal. Chem.*, vol. 53, no. 1, pp. 46–68, Jan. 2023, doi: 10.1080/10408347.2021.1934651.

[174] B. Buszewski and M. Szultka, “Past, Present, and Future of Solid Phase Extraction: A Review,” *Crit. Rev. Anal. Chem.*, vol. 42, no. 3, pp. 198–213, Jul. 2012, doi: 10.1080/07373937.2011.645413.

[175] N. M. Rice, H. M. N. H. Irving, and M. A. Leonard, “Nomenclature for liquid-liquid distribution (solvent extraction) (IUPAC Recommendations 1993),” *Pure Appl. Chem.*, vol. 65, no. 11, pp. 2373–2396, Jan. 1993, doi: 10.1351/pac199365112373.

[176] R. E. Clement and C. Hao, “Liquid–Liquid Extraction,” in *Comprehensive Sampling and Sample Preparation*, Elsevier, 2012, pp. 51–63. doi: 10.1016/B978-0-12-381373-2.00063-6.

[177] M. Rutkowska, J. Płotka-Wasylka, M. Sajid, and V. Andruch, “Liquid–phase

microextraction: A review of reviews," *Microchem. J.*, vol. 149, p. 103989, Sep. 2019, doi: 10.1016/j.microc.2019.103989.

[178] Y. Yamini, M. Rezazadeh, and S. Seidi, "Liquid-phase microextraction – The different principles and configurations," *TrAC - Trends Anal. Chem.*, vol. 112, pp. 264–272, Mar. 2018, doi: 10.1016/j.trac.2018.06.010.

[179] M. Rezaee, Y. Assadi, M.-R. Milani Hosseini, E. Aghaee, F. Ahmadi, and S. Berijani, "Determination of organic compounds in water using dispersive liquid–liquid microextraction," *J. Chromatogr. A*, vol. 1116, no. 1–2, pp. 1–9, May 2006, doi: 10.1016/J.CHROMA.2006.03.007.

[180] A. Zgoła-Grześkowiak and T. Grześkowiak, "Dispersive liquid-liquid microextraction," *TrAC Trends Anal. Chem.*, vol. 30, no. 9, pp. 1382–1399, Oct. 2011, doi: 10.1016/j.trac.2011.04.014.

[181] J. L. Pérez Pavón, S. Herrero Martín, C. García Pinto, and B. Moreno Cordero, "Determination of trihalomethanes in water samples: A review," *Anal. Chim. Acta*, vol. 629, no. 1–2, pp. 6–23, Nov. 2008, doi: 10.1016/j.aca.2008.09.042.

[182] M. Saraji and M. K. Boroujeni, "Recent developments in dispersive liquid–liquid microextraction," *Anal. Bioanal. Chem.*, vol. 406, no. 8, pp. 2027–2066, Mar. 2014, doi: 10.1007/s00216-013-7467-z.

[183] S. Ozcan, A. Tor, and M. E. Aydin, "Determination of polycyclic aromatic hydrocarbons in waters by ultrasound-assisted emulsification-microextraction and gas chromatography–mass spectrometry," *Anal. Chim. Acta*, vol. 665, no. 2, pp. 193–199, Apr. 2010, doi: 10.1016/j.aca.2010.03.047.

[184] S.-Y. Wei, M.-I. Leong, Y. Li, and S.-D. Huang, "Development of liquid phase microextraction based on manual shaking and ultrasound-assisted emulsification method for analysis of organochlorine pesticides in aqueous samples," *J. Chromatogr. A*, vol. 1218, no. 51, pp. 9142–9148, Dec. 2011, doi: 10.1016/j.chroma.2011.10.084.

[185] J. Cheng, G. Matsadiq, L. Liu, Y.-W. Zhou, and G. Chen, "Development of a novel ultrasound-assisted surfactant-enhanced emulsification microextraction method and its application to the analysis of eleven polycyclic aromatic hydrocarbons at trace levels in water," *J. Chromatogr. A*, vol. 1218, no. 18, pp. 2476–2482, May 2011, doi: 10.1016/j.chroma.2011.02.049.

[186] X. You, S. Wang, F. Liu, and K. Shi, "Ultrasound-assisted surfactant-enhanced emulsification microextraction based on the solidification of a floating organic droplet used for the simultaneous determination of six fungicide residues in juices and red wine," *J. Chromatogr. A*, vol. 1300, pp. 64–69, Jul. 2013, doi: 10.1016/j.chroma.2013.02.038.

[187] G. Lasarte-Aragonés, R. Lucena, S. Cárdenas, and M. Valcárcel, "Effervescence assisted dispersive liquid–liquid microextraction with extractant removal by magnetic nanoparticles," *Anal. Chim. Acta*, vol. 807, pp. 61–66, Jan. 2014, doi: 10.1016/j.aca.2013.11.029.

[188] M. A. Farajzadeh and M. R. A. Mogaddam, "Air-assisted liquid–liquid microextraction method as a novel microextraction technique; Application in extraction and preconcentration of phthalate esters in aqueous sample followed by gas chromatography–flame ionization detection," *Anal. Chim. Acta*, vol. 728, pp.

31–38, May 2012, doi: 10.1016/j.aca.2012.03.031.

[189] S. Topal, M. Şaylan, B. T. Zaman, and S. Bakırdere, "Determination of trace cadmium in saliva samples using spray assisted droplet formation-liquid phase microextraction prior to the measurement by slotted quartz tube-flame atomic absorption spectrophotometry," *J. Trace Elem. Med. Biol.*, vol. 68, p. 126859, Dec. 2021, doi: 10.1016/j.jtemb.2021.126859.

[190] P. N. Diridiri, S. E. Bodur, A. Bayraktar, Ö. T. Günkara, and S. Bakırdere, "Determination of copper ion at trace levels in apple tea samples by simultaneous complexation and spray assisted microextraction method prior to detection by flame atomic absorption spectrophotometry," *Food Chem.*, vol. 441, p. 138243, May 2024, doi: 10.1016/j.foodchem.2023.138243.

[191] O. Sağsöz, B. Arvas, B. T. Zaman, Ç. Yolaçan, and S. Bakırdere, "Determination of trace cobalt ions in bottled drinking water samples from Fiji Island by spray-assisted fine droplet formation-liquid phase microextraction based on simultaneous complexation and extraction before flame atomic absorption spectrometer measu," *Environ. Monit. Assess.*, vol. 195, no. 2, p. 313, Feb. 2023, doi: 10.1007/s10661-023-10943-1.

[192] S. Oflu, S. Erarpat, B. T. Zaman, Ö. T. Günkara, S. Bakırdere, and F. Turak, "Combination of quadrupole isotope dilution mass spectrometry with simultaneous derivatization and spray assisted droplet formation-liquid phase microextraction for the determination of methamphetamine in human urine and serum samples by gas chromatography," *J. Pharmacol. Toxicol. Methods*, vol. 119, p. 107207, Jan. 2023, doi: 10.1016/j.vascn.2022.107207.

[193] S. Oflu *et al.*, "Quantification of trace fenuron in waste water samples by matrix matching calibration strategy and gas chromatography–mass spectrometry after simultaneous derivatization and preconcentration," *Environ. Monit. Assess.*, vol. 195, no. 9, p. 1063, Sep. 2023, doi: 10.1007/s10661-023-11575-1.

[194] S. Bodur, S. Erarpat, Ö. F. Tutar, and S. Bakırdere, "Spray assisted preconcentration method combined with HPLC – Continuous flow hydride generation – FAAS for inorganic arsenic speciation in olive oil samples," *J. Food Compos. Anal.*, vol. 123, p. 105531, Oct. 2023, doi: 10.1016/j.jfca.2023.105531.

[195] M. Shirani, M. Faraji, and M. Soylak, "Microextraction in food and beverage: Applications of food and beverages by liquid-liquid microextraction," in *Reference Module in Chemistry, Molecular Sciences and Chemical Engineering*, Elsevier, 2023. doi: 10.1016/B978-0-443-15978-7.00003-5.

[196] R. A. Sheldon, "Metrics of Green Chemistry and Sustainability: Past, Present, and Future," *ACS Sustain. Chem. Eng.*, vol. 6, no. 1, pp. 32–48, Jan. 2018, doi: 10.1021/acssuschemeng.7b03505.

[197] K. Sood, Y. Saini, and K. K. Thakur, "Ionic liquids in catalysis: A review," *Mater. Today Proc.*, vol. 81, pp. 739–744, 2023, doi: 10.1016/j.matpr.2021.04.225.

[198] A. Shishov, A. Pochivalov, L. Nugbienyo, V. Andruch, and A. Bulatov, "Deep eutectic solvents are not only effective extractants," *TrAC Trends Anal. Chem.*, vol. 129, p. 115956, Aug. 2020, doi: 10.1016/j.trac.2020.115956.

[199] G. Lestari, M. Alizadehgiashi, M. Abolhasani, and E. Kumacheva, "Study of Extraction and Recycling of Switchable Hydrophilicity Solvents in an Oscillatory

Microfluidic Platform," *ACS Sustain. Chem. Eng.*, vol. 5, no. 5, pp. 4304–4310, May 2017, doi: 10.1021/acssuschemeng.7b00339.

[200] P. G. Jessop, D. J. Heldebrant, X. Li, C. A. Eckert, and C. L. Liotta, "Reversible nonpolar-to-polar solvent," *Nature*, vol. 436, no. 7054, pp. 1102–1102, Aug. 2005, doi: 10.1038/4361102a.

[201] U. Alshana, M. Hassan, M. Al-Nidawi, E. Yilmaz, and M. Soylak, "Switchable-hydrophilicity solvent liquid-liquid microextraction," *TrAC Trends Anal. Chem.*, vol. 131, p. 116025, Oct. 2020, doi: 10.1016/j.trac.2020.116025.

[202] Y. Zhang, R. Fu, Q. Lu, T. Ren, X. Guo, and X. Di, "Switchable hydrophilicity solvent for extraction of pollutants in food and environmental samples: A review," *Microchem. J.*, vol. 189, p. 108566, Jun. 2023, doi: 10.1016/j.microc.2023.108566.

[203] J. R. Vanderveen, J. Durelle, and P. G. Jessop, "Design and evaluation of switchable-hydrophilicity solvents," *Green Chem.*, vol. 16, no. 3, pp. 1187–1197, Feb. 2014, doi: 10.1039/c3gc42164c.

[204] G. Lasarte-Aragonés, R. Lucena, S. Cárdenas, and M. Valcárcel, "Use of switchable solvents in the microextraction context," *Talanta*, vol. 131, pp. 645–649, Jan. 2015, doi: 10.1016/j.talanta.2014.08.031.

[205] B. Y. Durak, D. S. Chormey, M. Firat, and S. Bakirdere, "Validation of ultrasonic-assisted switchable solvent liquid phase microextraction for trace determination of hormones and organochlorine pesticides by GC–MS and combination with QuEChERS," *Food Chem.*, vol. 305, p. 125487, Feb. 2020, doi: 10.1016/j.foodchem.2019.125487.

[206] Z. Tekin, S. Erarpat, A. Şahin, D. Selali Chormey, and S. Bakırdere, "Determination of Vitamin B12 and cobalt in egg yolk using vortex assisted switchable solvent based liquid phase microextraction prior to slotted quartz tube flame atomic absorption spectrometry," *Food Chem.*, vol. 286, pp. 500–505, Jul. 2019, doi: 10.1016/J.FOODCHEM.2019.02.036.

[207] S. K. Shahvandi, M. H. Banitaba, H. Ahmar, and P. Karimi, "A novel temperature controlled switchable solvent based microextraction method: Application for the determination of phthalic acid esters in water samples," *Microchem. J.*, vol. 152, p. 104300, Jan. 2020, doi: 10.1016/j.microc.2019.104300.

[208] S. Li *et al.*, "Sensitive determination of polychlorinated biphenyls from beverages based on switchable solvent microextraction: A robust methodology," *Chemosphere*, vol. 297, p. 134185, Jun. 2022, doi: 10.1016/j.chemosphere.2022.134185.

[209] M. Niwa, "Derivatization and Labeling Techniques," in *Reference Module in Chemistry, Molecular Sciences and Chemical Engineering*, Elsevier, 2018. doi: 10.1016/B978-0-12-409547-2.13970-8.

[210] F. Orata, *Derivatization reactions and reagents for gas chromatography analysis. Advanced gas chromatography-Progress in agricultural, biomedical and industrial applications*. 2012.

[211] D. R. Parkinson, "Analytical Derivatization Techniques," *Ref. Modul. Chem. Mol. Sci. Chem. Eng.*, Jan. 2014, doi: 10.1016/B978-0-12-409547-2.11454-4.

[212] S. Görög, "Derivatization of Analytes," in *Reference Module in Chemistry, Molecular Sciences and Chemical Engineering*, Elsevier, 2018. doi:

10.1016/B978-0-12-409547-2.14229-5.

[213] H. Kataoka, “Amines: Gas Chromatography,” in *Reference Module in Chemistry, Molecular Sciences and Chemical Engineering*, Elsevier, 2014. doi: 10.1016/B978-0-12-409547-2.10941-2.

[214] S. Görög, “Derivatization of Analytes,” in *Reference Module in Chemistry, Molecular Sciences and Chemical Engineering*, Elsevier, 2019, pp. 42–52. doi: 10.1016/B978-0-12-409547-2.14229-5.

[215] R. Michalski, M. Jabłońska-Czapla, A. Łyko, and S. Szopa, “Hyphenated Methods for Speciation Analysis,” in *Encyclopedia of Analytical Chemistry*, Wiley, 2000, pp. 1–17. doi: 10.1002/9780470027318.a9291.

[216] D. M. Templeton *et al.*, “Guidelines for terms related to chemical speciation and fractionation of elements. Definitions, structural aspects, and methodological approaches (IUPAC Recommendations 2000),” *Pure Appl. Chem.*, vol. 72, no. 8, pp. 1453–1470, Jan. 2000, doi: 10.1351/pac200072081453.

[217] A. Gonzalvez, M. L. Cervera, S. Armenta, and M. de la Guardia, “A review of non-chromatographic methods for speciation analysis,” *Anal. Chim. Acta*, vol. 636, no. 2, pp. 129–157, Mar. 2009, doi: 10.1016/j.aca.2009.01.065.

[218] O. F. X. Donard and J. A. Caruso, “Trace metal and metalloid species determination: evolution and trends,” *Spectrochim. Acta Part B At. Spectrosc.*, vol. 53, no. 2, pp. 157–163, Feb. 1998, doi: 10.1016/S0584-8547(98)00092-5.

[219] L. Liu, B. He, Z. Yun, J. Sun, and G. Jiang, “Speciation analysis of arsenic compounds by capillary electrophoresis on-line coupled with inductively coupled plasma mass spectrometry using a novel interface,” *J. Chromatogr. A*, vol. 1304, pp. 227–233, Aug. 2013, doi: 10.1016/j.chroma.2013.07.034.

[220] D. Templeton, “Speciation in Metal Toxicity and Metal-Based Therapeutics,” *Toxics*, vol. 3, no. 2, pp. 170–186, Apr. 2015, doi: 10.3390/toxics3020170.

[221] A. Olushola Sunday, B. Abdullahi Alafara, and O. Godwin Oladele, “Toxicity and speciation analysis of organotin compounds,” *Chem. Speciat. Bioavailab.*, vol. 24, no. 4, pp. 216–226, Jan. 2012, doi: 10.3184/095422912X13491962881734.

[222] A. Kot and J. Namiesnik, “The role of speciation in analytical chemistry,” *TrAC Trends Anal. Chem.*, vol. 19, no. 2–3, pp. 69–79, Mar. 2000, doi: 10.1016/S0165-9936(99)00195-8.

[223] G. E. Batley and S. C. Apte, “Elemental Speciation in Waters, Sediments, and Soils,” in *Reference Module in Chemistry, Molecular Sciences and Chemical Engineering*, Elsevier, 2017. doi: 10.1016/B978-0-12-409547-2.14264-7.

[224] S. Bakirdere, Ed., *Speciation Studies in Soil, Sediment and Environmental Samples*. CRC Press, 2013. doi: 10.1201/b15501.

[225] C. Reimann, A. Grimstvedt, B. Frengstad, and T. E. Finne, “White HDPE bottles as source of serious contamination of water samples with Ba and Zn,” *Sci. Total Environ.*, vol. 374, no. 2–3, pp. 292–296, Mar. 2007, doi: 10.1016/j.scitotenv.2006.12.035.

[226] R. Cornelis, J. Caruso, H. Crews, and K. Heumann, *Handbook of elemental speciation, Handbook of elemental speciation II: Species in the environment, food, medicine and occupational health*. Wiley, 2005. doi: 10.1002/0470856009.

[227] J. N. Kamau, “Elemental Speciation—Overview,” in *Reference Module in Chemistry, Molecular Sciences and Chemical Engineering*, Elsevier, 2018. doi: 10.1016/B978-0-12-409547-2.14386-0.

[228] P. Rodríguez-González, J. M. Marchante-Gayón, J. I. García Alonso, and A. Sanz-Medel, “Isotope dilution analysis for elemental speciation: a tutorial review,” *Spectrochim. Acta Part B At. Spectrosc.*, vol. 60, no. 2, pp. 151–207, Feb. 2005, doi: 10.1016/j.sab.2005.01.005.

[229] E. H. Evans and R. Clough, “Isotope Dilution Analysis,” in *Encyclopedia of Analytical Science*, Elsevier, 2005, pp. 545–553. doi: 10.1016/B0-12-369397-7/00301-0.

[230] A. Stracke, E. E. Scherer, and B. C. Reynolds, “Application of Isotope Dilution in Geochemistry,” in *Treatise on Geochemistry*, Elsevier, 2014, pp. 71–86. doi: 10.1016/B978-0-08-095975-7.01404-2.

[231] P. Rodríguez-González and J. I. García Alonso, “Isotope Dilution Mass Spectrometry,” in *Reference Module in Chemistry, Molecular Sciences and Chemical Engineering*, Elsevier, 2018. doi: 10.1016/B978-0-12-409547-2.14387-2.

[232] E. Roth, “Critical evaluation of the use and analysis of stable isotopes (Technical Report),” *Pure Appl. Chem.*, vol. 69, no. 8, pp. 1753–1828, Jan. 1997, doi: 10.1351/pac199769081753.

[233] D. G. Chapman, “The Estimation of Biological Populations,” *Ann. Math. Stat.*, vol. 25, no. 1, pp. 1–15, Mar. 1954, doi: 10.1214/aoms/1177728844.

[234] J. Meija and Z. Mester, “Paradigms in isotope dilution mass spectrometry for elemental speciation analysis,” *Anal. Chim. Acta*, vol. 607, no. 2, pp. 115–125, Jan. 2008, doi: 10.1016/j.aca.2007.11.050.

[235] K. G. Heumann, S. M. Gallus, G. Rädlinger, and J. Vogl, “Precision and accuracy in isotope ratio measurements by plasma source mass spectrometry,” *J. Anal. At. Spectrom.*, vol. 13, no. 9, p. 1001, Jan. 1998, doi: 10.1039/a801965g.

[236] T. Zhang *et al.*, “Determination of serum glucose by isotope dilution liquid chromatography-tandem mass spectrometry: a candidate reference measurement procedure,” *Anal. Bioanal. Chem.*, vol. 408, no. 26, pp. 7403–7411, Oct. 2016, doi: 10.1007/s00216-016-9817-0.

[237] J. Vogl and W. Pritzkow, “Isotope dilution mass spectrometry - A primary method of measurement and its role for RM certification,” *Mapan - J. Metrol. Soc. India*, vol. 25, no. 3, pp. 135–164, Sep. 2010, doi: 10.1007/s12647-010-0017-7.

[238] J. Vogl, “Measurement uncertainty in single, double and triple isotope dilution mass spectrometry,” *Rapid Commun. Mass Spectrom.*, vol. 26, no. 3, pp. 275–281, Feb. 2012, doi: 10.1002/rcm.5306.

[239] L. G. Mackay, C. P. Taylor, R. B. Myors, R. Hearn, and B. King, “High accuracy analysis by isotope dilution mass spectrometry using an iterative exact matching technique,” *Accredit. Qual. Assur.*, vol. 8, no. 5, pp. 191–194, May 2003, doi: 10.1007/s00769-003-0622-z.

[240] R. Demirel, S. Erarpat, S. Bodur, Ö. T. Günkara, S. Bakırdere, and F. Turak, “Synthesis of Isotopic Labelled Paracetamol Benzoate- d3 and Its Application in the Determination of Paracetamol,” *ChemistrySelect*, vol. 8, no. 13, Apr. 2023, doi:

10.1002/slct.202203851.

[241] S. Bodur *et al.*, "A sensitive determination method for trace bisphenol A in bottled water and wastewater samples: Binary solvent liquid phase microextraction-quadrupole isotope dilution-gas chromatography-mass spectrometry," *Microchem. J.*, vol. 159, p. 105532, Dec. 2020, doi: 10.1016/j.microc.2020.105532.

[242] M. A. Bezerra *et al.*, "Simultaneous optimization of multiple responses and its application in Analytical Chemistry – A review," *Talanta*, vol. 194, pp. 941–959, Mar. 2019, doi: 10.1016/j.talanta.2018.10.088.

[243] M. A. Bezerra, R. E. Santelli, E. P. Oliveira, L. S. Villar, and L. A. Escaleira, "Response surface methodology (RSM) as a tool for optimization in analytical chemistry," *Talanta*, vol. 76, no. 5, pp. 965–977, Sep. 2008, doi: 10.1016/j.talanta.2008.05.019.

[244] S. L. C. Ferreira *et al.*, "Multivariate optimization techniques in analytical chemistry - an overview," *Microchem. J.*, vol. 140, pp. 176–182, Jul. 2018, doi: 10.1016/j.microc.2018.04.002.

[245] G. Hanrahan, J. Zhu, S. Gibani, and D. G. Patil, "CHEMOMETRICS AND STATISTICS | Experimental Design," in *Encyclopedia of Analytical Science*, Elsevier, 2005, pp. 8–13. doi: 10.1016/B0-12-369397-7/00079-0.

[246] L. A. Sarabia, M. C. Ortiz, and M. S. Sánchez, "Response Surface Methodology," in *Comprehensive Chemometrics*, Elsevier, 2020, pp. 287–326. doi: 10.1016/B978-0-12-409547-2.14756-0.

[247] S. L. C. Ferreira, "Experimental Design," in *Reference Module in Chemistry, Molecular Sciences and Chemical Engineering*, Elsevier, 2018. doi: 10.1016/B978-0-12-409547-2.14536-6.

[248] S. L. C. Ferreira *et al.*, "Box-Behnken design: An alternative for the optimization of analytical methods," *Anal. Chim. Acta*, vol. 597, no. 2, pp. 179–186, Aug. 2007, doi: 10.1016/j.aca.2007.07.011.

[249] D. B. Hibbert, "Experimental Design in Chromatography: A Tutorial Review," *J. Chromatogr. B*, vol. 910, pp. 2–13, Dec. 2012, doi: 10.1016/J.JCHROMB.2012.01.020.

[250] S. Erarpat, C. Demir, M. Öner, and S. Bakırdere, "Chromium speciation by the combination of high-performance liquid chromatography and inductively coupled plasma-optical emission spectrometry," *Environ. Monit. Assess.*, vol. 194, no. 10, p. 690, Oct. 2022, doi: 10.1007/s10661-022-10395-z.

[251] S. Erarpat, S. Bodur, Ö. T. Günkara, and S. Bakırdere, "Combination of high performance liquid chromatography and flame atomic absorption spectrophotometry using a novel nebulizer interface supported T shaped slotted quartz tube for the determination of Vitamin B12," *J. Pharm. Biomed. Anal.*, vol. 217, p. 114855, Aug. 2022, doi: 10.1016/j.jpba.2022.114855.

[252] S. Erarpat, S. Bodur, M. Öner, Ö. T. Günkara, and S. Bakırdere, "Quadruple isotope dilution gas chromatography-mass spectrometry after simultaneous derivatization and spraying based fine droplet formation liquid phase microextraction method for the accurate and sensitive quantification of chloroquine phosphate in human," *J. Chromatogr. A*, vol. 1651, p. 462273, Aug. 2021, doi: 10.1016/j.chroma.2021.462273.

[253] S. Erarpat, S. Bodur, M. Öner, Ö. T. Günkara, and S. Bakırdere, “A simple and efficient derivatization strategy combined with switchable solvent liquid–liquid microextraction hydroxychloroquine methyl acetate-d3-based quadruple isotope dilution gas chromatography mass spectrometry for the determination of hydroxychloro,” *Rapid Commun. Mass Spectrom.*, vol. 36, no. 12, Jun. 2022, doi: 10.1002/rcm.9282.

[254] B. Markiewicz, I. Komorowicz, A. Sajnóg, M. Belter, and D. Barałkiewicz, “Chromium and its speciation in water samples by HPLC/ICP-MS – technique establishing metrological traceability: A review since 2000,” *Talanta*, vol. 132, pp. 814–828, Jan. 2015, doi: 10.1016/j.talanta.2014.10.002.

[255] X. Guo, W. Liu, X. Bai, X. He, and B. Zhang, “Speciation of chromium in chromium yeast,” *World J. Microbiol. Biotechnol.*, vol. 30, no. 12, pp. 3245–3250, Dec. 2014, doi: 10.1007/s11274-014-1751-8.

[256] M. Jabłońska-Czapla and S. Szopa, “Arsenic, antimony and chromium speciation using HPLC-ICP-MS in selected river ecosystems of Upper Silesia, Poland – a preliminary study and validation of methodology,” *Water Supply*, vol. 16, no. 2, pp. 354–361, Apr. 2016, doi: 10.2166/ws.2015.146.

[257] J. Sun, Z. Yang, H. Lee, and L. Wang, “Simultaneous speciation and determination of arsenic, chromium and cadmium in water samples by high performance liquid chromatography with inductively coupled plasma mass spectrometry,” *Anal. Methods*, vol. 7, no. 6, pp. 2653–2658, 2015, doi: 10.1039/C4AY02813A.

[258] F. A. Byrdy, L. K. Olson, N. P. Vela, and J. A. Caruso, “Chromium speciation by anion-exchange high-performance liquid chromatography with both inductively coupled plasma atomic emission spectroscopic and inductively coupled plasma mass spectrometric detection,” *J. Chromatogr. A*, vol. 712, no. 2, pp. 311–320, Oct. 1995, doi: 10.1016/0021-9673(95)00528-U.

[259] J. Prokisch, B. Kovács, Z. Gyódri, and J. Loch, “Interfacing ion chromatography with inductively coupled plasma atomic emission spectrometry for the determination of chromium(III) and chromium(VI),” *J. Chromatogr. A*, vol. 683, no. 1, pp. 253–260, Oct. 1994, doi: 10.1016/S0021-9673(94)89122-2.

[260] A. N. Tang, D. Q. Jiang, Y. Jiang, S. W. Wang, and X. P. Yan, “Cloud point extraction for high-performance liquid chromatographic speciation of Cr(III) and Cr(VI) in aqueous solutions,” *J. Chromatogr. A*, vol. 1036, no. 2, pp. 183–188, May 2004, doi: 10.1016/j.chroma.2004.02.065.

[261] I. Ali and H. Y. Aboul-Enein, “Speciation of arsenic and chromium metal ions by reversed phase high performance liquid chromatography,” *Chemosphere*, vol. 48, no. 3, pp. 275–278, Jul. 2002, doi: 10.1016/S0045-6535(02)00085-1.

[262] C. S. Kesava Raju, L. L. Yu, J. E. Schiel, and S. E. Long, “A simple and sensitive LC-ICP-MS method for the accurate determination of vitamin B12 in fortified breakfast cereals and multivitamin tablets,” *J. Anal. At. Spectrom.*, vol. 28, no. 6, pp. 901–907, May 2013, doi: 10.1039/c3ja30383g.

[263] P. Viñas, N. Campillo, I. L. García, and M. H. Córdoba, “Speciation of vitamin B12 analogues by liquid chromatography with flame atomic absorption spectrometric detection,” *Anal. Chim. Acta*, vol. 318, no. 3, pp. 319–325, Jan. 1996, doi: 10.1016/0003-2670(95)00445-9.

[264] E. Psillakis and N. Kalogerakis, “Developments in single-drop microextraction,” *TrAC Trends Anal. Chem.*, vol. 21, no. 1, pp. 54–64, Jan. 2002, doi: 10.1016/S0165-9936(01)00126-1.

[265] S. Bodur, S. Erarpat, Ö. T. Günkara, and S. Bakırdere, “Accurate and sensitive determination of hydroxychloroquine sulfate used on COVID-19 patients in human urine, serum and saliva samples by GC-MS,” *J. Pharm. Anal.*, vol. 11, no. 3, pp. 278–283, Jun. 2021, doi: 10.1016/j.jpha.2021.01.006.

[266] D. S. Chormey and S. Bakirdere, “Principles and Recent Advancements in Microextraction Techniques,” *Compr. Anal. Chem.*, vol. 81, pp. 257–294, 2018, doi: 10.1016/bs.coac.2018.03.011.

[267] K. Kaewkhao, K. Chotivanich, M. Winterberg, N. P. Day, J. Tarning, and D. Blessborn, “High sensitivity methods to quantify chloroquine and its metabolite in human blood samples using LC–MS/MS,” *Bioanalysis*, vol. 11, no. 5, pp. 333–347, Mar. 2019, doi: 10.4155/bio-2018-0202.

[268] D. Lejeune *et al.*, “Simultaneous determination of monodesethylchloroquine, chloroquine, cycloguanil and proguanil on dried blood spots by reverse-phase liquid chromatography,” *J. Pharm. Biomed. Anal.*, vol. 43, no. 3, pp. 1106–1115, Feb. 2007, doi: 10.1016/j.jpba.2006.09.036.

[269] A. Daneshfar, T. Khezeli, and M. H. Manafi, “Determination of anti-malaria agent chloroquine using single drop liquid-liquid-liquid microextraction,” *J. Sep. Sci.*, vol. 32, no. 4, pp. 511–516, Feb. 2009, doi: 10.1002/jssc.200800483.

[270] F. C. Churchill, D. L. Mount, and I. K. Schwartz, “Determination of chloroquine and its major metabolite in blood using perfluoroacylation followed by fused-silica capillary gas chromatography with nitrogen-sensitive detection,” *J. Chromatogr. B Biomed. Sci. Appl.*, vol. 274, pp. 111–120, Jan. 1983, doi: 10.1016/S0378-4347(00)84414-X.

[271] F. Kapukıran, M. Fırat, D. S. Chormey, S. Bakırdere, and N. Özdoğan, “Accurate and Sensitive Determination Method for Procymidone and Chlorflurenol in Municipal Wastewater, Medical Wastewater and Irrigation Canal Water by GC–MS After Vortex Assisted Switchable Solvent Liquid Phase Microextraction,” *Bull. Environ. Contam. Toxicol.*, vol. 102, no. 6, pp. 848–853, Apr. 2019, doi: 10.1007/s00128-019-02618-w.

[272] M. Fırat and E. G. Bakırdere, “An accurate and sensitive analytical strategy for the determination of palladium in aqueous samples: slotted quartz tube flame atomic absorption spectrometry with switchable liquid–liquid microextraction after preconcentration using a Schiff base ligand,” *Environ. Monit. Assess.*, vol. 191, no. 3, p. 129, Mar. 2019, doi: 10.1007/s10661-019-7252-3.

[273] F. Parvinizadeh and A. Daneshfar, “Fabrication of a magnetic metal–organic framework molecularly imprinted polymer for extraction of anti-malaria agent hydroxychloroquine,” *New J. Chem.*, vol. 43, no. 22, pp. 8508–8516, 2019, doi: 10.1039/C9NJ01385G.

[274] L.-Z. Wang *et al.*, “Method development and validation for rapid quantification of hydroxychloroquine in human blood using liquid chromatography–tandem mass spectrometry,” *J. Pharm. Biomed. Anal.*, vol. 61, pp. 86–92, Mar. 2012, doi: 10.1016/j.jpba.2011.11.034.

[275] A. R. M. de Oliveira, C. D. Cardoso, and P. S. Bonato, “Stereoselective determination of hydroxychloroquine and its metabolites in human urine by liquid-phase microextraction and CE,” *Electrophoresis*, vol. 28, no. 7, pp. 1081–1091, Apr. 2007, doi: 10.1002/elps.200600420.

[276] B. Charlier *et al.*, “Development of a novel ion-pairing HPLC-FL method for the separation and quantification of hydroxychloroquine and its metabolites in whole blood,” *Biomed. Chromatogr.*, vol. 32, no. 8, Aug. 2018, doi: 10.1002/bmc.4258.

[277] U. Balçık, D. S. Chormey, M. F. Ayyıldız, and S. Bakırdere, “Liquid phase microextraction based sensitive analytical strategy for the determination of 22 hazardous aromatic amine products of azo dyes in wastewater and tap water samples by GC-MS system,” *Microchem. J.*, vol. 155, p. 104712, Jun. 2020, doi: 10.1016/j.microc.2020.104712.

[278] A. V. Herrera-Herrera, M. Asensio-Ramos, J. Hernández-Borges, and M. Á. Rodríguez-Delgado, “Dispersive liquid-liquid microextraction for determination of organic analytes,” *TrAC Trends Anal. Chem.*, vol. 29, no. 7, pp. 728–751, Jul. 2010, doi: 10.1016/J.TRAC.2010.03.016.

[279] F. Aydin, E. Yilmaz, and M. Soylak, “Vortex assisted deep eutectic solvent (DES)-emulsification liquid-liquid microextraction of trace curcumin in food and herbal tea samples,” *Food Chem.*, vol. 243, pp. 442–447, Mar. 2018, doi: 10.1016/j.foodchem.2017.09.154.

[280] M. Rezaee, Y. Yamini, S. Shariati, A. Esrafili, and M. Shamsipur, “Dispersive liquid–liquid microextraction combined with high-performance liquid chromatography-UV detection as a very simple, rapid and sensitive method for the determination of bisphenol A in water samples,” *J. Chromatogr. A*, vol. 1216, no. 9, pp. 1511–1514, Feb. 2009, doi: 10.1016/j.chroma.2008.12.091.

[281] R. Fritsche-Guenther *et al.*, “Optimized Workflow for On-Line Derivatization for Targeted Metabolomics Approach by Gas Chromatography-Mass Spectrometry,” *Metabolites*, vol. 11, no. 12, p. 888, Dec. 2021, doi: 10.3390/metabo11120888.

[282] H. E. H. Ahmed, A. M. A. Mohammed, and M. Soylak, “A magnetic solid phase extraction procedure for Pb(II) at trace levels on magnetic Luffa@TiO2 in food and water samples,” *Food Chem.*, vol. 428, p. 136794, Dec. 2023, doi: 10.1016/j.foodchem.2023.136794.

[283] A. Peña-Alvarez, E. Ramírez-Maya, and L. Á. Alvarado-Suárez, “Analysis of capsaicin and dihydrocapsaicin in peppers and pepper sauces by solid phase microextraction–gas chromatography–mass spectrometry,” *J. Chromatogr. A*, vol. 1216, no. 14, pp. 2843–2847, Apr. 2009, doi: 10.1016/j.chroma.2008.10.053.

[284] M. Consolación Rodríguez-Palazón, N. Arroyo-Manzanares, P. Viñas, and N. Campillo, “Metabolomic study of capsaicinoid compounds in urine samples by dispersive liquid–liquid microextraction and ultra-high performance liquid chromatography with quadrupole time-of-flight mass spectrometry,” *Microchem. J.*, vol. 178, p. 107373, Jul. 2022, doi: 10.1016/j.microc.2022.107373.

[285] Q. Lu, H. Guo, D. Li, and Q. Zhao, “Determination of capsaicinoids by magnetic solid phase extraction coupled with UPLC-MS/MS for screening of gutter oil,” *J. Chromatogr. B*, vol. 1158, p. 122344, Nov. 2020, doi: 10.1016/j.jchromb.2020.122344.

[286] S. Chanthai, J. Juangsamoot, C. Ruangviriyachai, and S. Techawongstien, “Determination of Capsaicin and Dihydrocapsaicin in Some Chilli Varieties using Accelerated Solvent Extraction Associated with Solid-Phase Extraction Methods and RP-HPLC-Fluorescence,” *E-Journal Chem.*, vol. 9, no. 3, pp. 1550–1561, 2012, doi: 10.1155/2012/380574.

# PUBLICATIONS FROM THE THESIS

## Papers

**1.** S. Erarpat, S. Bodur, M. Öner, Ö.T. Günkara and S. Bakırdere, "Quadruple isotope dilution gas chromatography-mass spectrometry after simultaneous derivatization and spraying based fine droplet formation liquid phase microextraction method for the accurate and sensitive quantification of chloroquine phosphate in human serum, urine and saliva samples at trace levels," *J. Chromatogr. A,* vol 1651, p. 462273, 2021.

**2.** S. Erarpat, C. Demir, M. Öner and S. Bakırdere, "Chromium speciation by the combination of high-performance liquid chromatography and inductively coupled plasma-optical emission spectrometry," *Environ. Monit. Assess.,* vol 194(10), p. 690, 2022.

**3.** S. Erarpat, S. Bodur, Ö.T. Günkara and S. Bakırdere, "Combination of high-performance liquid chromatography and flame atomic absorption spectrophotometry using a novel nebulizer interface supported T shaped slotted quartz tube for the determination of Vitamin B12," *J. Pharm. Biomed. Anal.,* vol 217, p. 114855, 2022.

**4.** S. Erarpat, S. Bodur, M. Öner, Ö.T. Günkara and S. Bakırdere, "A simple and efficient derivatization strategy combined with switchable solvent liquid–liquid microextraction hydroxychloroquine methyl acetate-d3-based quadruple isotope dilution gas chromatography mass spectrometry for the determination of hydroxychloroquine sulfate in biological fluids," *Rapid Commun. Mass Spectrom.,* vol 36(12), p. e9282, 2022.

## Conference papers

**1.** S. Erarpat, C. Demir, M. Öner and S. Bakırdere, "Chromium Speciation in Soil, Water and Grass Samples by HPLC-ICP-OES," in 4$^{th}$ International Environmental Chemistry Congress, Antalya, 2022, pp 36.

**2.** S. Erarpat, S. Bodur, Ö.T. Günkara and S. Bakırdere, "Determination of Vitamin B12 in Vitamin Tablets by High Performance Liquid Chromatography Combined with Flame Atomic Absorption Spectrophotometry with a Novel Nebulizer Interface Supported T-

Shaped Slotted Quartz Tube," in 33rd International Symposium on Pharmaceutical and Biomedical Analysis, Ankara, 2023, pp 80.

**Projects**

**1.** 8946, SARS-CoV-2 (COVID-19) Tedavisinde Kullanılan Klorokin ve Hidroksiklorokin Kimyasallarının Kan, İdrar ve Tükürük Örneklerinde Yüksek Doğruluk ve Duyarlılıkta Hızlı Tayinlerine Yönelik İzotop Seyreltme Esaslı Analitik Yöntem Geliştirilmesi, TÜSEB Project (2020-CV-01 Call), Assistant Staff, Project Participitation/Departure Dates: 01.06.2020 – 01.02.2021, Project Start/End Dates: 01.06.2020 – 01.02.2021.

**2.** 122Z041, Biyolojik, Çevre ve Gıda Örneklerinde Bulunan Kapsaisinin Mikroekstraksiyon Yöntemleri ile Birleştirilmiş Dörtlü İzotop Seyreltme Kütle Spektrometresi ile Eser Seviyelerde Yüksek Doğruluk ve Duyarlılıkta Tayini, 1001 TÜBİTAK Project, Researcher, Project Participitation/Departure Dates: 15.04.2022 – 15.05.2024, Project Start/End Dates: 15.04.2022 – 15.05.2024.